NORTHWESTERN UNIVERSITY

Constrained Geometry Organoactinide Complexes: Scope and Mechanism of Intramolecular

Hydroamination/Cyclization of Primary and Secondary Amines

A DISSERTATION

SUBMITTED TO THE GRADUATE SCHOOL
IN PARTIAL FULFILLMENT OF THE REQUIREMENTS

for the degree

DOCTOR OF PHILOSOPHY

FIELD OF CHEMISTRY

By

Bryan D. Stubbert

EVANSTON, ILLINOIS

DECEMBER 2006

ABSTRACT

Constrained Geometry Organoactinide Complexes: Scope and Mechanism of Intramolecular Hydroamination/Cyclization of Primary and Secondary Amines

Bryan D. Stubbert

In Chapter 1, a series of "constrained geometry" organoactinide complexes, $(CGC)An(NMe)_2$ ($CGC = Me_2Si(\eta^5-Me_4C_5)(^tBuN)$; An = Th, **1**; U, **2**), prepared via efficient in situ, two-step protodeamination routes in good yields and high purity, is presented. Both **1** and **2** are quantitatively converted to the neutrally charged, solvent-free dihalides (**1-Cl$_2$**, **2-Cl$_2$** and **1-I$_2$**, **2-I$_2$**) with excess $Me_3Si–X$ (X = Cl, I) in non-coordinating solvents. Characterization of **1** and **2** by single crystal X-ray diffraction reveals substantially increased metal coordinative unsaturation vs. the corresponding $Me_2SiCp''_2AnR_2$ ($Cp'' = \eta^5-Me_4C_5$; An = Th, R = $CH_2(SiMe_3)$, **3**; An = U, R = CH_2Ph, **4**) and Cp'_2AnR_2 ($Cp' = \eta^5-Me_5C_5$; An = Th, R = $CH_2(SiMe_3)$, **5**; An = U, R = $CH_2(SiMe_3)$, **6**) complexes. Complexes **1**-**6** exhibit broad applicability for the intramolecular hydroamination (HA) of diverse C–C unsaturations, including terminal and internal aminoalkenes (primary and secondary amines), aminoalkynes (primary and secondary amines), aminoallenes, and aminodienes. Large turnover frequencies (N_t up to 3000 h^{-1}) and high regioselectivities (≥ 95%) are observed throughout. With several noteworthy exceptions, reactivity trends track relative 5f ionic radii and ancillary ligand coordinative unsaturation. Reactivity patterns and activation parameters are consistent with a reaction pathway proceeding via turnover-limiting C=C/C≡C insertion into the An–N σ-bond.

In Chapter 2, a detailed mechanistic study of intramolecular HA/cyclization catalyzed by tetravalent organoactinide and organozirconium complexes is presented. A series of selectively substituted complexes, $(CGC)M(NR_2)Cl$ (M = Th, **1-Cl**; U, **2-Cl**; R = $SiMe_3$; M = Zr, R = Me, **3-Cl**) and $(CGC)An(NMe_2)OAr$ (An = Th, **1-OAr**; An = U, **2-OAr**), has been prepared via in situ protodeamination (complexes **1**-**2**) or salt metathesis (**3-Cl**) in high purity and excellent yield, and are found to be active precatalysts for intramolecular primary and secondary aminoalkyne and aminoalkene hydroamination/cyclization. Substrate reactivity trends, rate laws, and activation parameters for cyclizations mediated by these complexes are virtually identical to those of more conventional $(CGC)MR_2$ (**1-3**), $(Me_2SiCp''_2)UBn_2$ (**4**), Cp'_2AnR_2 (**5-6**) and analogous organolanthanide complexes. Deuterium KIE measured at 25 °C in C_6D_6 for aminoalkene $D_2NCH_2C(CH_3)_2CH_2CHCH_2$ (**11**-d_2) with precatalysts **2** and **2-Cl** indicate k_H/k_D = 3.3(5) and 2.6(4), respectively. This provides strong evidence in these systems for turnover-limiting C–C insertion into an M–N(H)R σ-bond in the transition state. Related complexes $(Me_2SiCp''_2)U(CH_2Ph)(Cl)$ (**4-Cl**) and $Cp'_2An(R)(Cl)$ (An = Th, **5-Cl**; An = U, **6-Cl**) are also found to be effective precatalysts for this transformation. Additional arguments in favor of M–N(H)R intermediates vs. M=NR intermediates are presented.

Tobin J. Marks

ACKNOWLEDGEMENTS

I would like to thank my advisor, Professor Tobin Marks, for his support and guidance throughout my 5 ½ years in his research group. From my stint as zero-year until completion of this thesis, Tobin made himself available to me for questions, suggestions, and advice, both within chemistry and beyond. I have tried to learn as much as possible by following his example of meticulously attacking every problem with diligence, creativity, and enthusiasm. His mentorship has been and continues to be an invaluable part of my education, for which I will always be grateful.

I would also like to thank the members of my doctoral committee – Professors Lambert, Stair, and Ibers – for their scrutiny of my written work and presentations. In addition, several members of the faculty in the Inorganic Division have added a great deal to my development as a research scientist. Jim Ibers has provided a delightful combination of comic relief and keen observation in BIP and seminars alike. Hilary Godwin and Tom Meade have repeatedly offered their time in providing support and encouragement for my career after Northwestern, where their input has often been uplifting. Finally, I would like to thank Professor Fred Basolo for his advice in chemistry and in life, but above all, for his friendship. When I volunteered to orchestrate BIP in my 5th year of graduate school, I had some reservations about the level of commitment in trying to restore a great tradition. While I learned and gained many things in my role as

BIPmeister, the friendship that developed with Fred quickly became far more important than any other aspect of BIP, and I will always remember it fondly.

My labmates and friends from the Marks group have also been instrumental in my research progress. From the day that Nikki Edelman greeted me in G Wing, the senior members of the group served as a collective student mentor as I tried to get my equipment and project up and running. In particular, I would like to thank Nikki, Matt Metz, Mike Douglass, Hongsang Ahn, Sukwon Hong, Amber Kawaoka, Nick Stahl, Graham Abramo, Aswini Dash, Sven Schneider, Neng Guo, Mike Salata, Neeraj Saraiya, Holming Yuen, Smruti Amin, Milko van der Boom, and Antonio Facchetti for their camaraderie, even after departure (theirs or my own). The other hydroelementation types – Douglass, Amber, Sukwon, Jaesang Ryu, Masataka Oishi, Jiuqing Zhao, Holming, Bruce Xianghua Yu – are owed a special thanks for making our marathon f-element meetings (and sub-subgroup as a whole) an interesting adventure that, at times, seemed to last forever. A special thanks to Tryg Jensen is also in order for *acting* as a mentor during my zero-year, but more so for being a friend and roommate. Along with Eli Sone, John Magyar, Scott Barry, and Pete Dinolfo, Tryg was part of my everyday life when Rebecca Landry became a truly permanent fixture in my life. Some of Rebecca's friends and roommates – Heather Izumi, Katy Splan, Ryan and Maria Bailey, Aaron and Andrea Massari, Emily Weiss, and Beth Litzinger – were also mine and I thank them for putting up with "the couple" and for letting us spend so much time together as part of such a special group.

Last but certainly not least, I would like to thank my parents and family for being an important part of my formal and informal educations. Pop showed me what hard work really is

(long before I saw Tobin in action), and without my Mom, I might not have survived to high school. My brother Sean is my best friend that I didn't marry, and both he and my brother Eric continue to shape who I am today. Rebecca's family has also supported me and even tried to find interest in all of this chemistry that fascinates me and keeps their daughter and sister far away. I would also like to give special thanks to my wife, Rebecca, for being my best friend and for bringing our beautiful son Reid into our lives. I am also grateful to Reid for bringing us so much joy, for helping me stay awake, and forcing me to work with a baby in one hand and a keyboard in the other. Thank you all for being my family and for building the world around me.

DEDICATION

To my Mom and Rebecca

Thank you for making me believe,

for helping me get here,

and for staying with me as I finished

TABLE OF CONTENTS

LISTS OF TABLES

Chapter 1

Chapter 2

Appendix

LISTS OF CHARTS, FIGURES, AND SCHEMES

Chapter 1

Constrained Geometry Organoactinides as Versatile Catalysts for the Intramolecular Hydroamination/Cyclization of Primary and Secondary Amines Having Diverse Tethered C–C Unsaturation
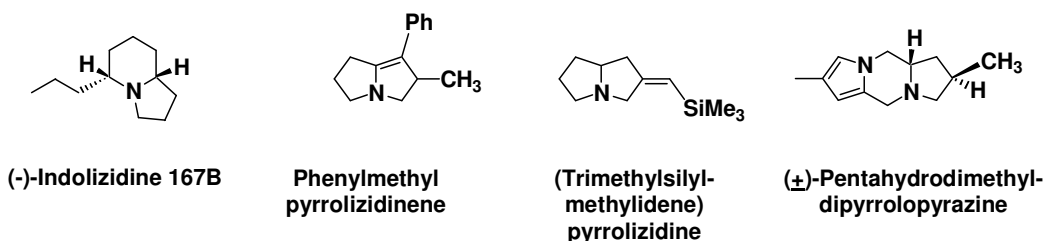
Abstract

A series of "constrained geometry" organoactinide complexes, $(CGC)An(NMe)_2$ ($CGC = Me_2Si(\eta^5\text{-}Me_4C_5)(^tBuN)$; An = Th, **1**; U, **2**), has been prepared via efficient in situ, two-step protodeamination routes in good yields and high purity. Both **1** and **2** are quantitatively converted to the neutrally charged, solvent-free dichlorides (**1-Cl$_2$**, **2-Cl$_2$**) and slightly more soluble diiodides (**1-I$_2$**, **2-I$_2$**) with excess $Me_3Si–X$ (X = Cl, I) in non-coordinating solvents. The new complexes were characterized by NMR spectroscopy, elemental analysis, and (for **1** and **2**) single crystal X-ray diffraction, revealing substantially increased metal coordinative unsaturation vs. the corresponding $Me_2SiCp''_2AnR_2$ ($Cp'' = \eta^5\text{-}Me_4C_5$; An = Th, R = $CH_2(SiMe_3)$, **3**; An = U, R = CH_2Ph, **4**) and Cp'_2AnR_2 ($Cp' = \eta^5\text{-}Me_5C_5$; An = Th, R = $CH_2(SiMe_3)$, **5**; An = U, R = $CH_2(SiMe_3)$, **6**) complexes. Complexes **1-6** exhibit broad applicability for the intramolecular hydroamination (HA) of diverse C–C unsaturations, including terminal and internal aminoalkenes (primary and secondary amines), aminoalkynes (primary and secondary amines), aminoallenes, and aminodienes. Large turnover frequencies (N_t up to 3000 h^{-1}) and high regioselectivities ($\geq$ 95%) are observed throughout, along with moderate to high diastereoselectivities (up to 90% *trans* ring closures). With several noteworthy exceptions, reactivity trends track relative 5f ionic radii and ancillary ligand coordinative unsaturation. Reactivity patterns and activation parameters are consistent with a reaction pathway proceeding via turnover-limiting C=C/C≡C insertion into the An–N σ-bond.

Introduction

The regioselective formation of C–N bonds is an important transformation in chemistry and biology, attracting considerable interest in both academic and industrial research.[1] Hydroamination (HA), defined as the formal addition of an N–H bond across a unit of C–C unsaturation,[2] is an atom-economical route to constructing both simple and complex organonitrogen skeletons and is capable of doing so efficiently and with high selectivity. Initially dominated by studies involving lanthanides,[3,4] current *intramolecular* HA/cyclization research activity is wide-ranging[2] and spans the entire Periodic Table,[5,6] from Ca[7] to the coinage metals.[8] While late transition metal catalysts generally enjoy greater functional group tolerance, they often require acidic conditions and *N*-protected amines, and may be further plagued by low efficiency and short catalyst lifetimes.[2] Early transition metal catalysts typically exhibit enhanced activity, however, with one noteworthy exception,[5g] these electrophilic catalysts normally have limited functional group tolerance and sluggish reaction rates vs. larger, more electrophilic organolanthanide catalysts.[2,5]

Beginning with terminal aminoalkenes,[3u,v] intramolecular organolanthanide-catalyzed HA/cyclization processes have been extensively investigated (Scheme 1),[2d,3,4] typically displaying near-quantitative yields in addition to high regio- and diastereoselectivities (> 95%) in addition to moderate/good enantioselectivities (up to 95%).[2b-d;3b-d,q-r;4b,d,h-l;9] The highly exothermic intramolecular HA/cyclization of simple aminoalkynes proceeds with surprising ease for both terminal and 1,2-disubstituted alkynes when catalyzed by organolanthanide complexes.[3n,s] Furthermore, single amines tethered to C=C and C≡C linkages undergo cascade

reactions involving sequential C–N/C–C bond fusions with high regioselection to afford

indolizidine, pyrrole, pyrrolizidine, and pyrazine scaffolds, while selectively retaining

unsaturations amenable to subsequent functionalization.[3k,l,o;4n,o] Initial difficulties in directly

adding N–H bonds across

| (-)-Indolizidine 167B | Phenylmethyl pyrrolizidinene | (Trimethylsilyl-methylidene) pyrrolizidine | (±)-Pentahydrodimethyl-dipyrrolopyrazine |

1,2-disubstituted C=C linkages[3i,u;4s,t] were overcome via implementation of more open, thermally

robust organolanthanide structures at high temperatures.[3b,h;4o] En route to such advances,

heterocyclic skeletons of greater structural complexity were accessed from allenic[3h,i,k] and

dienic[3c,f] substrates. In all cases, the tunable ionic radii of the Ln series (Table 1)[10] proved vital to

understanding those kinetic and mechanistic factors governing HA ring closure. Furthermore, the

possibility of broadening the scope of this powerful C–N bond-forming methodology by tuning

ancillary ligand architecture motivated the exploratory synthesis of additional catalyst classes.

With open coordination spheres having documented applications throughout the Periodic

Table,[11] the "constrained geometry" ligand ("CGC") was applied to organolanthanides. The
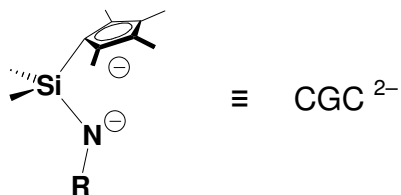
$$\equiv \quad CGC^{2-}$$

Table 1. Comparison of ionic radii for relevant lanthanide and actinide ions. See ref 10.

| Ion	Coordination No.	Ionic Radius (Å)
Th^{4+}	9	1.09
U^{4+}	9	1.05
La^{3+}	8	1.16
Sm^{3+}	8	1.079
Y^{3+}	8	1.019
Lu^{3+}	8	0.977

resulting catalysts are particularly efficacious for activating sterically encumbered and otherwise less-reactive amine substrates, especially when combined with larger radius lanthanides.[3a-j]

Actinide (An) and Ln chemistries differ primarily in the degree of covalency and extent of f-orbital participation in bonding and reactivity.[12,13] Unlike the poorly shielded and primarily non-bonding Ln 4f orbitals, limited involvement of An 6d and 5f orbitals has been invoked to explain observed molecular geometries and stabilities, as well as unique chemical reactivity patterns,[14] and has been ascribed to the increased importance of relativistic effects[12a,h-l] and improved shielding of the 5f orbitals. Although 6d and 5f orbital participation is still *relatively* modest, the degree of bond covalency is significantly enhanced over lanthanides,[12] presenting unique possibilities for new and interesting reactivity modalities. In light of the broad scope of substrates amenable to intramolecular HA/cyclization catalyzed by organolanthanides[2d,3,4] along with the intriguing similarities and differences between 4f- and 5f-element organometallic chemistries,[12] the investigation of organoactinide HA/cyclization catalysts having increased coordinative unsaturation, along with an additional covalently bonded ligand (vs. Ln), offers an
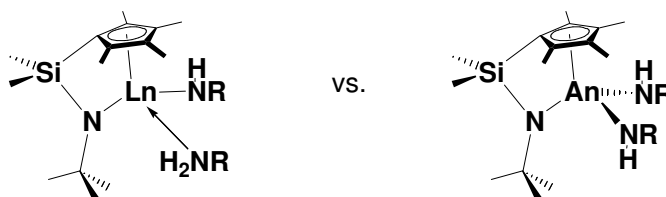

ideal opportunity to examine the roles of bond covalency, ionic radius, metal oxidation state, and ancillary ligation, as well as the mechanistic significance of these factors.

Scheme 1. Scope of intramolecular HA/cyclization mediated by organo-4f-element catalysts (see refs. 2d, 3, and 4).
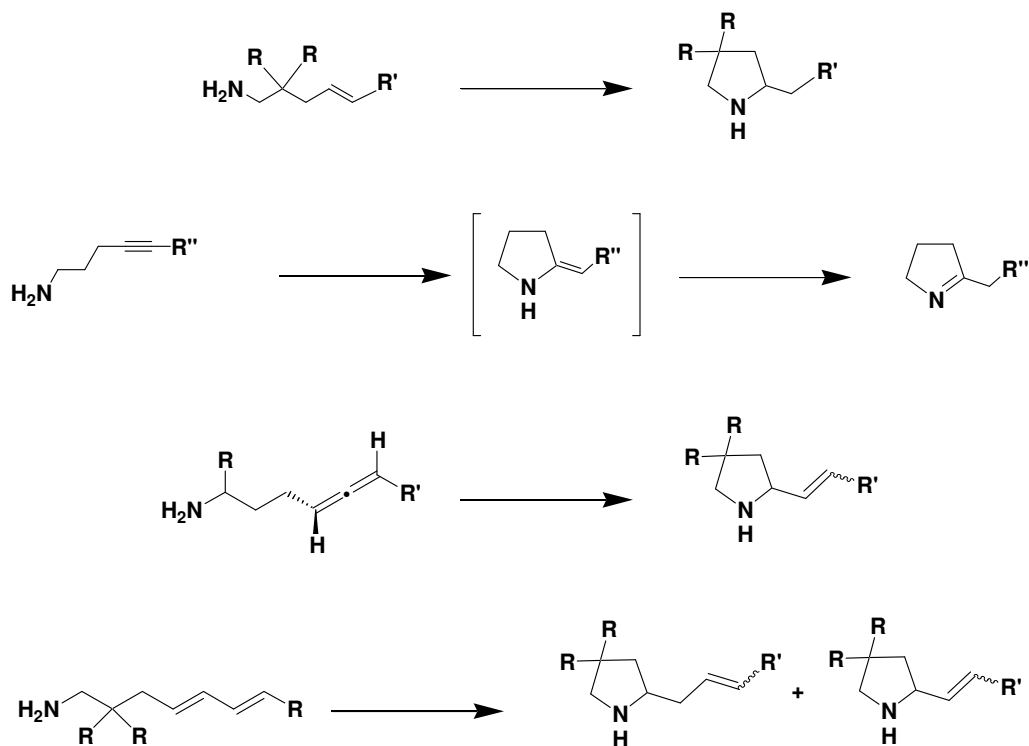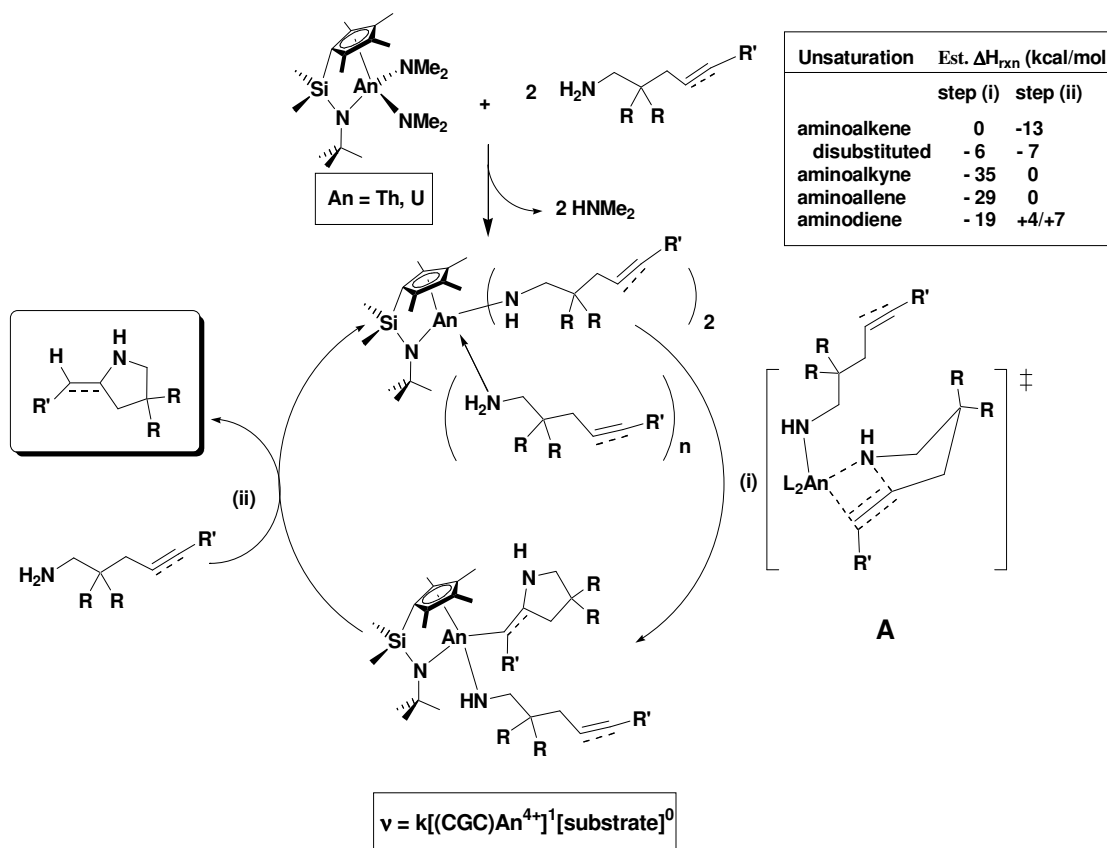
We previously communicated the synthesis and characterization of several members of a new class of CGC organoactinide complexes, along with initial investigations of their catalytic competence for intramolecular HA/cyclization.[15] From these preliminary results, we envisioned a mechanistic pathway as depicted in Scheme 2, with an insertive transition state such as A. In this Chapter, we report improved syntheses

A
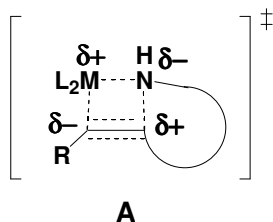
of (CGC)An‹ complexes and a detailed investigation of their catalytic intramolecular HA/cyclization activity with respect to a broad series of representative substrates. We compare/contrast with less open organoactinide complexes and discuss these results relative to electrophilic organolanthanide and group 4 metal catalysts. The scope of organoactinide-catalyzed HA/cyclization established includes 1,2-disubstituted alkenes, allenes, and diene C–C unsaturations tethered to 1° amines. Furthermore, we show that 2° aminoalkenes and aminoalkynes are rapidly converted to 3° pyrrolidine and enamine heterocycles, *requiring* the agency of an M–N σ-bonded intermediate in the insertive transition state (**A**, Scheme 2). A companion contribution presents a detailed mechanistic investigation of (CGC)An‹-mediated hydroamination.[16]

Scheme 2. Proposed mechanism for the intramolecular HA/cyclization of C–C unsaturations tethered to 1° and 2° amines, including alkene, alkyne, allene, and diene substrates under mild conditions in C_6D_6 or C_7D_8. This mechanistic scenario is consistent with the observed rate law, $\nu \sim [(CGC)An]^1[substrate]^0$, and is similar to the σ-bond insertive pathway proceeding through an $L_2Ln–N(H)R$ intermediate proposed for organolanthanide-catalyzed HA/cyclization processes (see refs 2-4).

Unsaturation	Est. ΔH_{rxn} (kcal/mol)	
	step (i)	step (ii)
aminoalkene	0	-13
disubstituted	- 6	- 7
aminoalkyne	- 35	0
aminoallene	- 29	0
aminodiene	- 19	+4/+7

$$\nu = k[(CGC)An^{4+}]^1[substrate]^0$$

Experimental

General Considerations.

All manipulations of air-sensitive materials were carried out with rigorous exclusion of oxygen and moisture in flame- or oven-dried Schlenk-type glassware on a dual-manifold Schlenk line, interfaced to a high-vacuum manifold (10^{-6} Torr), or in a nitrogen-filled Vacuum Atmospheres glovebox with a high capacity recirculator (< 2 ppm of O_2). Argon (Matheson, prepurified) was purified by passage through a MnO oxygen-removal column and a Davison 4A molecular sieve column. All solvents were dried and degassed over Na/K alloy and transferred in vacuo immediately prior to use. Commercially available materials were purchased from Aldrich, Lancaster, or Fisher (Acros) and used without further purification unless otherwise noted. $Th(C_2O_4)_2 \cdot 6H_2O$ was precipitated from an acidic aqueous solution of $Th(NO_3)_4 \cdot 4H_2O$ with oxalic acid and converted to anhydrous ThO_2 by thermolysis and oxidation in dry air at 450 °C. [17] Anhydrous $ThCl_4$ was then prepared by slowly passing a stream of CCl_4 vapor in N_2 over ThO_2 at 500 ºC.[17] The extremely air- and moisture-sensitive reagents UCl_4,[18] $U(NMe_2)_4$,[19] $Th(NMe_2)_4$,[20] $Me_2SiCp''_2Th[CH_2(SiMe_3)]_2$ (**3**),[21] $Me_2SiCp''_2U(CH_2Ph)_2$ (**4**),[22] Cp'_2ThR_2 (**5**), and Cp'_2UR_2 (**6**) ($Cp' = \eta^5\text{-}C_5Me_5$; $R = CH_2(SiMe_3)$],[23] as well as H_2CGC,[24] aminoalkenes **7**, **9**, **11**, **13**, **15**, **17**, **19**, **21**, **23**, **27**, **29**, **31**,[3b,c;25] aminoallenes **43**, **45**, **47**, [3j] and aminodienes **49**, **51**, **53**[3c] were prepared according to literature procedures. Aminoalkynes **25**, **33**, **35**, **37**, and **39** were prepared according to literature procedures[3n] or according to the general method detailed below for **41** (in improved overall yield). All substrates for catalytic experiments were dried at least three times as solutions in benzene-d_6 or toluene-d_8 over freshly-activated Davison 4A molecular

sieves and were degassed by repeated freeze-pump-thaw cycles. Aminoalkynes were pre-dried by stirring over BaO overnight as C_6D_6 solutions before rigorous drying over freshly activated molecular sieves. Substrates were then stored under Ar in vacuum-tight storage flasks.

Physical and Analytical Measurements.

NMR spectra were recorded on a ^{UNITY}Inova-500 (FT, 500 MHz, ^{1}H; 125 MHz, ^{13}C) instrument.   Chemical shifts (δ) for ^{1}H and ^{13}C spectra are referenced to internal solvent resonances and reported relative to Me_4Si. NMR experiments on air-sensitive samples were conducted in Teflon valve-sealed tubes (J. Young). EI-HRMS data were obtained using a Thermo Finnigan MAT-XL900 spectrometer at 70 eV. Elemental analyses on air-sensitive samples were performed by the Micro-Mass Facility at U. of California, Berkeley; air-stable samples were analyzed by Midwest Microlabs, Indianapolis, IN.

(CGC)Th(NMe$_2$)$_2$ (1). A small flip-frit apparatus with a magnetic stir bar was charged in the glovebox with $ThCl_4$ (5.00 g, 13.4 mmol) and $LiNMe_2$ (2.65 g, 52.0 mmol; 3.9 equiv). After evacuating under high-vacuum, pentane (10 mL) and THF (60 mL) were condensed onto the solids at -196 ºC. The stirring mixture was allowed to slowly warm to 20 ºC under Ar and allowed to react for an additional 24 h before removing all volatiles in vacuo. Pentane (30 mL) was condensed onto the resulting oily residue at -78 ºC and then allowed to warm to 20 ºC under Ar. After stirring overnight, the pale-yellow pentane solution was filtered and concentrated in vacuo to afford an off-white solid that was further dried under high-vacuum to afford 1.895 g of

a roughly 1:1 mixture of $Th(NMe_2)_4$ and $Li[Th(NMe_2)_5](THF)_n$. as determined by ^{1}H NMR spectroscopy (ca. 4.64 mmol of "$Th(NMe_2)_4$", 35% yield).[19]

A 100 mL round bottom flask in the glovebox containing the isolated mixture (homoleptic amide + ate complex), magnetic stir bar, and high-vacuum adapter was charged with pentane (15 mL) and H_2CGC (1.18 g, 4.67 mmol) at 20 ℃. The flask was moved to the high-vacuum manifold where volatile byproduct $HNMe_2$ was periodically removed via Ar flush and/or partial evacuation over 3 d. Complete evacuation of volatiles, followed by condensation of fresh solvent (either pentane or toluene) into the reaction flask at -196 ℃, was carried out once every 12 h. Reaction progress can be monitored by ^{1}H NMR spectroscopy. The product was next isolated by extraction with pentane (2 x 25 mL) and filtration. The solution was concentrated to a volume of ca. 10 mL, and **1** was isolated by slow cooling to -78 ℃. Collection of the colorless powder on a glass frit afforded 1.94 g of **1** (74% yield based on "$Th(NMe_2)_4$"). ^{1}H NMR (C_6D_6, 500 MHz, 25 ℃): δ 2.81 (s, 12 H, N(CH_3)$_2$), 2.20 (s, 6 H, $C_5(CH_3)_4$), 2.02 (s, 6 H, $C_5(CH_3)_4$), 1.30 (s, 9 H, NC(CH_3)$_3$), 0.67 (s, 6 H, Si(CH_3)$_2$).

(CGC)U(NMe₂)₂ (2). The one-pot preparative route to $(CGC)An(NR_2)_2$ complexes is detailed here for complex **2**. A 250 mL sidearm flask with a magnetic stir bar was charged in the glovebox with UCl_4 (3.00 g, 7.90 mmol) and $LiNMe_2$ (1.57 g, 30.8 mmol, 3.9 equiv). The flask was evacuated under high-vacuum before condensing pentane (20 mL) and THF (80 mL) onto the solids at -78 ℃. The dark red mixture was protected from light and allowed to warm slowly with stirring to 20 ℃ under Ar. After 20 h, the volatiles were removed in vacuo and replaced

with pentane (80 mL) at -78 ºC. The mixture was warmed to 20 ºC, and a solution of H_2CGC (2.35 g, 9.34 mmol; 1.18 equiv) in pentane (5 mL) was added by syringe through the sidearm under a rapid Ar purge. Byproduct $HNMe_2$ was periodically removed via Ar flow and/or partial evacuation over 2 d. Complete evacuation of volatiles, followed by condensation of fresh pentane into the flask at -196 ºC, was carried out once every 6-12 h. Reaction progress may be monitored by ^1H NMR spectroscopy. Product **2** is isolated and purified by filtration, followed by concentration to a volume of < 10 mL and slow cooling to -78 ºC. Decantation of the mother liquor afforded 3.20 g of brown microcrystalline **2** in 71% yield (from UCl_4). ^1H NMR (C_6D_6, 500 MHz, 25 ºC): δ 22.24 (s, 12 H, N(CH_3)$_2$), 15.28 (s, 6 H, $C_5(CH_3)_4$), 1.31 (s, 6 H, $C_5(CH_3)_4$), -18.93 (s, 9 H, NC(CH_3)$_3$), -22.08 (s, 6 H, Si(CH_3)$_2$).

(CGC)ThCl$_2$ (1-Cl$_2$). A 100 mL round-bottom reaction flask was charged in the glove box with **1** (0.911 g, 1.60 mmol) and pentane (25 mL) before adding trimethylchlorosilane (1.2 mL, 9.5 mmol) by syringe, immediately producing a colorless precipitate. The flask was then attached to the vacuum line, and the solution stirred overnight at 20 ºC. The colorless **1-Cl$_2$** powder is formed in quantitative yield as assessed by ^1H NMR spectroscopy. The product was purified by drying under high vacuum (10^{-6} Torr) and/or by washing with pentane to remove the $Me_3Si-NMe_2$ byproduct. The very fine colorless powder was collected and isolated in 81% yield (0.717 g, 1.30 mmol). ^1H NMR (THF-d_8, 500 MHz, 25 ºC): δ 2.38 (s, 6 H, $C_5(CH_3)_4$), 2.08 (s, 6 H, $C_5(CH_3)_4$), 1.27 (s, 9 H, NC(CH_3)$_3$), 0.48 (s, 6 H, Si(CH_3)$_2$). EIMS m/z (M$^{+•}$) 552. Anal. Calcd. C, 32.61; H, 4.93; N, 2.54. Found: C, 33.43; H, 5.05; N, 2.76.

(CGC)UCl$_2$ (2-Cl$_2$). This compound was prepared from **2** by an identical procedure to that employed for **1-Cl$_2$**. The very fine orange **2-Cl$_2$** powder was isolated in 84% yield, although conversion is quantitative by ^{1}H NMR spectroscopy. ^{1}H NMR (THF-d_8, 500 MHz, 25 ºC): δ 28.73 (s, 9 H, NC(CH$_3$)$_3$), 21.41 (s, 6 H, C$_5$(CH$_3$)$_4$), 7.64 (s, 6 H, C$_5$(CH$_3$)$_4$), -32.05 (s, 6 H, Si(CH$_3$)$_2$). EIMS *m/z* (M$^{+\bullet}$) 557. Anal. Calcd. C, 32.26; H, 4.87; N, 2.51. Found: C, 32.07; H, 4.91; N, 2.37.

(CGC)ThI$_2$ (1-I$_2$). This compound was prepared from **1** by an identical procedure to that employed for **1-Cl$_2$** using up to ten-fold excess of trimethyliodosilane. The very fine colorless **1-I$_2$** powder was obtained quantitatively (^{1}H NMR spectroscopy) and used without further purification. ^{1}H NMR (THF-d_8, 500 MHz, 25 ºC): δ 2.65 (s, 6 H, C$_5$(CH$_3$)$_4$), 2.21 (s, 6 H, C$_5$(CH$_3$)$_4$), 1.38 (s, 9 H, NC(CH$_3$)$_3$), 0.55 (s, 6 H, Si(CH$_3$)$_2$).

(CGC)UI$_2$ (2-I$_2$). This compound was prepared from **2** by an identical procedure to that employed for **1-Cl$_2$** using up to ten-fold excess of trimethyliodosilane. The very fine orange **2-I$_2$** powder was obtained quantitatively (^{1}H NMR spectroscopy) and used without further purification. ^{1}H NMR (THF-d_8, 500 MHz, 25 ºC): δ 36.45 (s, 6 H, Si(CH$_3$)$_2$) 17.83 (s, 9 H, NC(CH$_3$)$_3$), 7.53 (s, 6 H, C$_5$(CH$_3$)$_4$), -46.47 (s, 6 H, C$_5$(CH$_3$)$_4$).

N-methyl-2,2-diphenyl-4-penten-1-amine (21). A 250 mL round bottom flask with a magnetic stirbar was charged with 2,2-diphenyl-4-penten-1-amine[25b] (4.28 g, 18.0 mmol) and ethyl formate (25 mL). The solution was heated at reflux for 24 h and then concentrated in vacuo

to yield a pale yellow oil. Et_2O (30 mL) was added to dissolve the oil, and the solution was slowly added dropwise to a rapidly stirred suspension of LAH (2.15 g, 56.7 mmol) in a 200 mL sidearm flask at 0 °C. After complete addition, the cold bath was removed, and the stirring mixture was allowed to warm to 20 ºC overnight before heating at reflux for 9 h. The reaction mixture was next quenched with a basic N-N-3N workup[3c] in a 0 ºC bath. The solids were removed by filtration, and Et_2O was removed in vacuo, leaving a pale yellow oil. The oil was purified by Kugelrohr distillation (120 °C, 40 mTorr). Yield: 4.38 g, 96.7%. Anal. Calcd. $C_{18}H_{21}N$, 86.01% C, 8.42% H, 5.57% N; Found 86.15% C, 8.33% H, 5.57% N. EI-HRMS theor. mass 251.1669, found 251.1667. ^{1}H and ^{13}C NMR spectra agree with literature data.[5f]

***N*-methyl-5-phenyl-4-pentyn-1-amine (25)**.[26]   A 250 mL round bottom flask containing a magnetic stirbar was charged with 5-phenyl-4-pentyn-1-amine (1.15 g, 7.22 mmol), ethyl formate (50 mL), and 4 Å molecular sieves (ca. 1 g). A reflux condenser was attached to the flask, and the mixture was heated at reflux under N_2 for 1 d. The mixture was then allowed to cool to 20 ºC and filtered through Celite to remove the crushed molecular sieves. The solids were washed with Et_2O (20 mL), and the combined solutions were concentrated in vacuo to afford the crude intermediate imine. Next, a suspension of LAH (0.78 g, 21 mmol) and Et_2O (80 mL) was stirred in a 250 mL sidearm flask at 0 ºC under N_2 before adding the crude intermediate dropwise as an ethereal solution (20 mL) over 15 min. After complete addition, the mixture was stirred at 0 ºC for an additional 15 min before removing the bath and allowing it to warm to 20 ºC over 1 d. The crude product was then quenched and isolated via a basic N-N-3N workup[3c] (N = 0.5 mL

H_2O) in a 0 °C bath. The colorless solids were removed by filtration, and the volatiles were removed in vacuo. The crude, pale yellow oil was purified by Kugelrohr distillation (80 °C, 0.2 Torr). Yield: 2.00 g, 11.5 mmol, 55% (4 steps from 5-hexyn-1-ol). ^{1}H NMR (C_6D_6, 500 MHz, 25 ºC): δ 7.50 (d, 2 H, J = 6.5 Hz, *meta*-Ph), 7.01-6.95 (m, 3 H, *ortho*- and *para*-Ph), 2.48 (q, 2 H, J = 6.5 Hz, CH_2N), 2.38-2.30 (m, 2 H, J = 7.0 Hz, CH_2CH_2N), 1.60-1.55 (m, 2 H, J = 7.0 Hz, CH_2C≡C), 0.16 (br s, 2 H, CH_2NHCH_3).

6-Phenyl-5-hexyn-1-amine (41).   The reagent 6-phenyl-5-hexyn-1-ol was prepared under Sonagashira conditions according to the method of Molinaro and Jamison[27] in Et_3N (100 mL) using iodobenzene (2.2 mL, 4.0 g, 19.6 mmol) and 5-hexyn-1-ol (2.05 g, 20.9 mmol), in addition to catalytic amounts of CuI (0.22 g, 1.6 mmol) and $Pd(PPh_3)_4$ (0.25 g, 0.22 mmol), with heating at 60 ºC overnight. The crude product was isolated by diluting with Et_2O and filtering through a Celite pad prior to aqueous work-up that included washing with 1 M HCl followed by neutralization with saturated $NaHCO_3$. The combined organic phases were dried over $MgSO_4$, filtered, and concentrated in vacuo to afford the crude, orange oil in quantitative yield. The crude product was characterized by ^{1}H and ^{13}C NMR spectroscopy[26] and was used below without further purification in the preparation of 6-phenyl-5-hexyn-1-mesylate.

A 250 mL round bottom flask containing the crude 6-phenyl-5-hexyn-1-ol and a magnetic stirbar was charged with Et_3N (10 mL) and purged with N_2 for 15 min before capping with a Suba seal and affixing an N_2 inlet. CH_2Cl_2 (75 mL) was added by syringe, and the solution was stirred under N_2 atmosphere while cooling in a 0 °C bath. Mesyl chloride (2.3 mL, 30 mmol)

was slowly added by syringe over 5 min, quickly forming a cream-colored suspension, and the mixture was stirred at 0 °C for an additional 90 min. The reaction mixture was then poured into ice water (300 mL) and separated. The organic phase was then washed sequentially with 1 M HCl (100 mL), saturated NaHCO$_3$ solution (50 mL), and brine (75 mL). The combined organic phases were dried over MgSO$_4$, filtered, and concentrated in vacuo to afford the crude mesylate as an orange oil in quantitative yield. ^{1}H NMR (CDCl$_3$, 500 MHz, 25 °C): δ 7.41 (d, 2 H, J = 3.5 Hz, *meta*-Ph), 7.31-7.29 (m, 3 H, *ortho*- and *para*-Ph), 4.32 (t, 2 H, J = 6.2 Hz, *CH$_2$*OMs), 3.03 (s, 3 H, OSO$_2$*CH$_3$*), 2.50 (t, 2 H, J = 7.5 Hz, *CH$_2$*C≡C), 1.97 (quintet, 2 H, J = 6.9 Hz, *CH$_2$*CH$_2$OMs), 1.76 (quintet, 2 H, *CH$_2$*CH$_2$C≡C). ^{13}C NMR (CDCl$_3$, 125 MHz, 25 °C): δ 131.69 (*meta*-Ph), 128.42 (*para*-Ph), 127.91 (*ortho*-Ph), 123.80 (*ipso*-Ph), 89.12 (C≡*C*Ph), 81.57 (C≡*C*CH$_2$), 69.69 (OSO$_2$*CH$_3$*), 37.56 (*CH$_2$*OMs), 28.42 (*CH$_2$*CH$_2$OMs), 24.74 (*CH$_2$*CH$_2$C≡C, 19.00 (*CH$_2$*C≡C).

A 250 mL round bottom flask containing the crude 6-phenyl-5-hexyn-1-mesylate and a magnetic stirbar was charged with NaN$_3$ (3.60 g, 55.4 mmol) and DMF (50 mL) before capping with a Suba seal, affixing an N$_2$ inlet, and stirring overnight in a 60 °C oil bath. The reaction mixture was then poured into water (500 mL) and extracted with Et$_2$O (3 x 50 mL). The combined ether layers were then dried over MgSO$_4$, filtered, and concentrated in vacuo to afford the crude azide as an orange oil. ^{1}H NMR (CDCl$_3$, 500 MHz, 25 °C): δ 7.42-7.39 (m, 2 H, J = 4.5 Hz, *meta*-Ph), 7.31-7.28 (m, 3 H, J = 3.0 Hz, *ortho*- and *para*-Ph), 3.36 (t, 2 H, J = 6.8 Hz, *CH$_2$*N$_3$), 2.48 (m, 2 H, J = 6.8 Hz, *CH$_2$*CH$_2$N$_3$), 1.81 (m, 2 H, J = 6.7 Hz, *CH$_2$*CH$_2$C≡C), 1.71 (m, 2 H, J = 7.3 Hz, *CH$_2$*C≡C). ^{13}C NMR (CDCl$_3$, 125 MHz, 25 °C): δ 131.69 (*meta*-Ph), 128.38

(*para*-Ph), 127.83 (*ortho*-Ph), 123.90 (*ipso*-Ph), 89.40 (C≡CPh), 81.39 (C≡CCH$_2$), 51.19 (*CH$_2$*N$_3$), 28.18 (*CH$_2$*CH$_2$N$_3$), 25.95 (*CH$_2$*CH$_2$C≡C, 19.15 (*CH$_2$*C≡C).

A 200 mL sidearm flask with a magnetic stirbar was charged with LiAlH$_4$ (0.73 g, 19.2 mmol). Under an N$_2$ atmosphere, Et$_2$O (100 mL) was added by syringe, and the flask was cooled in a 0 ºC bath while a 25 mL solution of the crude azide in Et$_2$O was slowly added dropwise over 30 min to the rapidly stirring LAH suspension. After an additional 30 min at 0 ºC, the stirred mixture was allowed to warm slowly to 20 ºC over 2 h. The reaction was then quenched with a basic N-N-3N workup (N = 0.5 mL H$_2$O) in a 0 ºC bath and stirred at 20 ºC for 2 h while exposed to air. The solids were removed by filtration, and the volatiles were removed in vacuo, leaving the crude, pale yellow oil. The oil was purified by Kugelrohr distillation (95 °C, 0.04 Torr). Yield: 2.00 g, 11.5 mmol, 55% (4 steps from 5-hexyn-1-ol). The product ^{1}H and ^{13}C NMR spectra agree with literature[3n] data.

Kinetic Studies of Hydroamination Reactions.

In a typical experiment, the precatalyst (ca. 1-6 mg, 2-11 μmol) and the internal standard Si(*p*-tolyl)$_4$ (ca. 2-5 mg, 5-12 μmol) were dissolved in C$_6$D$_6$ (0.80 mL) and added to a Teflon-valved NMR tube in the glove box. A preliminary ^{1}H NMR spectrum was recorded to verify the relative concentrations of precatalyst and standard. The NMR tube was then attached to a high vacuum manifold via a glass adapter with a secondary Teflon valve and was placed in a -78 ºC bath before evacuating to ca. 5 x 10^{-6} Torr and resealing. The upper portion of the valve was then backfilled with Ar, and a 1 M solution of substrate in C$_6$D$_6$ (0.20 mL) was added to the adapter

under a flush of Ar. The primary valve was next opened and the substrate solution pulled into the NMR tube, freezing the substrate solution just above the precatalyst solution. After evacuating and backfilling the tube with Ar three times, the valve was closed. The sample remained frozen in the -78 ºC bath until thawing and placing directly into the Varian [UNITY]Inova 500 MHz NMR spectrometer, pre-equilibrated at 25.0 ºC ($\pm$ 0.2 ºC), calibrated with a neat ethylene glycol standard. Data were obtained with only a single transient to avoid signal saturation, and substrate and/or product concentrations were determined relative to the intensity of an internal standard resonance, typically downfield of C_6D_5H in the aromatic region of $Si(p\text{-tolyl})_4$ (7.74 ppm), over three or more half-lives. All data were fit by least-squares analysis according to eq. 1, where C_o is the initial concentration of substrate and t is time. The turnover frequency (N_t) was calculated according to eq. 2, where E is the normalized substrate:catalyst ratio determined from the relative intensities of non-overlapping resonances in each ^{1}H NMR spectrum, typically with $\pm$ 5% precision.

$$C = mt + C_0 \tag{1}$$

$$N_t = \left(\frac{m}{-C_0} \right) E \tag{2}$$

X-ray diffraction studies. Single crystals of compounds **1a** and **2a** suitable for diffraction[15] were grown by cooling concentrated pentane solutions in a -40 ºC freezer for several days. The mother liquor was removed and the crystals were covered with Infineum V8512 (aka, Paratone-N) oil in an N_2-filled glove box immediately prior to mounting on a goniometer head. Data were collected under a cold (-120 ºC) N_2 stream using a Bruker SMART-1000 CCD area detector with

graphite monochromated MoK$_\alpha$ radiation. Complexes **1** and **2** crystallize in space groups P$\bar{1}$ and P2$_1$/n, respectively.[15] The structures were solved by direct methods and expanded using Fourier techniques, non-hydrogen atoms were refined anisotropically, and hydrogen atoms were included but not refined. All calculations were performed using the Shelxtl for WindowsNT software package.[28] Centroid distances and angles were obtained using the program ORTEP-3 for Windows, available as a free download.[29]

Results

In this section we begin with an account of (CGC)AnX$_2$ synthesis, molecular structures, and reaction chemistry. We then discuss the intramolecular HA/cyclization of representative terminal and internal aminoalkene, aminoalkyne, aminoallene, and aminodiene substrates mediated by constrained geometry organoactinide complexes, as well as by other organoactinides of progressively less coordinative unsaturation. Catalytic reactions with terminal and 1,2-disubstituted 1° and 2° aminoalkenes are discussed in detail. Intramolecular terminal and 1,2-disubstituted alkyne HA/cyclization with both 1° and 2° amines is then described, followed by extension of the reaction scope to an illustrative selection of aminoallenes and aminodienes. The effects of both metal ionic radius and ancillary ligation are analyzed in each instance, along with relevant kinetic and activation parameters for ring closure involving each C–C unsaturation.

(CGC)AnX$_2$ Synthesis and Characterization

Constrained geometry organoactinide complexes **1** and **2** are prepared in good yields (ca. 70%) and high purity from AnCl$_4$ reagents via an improved, general procedure using the corresponding in situ generated homoleptic tetrakis(dialkylamido)actinide complexes, followed by protodeaminative substitution with the diprotic H$_2$CGC proligand (eq. 3). NMR-scale syntheses proceed in quantitative yield and in >95% purity (^{1}H NMR spectroscopy), indicating that the yield-limiting step in (CGC)An(NR$_2$)$_2$ preparation is precipitation and crystallization from alkane or aromatic solvents. Yields are optimized by incorporating a slight stoichiometric excess of H$_2$CGC, counteracting the formation of ate complex contaminants (i.e., Li[An(NMe$_2$)$_5$(THF)$_n$], An = Th, U) and driving the product-forming equilibrium to the right (eq. 3). Pentane-insoluble impurities

AnCl$_4$ $\xrightarrow{\begin{array}{l}\text{(i) 4 LiNMe}_2\text{ in THF}\\\text{(ii) pentane, -LiCl (s)}\\\text{(iii) H}_2\text{CGC, pentane}\end{array}}$ An(NR$_2$)$_4$ + H$_2$CGC $\rightleftharpoons$ [(CGC)An(NR$_2$)$_2$] + 2 HNR$_2$ **(3)**

1, (CGC)Th(NMe$_2$)$_2$, colorless powder
2, (CGC)U(NMe$_2$)$_2$, brown microcrystals
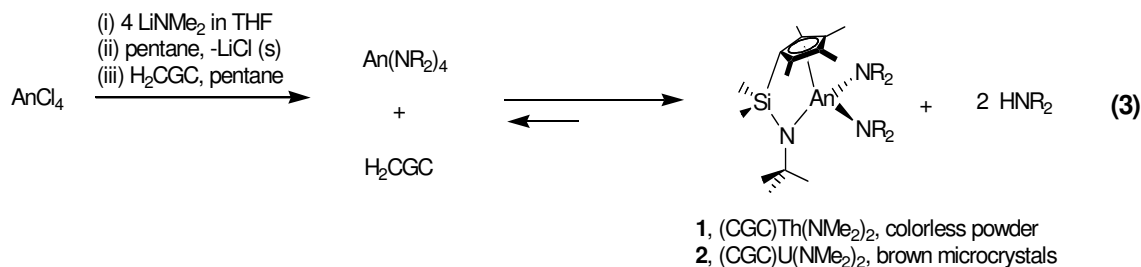
(primarily residual LiCl) are removed by filtration prior to -78 ºC recrystallization to afford analytically-pure (CGC)An(NMe$_2$)$_2$ complexes **1** and **2**. The absence of coordinated Lewis bases in the final products allows direct application as precatalysts without further purification.[3a,u;30] The solid-state structures of **1** and **2** determined by single-crystal X-ray diffraction (Figure 1) are discussed below in the context of their substantially more open ligand frameworks and the impact on catalytic properties (vide infra).

Figure 1. Solid-state structures of (CGC)An(NMe₂)₂ complexes and selected bond distances (Å) and angles (°). (a) Complex 1, distances: Cp″(centroid)–Th, 2.498; Th–N1, 2.315(4); Th–N2, 2.266(5); Th–N3, 2.273(5). Angles: N2–Th–N3, 107.6(2); N1–Th–N2, 114.0(2); N1–Th–N3, 112.8(2). (b) Complex 2, distances: Cp″(centroid)–U, 2.425; U–N1, 2.278(4); U–N2, 2.207(4); U–N3, 2.212(4). Angles: N2–U–N3, 109.6(2); N1–U–N2, 111.0(2); N1–U–N3, 114.2(2). Ellipsoids are drawn at 50% probability (see ref. 15).
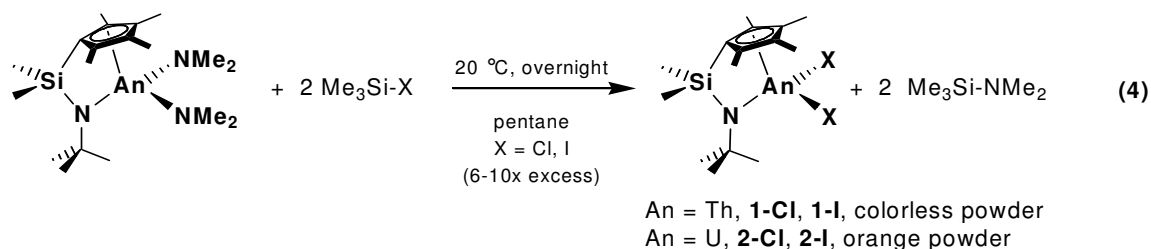
(a)
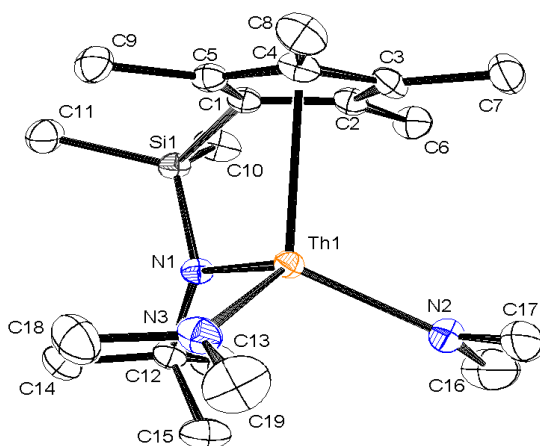
(b)
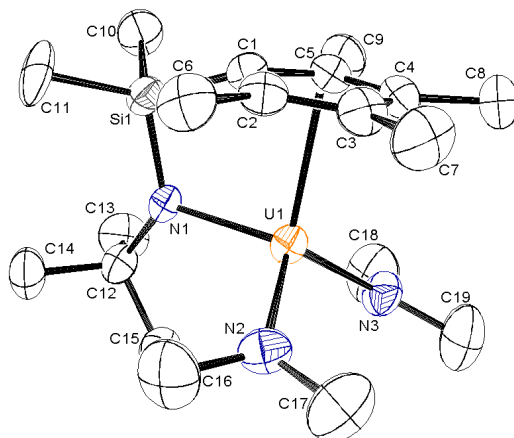
Neutrally charged Lewis base-free halide complexes **1-Cl₂**, **2-Cl₂**, **1-I₂**, and **2-I₂** are cleanly prepared by reaction of **1** or **2** with a 6-10-fold excess of Me₃Si–X (X = Cl, I; eq. 4) in non- coordinating solvents. The dihalides are isolated cleanly and quantitatively from pentane as

An = Th, **1-Cl**, **1-I**, colorless powder
An = U, **2-Cl**, **2-I**, orange powder

fine powders. Although the solubility of diiodides **1-I₂** and **2-I₂** is greater than that of dichlorides **1-Cl₂** and **2-Cl₂** in Et₂O and THF, insolubility in suitable, non-coordinating solvents precludes cryoscopic molecular weight determination.

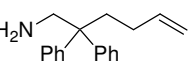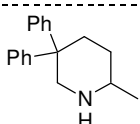**Catalytic Intramolecular Hydroamination/Cyclization. Substrate and Catalyst Trends.**
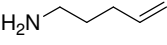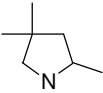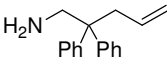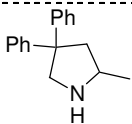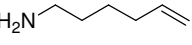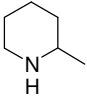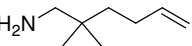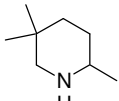
In this section, we present the results of catalytic intramolecular HA studies for a range of C–C unsaturations, revealing an impressive scope rivaled only by organolanthanide catalysts. Substrates surveyed with precatalysts **1**-**6** include primary (**7**-**18**) and secondary (**19**-**24**) terminal aminoalkenes, primary internal (**27**-**32**) aminoalkenes, primary (**33**-**42**) and secondary (**25**-**26**) aminoalkynes, primary aminoallenes (**43**-**48**), and primary aminodienes (**49**-**54**).

Aminoalkenes. Intramolecular hydroamination/cyclization of terminal as well as 1,2-disubstituted (internal) amino-olefins is effectively mediated by (CGC)An‹ complexes. Results for simple 1° amine substrates are presented first, followed by 2° amines and internal olefins. The

scope of precatalyst **1**- and **2**-mediated terminal aminoalkene HA is summarized in Table 2. Thus, unsubstituted substrate **7** is converted to exocyclic pyrrolidine **8** by either **1** or **2** at roughly comparable N_ts, although rather sluggishly at 60 ºC (Table 2, entries 1, 2). Introduction of geminal dimethyl substituents in **9** → **10** cyclization (Table 2, entries 3, 4) effects a reactivity increase of ca. 10× for **1** ($N_t = 15$ h^{-1}, An = Th) vs. **2** ($N_t = 2.5$ h^{-1}, An = U) at 25 ºC. A similar, though more pronounced effect is observed for **11** → **12**, where geminal disubstitution effects are enhanced by phenyl substitution (Table 2, entries 5, 6). Here precatalyst **1** effects HA/cyclization with remarkable efficiency at 25 ºC -- $N_t = 1460$ h^{-1} as compared to the impressive $N_t = 430$ h^{-1} for **2**. Again, the Th-based complex mediates the transformation with markedly greater efficiency, presumably owing to the larger ionic radius (Table 1, vide infra). Larger piperidine rings are also accessible using the present organoactinide precatalysts. Again, the marked influence of geminal dialkyl substitution is evident, effecting a ca. 10× increase in N_t on going from substrate **13** to **15** to **17**, when mediated by **1** for R = H < Me < Ph (entries 7, 9, 11). The formation of five-membered pyrrolidine vs. six-membered piperidine rings is significantly more efficient in most cases for either Th or U, with the notable exception of substrate **15**, where HA/cyclization proceeds *faster* for **2** than for **1** (at 25 ºC for An = U vs. 60 ºC for An = Th). Compared with substrate **9** ($N_t = 2.5$ h^{-1} at 25 ºC; Table 2, entry 4), this pronounced difference in reactivity is intriguing and may reflect Th vs. U electronic properties or unique steric factors introduced by the CGC ancillary ligand (vide infra). This effect also obtains for R = Ph substitution in substrate **17**, where $N_t = 4.8$ h^{-1} at 25 ºC (Table 2, entry 12). The results for **13** and **17** cyclization to piperidines **14** and **18**, respectively (Table 2, entries 7, 8, 11, 12),

Table 2. Aminoalkene HA/ cyclization processes catalyzed by (CGC)An‹ complexes **1** and **2** in C₆D₆ showing the effects of ionic radius on N_t.
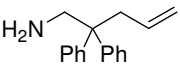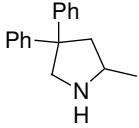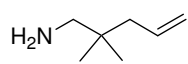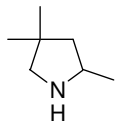
Entry	Substrate	Product[a]	Precatalyst	N_t, h^{-1} (°C)[b]
1.			(CGC)Th(NMe$_2$)$_2$	0.3 (60)
2.	H_2N ... **7**	**8**	(CGC)U(NMe$_2$)$_2$	0.3 (60)
3.			(CGC)Th(NMe$_2$)$_2$	15 (25)
4.	H_2N ... **9**	**10**	(CGC)U(NMe$_2$)$_2$	2.5 (25)
5.		Ph Ph	(CGC)Th(NMe$_2$)$_2$	1460 (25)
6.	H_2N Ph Ph **11**	**12**	(CGC)U(NMe$_2$)$_2$	430 (25)
7.			(CGC)Th(NMe$_2$)$_2$	0.2 (60)
8.	H_2N ... **13**	**14**	(CGC)U(NMe$_2$)$_2$	0.2 (60)
9.			(CGC)Th(NMe$_2$)$_2$	12 (60)
10.	H_2N ... **15**	**16**	(CGC)U(NMe$_2$)$_2$	15 (25)
11.		Ph Ph	(CGC)Th(NMe$_2$)$_2$	4.3 (25)
12.	H_2N Ph Ph **17**	**18**	(CGC)U(NMe$_2$)$_2$	4.8 (25)

[a]Yields ≥ 95% by ^{1}H NMR spectroscopy. [b]Determined by ^{1}H NMR spectroscopy.

parallel those for pyrrolidine formation and suggest that similar Th and U losses in cyclization efficiency are operative upon increasing the product ring size from five to six members.

The consequences of (CGC)An‹ steric openness relative to more encumbered actinocene complexes, are particularly evident in Table 3. Here, transformations **9 → 10** (entries 7- 10) and **11 → 12** (entries 1- 6), are compared for precatalysts **1-6**. Note that $Cp'_2An‹$ complexes **5** and **6** display markedly diminished efficiencies and require heating at 60 ºC for useful HA/cyclization of the two most reactive aminoalkene substrates **9** (N_t = 0.4 h^{-1}, An = Th; N_t = 0.2 h^{-1}, An = U; entries 9 and 10) and **11** (N_t = 2.8 h^{-1}, An = Th; N_t = 1.0 h^{-1}, An = U; entries 5 and 6). This reactivity-coordinative unsaturation trend is evident in comparing these results with those for precatalysts **3** and **4** having intermediate $Me_2SiCp''_2An‹$ ancillary ligation. With extremely reactive substrate **11** (N_t = 120 h^{-1}, An = Th; N_t = 29 h^{-1}, An = U at 25 ºC; entries 3 and 4), the greater than 10× reactivity difference between complexes **1** vs. **3** and **2** vs. **4** is illustrative of the importance of the ancillary ligation and substrate accessibility to the catalytic center. A representative plot of normalized [substrate]:[An] ratio vs. time (Figure 2a) was determined from the ^{1}H NMR spectral intensities of precatalyst + (p-tolyl)$_4$Si internal standard solutions. The slope of the plot is constant in all cases, indicating zero-order dependence on [substrate]. Near complete conversion (low [substrate]), some departure from linearity is observed. However, plots of multiple catalytic runs with a single loading of precatalyst in a single NMR tube (Figure 2b) indicate that this deviation is not caused by catalyst deactivation, but rather by competitive inhibitory binding of substrate or product, interfering with turnover-limiting C=C insertion into the An–N bond.[2d,3u]

Table 3. Aminoalkene HA/cyclization of substrates **9** and **11** processes catalyzed by organoactinide complexes **1**-**6**. Comparison of N_t as a function of metal ionic radius and ancillary ligand environment in C_6D_6.

Entry	Substrate	Product[a]	Precatalyst	N_t, h^{-1} (°C)[b]
1.			$(CGC)Th(NMe_2)_2$	1460 (25)
2.			$(CGC)U(NMe_2)_2$	430 (25)
3.	**11**	**12**	$(Me_2SiCp''_2)ThR_2$	120 (25)
4.			$(Me_2SiCp''_2)UBn_2$	29 (25)
5.			Cp'_2ThR_2	2.8 (60)
6.			Cp'_2UR_2	1.0 (60)
7.			$(CGC)Th(NMe_2)_2$	15 (25)
8.			$(CGC)U(NMe_2)_2$	2.5 (25)
9.	**9**	**10**	Cp'_2ThR_2	0.4 (60)
10.			Cp'_2UR_2	0.2 (60)

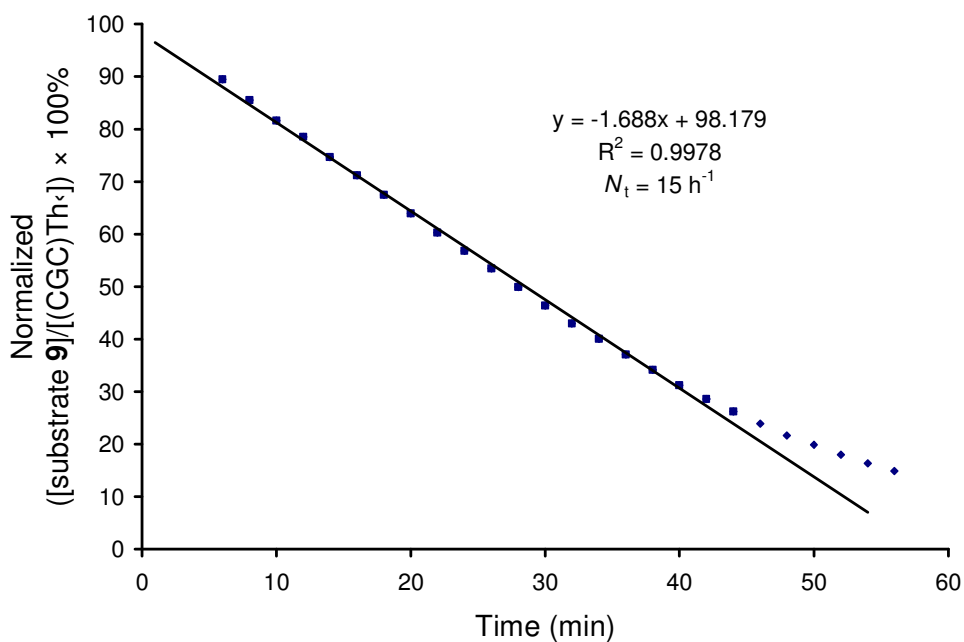[a]Yields $\geq$ 95% by ^{1}H NMR spectroscopy. [b]Determined by ^{1}H NMR spectroscopy.

The cyclization of more complex 2º amine substrates to form products containing 3º amine skeletons was also explored for (CGC)An‹ complexes **1** and **2** (Table 4). Aminodiene **19** undergoes initial HA and cyclization to form the intermediate 2º amine **20a** with an efficiency analogous to that for structurally similar substrate **9** (N_t = 12 h^{-1}, An = Th and N_t = 1.5 h^{-1}, An = U; Table 4 entries 1, 2). Interestingly, subsequent reaction at 100 ºC cleanly converts **20a** to bicyclic **20b** in quantitative yield (eq. 5). The 2º amine
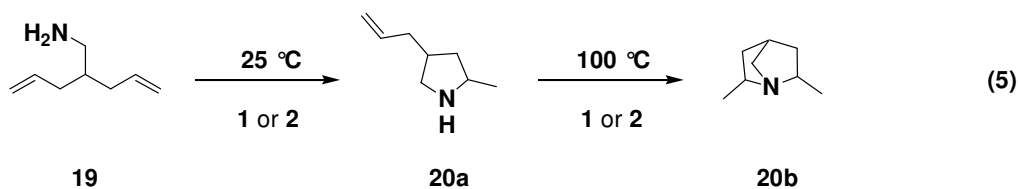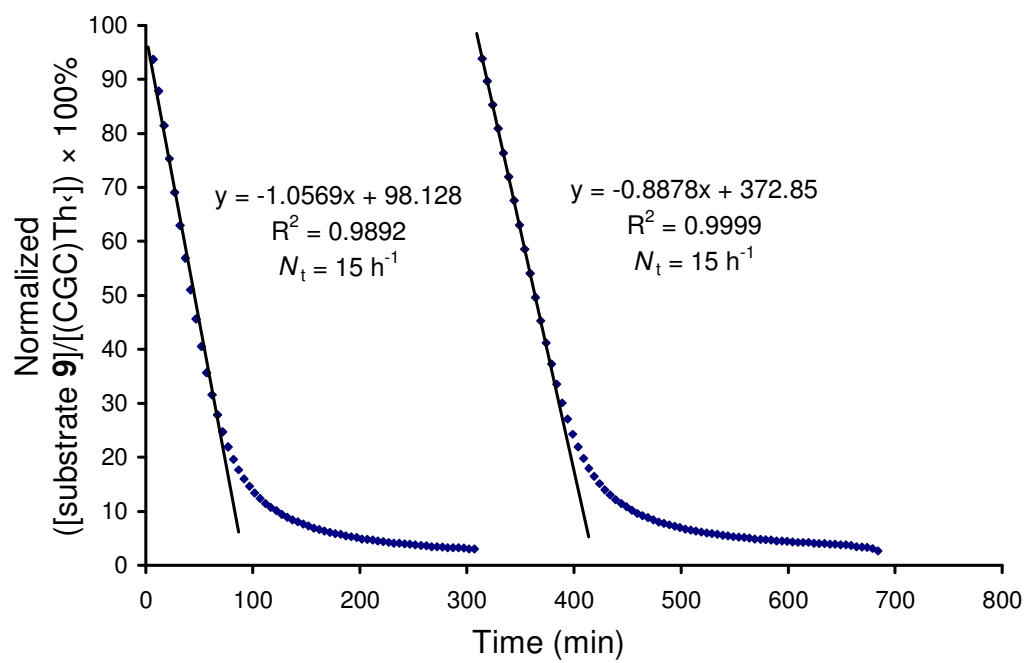

analog of substrate **11**, *N*-methyl substrate **21**, displays the greatest turnover frequency of all aminoalkene transformations in Table 4 and proceeds smoothly at 60 ºC (N_t = 0.6 h^{-1}, An = Th; N_t = 0.8 h^{-1}, An = U; entries 5, 6). Sterically more encumbered **23** bears an *N*- benzyl substituent and requires 100 ºC reaction temperatures to achieve significant rates (N_t = 0.1 h^{-1}; Table 4, entries 7, 8). The steric and electronic obstacles presented by **23** are reflected in the sluggish turnover frequency and its sluggish protonolytic activation of precatalysts **1** and **2** at 60 ºC (typically instantaneous at -78 ºC in C$_7$D$_8$). Also note that the **25** → **26** conversion proceeds at turnover frequencies (N_t = 80 h^{-1}, An = Th; N_t = 120 h^{-1}, An = U; Table 4, entries 9, 10) far greater than those for analogous 1º aminoalkyne **39** at 25 ºC (vide infra).

Figure 2. Kinetic plots for representative HA/cyclization of aminoalkenes. (a) Plot of the normalized ([aminoalkene **9**]/[(CGC)Th‹]) ratio × 100% ([(CGC)Th‹] from precatalyst **1** relative to Si(p-tolyl)$_4$ internal standard) at 25 ºC in C$_6$D$_6$. The line depicts the least-squares fit, with N_t determined from the slope of the line according to eqs. 1 and 2. (b) Plot of ([aminoalkene **9**])/[(CGC)Th‹]) × 100% (normalized to Si(p-tolyl)$_4$ internal standard) over two consecutive catalytic runs under identical conditions. Following completion of the first HA/cyclization reaction, all volatiles were removed in vacuo (including product **10**; 10^{-6} Torr) and replaced with fresh C$_6$D$_6$ solvent and fresh substrate **9** (see Experimental Section for complete details).
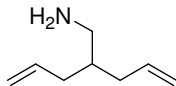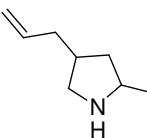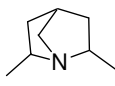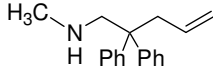
(a)

$y = -1.688x + 98.179$
$R^2 = 0.9978$
$N_t = 15\ h^{-1}$

(b)

Y-axis: Normalized ([substrate **9**]/[((CGC)Th‹]) × 100%

X-axis: Time (min)

$y = -1.0569x + 98.128$
$R^2 = 0.9892$
$N_t = 15\ h^{-1}$

$y = -0.8878x + 372.85$
$R^2 = 0.9999$
$N_t = 15\ h^{-1}$
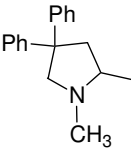
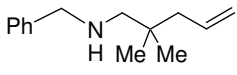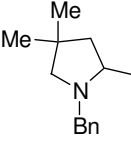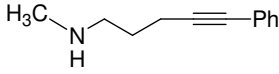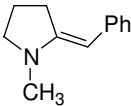The scope of organoactinide-mediated 1,2-disubstituted (internal) aminoalkene HA/cyclization was also investigated (Table 5). These transformations are most efficient for "activated" styrene conversion $27 \rightarrow 28$, where (CGC)An‹ precatalysts 1 and 2 effect cyclization under mild conditions with reasonable efficiency (N_t = 1.3 h^{-1}, An = Th; N_t = 0.9 h^{-1}, An = U; entries 1, 2). Ancillary ligation effects on the HA/cyclization were also explored, with significantly lower turnover frequencies observed using more coordinatively saturated Me$_2$SiCp"$_2$An‹ and Cp'$_2$An‹ precatalysts **3-6** (Table 5, entries 1-6). At 100 ºC, *ansa*-metallocenes **3** and **4** afford **28** at reasonable rates (N_t = 5.8 h^{-1} and 7.0 h^{-1} for **3** and **4**, respectively; entries 3, 4) whereas unbridged actinocenes are sluggish (N_t = 0.2 h^{-1} and 0.5 h^{-1} for **4** and **6**, respectively; entries 5, 6). With unactivated substrates, transformations $29 \rightarrow 30$ and $31 \rightarrow 32$ proceed only at elevated temperatures (100 ºC). Pyrrolidine product 30 is obtained with similar N_t values for both **1** and **2** (N_t = 0.6 h^{-1}, An = Th; N_t = 0.2 h^{-1}, An = U; Table 5, entries 7, 8), while piperidine **32** formation proceeds with similar efficiency for 1 (N_t = 0.2 h^{-1}, An = Th; Table 5, entry 9). As for transformation $15 \rightarrow 16$, precatalyst **2** mediates $31 \rightarrow 32$ (N_t = 2.2 h^{-1}, An = U; Table 5, entry 10) with far greater efficiency than $29 \rightarrow 30$, in accord with (CGC)U‹ catalyst-substrate specificity effects observed with geminal dimethylpiperidine formation (Table 2, entries 9-12; vide infra).

Table 4. Organoactinide-catalyzed HA/cyclization of secondary amine substrates tethered to alkene and alkyne C–C unsaturations. Comparison of N_t as a function of metal ionic radius in C_6D_6.
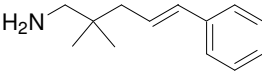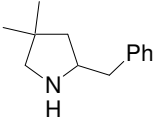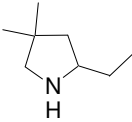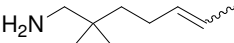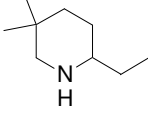
Entry	Substrate	Product[a]	Precatalyst	N_t, h^{-1} (°C)[b]
1.			$(CGC)Th(NMe_2)_2$	12 (25)
2.	**19**	**20a**	$(CGC)U(NMe_2)_2$	1.5 (25)
3.			$(CGC)Th(NMe_2)_2$	0.1 (100)
4.		**20b**	$(CGC)U(NMe_2)_2$	0.1 (100)
5.			$(CGC)Th(NMe_2)_2$	0.5 (60)
6.	**21**	**22**	$(CGC)U(NMe_2)_2$	0.9 (60)
7.			$(CGC)Th(NMe_2)_2$	0.1 (100)
8.	**23**	**24**	$(CGC)U(NMe_2)_2$	0.1 (100)
9.			$(CGC)Th(NMe_2)_2$	80 (25)
10.	**25**	**26**	$(CGC)U(NMe_2)_2$	120 (25)

[a]Yields $\geq$ 95% by ^{1}H NMR spectroscopy. [b]Determined by ^{1}H NMR spectroscopy.

Representative terminal aminoalkene conversion **17** → **18**, mediated by Th catalyst **1** was examined over a broad temperature range, and from Eyring and Arrhenius analyses,[31] $\Delta H^{\ddagger} = 12.6(5)$ kcal/mol, $\Delta S^{\ddagger} = -30(1)$ eu, and $E_a = 13.3(7)$ kcal/mol are obtained from 25°-82 °C. For comparison with internal aminoalkene substrates, the **27** → **28** HA/cyclization promoted by precatalyst 2 was similarly investigated between 44°-84 °C, affording $\Delta H^{\ddagger} = 16(2)$ kcal/mol, $\Delta S^{\ddagger} = -30(7)$ eu, and $E_a = 17(2)$ kcal/mol (Table 9).

Aminoalkynes. Terminal and 1,2-disubstituted (internal) aminoalkyne hydroamination/cyclization is effectively mediated by organoactinide complexes **1-6**. As for organo-4f-element catalysts,[2d;3n,s] this transformation is efficient and highly regioselective at room temperature. The scope of the present aminoalkyne HA/cyclizations includes five- and six-membered ring formation. Conversion **33** → **34** was examined with precatalysts **1-6** to explore the effects of ligand environment (Table 6, entries 1-6). The (CGC)An‹ framework is by far the most efficient in mediating this transformation, proceeding rapidly at 25 °C ($N_t = 82$ h^{-1}, An = Th; $N_t = 3000$ h^{-1}, An = U; Table 6, entries 1, 2). Interestingly, in the case of more coordinatively saturated precatalysts **3-6**, N_t at 60 °C increases with decreasing steric openness ($N_t = 149$ h^{-1}, **3**; $N_t = 190$ h^{-1}, **5**; $N_t = 9.8$ h^{-1}, **4**; $N_t = 15.8$ h^{-1}, **6**; Table 6, entries **4-6**), although not for (CGC)An‹ catalysts **1** and **2**. Additionally, the superiority of the (CGC)An‹ catalyst framework over Cp'$_2$An‹ is evident for substrates **35** (An = U; Table 6, entries 8, 9) and **39** (An = Th; Table 6, entries 12, 14), where (CGC)An‹ N_t values are far greater.

Table 5. Organoactinide-mediated HA/cyclization of 1,2-disubstituted aminoalkene substrates in C_6D_6 catalyzed by **1-6**. Comparison of N_t as a function of metal ionic radius and ancillary ligand environment in C_6D_6.

Entry	Substrate	Product[a]	Precatalyst	N_t, h^{-1} (°C)[b]
1.			$(CGC)Th(NMe_2)_2$	1.3 (60)
2.			$(CGC)U(NMe_2)_2$	0.9 (60)
3.	**27**	**28**	$(Me_2SiCp''_2)ThR_2$	5.8 (100)
4.			$(Me_2SiCp''_2)UBn_2$	7.0 (100)
5.			Cp'_2ThR_2	0.2 (100)[c]
6.			Cp'_2UR_2	0.5 (100)
7.			$(CGC)Th(NMe_2)_2$	0.6 (100)
8.	**29**	**30**	$(CGC)U(NMe_2)_2$	0.2 (100)
9.			$(CGC)Th(NMe_2)_2$	0.2 (100)
10.	**31**	**32**	$(CGC)U(NMe_2)_2$	2.2 (100)

[a]Yields $\geq$ 90% by ^{1}H NMR spectroscopy. [b]Determined by ^{1}H NMR spectroscopy.
[c]Polymeric byproduct precipitate observed. Single product detected in solution by ^{1}H NMR spectroscopy and GC/MS.

The scope of organoactinide-mediated aminoalkyne HA/cyclization and An^{4+} ionic radius effects are summarized in Table 6. As noted above, conversion of Me_3Si-substituted **33** is most efficient for both An = Th and U, likely owing to $-SiMe_3$ group transition state electronic stabilization (vide infra). Unsubstituted terminal alkyne **35** is rapidly cyclized/tautomerized to **36**, especially by **2**, where N_t is ca. $10^3\times$ greater than for **1** (N_t = 7.8 h^{-1}, An = Th; N_t = 1210 h^{-1}, An = U at 25 ºC; Table 6, entries 7, 8). More sterically-demanding **37** → **38** conversion (Table 6, entries 10, 11) proceeds rapidly, although with considerably less efficiency with **2** than with **1** (nearly 10×), clearly indicating finely-controlled steric and electronic requirements. Electronically-assisted transformation **39** → **40** (vide infra) exhibits decreased N_t vs. sterically less-encumbered substrates **35** and **37** for **2** but, for precatalyst **1**, only vs. **35** (N_t = 4.3 h^{-1}, An = Th; N_t = 51 h^{-1}, An = U at 25 ºC; Table 6, entries 12, 13). The relative rates of aminoalkyne HA/cyclization vary differently for **1** and **2**, with $-SiMe_3 > -H > -Ph > -Me$ for An = Th, and $-SiMe_3 > -H \gg -Me > -Ph$ for An = U. The HA/cyclization of **41**, yielding benzyl-substituted tetrahydropyridine **42**, proceeds less efficiently, requiring higher temperatures (N_t = 1.4 h^{-1}, An = Th; N_t = 5.0 h^{-1}, An = U at 60 ºC; Table 6, entries 15, 16). As observed with aminoalkenes, metal ionic radius effects diminish considerably in closures to larger-ring products. Plots of [substrate]:[An] vs. time (e.g., Figure 3) again exhibit deviations from linearity at low [substrate] which is attributed to product inhibition[2d] at high conversion. Additionally, representative transformation **37** → **38**, mediated by Th complex **1**, was examined over a 50 ºC temperature window to yield[31] $\Delta H^{\ddagger}$ = 14(2) kcal/mol, $\Delta S^{\ddagger}$ = -27(5) eu, and E_a = 15(2) kcal/mol (Table 9).

Table 6. HA/cyclization results with aminoalkyne substrates mediated by organoactinide precatalysts **1**-**6** in C_6D_6.

Entry	Substrate	Product[a]	Precatalyst	N_t, h^{-1} (°C)[b]
1.			$(CGC)Th(NR_2)_2$	82 (25)
2.			$(CGC)U(NR_2)_2$	3000 (25)
3.	**33** H_2N—≡—$SiMe_3$	**34**	$(Me_2SiCp''_2)ThR_2$	149 (60)
4.			$(Me_2SiCp''_2)UBn_2$	9.8 (60)
5.			Cp'_2ThR_2	190 (60)
6.			Cp'_2UR_2	15.8 (60)
7.	**35** H_2N—≡—H	**36**	$(CGC)Th(NR_2)_2$	7.8 (25)
8.			$(CGC)U(NR_2)_2$	1210 (25)
9.			Cp'_2UMe_2	26 (25)
10.	**37** H_2N—≡—Me	**38**	$(CGC)Th(NR_2)_2$	2.2 (25)
11.			$(CGC)U(NR_2)_2$	170 (25)
12.	**39** H_2N—≡—Ph	**40**	$(CGC)Th(NR_2)_2$	4.3 (25)
13.			$(CGC)U(NR_2)_2$	51 (25)
14.			Cp'_2ThMe_2	0.8 (60)
15.	**41** H_2N—≡—Ph	**42**	$(CGC)Th(NR_2)_2$	1.4 (60)
16.			$(CGC)U(NR_2)_2$	5.0 (60)

[a]Yields ≥ 95% by ^{1}H NMR spectroscopy and GC/MS. [b]Determined by ^{1}H NMR spectroscopy.
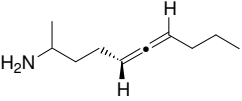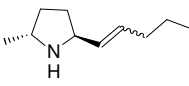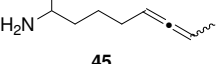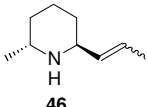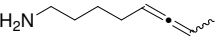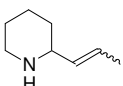
Aminoallenes. Intramolecular hydroamination/cyclization of 1,3-disubstituted (internal) aminoallenes is mediated with high regioselectivity by (CGC)An‹ complexes. As for organo-4f-element catalysts,[2d;3h,i,k] such transformations are efficient, highly regioselective, and moderately to highly diastereoselective. The scope of aminoallene HA/cyclization was explored for both five- and six-membered ring products (Table 7). Cyclization of internal aminoallenes **43**, **45**, and **47** proceeds with >90% regioselectivity in forming smaller-ring pyrrolidine or piperidine (kinetically favored) products **44**, **46**, and **48**, with 60-90% *trans*-selective product diastereoselectivities (Table 7, entries 1-8). For conversion **43** → **44**, the effect of ancillary ligand openness on both N_t and diastereoselectivity was explored for precatalysts **1**-**6**. Selectivity for *trans* product **44** is comparable for either An = Th or U, regardless of ancillary ligation, although selectivity falls noticeably from (CGC)An‹ to more congested Me$_2$SiCp″$_2$An‹ and Cp′$_2$An‹ frameworks (90:10 *trans*:*cis*, **1**; 80:20, **2**; 60:40, **3** and **4**; 70:30, **5**; 65:35, **6**; Table 7, entries 1-6). The rate of this transformation varies far more upon opening or closing the actinide coordination geometry, with precatalyst **2** exhibiting superior activity vs. **4** and **6**, which require 100 ºC reaction temperatures for moderate rates (N_t = 29 h^{-1}, **2**, 25 ºC; N_t = 0.3 h^{-1}, **4**, 25 ºC; N_t = 0.8 h^{-1}, **6**, 100 ºC; Table 7, entries 2, 4, 6). A similar trend is evident for An = Th, where precatalyst **1** is far more efficient than either **3** or **5** (N_t = 2.7 h^{-1}, **1**, 25 ºC; N_t = 0.03 h^{-1}, **4**, 25 ºC; N_t = 0.3 h^{-1}, **5**, 100 ºC; Table 7, entries 1, 3, and 5).

Figure 3. Plot of the normalized ([aminoalkyne **37**]/[(CGC)U‹]) ratio × 100% ([(CGC)U‹] from precatalyst **2** relative to Si(p-tolyl)$_4$ internal standard) at 25 °C in C_6D_6. The line depicts the least-squares fit, and N_t is determined from the slope of the line according to eqs. 1 and 2.

$y = -9.5526x + 113.99$
$R^2 = 0.9898$
$N_t = 170\ h^{-1}$
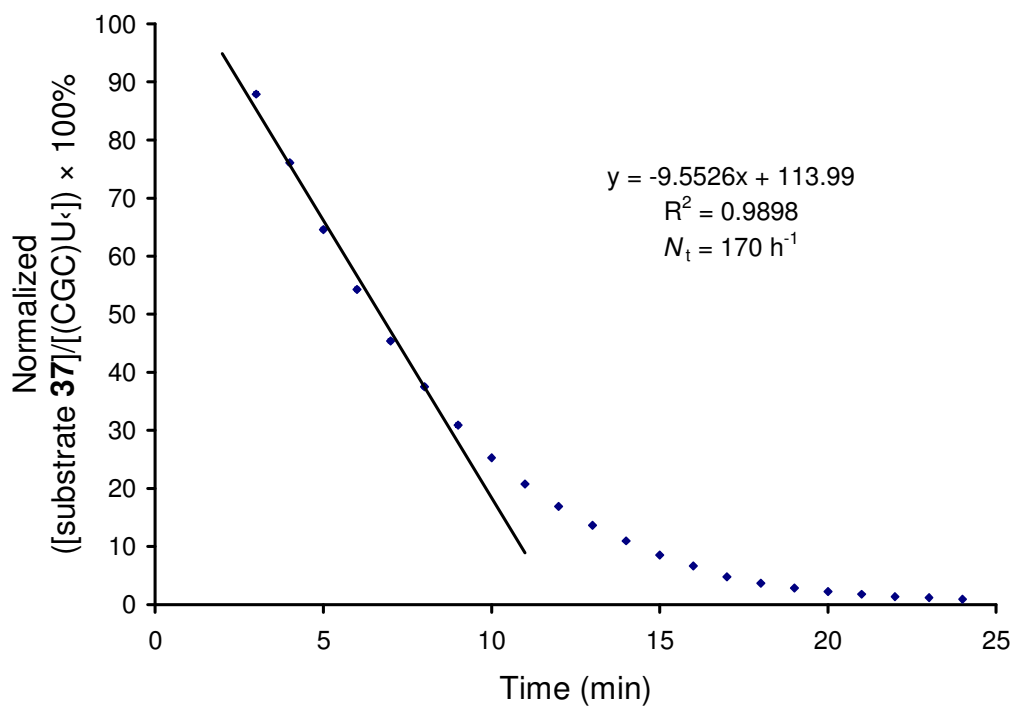
The effect of An^{4+} ionic radius on rate and selectivity was also investigated for (CGC)An‹-promoted aminoallene HA/cyclization reactions (Table 7, entries 1, 2, 7-10). The aforementioned **43** → **44** conversion proceeds smoothly at 25 ºC when mediated by either **1** or **2**, although ca. 10× more efficiently for An = U with N_t = 2.7 h^{-1}, An = Th; N_t = 29 h^{-1}, An = U (Table 7, entries 1, 2). Diastereoselectivities here are comparable, with **1** displaying slightly greater selectivity (90:10 *trans*:*cis* vs. 80:20). In the case of cyclization to piperidine **46**, diastereoselectivities are again similar but with **2** exhibiting somewhat greater selectivity at 60 °C (75:25 *trans*:*cis* vs. 60:40; Table 8, entries 7, 8). Furthermore, ca. 10× rate enhancement is again observed for An = U vs. An = Th, while for **47** → **48**, precatalysts **1** and **2** effect sluggish conversion for this aminoallene substrate at 100 °C (N_t = 0.01 h^{-1}, An = Th; N_t = 0.1 h^{-1}, An = U; Table 7, entries 9, 10). Activation parameters for the present aminoallene HA/cyclizations were quantified for representative transformation **43** → **44** mediated by Th complex **1** between 25º-68 ºC. From Eyring and Arrhenius analyses,[31] $\Delta H^{\ddagger}$ = 13(2) kcal/mol, $\Delta S^{\ddagger}$ = -29(6) eu, and E_a = 14(2) kcal/mol (Table 9).

Table 7. HA/cyclization results with aminoallene substrates in C_6D_6 mediated by organoactinide precatalysts **1**-**6**.

Entry	Substrate	Product[a]	Precatalyst	*trans*:*cis*[b]	N_t, h^{-1} (°C)[c]
1.			$(CGC)Th(NMe_2)_2$	90:10	2.7 (25)
2.			$(CGC)U(NMe_2)_2$	80:20	29 (25)
3.	**43**	**44**	$(Me_2SiCp''_2)ThR_2$	60:40	0.03 (25)
4.			$(Me_2SiCp''_2)UBn_2$	60:40	0.3 (25)
5.			Cp'_2ThR_2	70:30	0.3 (100)[d]
6.			Cp'_2UR_2	65:35	0.8 (100)
7.	**45**	**46**	$(CGC)Th(NMe_2)_2$	60:40	0.1 (60)
8.			$(CGC)U(NMe_2)_2$	75:25	1.3 (60)
9.	**47**	**48**	$(CGC)Th(NMe_2)_2$		0.01 (60)
10.			$(CGC)U(NMe_2)_2$		0.1 (60)
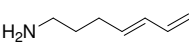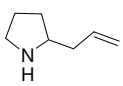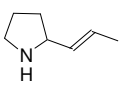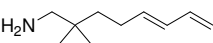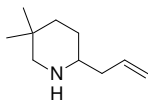
[a]Yields $\geq$ 95% by ^1H NMR spectroscopy and GC/MS. [b]Determined by ^1H NMR spectroscopy. [c]Determined in situ by ^1H NMR spectroscopy. [d]Byproduct precipitate observed. Single set of isomers detected in solution by ^1H NMR spectroscopy .

Aminodienes. Intramolecular HA/cyclization of terminal and 1,4-disubstituted aminodienes is effectively mediated by (CGC)An‹ complexes. As for organo-4f-element catalysts,[2d;3c,f] such transformations are efficient and exhibit moderate/high regioselectivity at moderate temperatures. The scope spans pyrrolidine and piperidine skeletons with products evidencing mixed regioselectivities (Table 8), where rate and selectivity vary with actinide identity. Complexes **1** and **2** mediate aminodiene **49** to allylpyrrolidine **50a** conversion, along with small quantities of (1-propenyl)pyrrolidine byproduct **50b** with $N_t = 3.0$ h^{-1}, 98:2 **a:b**, An = Th; $N_t = 29$ h^{-1}, 93:7 **a:b**, An = U (Table 8, entries 1, 2). Cyclization **51** → **52a/b** is highly regioselective when promoted by **1** and proceeds more rapidly than **49** → **50a/b** at 60 ºC, owing to the geminal dimethyl substitution (Table 8, entry 7). As with substrates having similar structural characteristics (**15** and **31**, vide infra), this transformation is considerably more rapid than with An = Th or with **2** in the **49** → **50a/b** conversion ($N_t = 19.9$ h^{-1}, 81:19 **a:b**, An = U at 60 ºC; Table 8, entry 8). Conversion of styrenic substrate **53** to 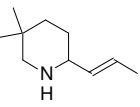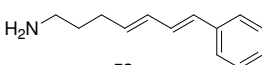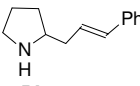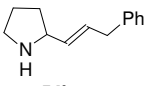pyrrolidines **54a** and **54b** proceeds with considerably lower N_t values vs. substrates **49** and **51**, as well as with diminished regioselectivity ($N_t = 0.02$ h^{-1}, 69:31 **a:b**, An = Th; $N_t = 0.3$ h^{-1}, 79:21 **a:b**, An = U; Table 8, entries 9, 10).

The influence of actinide ancillary ligation was also investigated for aminodiene HA/cyclization (Table 8, entries 1-6). Both *ansa*-metallocene Me$_2$SiCp″$_2$Th‹ (**3**) and unbridged Cp′$_2$Th‹ (**5**) promote transformation **49** → **50a/b** with moderate regioselectivity (71:29 **a:b**, **3**; 76:24 **a:b**, **5**; Table 8, entries 3, 5), whereas the An = U congeners exhibit moderate but *opposing* regioselectivity (15:85 **a:b**, **4**; 35:65 **a:b**, **6**; Table 8, entries 4, 6). Regarding conversion rates, note that the Cp′$_2$An‹ catalysts require 80 ºC to achieve sluggish activity relative to the more
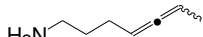
Table 8. HA/cyclization results with aminodiene substrates in C_6D_6 promoted by organoactinide precatalysts **1**-**6**.

Entry	Substrate	Products[a]		Precatalyst	Product Ratio[b]	N_t, h^{-1} (°C)[c]
1.				(CGC)Th(NMe$_2$)$_2$	98:2	3.0 (60)
2.				(CGC)U(NMe$_2$)$_2$	93:7	5.5 (60)
3.	H$_2$N (**49**)	**50a**	**50b**	(Me$_2$SiCp"$_2$)ThR$_2$	71:29	1.9 (60)
4.				(Me$_2$SiCp"$_2$)UBn$_2$	15:85	0.8 (60)
5.				Cp'$_2$ThR$_2$	76:24	0.2 (80)
6.				Cp'$_2$UR$_2$	35:65	0.2 (80)
7.	H$_2$N (**51**)	**52a**	**52b**	(CGC)Th(NMe$_2$)$_2$	93:7	6.1 (60)
8.				(CGC)U(NMe$_2$)$_2$	81:19	19.9 (60)
9.	H$_2$N (**53**)	**54a**	**54b**	(CGC)Th(NMe$_2$)$_2$	69:31	0.02 (60)
10.				(CGC)U(NMe$_2$)$_2$	79:21	0.3 (60)

[a]Yields $\geq$ 95% by ^{1}H NMR spectroscopy and GC/MS. [b]Determined by ^{1}H NMR spectroscopy. [c]Determined in situ by ^{1}H NMR spectroscopy.

open organoactinide catalysts (N_t = 0.2 h^{-1}, An = Th and U; Table 8, entries 5, 6). While similar steric concerns may be an issue for Me$_2$SiCp″$_2$U‹-mediated formation of **50**, N_t is comparable for both **1** and **3** (N_t = 1.9 h^{-1}, An = Th; N_t = 0.8 h^{-1}, An = U; Table 8, entries 3, 4). Activation parameters for representative aminodiene HA/cyclization **49** → **50a/b** promoted by complex **2** are: $\Delta H^{\ddagger}$ = 19(3) kcal/mol, $\Delta S^{\ddagger}$ = -16(9) eu, and E$_a$ = 19(3) kcal/mol between 40 ºC and 82 ºC.[31] Activation parameters for all organoactinide-catalyzed intramolecular HA/cyclization reactions are summarized in Table 9.

Table 9. Summary of organolanthanide- and organoactinide-mediated HA/cyclization activation parameters calculated from standard Eyring and Arrhenius analyses. Data obtained using $Cp'_2Ln[CH(SiMe_3)_2]$ (Ln = La, Sm, Lu) and **1** or **2** as noted over a 40-55 ºC temperature range in C_6D_6 for each class of C–C unsaturation. The columns listed as step (i), C–C insertion into M–N bond, and step (ii), protonolysis of cyclized substrate, refer to the proposed mechanism depicted in Scheme 1.

Unsaturation	Est. ΔH_{rxn} (kcal/mol)		Precatalyst	Substrate	$\Delta H^{\ddagger}$ (kcal/mol)	$\Delta S^{\ddagger}$ (eu)	E_a (kcal/mol)
	step (i)	step (ii)					
aminoalkene	0	- 13	$Cp'_2La[CH(SiMe_3)_2]$[3v]	9	12.7(5)	- 27(2)	13.4(5)
			$(CGC)Th(NMe_2)_2$	17	12.6(5)	- 30(1)	13.3(7)
disubstituted aminoalkene	- 6	- 7	$Cp'_2La[CH(SiMe_3)_2]$[3c]	29	16(2)	- 28(7)	17(2)
			$(CGC)U(NMe_2)_2$	27	18(2)	- 25(5)	18(2)
aminoalkyne	- 35	0	$Cp'_2Sm[CH(SiMe_3)_2]$[3o]	35	11(8)	- 27(6)	--
			$(CGC)Th(NMe_2)_2$	37	14(2)	- 27(5)	15(2)
aminoallene	- 29	0	$Cp'_2LuCH(SiMe_3)_2]$[3j]	H_2N (allene structure)	13(2)	- 29(6)	14(2)
			$(CGC)Th(NMe_2)_2$	43	17(1)	- 16(4)	18(1)
aminodiene	- 19	+4/+7	$Cp'_2LaCH(SiMe_3)_2]$[3d]	49	19(3)	- 16(9)	19(3)
			$(CGC)U(NMe_2)_2$	49	10.4(4)	- 33(1)	10.4(4)

Discussion

We first discuss synthetic and characterization aspects of $(CGC)An(NMe_2)_2$ chemistry relating to catalytic intramolecular HA/cyclization reactivity and selectivity. The significance of metal ionic radius and ancillary ligation for catalysis are discussed. Reactivity trends for intramolecular C–N bond forming processes are analyzed, along with basic mechanistic insights and comparisons with transformations mediated by organo-4f-element and organo-transition metal catalysts. A detailed mechanistic analysis of (CGC)An-mediated intramolecular HA reactions is presented in a companion contribution.[16]

Precatalyst Synthesis and Characterization. Protodeamination routes to d- and f-block metal complexes avoid coordinating solvents and undesired "ate" byproducts.[32] For example, $Cp_2An(NR_2)_2$ actinocenes have been prepared in this manner from the corresponding homoleptic $An(NR_2)_4$ reagents and excess HCp (eq. 6).[19,20,33] However, activation of more encumbered rings (e.g., HCp′) has been less successful, even at elevated temperatures, presumably reflecting unfavorable steric interactions and diminished Brønsted acidity (eq. 7).[23] For the present H_2CGC proligand, HCp″ steric bulk is partially offset by chelation in the final complex.[13] Interestingly, in the synthesis of $(CGC)Ln–N(SiMe_3)_2$ organolanthanides (Ln = Nd, Sm, Yb, Lu), initial $HN(SiMe_3)_2$ displacement and concomitant ligand binding is found to proceed via the $HN(^tBu)$

$$An(NR_2)_4 \quad + \quad 2 \quad \text{(cyclopentadiene)} \quad \longrightarrow \quad \text{Cp}_2An(NR_2)_2 \quad + \quad 2\ HNR_2 \qquad (6)$$

$$An(NR_2)_4 \quad + \quad 2 \quad \text{(pentamethylcyclopentadiene)} \quad \overset{\times}{\longrightarrow} \quad \text{Cp*}_2An(NR_2)_2 \quad + \quad 2\ HNR_2 \qquad (7)$$
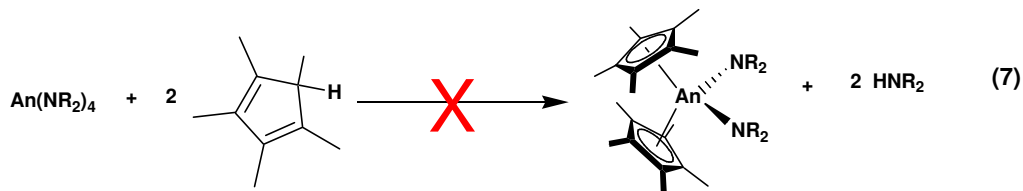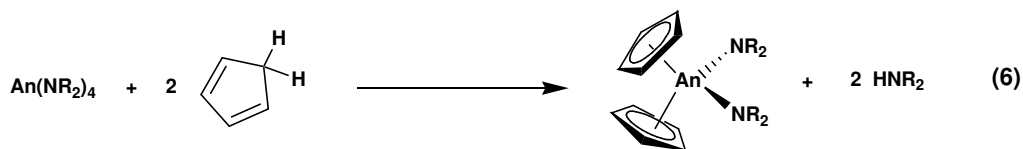
moiety,[31] likely reflecting unfavorable steric interactions (eq. 8). The HCp″ group subsequently coordinates via a second protodeamination, both requiring prolonged reflux and $HN(SiMe_3)_2$ byproduct removal in vacuo.

$$Ln[N(SiMe_3)_2]_3 + H_2CGC \rightleftharpoons \cdots \rightleftharpoons \cdots \qquad (8)$$
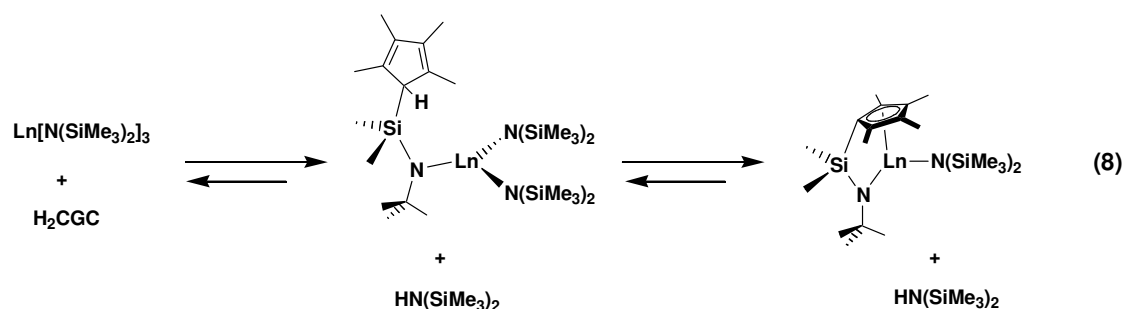
Constrained geometry organoactinide complexes **1** and **2** are conveniently prepared in good yield and high purity from $AnCl_4$ via one-pot in situ generation of the corresponding tetrakisdialkylamide reagents, followed by addition of the H_2CGC proligand (eq. 3). In earlier (CGC)An(NRR')_2 work, similar results were obtained using sublimed, isolated homoleptic amidoactinides. Likewise, LiCl byproduct removal and isolation of the crude "$An(NR_2)_4$" prior to reaction with H_2CGC is equally successful (see Experimental Section for **1**). NMR-scale syntheses monitored in situ indicate that crude or pure $An(NR_2)_4$ protonolysis with H_2CGC is

essentially quantitative in benzene-d_6 and that appreciable (CGC)An(NR$_2$)$_2$ solubility in hydrocarbon solvents limits the isolated yields of analytically pure **1** and **2**. The highest yield was obtained for (CGC)U(NEtMe)$_2$, which presumably combines –NMe$_2$ compactness with –NEt$_2$ steric screening (preventing formation of U(NEtMe$_2$)$_4$ "ate" contaminants) to promote crystallization in analytical purity and ca. 80% yield from UCl$_4$. In all cases, optimized yields are obtained by incorporating a slight H$_2$CGC excess to counteract ate contaminant formation and to drive the protodeamination equilibrium to the right (eq. 9). Contrary to (CGC)Ln–N(SiMe$_3$)$_2$ chemistry, the order of ligand attachment (determined in situ by ^{1}H NMR spectroscopy) more closely follows the expected thermodynamic pathway of protonolysis whereby the more acidic HCp″ moiety (pK_a ~ 24) binds to the An center first, followed by the HN(^{t}Bu) moiety (pK_a ~ 33),[34] likely owing to the smaller HNR$_2$ leaving groups employed for the tetravalent actinides.[32,33] Also note that the rate that equilibrium is reached parallels the byproduct amine volatility (rate: HNMe$_2$, bp 7 ºC >> HNEtMe, bp 35 ºC > HNEt$_2$, bp 55 ºC).
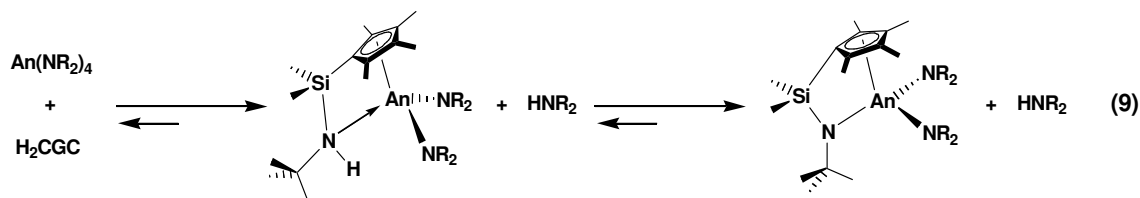
In the case of complexes **1** and **2** (An = Th, U; R = Me), the "An(NR$_2$)$_4$" species most likely contain some "ate" contamination, e.g. Li[An(NMe$_2$)$_5$],[19,20,32a,33] resulting from insufficient –NMe$_2$ group steric screening. This leads to small amounts of byproduct, formulated as Li$_2$[Me$_2$Si(η^5-Me$_4$C$_5$)(^{t}BuN)], which, along with any other pentane-insoluble impurities, are removed by 20 ºC filtration prior to -78 ºC recrystallization, affording analytically-pure

(CGC)An(NMe$_2$)$_2$ products. The absence of coordinated Lewis bases here allows direct application of **1** and **2** as precatalysts in C–N bond-forming reactions without further purification or undesirable catalytic inhibition.[3a,u;30]

Single crystals of **1** and **2** suitable for diffraction studies were obtained by slow cooling of saturated pentane solutions. ORTEP depictions of the solid-state structures of **1** and **2** are shown in Figure 1. These complexes display a pseudo-tetrahedral geometry about the An^{4+} center along with a considerably more open coordination environment than previously characterized organoactinide complexes (Chart 1). The two An–NMe$_2$ distances within each complex are nearly identical (within 1σ) and similar to other An–N σ-bonded distances,[35] with average An–N bond lengths of 2.27(1) Å (**1**) and 2.21(1) Å (**2**). In comparison, the average Th–N distance of 2.25(3) Å in (η^5-Me$_7$C$_9$)$_2$Th(NMe$_2$)$_2$[35a] and the U–NEt$_2$ distance of 2.220(5) Å in (η^4-[(SiMe$_3$)NCH$_2$CH$_2$]$_3$N)U(NEt$_2$)[35b] differ only slightly from those in **1** and **2**, attributable to differences in interligand steric interactions (Chart 1). However, owing to the silyl moiety electron-withdrawing and α-anion stabilization properties,[36] in addition to geometric constraints imposed by the ligand structure, the An–N(^{t}Bu) σ-bond lengths are considerably longer (> 3σ) than their An–NR$_2$ counterparts in both **1** and **2**. This trend is also observed in a series tetravalent (triamidoamine)uranium complexes, namely (η^4-[(SiMe$_3$)NCH$_2$CH$_2$]$_3$N)U–X (X = Cl, Br, I, NEt$_2$, or Cp′),[35b,d] aryl-substituted Cp′$_2$U[N(H)Ar]$_2$ (Ar = 2,6-dimethylphenyl),[35c] and bis[8]annulene (η^8-COT)Th[N(SiMe$_3$)$_2$]$_2$[35e] complexes. Considering the difference in ionic radii between the two metals (Table 1),[10] note that this effect appears to be less pronounced in the Th–

N(^{t}Bu) bond length in **1** vs. the U–N(^{t}Bu) distance in **2**, perhaps a consequence of geometric constraints imposed by the chelating CGC^{2-} ligand. The Cp″ rings in **1** and **2** are coordinated to the respective actinide centers in an η^5 manner as indicated by the C–C bond lengths and Cp″(C)-An distances, without evidence for significant $\eta^5 \rightarrow \eta^3$ ring-slippage[37] (Figure 1).

Compared with previously characterized organoactinide complexes bearing similar ancillary ligation,[38] the solid-state structures of **1** and **2** indicate considerably greater metal center steric openness/coordinative unsaturation (Chart 2). The Cp(c)-An-L angles (L = N(^{t}Bu), Cp″, Cp′) of 91.3° and 93.3° determined for **1** and **2**, respectively, evidence considerably greater openness vs. **3** (118.3°),[21a] closely related "ate" complex Me$_2$SiCp″$_2$U(μ-Cl)$_4$[Li(TMEDA)]$_2$ (114.1°),[22] (HCp″)$_2$UMe$_2$ (134.3°),[38a] Cp′$_2$ThMe$_2$ (133.9°),[38b] or Cp′$_2$UMe$_2$ (140.5°),[38b] indicating enhanced An center accessibility. The less constrained Me$_2$SiCp″$_2$An‹ (**3** and **4)** and Cp′$_2$An‹ (**5** and **6**) ligand environments are quantifiably less accessible to incoming substrates by ca. 25° and 40°, respectively, vs. (CGC)An‹ **1** and **2**.

Compared to charge-neutral (CGC)Ln–E(SiMe$_3$)$_2$ (Ln = Sm, E = N; Ln = Lu, E = CH),[3j] complexes, the present organoactinide coordinative openness is greater, with larger lanthanide ions displaying Cp(c)-Ln-N(^{t}Bu) angles ranging from 95.3° (Sm) to 100.9° for Ln = Lu (Lu; Chart 2). This trend can be rationalized in terms of metal ionic

Chart 1

2.27(1) Å (avg)

NMe₂

Si   Th   NMe₂

N

2.315(4) Å

2.25(3) Å (avg)

NMe₂

Th   NMe₂

2.34(1) Å (avg)

Th

(Me₃Si)₂N   N(SiMe₃)₂

2.21(1) Å (avg)

NMe₂

Si   U   NMe₂

N

2.278(4) Å

2.220(5) Å

NEt₂

SiMe₃

Me₃Si   N   U   N

N   SiMe₃

2.271(3) Å

H   Me

N

Me

U   2.267(6) Å

H   N

Me

Me
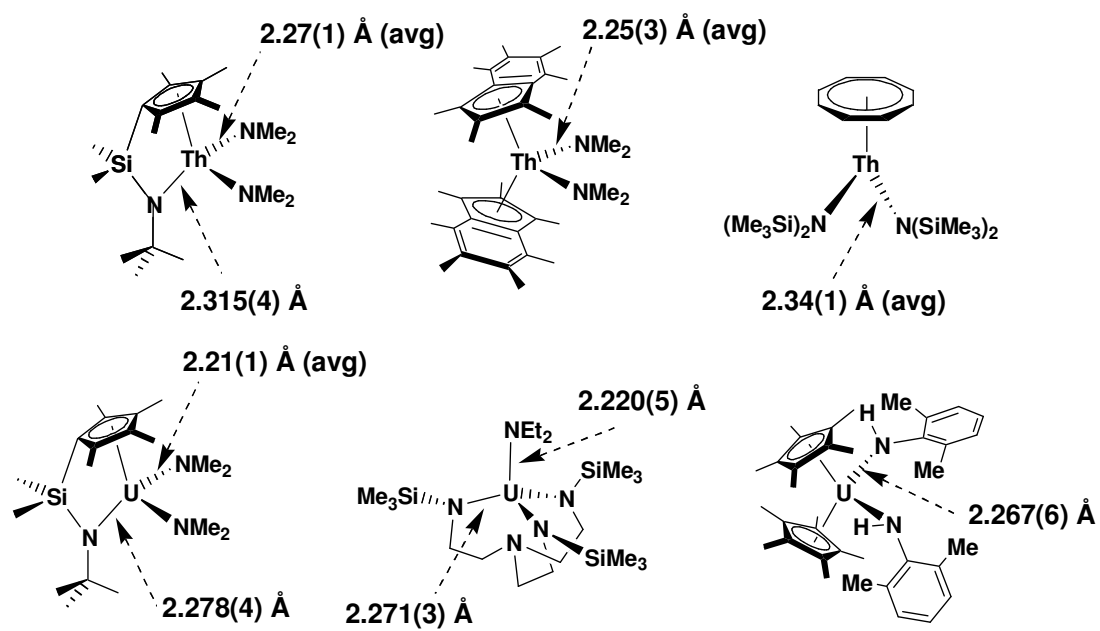
Chart 2
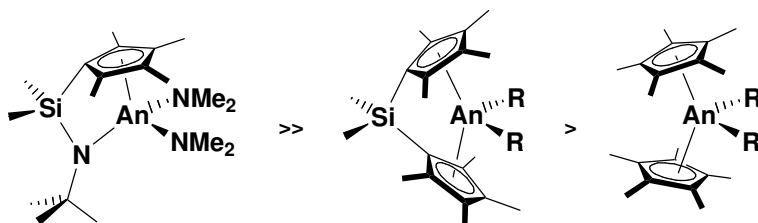
CGC Cp''(c)-M-N1 angle	
Th	91.3°
U	93.3°
Sm	95.3°
Zr	100.2°
Lu	100.9°
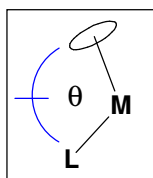
Cp(c)-An-Cp(c) angle	
Cp'$_2$ThMe$_2$	133.9°
Cp'$_2$UMe$_2$	140.5°
(HCp'')$_2$UMe$_2$	134.3°
(Me$_2$SiCp''$_2$)Th[CH$_2$(TMS)]$_2$	118.3°
(Me$_2$SiCp''$_2$)UCl$_4$(Li-TMEDA)$_2$	114.1°

radius, where eight- and nine-coordinate ionic radii[10] for selected Ln^{3+} and An^{4+} ions are listed in Table 1. Overall, trends in the Cp″(c)–An–N1 angle indicate that the steric openness in f-element CGC complexes increases in the order Lu << Sm < U < Th. Versus related tetravalent group 4 complexes, the considerably less open ∡ Cp(c)–M–N(^{t}Bu) of 100.2° in (CGC)Zr(NMe$_2$)$_2$,[39] among other factors, is in accord with the diminished catalytic activity in mediating aminoalkene HA/cyclization.[2]

Analytically-pure (CGC)AnX$_2$ (An = Th, **1-Cl$_2$** and **1-I$_2$**; An = U, **2-Cl$_2$** and **2-I$_2$**) dihalide complexes are prepared in quantitative yield by reaction of **1** or **2** with excess Me$_3$SiX reagents (eq. 4). These complexes are insoluble in non-coordinating solvents and precipitate immediately from solution as fine powders, allowing removal of the byproduct amine in vacuo or by suitable washing. This synthetic strategy is particularly useful for one-pot reactions, proceeding through the dihalides **1-X$_2$** and **2-X$_2$**. Although poor solubility precludes cryoscopic molecular weight determination, the open coordination spheres and frequent observation of d^0- and f-block bridging halide complexes[12,13,40] suggests that these complexes may exist as dimers or trimers (vide infra). ^{1}H NMR studies in THF-d_8 solution are in agreement with a single C_s-symmetric instantaneous species at 20 ºC, consistent with formation of a monomeric, fluxional THF adduct or symmetric [(CGC)An(μ–X)$_2$]$_2$ (**B**) or [(CGC)AnX(μ–X)]$_2$ (**C**) structures.

B   **C**   **D**
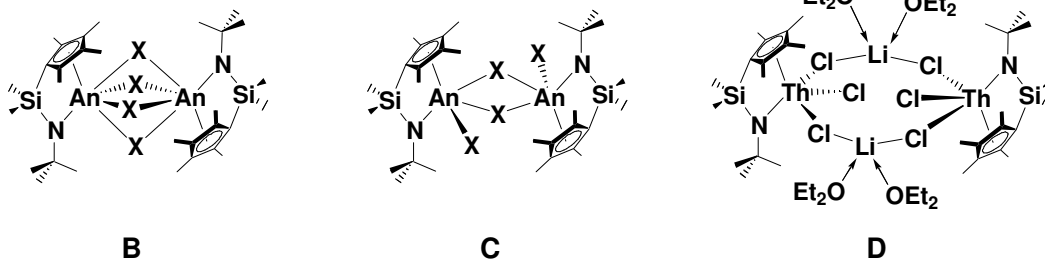
Interestingly, while the solubility of these dihalides in THF is typical of organoactinide halides, the solubility of **1-Cl$_2$** and **2-Cl$_2$** in diethyl ether or hydrocarbons is far less, prompting the synthesis of analogous diiodides **1-I$_2$** and **2-I$_2$**. These display improved solubility in diethyl ether, but not in hydrocarbons.

Closely related [(CGC)ThCl(μ–Cl)$_2$Li(OEt$_2$)$_2$]$_2$ was prepared in 43% yield via a traditional salt elimination route from ThCl$_4$ with Li$_2$CGC in diethyl ether[41] and exhibits solid-state structure **D**, with each Th center retaining an additional chloride ligand. While it is unlikely that catalytic activity would be observed for any of these species without the addition of a cocatalytic reagent (e.g., MAO and/or AlR$_3$),[42] the absence of residual Lewis bases in the coordination spheres of **1-Cl$_2$**, **2-Cl$_2$**, **1-I$_2$**, and **2-I$_2$** reduces the possibility of catalyst inhibition. Furthermore, base-free dihalide complexes **1-X$_2$** and **2-X$_2$** can be obtained from crude, AnCl$_4$-derived (CGC)An(NR$_2$)$_2$ complexes in high overall yield.

Catalytic C–N Bond Formation

The following focuses on (CGC)An‹ catalytic properties in mediating HA/cyclization of diverse primary and secondary amines, tethered to diverse of C–C unsaturations. Beginning with simple terminal aminoalkenes and progressing through additional substrate classes, the

expansive scope and powerful C–N bond-forming ability of (CGC)An‹ catalysts are placed in context with relevant literature and likely mechanistic scenarios.

Aminoalkenes. (CGC)An‹ complexes rapidly and regioselectively mediate intramolecular HA/cyclization of terminal and disubstituted aminoalkenes. Compared to other catalyst systems, the efficacy of precatalysts **1** and **2** is impressive, displaying comparable scope and activity to complexes of intermediate-sized Ln^{3+} ions stabilized by similar ligands[2d] and far-exceeding aminoalkene HA/cyclization rates mediated by group 4 catalysts, all of which require heating to ≥ 100 °C and/or Lewis acid activators.[5b,d,f,g] Organolanthanide-catalyzed aminoalkene conversion rates to the corresponding pyrrolidines and piperidines are highly dependent on ancillary ligation and ionic radius, with complexes offering greater access to the Ln center being the most active catalysts. For example, the **9** → **10** conversion promoted by trivalent $Cp'_2Ln–$ catalysts proceeds more rapidly with larger radius metals, i.e., La ($N_t = 95$ h^{-1}) > Sm (4.8 h^{-1}) > Lu (0.03 h^{-1}) at 25 °C. Expanding the degree of coordinative unsaturation yields a similar trend: (CGC)Lu– (90 h^{-1}) >> $Me_2Si(Cp'')(Cp)Lu–$ (4.2 h^{-1}) > $Me_2SiCp''_2Lu–$ (1.6 h^{-1}) > $Cp'_2Lu–$ (0.03 h^{-1}) at 25 °C.[3j,u;43] Examples of 1° aminoalkene HA/cyclizations mediated by early transition metal complexes are limited, proceeding similarly to the aforementioned Ln^{3+}, but with far less efficiency (e.g., with $Ti(NMe_2)_4$[5b] and chelated diamide **E**).[5d] Notably, cationic β-diketiminatoscandium complex **F** displays significantly increased catalytic activity vs. the neutral $LScMe_2$ analogue, most likely a consequence of the more accessible, more electrophilic metal center.[4f] Similar cationic group 4 species mediate HA/cyclization of 2° aminoalkenes, with apparent deactivation by 1° amine

E   **F**
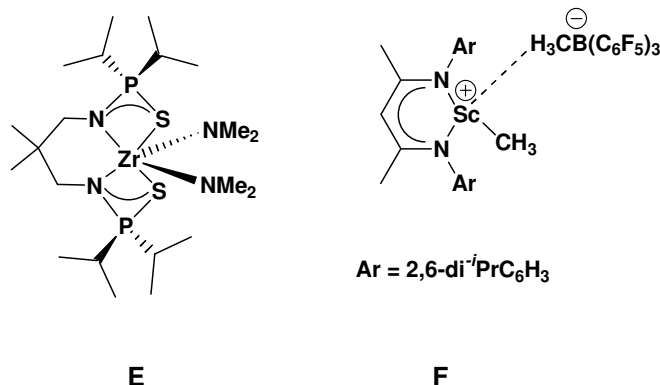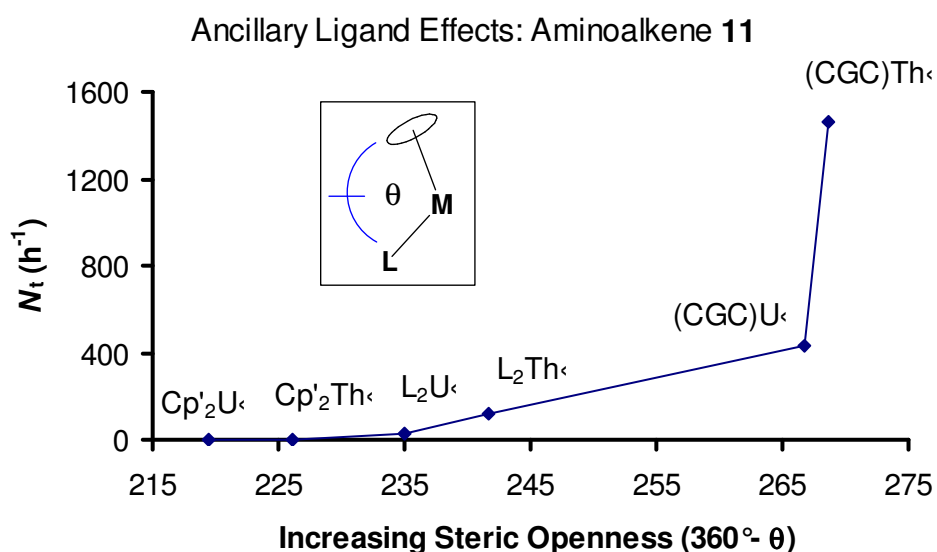
substrates (vide infra).[5f,g]

Reactivity patterns for organoactinide-mediated HA/cyclization of 1° aminoalkenes largely parallel those of other highly electrophilic catalysts with considerably greater activities than for group 4 catalysts.[5b,d,f,g] Terminal aminoalkene conversions are efficient and highly regioselective at room temperature, without an induction period,[44] exclusively providing exocyclic products. In general, larger, more unsaturated An complexes mediate this transformation most rapidly. Thus, (CGC)An‹ complexes **1** and **2** are the most active organoactinide catalysts yet discovered, with N_t increasing ca. 10× upon proceeding from Cp′$_2$An‹ $\rightarrow$ Me$_2$SiCp″$_2$An‹ $\rightarrow$ (CGC)An‹ (Chart 2). Interestingly, the most abrupt activity increase occurs from Cp′$_2$An‹ $\rightarrow$ Me$_2$SiCp″$_2$An‹, although the Cp(c)-An-L angles discussed above transition in roughly equal degrees, reflecting a remarkable sensitivity of this transformation to ancillary ligand openness. Nevertheless, the N_t increase on proceeding to more open precatalysts **1** and **2** is indeed significant, with greater thermal stability[21,22,45] than **3** and **4** and greater access to more demanding transformations (vide infra). This trend in increasing

activity with increasing coordinative unsaturation as indexed by $\measuredangle$ Cp(c)–M–L (Chart 2) is summarized graphically in Figure 4a for **11** → **12**, perhaps approaching an asymptotic limit.
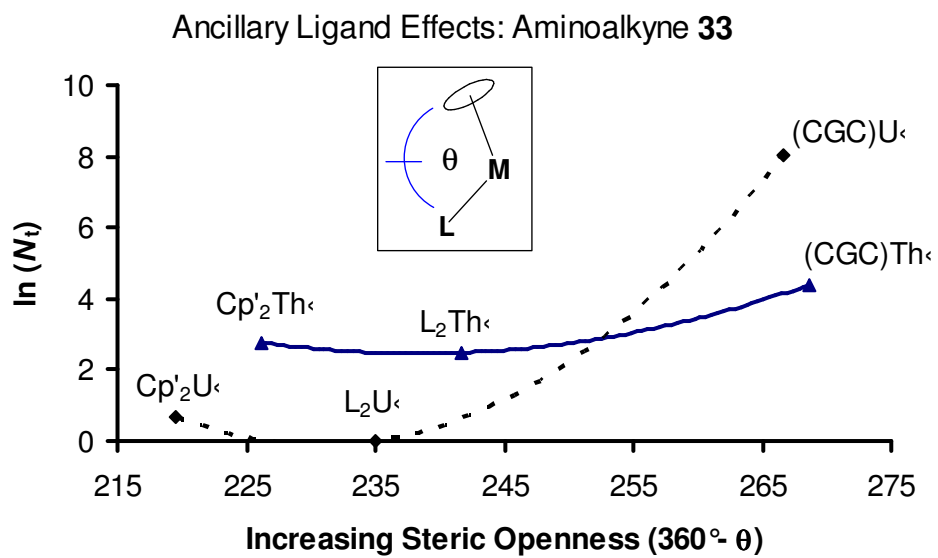
The scope of 1° aminoalkene HA/cyclization was further investigated with **1** and **2** to assess the importance of actinide ionic radius (Tables 1, 3). Overall, the data for the wide range of substrate structures and substitutions generally parallels 4f trends,[2d] namely that larger metal centers more rapidly mediate HA/cyclization, geminal dialkyl substitution accelerates cyclizations, and five-membered pyrrolidines form more rapidly than six-membered piperidines. The Thorpe-Ingold effect[46] in stabilizing the likely four-centered, insertive transition state (**A**) is pervasive here,[47,48] typically resulting in 100-fold rate enhancements upon geminal dialkyl substitution, exemplified by substrates **7** vs. **9**, **13** vs. **15**, and again for **9** vs. **11**, **15** vs. **17**. Interestingly, this is not the case for the **15** → **16** conversion promoted by **2**, where N_t is *greater* than that for **17** → **18**. Remarkably, **15** → **16** is also considerably more efficient than **9** → **10**, in spite of the five- to six-membered ring size increase, contrary to the Baldwin ring closure rules.[49] This interesting result is likely a consequence of the finely-tuned steric requirements for intramolecular HA/cyclization and is also observed for similar substrates when catalyzed by (CGC)U‹. Internal alkene **31** → **32** (Table 5) and conjugated 1,3-diene **51** → **52a/b** (Table 8) conversions, where each substrate possesses the same $H_2NCH_2C(Me)_2CH_2CH_2-$ structure adjacent to the C=C fragment, appear to create an almost enzyme-like[50] "sweet spot" for cyclization (e.g., eq. 10).

Figure 4. Plots of N_t vs. increasing steric openness (360°- θ; Chart 2) for intramolecular HA/cyclizations of (a) aminoalkene **11** → **12**, (b) aminoalkyne **33** → **34** (ln(N_t) vs. increasing openness), (c) aminoallene **43** → **44**, and (d) aminodiene **49** → **50** mediated by the indicated organoactinide complexes **1**-**6** (L₂An‹ corresponds to **3** and **4**, L^{2-} = [Me₂SiCp″₂]$^{2-}$) in C₆D₆ and extrapolated to 25 °C. Curves are drawn as a guide to the eye.

(a)

(b)
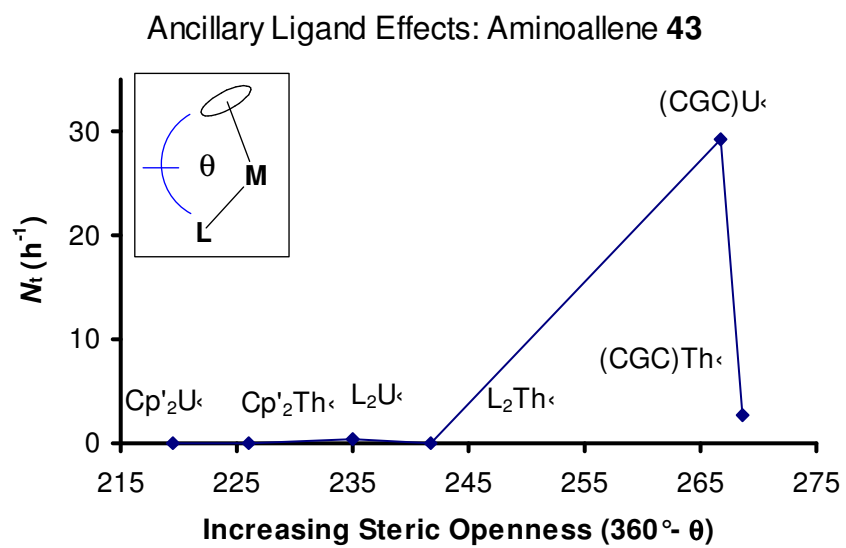

Ancillary Ligand Effects: Aminoalkyne **33**

(c)

Ancillary Ligand Effects: Aminoallene **43**

(d)

Ancillary Ligand Effects: Aminodiene **49**

$$G \longrightarrow G^{\ddagger} \tag{10}$$
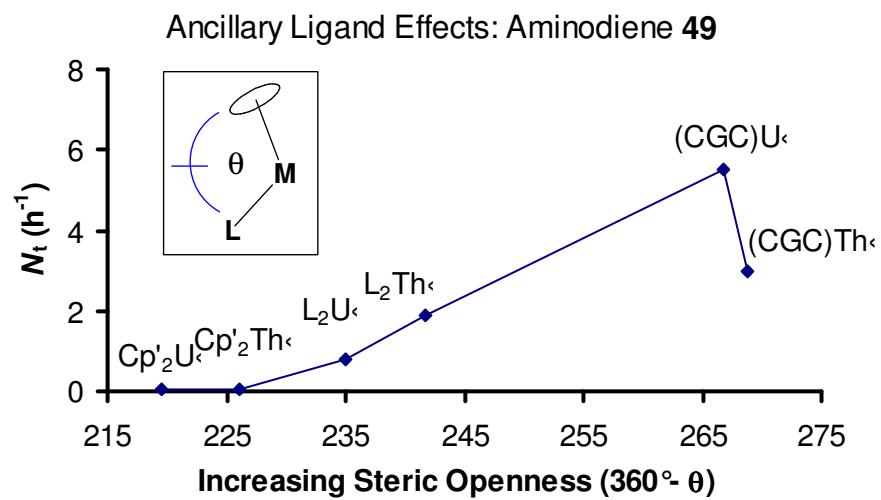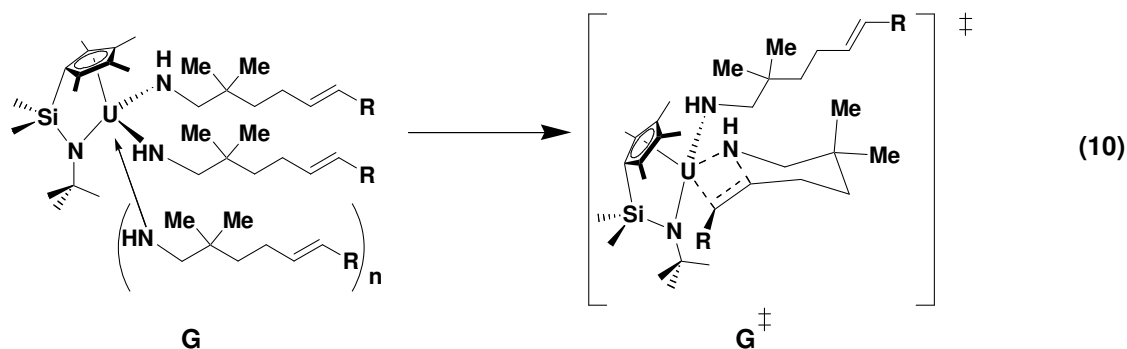
The catalytic addition of 2° N–H bonds across C=C functionality was also explored, with **1** and **2** typifying the ability of more open (CGC)An‹ complexes to mediate more sterically-demanding cyclizations. As expected from the structural similarity to **9**, simple 1° amine substrate **19** is rapidly converted to **20a** at 25 °C, with strained bicyclic **20b** requiring heating to 100 °C. An identical N_t is observed for **23 → 24** under similar conditions (Table 4), where more hindered *N*-benzyl substitution is combined with reduced N nucleophilicity. Less forcing conditions are required for less encumbered *N*-methyl substrates **21** and **25** (Table 4), indicating that steric factors are important, although the An^{4+} size dependence suggests that ancillary ligation openness is important. Note also the rate *enhancement* for **25 → 26** vs. analogous *N*-unprotected aminoalkyne **39 → 40** (Tables 5 and 7). In that 2° aminoalkenes present greater steric impediment to cyclization than their *N*-unprotected congeners (see structure **A**), this result is consistent with previously reported rate increases with decreasing Ln^{3+} ionic radius in aminoalkyne HA/cyclization (vide infra).[3n,s] A similar enhancement in activity is seen in sequential C–N/C–C bond-forming processes mediated by $Cp'_2Sm–$ catalysts (eq. 11).[31] Interestingly, in the case of $Cp'_2Sm–$, alkyne terminus phenyl substitution leads to a *decrease* in

(11)
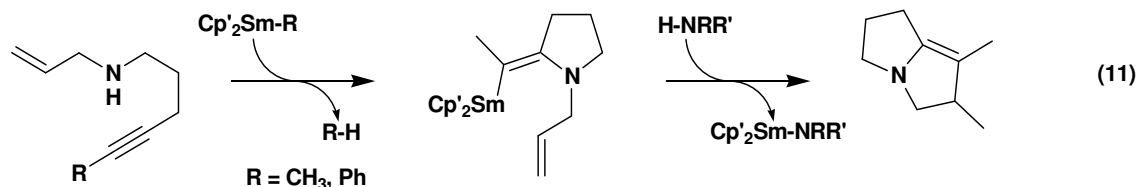
cyclization rate, indicative of unfavorable steric interactions during C–C insertion into the M–N bond in transition state **A**.

The competence of **1** and **2** in mediating facile *2° aminoalkene* transformations argues against an easily accessible An=NR intermediate/transition state in C–N bond formation (cf., Scheme 3).[51] Less plausible high-energy species such as **H** or **I** must be invoked in place of more plausible **J**. Ion pair **H**, presumably generated via unimolecular α-H$^+$ abstraction, features An-coordinated hypervalent N, while zwitterion **I** (by way of N-based electron pair transfer to the
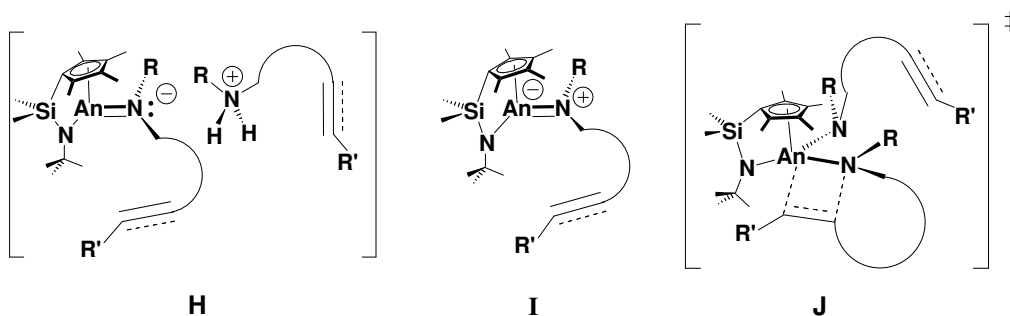
An–N bond) places a formal negative charge on electrophilic Th^{4+} or U^{4+} (no change in ^{1}H NMR paramagnetic shifts is observed vs. similar 1° amine HA/cyclization processes). In regard to possible radical pathways, the high regioselectivity observed for An-mediated cyclizations of 2° aminoalkene and aminoalkyne substrates is inconsistent with radical chain processes (eqs. 12 and 13).[52] Additionally, the required but energetically unfavorable An^{4+} → An^{3+} electron transfer/reduction for An–N(H)R homolysis (particularly for An = Th),[12,13] the rate dependence

on metal ionic radius, zero-order dependence on [substrate],[31] and pronounced effects of ancillary ligation on N_t and cyclization diastereoselectivity, all render radical pathways unlikely, especially in view of poor regioselectivity and overall yield in radical-mediated aminoalkene

(12)

R = H, Me, Ph

(13)

cyclizations.[52b,c] Results for cationic group 4 metal-catalyzed aminoalkene HA/cyclizations, where 1° aminoalkenes deactivate $L_2Ti–^+$ and $L_2Zr–^+$ catalysts,[5f,g] suggest that in these cases, neutral $L_2M=NR$ imido species are marginally reactive with respect to C=C insertion (eq. 14),

(14)

R' = Me, C$_6$F$_5$

unlike the highly reactive intermediate proposed in group 4 *intermolecular* HA. Additional experiments probing the detailed mechanism of intramolecular 1° and 2° amine HA/cyclization mediated by (CGC)An‹ and (CGC)Zr‹ catalysts are reported elsewhere.[16]

Regarding internal (1,2-disubstituted) aminoalkene HA/cyclizations, trends are similar to those observed for terminal olefinic substrates and those mediated by 4f catalysts.[2d] Specifically, Th-mediated transformations are generally more rapid than those of U^{4+}, and more open

(CGC)An‹ and Me$_2$SiCp″$_2$An‹ complexes are more active than Cp′$_2$An‹ catalysts (Table 5). Specifically, (CGC)An‹ catalysts are ~10× more active than the corresponding Me$_2$SiCp″$_2$An‹ catalysts. In conversion **27 → 28**, the electron-withdrawing phenyl ring plausibly stabilizes the δ$^-$ charge in proposed transition state **K** (R = Ph), thereby assisting turnover-limiting C=C insertion, despite unfavorable steric interactions (Table 4).[3e,12] Additional stabilization may be provided by arene ring π-coordination to the electrophilic L$_2$An‹ center (**K**). Studies of Ln-mediated
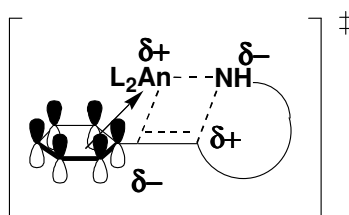
K

intermolecular substituted styrene HA invoked a similar pathway to explain the impressive anti-Markovnikov regioselectivity and X effects on rate (eq. 15).[3e] "Unactivated" substrates **29** and **31** are converted to **30** and **32**, respectively, at elevated temperatures (100 °C; Table 5) but otherwise closely follow patterns observed for **9 → 10** and **15 → 16**.

(15)
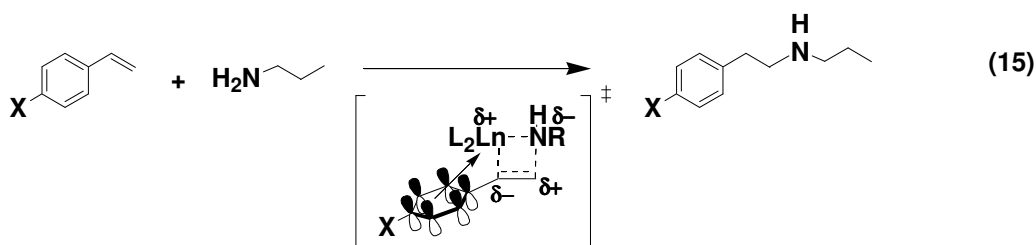
Aminoalkynes. The present (CGC)An‹ complexes rapidly and regioselectively catalyze aminoalkyne HA/cyclization under mild conditions. Previous observations with organolanthanide catalysts indicate extremely high activity for Ln complexes of *smaller* ionic radius.[3n,s] For example, **35** → **36** conversion is efficiently mediated at 21 °C by $Cp'_2Ln–R$ precatalysts with the observed relative rates Lu (5.3) > Sm (4.3) > Nd (1.5) > La (1). This trend is paralleled by the ca. 40× fall in activity upon opening the catalyst coordination sphere of $Cp'_2Sm–$ (77 h^{-1}) to $Me_2SiCp''_2Sm–$ (2 h^{-1}) in **39** → **40** HA/cyclization, exactly *contrary* to aminoalkene trends.[2d] Group 4 catalysts also mediate the intramolecular HA/cyclization of highly reactive aminoalkynes, displaying greater reactivity with M = Ti than with M = Zr, although electronic considerations and ancillary ligand steric requirements are less clearly defined.[2a,h-n] Rates with Ti^{4+} complexes (proposed to proceed through a [2 + 2] cycloaddition pathway; Scheme 3) are, in some cases, comparable to those of Ln^{3+} complexes.[2]

Consistent with these observations, intramolecular aminoalkyne HA/cyclization mediated by **1** and **2** proceeds rapidly and regioselectively (Table 6). N_t values are comparable to or greater than those of $L_2Ln–$ catalysts.[3n] Thus, conversions **35** → **36** and **37** → **38** mediated by **2** proceed at ca. twice the rate of $Cp'_2Sm–$ catalysts, establishing **2** as the most efficient catalyst reported for this transformation. While the **2**-mediated conversion **33** → **34** is extremely rapid ($N_t \approx 3000$ h^{-1}, 25 °C), it is even more so when catalyzed by similarly-sized $L_2Ln–$ species.[3n,s] Regarding transition state **A** and the tendency of $Me_3Si–$ functionalities to stabilize α-carbanions and β-carbocations[36] and, therefore, to outweigh steric impediments to C≡C insertion, this difference in reactivity may reflect a reduced tendency for An^{4+} (vs. Ln^{3+}) ions to stabilize γ-agostic

interactions with proximate Si–C bonds,[12f] or, considering the presence of a second, covalently σ-bonded substrate moiety, reflect steric vs. electronic factor balance in the highly polarized transition state (vide infra). Notably, more electrophilic Th^{4+} appears to favor arene coordination/ transition state stabilization (as discussed above for **27** → **28**) more effectively than U^{4+}, perhaps reflecting differences in 5f-element bond covalency.[12,13] Moreover, the dispersion in rates with alkyne substitution for **1** (–SiMe$_3$ > –H > –Ph > –Me) vs. the more Cp′$_2$Sm-like[3n] behavior of **2** (–SiMe$_3$ >> –H >> –Me > –Ph), suggests a complex interplay of sterics and electronics.

Ancillary ligand effects on aminoalkyne HA/cyclization were also investigated with **1-6**. Reactivity patterns largely parallel the Cp′$_2$Ln– and Me$_2$SiCp″$_2$Ln– systems,[3n] with rates following the general trend Cp′$_2$An‹ > Me$_2$SiCp″$_2$An‹, and ca. 10× greater activity for the *larger* Th^{4+} center with each ligand set. However, a sharp deviation from this trend is observed with the markedly more open, coordinatively unsaturated (CGC)An‹ catalysts, with relative rates for **33** → **34** of roughly 82 (**1**):12 (**3**):16 (**5**) h^{-1} for An = Th and 3000 (**2**):1 (**4**):2 (**6**) h^{-1} for An = U. This reveals a remarkable increase in catalytic activity (> 10^3-fold; Figure 4b) with (CGC)An‹ catalysts and provides a dramatic demonstration of successfully combining the electronic and coordinative unsaturation characteristics of CGC ligation in organometallic catalysis.[11]

Aminoallenes. Intramolecular (CGC)An‹-mediated HA/cyclization of 1,3-disubstituted allenes covalently linked to 1° amines proceeds under mild conditions, displaying moderate *trans*-2,5-pyrrolidine and *trans*-2,6-piperidine diastereoselectivity along with > 90% regioselectivity. Compared to similar transformations effected by group 4[5i,j] and Ln complexes,[3h,i,k] (CGC)An‹

complexes display comparable activities and activity trends. The scope of such conversions previously investigated with organo-group 3 and -4f catalysts demonstrated impressive, regioselective routes to natural products.[3h] Mechanistic analysis revealed unusual dependence on Ln^{3+} ionic radius, with maximum N_ts for intermediate ionic radii, and an "alkyne-like" dependence on catalyst ancillary ligation, with (CGC)Y-catalyzed reactions exhibiting marked diminution of cyclization rates vs. $Cp'_2Y–$.[3i] Furthermore, group 4 catalysts with chelating bis(sulfonamide) ligands (likely providing greater steric openness and electrophilicity) exhibit striking enhancements in activity as well as scope over traditional group 4 metallocenes.[5i,j] Interestingly, regiospecificities for Ln- and Ti-based processes are reversed, with Ln^{3+} and An^{4+} catalysts selectively generating exocyclic rings (pathway **a**, eq. 16) vs. formation of endocyclic regioisomers with Ti^{4+} catalysts (pathway **b**, eq. 16);[3i,5i] both pathways are favorable within the
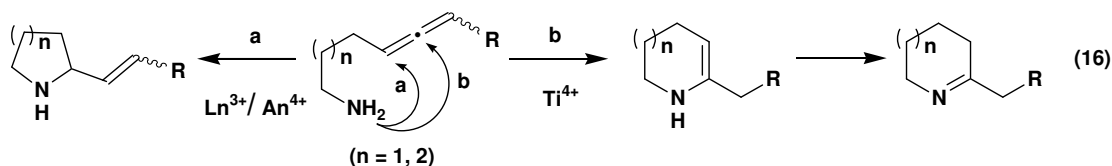
Baldwin ring-closure rules.[49] Zr-mediated transformations also operate via pathway **a** and cyclize 1,3,3-trisubstituted aminoallenes in moderate yields and with > 90% regioselectivity, although more sluggishly than similarly ligated Ti catalysts.[5j]

Overall, (CGC)An‹ catalyst selectivity and activity (Table 7) more closely resemble organolanthanide patterns than those of Ti/Zr- catalysts. However, comparing $Me_2SiCp''_2An‹$ vs. $Cp'_2An‹$ coordinative unsaturation, precatalysts **3**-**6** exhibit sluggish efficiencies and moderate diastereoselectivities, unlike the general trend observed with lanthanocenes (*increasing* reactivity

with *decreasing* coordinative unsaturation).[3i] Rather the An trend resembles smaller, tetravalent Ti/Zr patterns, suggesting that increased encumbrance introduced by an additional covalent σ-bond may impose greater steric constraints on transition state **A** and rate-limiting C=C insertion into the An–N bond (cf., **G**, **G**[‡], and **J**). Likewise, the additional bond covalency of An (vs. Ln) ions may help stabilize **A**. Qualitative comparison of coordinative unsaturation effects on N_t (according to the Cp(c)–M–L angle θ in Chart 2) is presented in Figure 4c for **43** → **44** conversion mediated by precatalysts **1**-**6**.

More striking are Me$_2$SiCp″$_2$An‹ → (CGC)An‹ ancillary ligand effects where cyclization rates are comparable to rapid, Cp′$_2$Ln-promoted reactions.[3i] With the exception of the "preorganized" aminoallene **43**, which exhibits a 10× rate enhancement for Cp′$_2$Sm– vs. (CGC)U‹-mediated cyclization, there is virtually no loss in activity from Cp′$_2$Ln– to (CGC)U‹ catalysts. However, the ca. 10× decrease in activity observed for **1** vs. **2** reflects a Ln-like dependence on ionic radius in the sterically-sensitive intramolecular 1,3-disubstituted allene HA/cyclization. Although substrates bearing geminal dialkyl substitutions were not investigated, the substantial increase in activity of both **1** and **2** for transformations **45** → **46** vs. **47** → **48** (Table 7) is consistent with more advantageous orientation of the reactive substrate moiety in the transition state owing to α-alkyl substitution.[46]

Although diastereoselectivity was not reported in detail for group 4 catalysts,[5i,j] organolanthanides consistently afford 2,5-*trans*-pyrrolidine and 2,6-*cis*-piperidine heterocyclic products.[3i] In all instances, organoactinide catalysts (Table 7, entries 1-8) consistently favor 2,5-*trans*-pyrrolidine (**43** → **44**, precatalysts **1**-**6**) and 2,6-*trans*-piperidine (**45** → **46**, precatalysts **1**

and **2**) diastereoselection. The former trend tracks that observed with organolanthanide catalysts and is explicable in terms of preferred orientation and minimization of unfavorable substrate-ancillary ligand steric repulsion. However, the latter result differs from L_2Ln- catalysts, likely reflecting the second, covalently bonded substrate interfering with C=C=C insertion at the An–N bond. Added steric obstruction in the already congested transition state (cf., **A** and **G**‡) is consistent with reduced diastereoselectivity and reduction in catalytic activity upon moving from coordinatively unsaturated (CGC)An‹ complexes, where diastereoselectivities up to 90% are achieved, to their less open **3-6** analogues, where diastereoselectivies are uniformly modest and reaction rates markedly more sluggish.

Aminodienes. While ample precedent exists for *intermolecular* 1,3-diene HA across the Periodic Table,[2k] there have been few investigations of the intramolecular variant of this useful transformation. Notably, scope and mechanism have been thoroughly examined for Ln catalysts with diverse ancillary ligands, from conventional Cp′$_2$Ln– to chiral bis(oxazolinato) complexes.[3c,d,f] These studies reveal a dependence on Ln^{3+} ionic radius and coordinative unsaturation that is far more pronounced than in aminoalkene intramolecular HA/cyclization, where larger, more accessible metal centers with more open coordination spheres are optimal for rate and regioselectivity. Although recent computational studies suggest that Ln–C σ-bond protonolysis following aminodiene cyclization may be turnover-limiting,[48,53] experimental data argue for turnover-limiting C–C unsaturation insertion into the Ln–N bond (Scheme 1).[3c,47]

Intramolecular 1,3-aminodiene HA/cyclization, involving both terminal and 1,4-disubstituted (internal) diene units, is effectively catalyzed by (CGC)An‹ complexes (Table 8). As for organo-4f-element catalysts, such transformations are efficient and highly regioselective. With the noteworthy exception of the **2**-promoted **51 → 52a/b** conversion (vide supra), relative ring-closure rates follow expected trends where smaller pyrrolidines form more rapidly from unsubstituted 1,3-dienes than do piperidines, and 1,4-disubstituted diene conversions are slow vs. terminal dienes.[3c] This trend is typical of ring-closing reactions in general,[44,49,54] and (CGC)An‹-catalyzed aminodiene HA is clearly governed by similar steric and electronic demands. Furthermore, product distributions typically favor thermodynamically *less* favored (~3 kcal/mol) terminal, monosubstituted olefinic products (**50a** and **52a**, Table 8). That product distributions are time-independent and favor the kinetic cyclization product (**a** in eq. 17), suggests that subsequent isomerization via reinsertion at the An center (**b** in eq. 17) is unimportant, in contrast
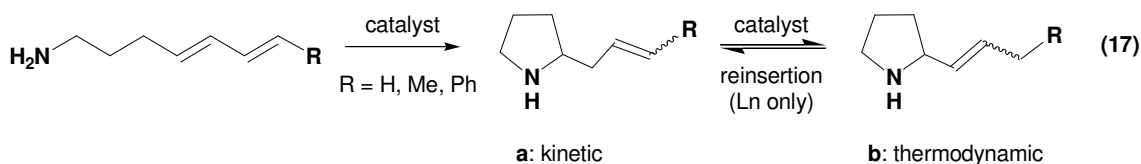
to most Ln-catalyzed transformations.[3d] This trend for Ln catalysts is explicable in terms of well-precedented η^3-allyl/benzyl intermediates (**L**)[12,13] and suggests that such intermediates are more stable for large Ln^{3+} ions than for similarly-sized An^{4+} ions, having two An–N σ-bonded substrates in the resting state (**M**).
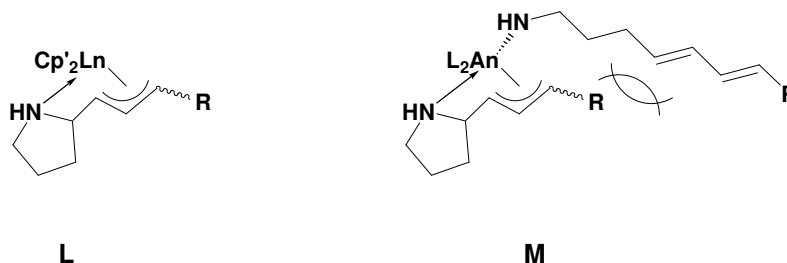
The effects of ancillary ligand openness as assayed by ∡ Cp(c)–M–L (Chart 2) on the present An-catalyzed process (Figure 4d) parallel those in organolanthanide catalysis and those generally seen in Ln- or An-catalyzed aminoalkene HA/cyclization.[2d,15] In contrast, the rate dependence on An^{4+} ionic radius (rate: U > Th) resembles more thermodynamically-favored N–H bond additions to aminoalkyne C≡C and aminoallene C=C=C units. From a Hammond postulate standpoint,[31,49] such behavior suggests a diene HA transition state more closely resembling reactants than products in each transformation class.

To rationalize organoactinide reactivity patterns for all HA reactions, it is beneficial to consider the estimated enthalpies associated with each class of cyclization (Table 9). For transformations where Scheme 1 step (i) is most exothermic vs. step (ii), the U^{4+}-catalyzed processes are more rapid; when steps (i) and (ii) are closest in exothermicity (i.e., 1,2-disubstituted alkenes), rate dependence on metal ionic radius is negligible. In qualitative terms, the softer, more electron-rich substrates (i.e., alkynes > allenes > dienes) more rapidly undergo insertion at the slightly softer[13] U^{4+} metal center, whereas the less soft alkene substrates more rapidly undergo insertion at the slightly harder[13] Th^{4+} metal center. This ordering does not hold

in organo-4f-element HA/cyclization,[2d] suggesting that increased bond covalency[12,13] may be operative in organoactinide vs. organolanthanide catalysis.

Mechanistic Implications

A priori, the present tetravalent organoactinide complexes could mediate catalytic intramolecular HA/cyclization via either of two distinct, limiting mechanistic scenarios: (1) a polar, highly organized four-centered, insertive transition state involving $L_2An\langle$ species possessing two An–N σ-bonds ("Ln-like"; Scheme 1), or (2) a [2 + 2] cycloaddition pathway proceeding via reactive $L_2An=NR$ species, analogous to that proposed for *intermolecular* alkyne HA with bulky amines, mediated by Cp_2MR_2, $Cp_2M=NR(THF)$, and Cp'_2AnMe_2 catalysts (M = Ti, Zr; An = Th, U) at elevated temperatures (Scheme 3).[2a,e,f,h-n;55,56] In group 4 cases, scenario (2) has been shown to involve a rapid pre-equilibrium between $Cp_2M[N(H)Ar]_2$ and $Cp_2M=NAr(H_2NAr)$ (**B**) species, followed by turnover-limiting [2 + 2] $RC\equiv CR'$ cycloaddition to the $Cp_2M=NAr$ species (step (ii), Scheme 3), in agreement with the observed rate law (eq. 18a).[55] Slightly different kinetics were reported for Cp'_2AnMe_2-catalyzed intermolecular additions of bulky and unhindered aliphatic 1° amines to terminal alkynes, although with zero-order dependence on [alkyne] (rates were independent of alkyne identity) suggesting rapid $C\equiv C$ addition following turnover-limiting amine elimination, and with competing alkyne oligomerization processes.[56,57] Although inconsistent with non-catalytic $L_2An=NR$ chemistry,[12-14,22,38] an alternative scenario where an M=NR species forms irreversibly, followed by rapid $C\equiv C$ addition can also be envisioned (eq. 18b).

Scheme 3. Proposed [2 + 2] cycloaddition mechanistic pathway proceeding through an $L_2M=NAr$ intermediate (M = Ti, Zr) and consistent with the observed rate law ~ $[L_2M^{4+}]^1[alkyne]^1[amine]^{-1}$ in the *intermolecular* HA of alkynes with bulky (aromatic) amines (ref. 53). A similar pathway is proposed for Cp'_2An^{4+}-mediated processes displaying zero-order dependence on [alkyne] (see refs. 2 and 53-55).

$$\nu \sim [M]^1[\text{amine}]^{-1}[\text{alkyne}]^1 \qquad (18a)$$

$$\nu \sim [M]^1[\text{amine}]^0[\text{alkyne}]^0 \qquad (18b)$$
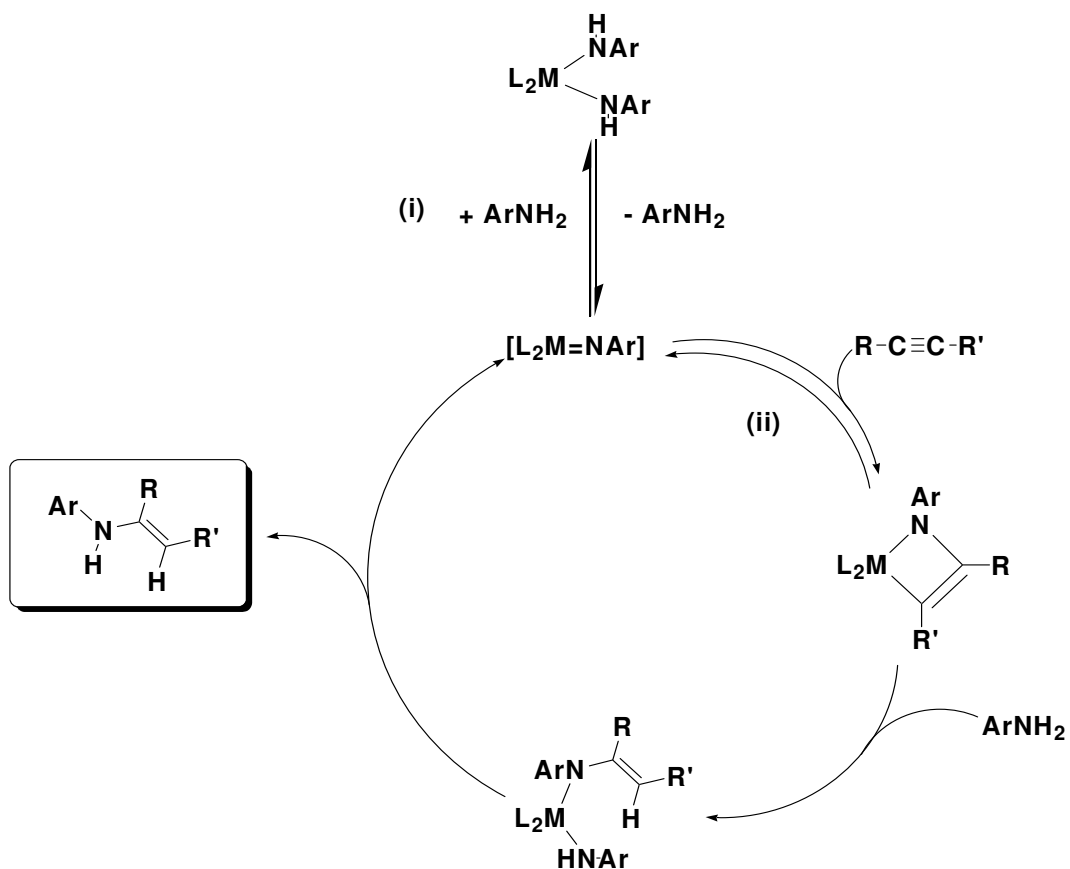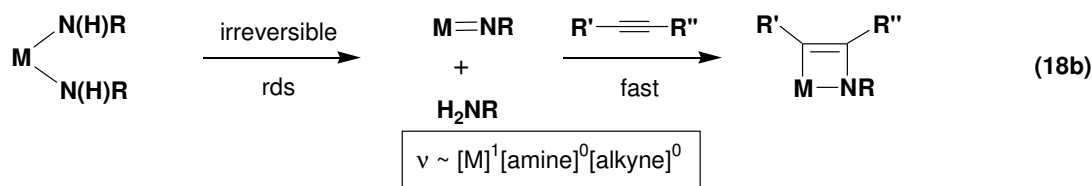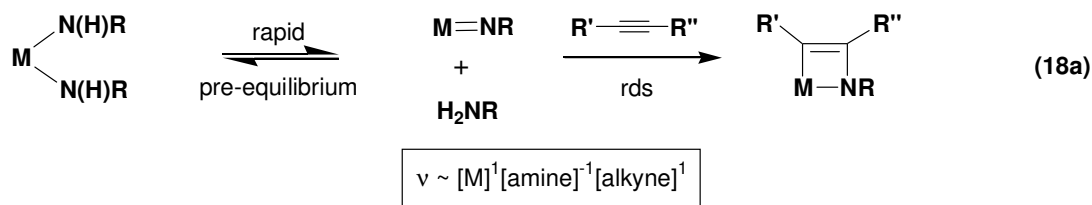
In contrast, more active cationic $U(NEt_2)_3{}^+BPh_4{}^-$ displays behavior similar to $Cp'_2An\langle$- and $Cp_2Zr\langle$-catalyzed intermolecular terminal alkyne HA with 1° amines, but also mediates $HNEt_2$ addition to $Me_3SiC{\equiv}CH$,[58] precluding an obvious An=NR intermediate. Moreover, cationic organozirconium and organotitanium complexes effect *intramolecular* aminoalkene HA/cyclizations, with scope limited to 2° amine substrates, again suggesting that a *neutral* $L_2M{=}NR$ species cannot be an intermediate (eq. 14).[5f,g] Note that monomeric tetravalent actinide imido complexes are normally observed with sterically encumbered (e.g., $Cp'_2An\langle$) ancillary ligands and result from bis(amido)actinide or related precursors (e.g., $Cp'_2An[N(H)Ar]_2$ or $Cp'_2An(Me)[N(H)Ar]$) at elevated temperatures via α-H elimination.[12-14,22,38,51,55,56] These considerations argue against the pathway of eq. 18b, where the predicted rate law, although in agreement with the presently observed (intramolecular HA/cyclization) rate law, assumes a stable, monomeric $L_2An{=}NR$ intermediate. Under the mild reaction conditions typical of HA/cyclizations reported here, involvement of $L_2An{=}NR$ intermediates seems unlikely considering the coordinative unsaturation of the $(CGC)An\langle$ species involved, the reactivity of

sterically unencumbered substrates, facile 2º amine cyclizations, absence of induction periods prior to catalytic turnover,[44] and rate differences observed for different C–C unsaturations. Furthermore, rate *acceleration* at low [substrate] ($L_2M=NR$ formation favored) and rate *deceleration* at high [substrate] ($L_2M[N(H)R]_2$ favored) seen in [2 + 2] cycloaddition pathways[55] are not observed here. On the contrary, (CGC)An‹-mediated intramolecular 1° or 2° amine HA/cyclizations display opposing behavior (namely, high [product] moderately inhibits catalytic turnover via competitive binding; Figures 2, 3),[2d,3v,15] and exhibit the rate law $\nu \sim [An]^1[amine]^0$ without an induction period, inconsistent with scenario (2) and signifying that turnover is not preceded by a rapid pre-equilibrium. Aminoalkene and aminoalkyne HA/cyclizations mediated by monosubstituted $L_2M(NR_2)X$ complexes, incapable of M=NR formation with 1° or 2° amine substrates,[16] further support mechanistic scenario (1), characterized by a highly organized transition state with turnover-limiting[53] C–C insertion into a σ-bonded M–N species (cf., **A**). This is also in agreement with DFT-level computational studies of organolanthanide-mediated HA/cyclization.[47]

Activation parameters derived for each C–C unsaturation (Table 9) also suggest a mechanistic pathway closely resembling that proposed for organolanthanide-mediated HA processes, where deviation from the generally preferred trivalent Ln^{3+} state is unlikely.[13] Activation parameters for the present (CGC)An‹-mediated HA/cyclizations are similar to those for the Cp'_2AnMe_2-mediated *intermolecular* terminal alkyne HA ($\Delta H^{\ddagger} = 11.7(3)$ kcal/mol, $\Delta S^{\ddagger} = -44.5(8)$ eu).[56] The more negative $\Delta S^{\ddagger}$ is not unexpected in comparison to *intramolecular* aminoalkene ($\Delta H^{\ddagger} = 12.6(2)$ kcal/mol, $\Delta S^{\ddagger} = -29.6(3)$ eu) and aminoalkyne HA/cyclization ($\Delta H^{\ddagger}$

= 13.9(2) kcal/mol, $\Delta S^{\ddagger}$ = -27(5) eu; Table 9) processes, and suggest that (CGC)An‹-catalyzed intramolecular HA/cyclizations proceed through an energetically-similar transition state to Ln-catalyzed HA/cyclization (**A**). Activation parameters for (CGC)An‹-catalyzed HA/cyclization are very similar to (< 3σ) Ln-catalyzed reactions (Table 9),[2d,3] in accord with similar, highly organized insertive transition states. Additional mechanistic data and arguments are presented in a companion manuscript.[16]

Conclusions

The catalytic competence of readily accessible constrained geometry (CGC)An(NR$_2$)$_2$ complexes in mediating intramolecular hydroamination/cyclization reactions of a large variety of primary and secondary amines tethered to multiple classes of terminal and disubstituted C–C unsaturations has been investigated in detail. Reaction scope includes aminoalkenes, aminoalkynes, aminoallenes, and aminodienes, with catalytic efficiencies comparable to the most active organolanthanide catalysts and *far exceeding* activities reported for tetravalent transition metal complexes. Reactivity trends reveal a marked dependence on An^{4+} ionic radius and ancillary ligation, with pronounced reactivity enhancement afforded by the CGC framework, regardless of C–C unsaturation. Experimentally-determined $\Delta H^{\ddagger}$, $\Delta S^{\ddagger}$, and E$_a$ parameters are similar to those for organolanthanide-mediated processes, consistent with highly-organized transition states exhibiting considerable bond-forming character. These facts, along with the rate law and other similarities to organolanthanide-catalyzed HA/cyclization processes, suggest a

"Ln-like" σ-bond insertive mechanistic pathway proceeding through an An–N(H)R intermediate (Scheme 2).

Chapter 2

Mechanistic Investigation of Intramolecular Aminoalkene and Aminoalkyne Hydroamination/Cyclization Catalyzed by Highly Electrophilic, Tetravalent Constrained Geometry 4d and 5f Complexes. Evidence for an M–N σ-Bonded Insertive Pathway
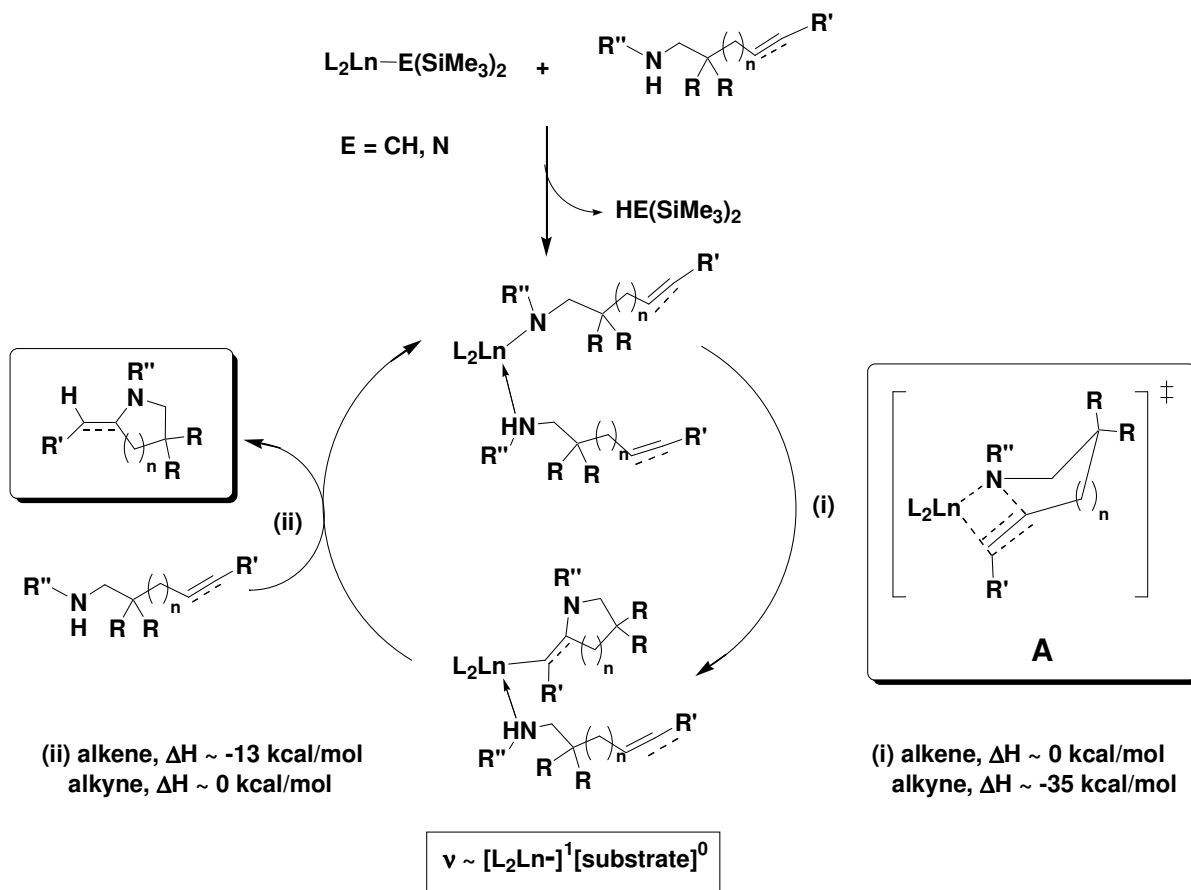
Abstract

A mechanistic study of intramolecular hydroamination/cyclization catalyzed by tetravalent organoactinide and organozirconium complexes is presented. A series of selectively substituted constrained geometry complexes, $(CGC)M(NR_2)Cl$ $(CGC = [Me_2Si(\eta^5\text{-}Me_4C_5)(^tBuN)]^{2-}$; M = Th, **1-Cl**; U, **2-Cl**; R = $SiMe_3$; M = Zr, R = Me, **3-Cl**) and $(CGC)An(NMe_2)OAr$ (An = Th, **1-OAr**; An = U, **2-OAr**) has been prepared via in situ protodeamination (complexes **1**-**2**) or salt metathesis (**3-Cl**) in high purity and excellent yield, and are found to be active precatalysts for intramolecular primary and secondary aminoalkyne and aminoalkene hydroamination/cyclization. Substrate reactivity trends, rate laws, and activation parameters for cyclizations mediated by these complexes are virtually identical to those of more conventional $(CGC)MR_2$ (M = Th, R = NMe_2, **1**; M = U, R = NMe_2, **2**; M = Zr, R = Me, **3**), $(Me_2SiCp''_2)UBn_2$ (**4**), Cp'_2AnR_2 (An = Th, **5**, An = U, **6**, R = CH_2SiMe_3) and analogous organolanthanide complexes. Deuterium KIE measured at 25 °C in C_6D_6 for aminoalkene $D_2NCH_2C(CH_3)_2CH_2CHCH_2$ (**11**-d_2) with precatalysts **2** and **2-Cl** indicate $k_H/k_D = 3.3(5)$ and $2.6(4)$, respectively. This provides strong evidence in these systems for turnover-limiting C–C insertion into an M–N(H)R σ-bond in the transition state. Related complexes $(Me_2SiCp''_2)U(CH_2Ph)(Cl)$ $(Cp'' = \eta^5\text{-}Me_4C_5$, **4-Cl**) and $Cp'_2An(R)(Cl)$ $(Cp' = \eta^5\text{-}Me_5C_5$; R = $CH_2(SiMe_3)$; An = Th, **5-Cl**; An = U, **6-Cl**) are also found to be effective precatalysts for this transformation. Additional arguments in favor of M–N(H)R intermediates vs. M=NR intermediates are presented.

Introduction

Hydroamination (HA), the atom-economical addition of an N–H bond across a C–C unsaturation,[1] is an important synthetic methodology for regiospecific C–N bond formation, a topic of considerable academic and industrial interest.[2] Research on this transformation pervades the Periodic Table,[1] with extensively studied organolanthanide-catalyzed intramolecular HA/cyclization playing a prominent role,[3,4] typically displaying near-quantitative yields in addition to high regio- and diastereoselectivities (>95%)[1d] and with enantioselectivities as high as 95%.[4b] Mechanistic experiments with rigorously trivalent lanthanide (Ln) catalysts on the intramolecular aminoalkene,[3v,w] aminoalkyne,[3m,o-q,t] aminoallene,[3i,j,l] internal olefin,[3c,h] and aminodiene[3d,g] HA/cyclization generally argue for turnover-limiting C=C/C≡C insertion into an L_2Ln-N σ-bond (Scheme 1). The observed rate law ($\nu \sim [Ln]^1[substrate]^0$), moderate $\Delta H^{\ddagger}$, and large negative $\Delta S^{\ddagger}$ are consistent with a highly ordered, polar **A**-like transition state,[1d] as are DFT calculations implicating an $L_2Ln[N(H)R](H_2NR)$ catalyst resting state and **A**-like species.[3a,x;5]

While growing interest in intramolecular aminoalkene[6] and aminoalkyne[7] HA/cyclization mediated by charge-neutral group 4 precatalysts has led to innovative catalyst design, many mechanistic details are not entirely understood. The pathway most often invoked is closely related to that proposed in the pioneering work of Bergman and co-workers (Scheme 2) for *intermolecular* alkyne (and allene) HA with bulky, primary $ArNH_2$ substrates, mediated by Cp_2ZrR_2 (R = Me, N(H)Ar) or $Cp_2Zr=NAr(THF)$ complexes at elevated temperatures.[8] This pathway involves a rapid pre-equilibrium (step (i), Scheme 2) between $Cp_2Zr[N(H)Ar]_2$ and $Cp_2Zr=NAr + H_2NAr$ (**B**) species, followed by turnover-limiting [2 + 2] RC≡CR′ cycloaddition

Scheme 1. Proposed σ-bond insertive mechanism for *intramolecular* aminoalkene and aminoalkyne HA/cyclization mediated by trivalent organolanthanide complexes. The pathway proposed for L_2Ln^{3+}-catalyzed *intermolecular* HA is similar, also proceeding through an L_2Ln–N(H)R σ-bonded species, leading to a transition state analogous to **A** (see ref. 1d).


$L_2Ln-E(SiMe_3)_2$ +

$E = CH, N$

$HE(SiMe_3)_2$

(i)

(ii)

A

(ii) alkene, ΔH ~ -13 kcal/mol
alkyne, ΔH ~ 0 kcal/mol

(i) alkene, ΔH ~ 0 kcal/mol
alkyne, ΔH ~ -35 kcal/mol

$\nu \sim [L_2Ln-]^1[substrate]^0$

(step (ii), Scheme 2), in agreement with the observed rate law ($\nu \sim [Zr]^1[alkyne]^1[amine]^{-1}$).
Similar kinetic studies on Cp'_2AnMe_2-catalyzed intermolecular addition of bulky and unhindered
primary aliphatic amines to terminal alkynes led Eisen and co-workers to propose a similar
pathway for $Cp'_2An\langle$ catalysts with rapid, irreversible [2 + 2] $RC\equiv CR'$ cycloaddition.[9]
Interestingly, neither $Cp_2Zr\langle$ nor $Cp'_2An\langle$ are active catalysts for primary amine additions in less
exothermic[1] intermolecular alkene HA.

In contrast to the above findings, more active cationic $U(NEt_2)_3{}^+BPh_4{}^-$ displays kinetic
behavior similar to $Cp'_2An\langle$- and $Cp_2Zr\langle$-catalyzed intermolecular terminal alkyne HA but effects
secondary $HNEt_2$ addition to $Me_3SiC\equiv CH$,[9a] arguing against an An=NR intermediate (vide
infra). Moreover, cationic organozirconium and organotitanium complexes effect related
intramolecular aminoalkene HA/cyclizations, with the reported scope limited *exclusively* to
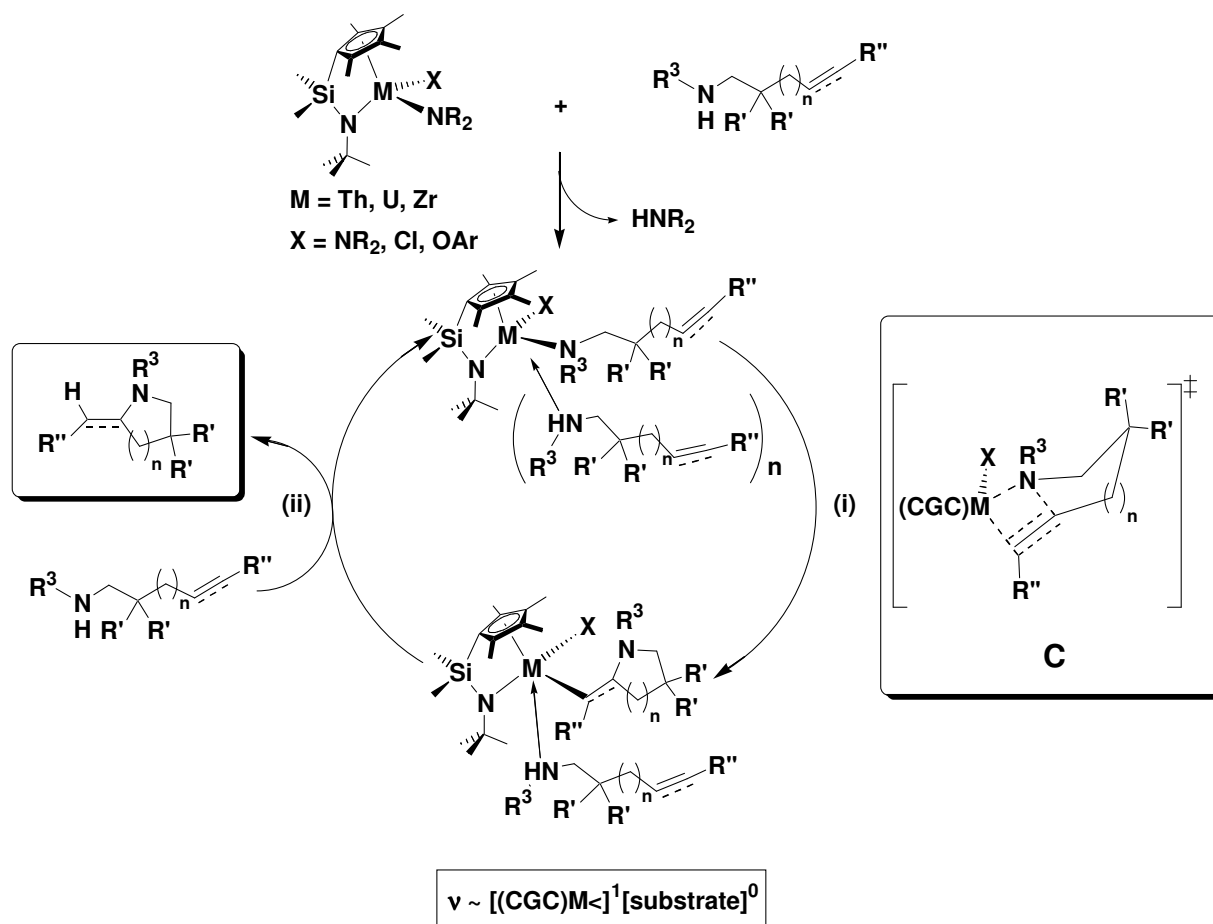secondary aminoalkenes, offering no obvious routes to $L_2M=NR$ species.

In a companion contribution, we report the rapid and regioselective intramolecular
HA/cyclization of primary and secondary amines having diverse tethered C–C unsaturations,
mediated by a new series of constrained geometry organoactinide complexes $(CGC)An(NMe_2)_2$
(An = Th, 1; An = U, 2).**[10]** The scope of C–C unsaturations was explored in depth for terminal
and disubstituted alkene, alkyne, allene, and diene substrates, revealing aminoalkene and
aminoalkyne turnover frequencies comparable to those of organolanthanide catalysts and
exceeding those of organo-group 4 catalysts.[10b] On the basis of substrate structure-reactivity
patterns and kinetic data paralleling organo-4f-element catalysis, a "Ln-like" mechanistic
scenario proceeding via a tetravalent An–N(H)R σ-bonded species (C) was tentatively suggested

Scheme 2. Proposed [2 + 2] cycloaddition mechanistic pathway proceeding through a Cp$_2$Zr=NAr intermediate **B** in *intermolecular* alkyne HA with bulky (aromatic) amines. A closely-related pathway is proposed for Cp$'_2$An‹-catalyzed alkyne HA (see refs. 8, 9 and eqs. 10).
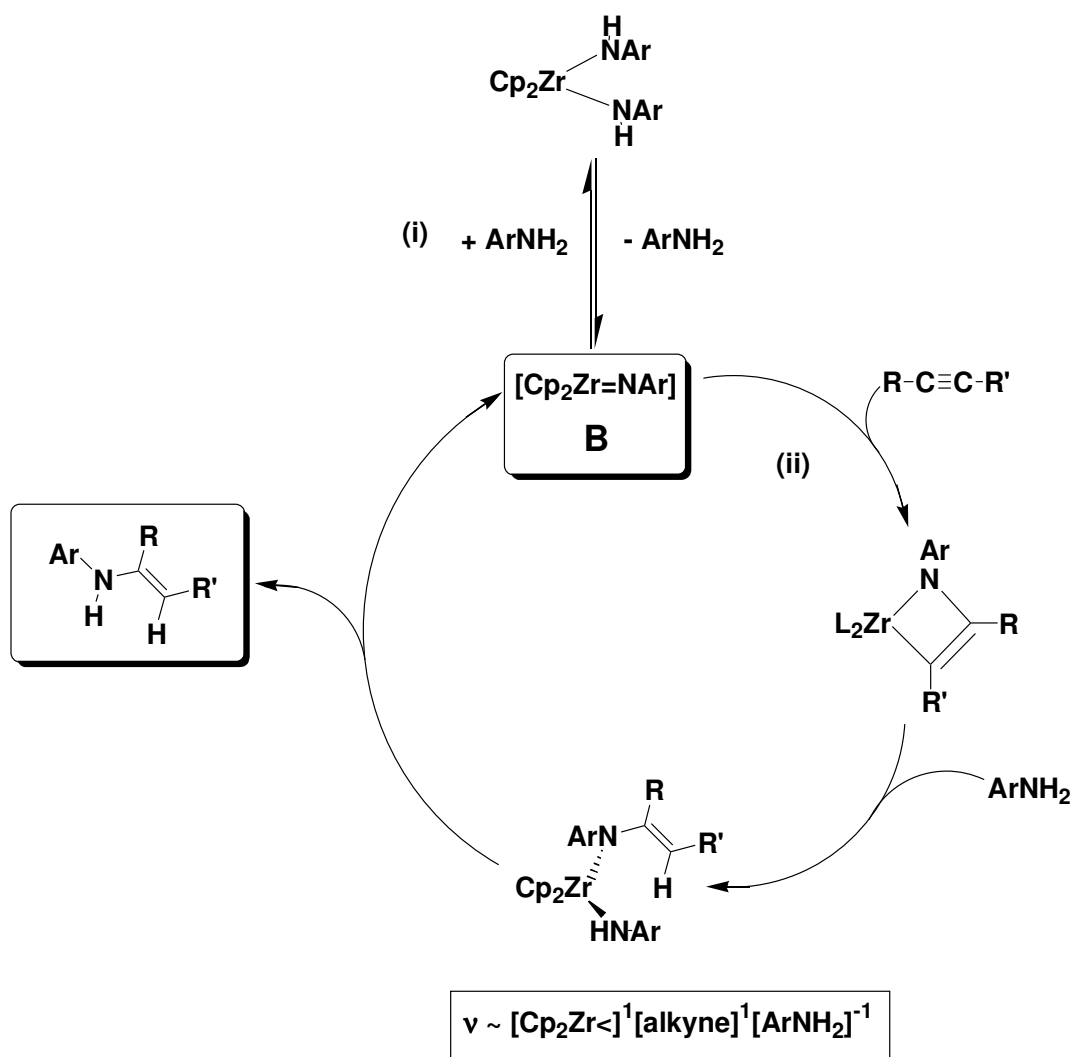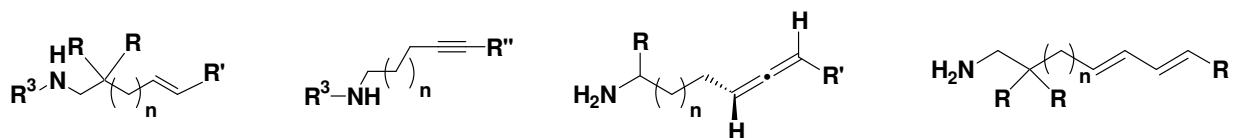
(Scheme 3). However, while this pathway is plausible for secondary aminoalkenes, cyclizations proceeding through An=NR species cannot a priori be precluded for primary aminoalkenes. These observations along with the paucity of mechanistic information on *intramolecular* HA/cyclization processes mediated by tetravalent group 4 metal centers and known group 4 vs. An^{4+} M–N bond polarity differences, prompted a mechanistic investigation. Herein we report evidence for turnover-limiting C=C/C≡C insertion at An–N(H)R species, supported by results with a series of monosubstituted $(CGC)An(NR_2)X$ complexes (X = non-labile ligand) that rapidly and regioselectively mediate intramolecular primary and secondary aminoalkene and aminoalkyne HA/cyclization. Selective substitution of a protonolytically non-labile X ligand for a protonolytically labile amide generates catalysts with only a single non-dative σ-bonded substrate moiety, unlikely to permit formation of An=NR species. Extension to analogous (CGC)Zr‹-catalyzed HA/cyclization reactions yields similar results. In most cases, the $(CGC)M(NR_2)X$ complexes effect HA reactions more rapidly than the corresponding $(CGC)MR_2$ complexes, further supporting the Scheme 3 pathway.

Scheme 3. Proposed σ-bond insertive mechanism for (CGC)M‹-catalyzed *intramolecular* HA/cyclization (M = Zr, Th, U) of terminal and disubstituted aminoalkenes, aminoalkynes, aminoallenes, and aminodienes. When X = NR$_2$, two substrate molecules enter the catalytic cycle and two HNR$_2$ are evolved during precatalyst activation (ref. 10).

Experimental

General Considerations.

All manipulations of air-sensitive materials were carried out with rigorous exclusion of oxygen and moisture in flame- or oven-dried Schlenk-type glassware on a dual-manifold Schlenk line, interfaced to a high-vacuum manifold (10^{-6} Torr), or in a nitrogen-filled Vacuum Atmospheres glovebox with a high capacity recirculator (< 2 ppm of O_2). Argon (Matheson, prepurified) was purified by passage through an MnO oxygen-removal column and a Davison 4A molecular sieve column. All solvents were dried and degassed over Na/K alloy and transferred in vacuo immediately prior to use. Commercially available materials were purchased from Aldrich, Lancaster, or Fisher (Acros) and used without further purification unless otherwise noted. $Th(C_2O_4)_2 \bullet 6H_2O$ was precipitated from an acidic aqueous solution of $Th(NO_3)_4 \bullet 4H_2O$ with oxalic acid and converted to anhydrous ThO_2 by thermolysis and oxidation in dry air at 450 °C. Anhydrous $ThCl_4$ was then prepared by slowly passing a stream of CCl_4 vapor in N_2 over ThO_2 at 500 ºC.[11] The extremely air- and moisture-sensitive reagents UCl_4,[12] $U[N(SiMe_3)_2]_3Cl$ and $Th[N(SiMe_3)_2]_3Cl$,[13] $(Me_2SiCp''_2)U(CH_2Ph)_2$ (**4**) and $(Me_2SiCp''_2)U(CH_2Ph)Cl$ (**4-Cl**),[14] Cp'_2AnR_2 ($Cp' = \eta^5\text{-}C_5Me_5$; $R = CH_2(SiMe_3)$; An = Th, **5**; An = U, **6**) and $Cp'_2An(R)Cl$ An = Th, **5-Cl**; An = U, **6-Cl**),[15] (CGC)$ZrMe_2$ (**3**) and (CGC)$ZrCl_2$,[16] H_2CGC [$Me_2Si(C_5Me_4H)(^tBuNH)$],[17] as well as substrates **7**, **9**, **13**, **15**,[11] and **11**[18] were prepared according to literature procedures. *N*-deuterated aminoalkene **11**-d_2 was prepared by shaking a CH_2Cl_2 solution of **11** with D_2O at least three times[19] and passing through a Celite plug to remove D_2O emulsions, followed by distillation and storage under N_2. ^1H NMR spectra indicate ≥95% isotopic enrichment. All

substrates for catalytic experiments were dried at least three times as solutions in benzene-d_6 over freshly-activated Davison 4A molecular sieves and were degassed repeatedly by freeze-pump-thaw cycles. Substrates were then stored under Ar in vacuum-tight storage flasks.

Physical and Analytical Measurements.

NMR spectra were recorded on a Varian [UNITY]Inova-500 (FT, 500 MHz, ^{1}H; 125 MHz, ^{13}C) instrument. Chemical shifts (δ) for ^{1}H and ^{13}C spectra are referenced to internal solvent resonances and reported relative to SiMe$_4$. NMR experiments on air-sensitive samples were conducted in Teflon valve-sealed tubes (J. Young). Elemental analyses on air-sensitive samples were performed by the Micro-Mass Facility at the University of California, Berkeley.

[(CGC)Th[N(SiMe₃)₂]Cl]₂ (1-Cl). Th[N(SiMe$_3$)$_2$]$_3$Cl was prepared according to the literature procedure[14] (without isolation) from ThCl$_4$ (0.51 g, 1.36 mmol) and NaN(SiMe$_3$)$_2$ (0.72 g, 3.93 mmol) in THF (40 mL) over 3 d in a 100 mL round-bottom reaction flask. Volatiles were removed in vacuo, and toluene (40 mL) was condensed onto the crude colorless mixture at -78 °C. After warming to 20 °C under Ar, a solution of H$_2$CGC (0.37 g, 1.5 mmol) in pentane (3 mL) was added by syringe. The flask was then heated in a 70 °C oil bath and stirred under argon for 16 h. The oil bath was removed, and the mixture was allowed to cool before filtering to remove NaCl, and then concentrating the pale yellow filtrate in vacuo to a total volume of ca. 5 mL. The resulting colorless powder, which precipitated from the solution at -78 °C, was collected by filtration and dried in vacuo to afford **1-Cl** in 83% yield (0.66 g, 0.97 mmol). ^{1}H NMR (C$_6$D$_6$,

500 MHz, 20 ºC): δ 2.35 (s, 3 H, C$_5$(CH$_3$)$_4$), 2.28 (s, 3 H, C$_5$(CH$_3$)$_4$), 2.20 (s, 3 H, C$_5$(CH$_3$)$_4$), 2.04 (s, 3 H, C$_5$(CH$_3$)$_4$), 1.41 (s, 9 H, NC(CH$_3$)$_3$), 0.61 (s, 3 H, Si(CH$_3$)$_2$), 0.59 (s, 3 H, Si(CH$_3$)$_2$), 0.38 (s, 3 H, N[Si(CH$_3$)$_3$]$_2$), 0.23 (s, 3 H, N[Si(CH$_3$)$_3$]$_2$). Anal. Calcd. C, 37.24; H, 6.70; N, 4.14. Found: C, 37.14; H, 6.95; N, 4.22. Single crystals of **1-Cl** suitable for X-ray diffraction analysis were grown by cooling a concentrated pentane solution to -30 °C over several days.

(CGC)U[N(SiMe$_3$)$_2$]Cl (2-Cl).   The title compound was prepared in a manner analogous to that employed for **1-Cl** in 85% yield (0.75 g, 1.1 mmol), by generating U[N(SiMe$_3$)$_2$](Cl) at 20 °C from UCl$_4$ (0.50 g, 1.32 mmol) and NaN(SiMe$_3$)$_2$ (0.73 g, 3.98 mmol) in 24 h, followed by treatment with a pentane solution of H$_2$CGC (0.33 g, 1.3 mmol) at 70 °C for 16 h. ^{1}H NMR (C$_6$D$_6$, 500 MHz, 20 ºC): δ 82.88 (s, 3 H), 56.28 (s, 3 H), 23.35 (s, 9 H, NC(CH$_3$)$_3$), -8.97 (s, 3 H), -9.55 (s, 3 H), -10.51 (br s, 9 H, N[Si(CH$_3$)$_3$]$_2$), -32.61 (br s, 9 H, N[Si(CH$_3$)$_3$]$_2$), -50.53 (s, 3 H), -67.14 (s, 3 H). Anal. Calcd. C, 36.91; H, 6.64; N, 4.10. Found: C, 36.52; H, 6.72; N, 4.08. Single crystals of **2-Cl** suitable for X-ray diffraction analysis were grown from a concentrated pentane solution at -30 °C over several days.

(CGC)Th(NMe$_2$)OAr (1-OAr).   A 25 mL round-bottom flask was charged in the glovebox with a magnetic stir bar, (CGC)Th(NMe$_2$)$_2$ (0.145 g, 0.254 mmol), and 2,6-di-*tert*-butylphenol (0.056 g, 0.270 mmol, 1.1 equiv.). Toluene (15 mL) was condensed in vacuo onto the solids at -78 °C, and the mixture was allowed to warm to 20 °C under Ar. After stirring at 20 °C for 1 h, volatiles were removed in vacuo, and pentane (15 mL) was condensed onto the solids at -78 °C.

The mixture was warmed to 20 °C under Ar and filtered to remove a fine precipitate, likely (CGC)Th(OAr)$_2$ (suggested by ^{1}H NMR spectroscopy). The pentane solution was then concentrated to a volume of 3 mL and slowly cooled in a -30 °C freezer to afford colorless crystals of **1-OAr** in 86% yield (0.16 g, 0.22 mmol). This compound can also be prepared in situ and used directly in catalytic reactions, with identical results and without interference from small amounts (5-10 mol%) of (CGC)Th(OAr)$_2$ byproduct. ^{1}H NMR (C$_6$D$_6$, 500 MHz, 20 °C): δ 7.30 (d, 2 H, *meta*-C$_6$H$_3$), 6.90 (t, 1 H, *para*-C$_6$H$_3$), 2.91 (s, 6 H, N(*CH$_3$*)$_2$), 2.31 (s, 3 H, C$_5$(*CH$_3$*)$_4$), 2.19 (s, 3 H, C$_5$(*CH$_3$*)$_4$), 2.07 (s, 3 H, C$_5$(*CH$_3$*)$_4$), 1.90 (s, 3 H, C$_5$(*CH$_3$*)$_4$), 1.49 (s, 18 H, (*^{t}Bu*)$_2$C$_6$H$_3$), 1.32 (s, 9 H, NC(*CH$_3$*)$_3$), 0.73 (s, 3 H, Si(*CH$_3$*)$_2$), 0.65 (s, 3 H, Si(*CH$_3$*)$_2$). Single crystals of **1-OAr** suitable for X-ray diffraction analysis were grown by cooling a concentrated pentane solution to -30 °C over several days.

(CGC)U(NMe$_2$)OAr (2-OAr).   The title compound was prepared in a manner analogous to that employed for **1-OAr** in 92% yield (0.12 g, 0.16 mmol) from (CGC)U(NMe$_2$)$_2$ (0.151 g, 0.174 mmol) and 2,6-di-*tert*-butylphenol (0.066 g, 0.320 mmol, 1.8 equivalents) in an orange toluene solution (15 mL). Unlike **1-OAr**, the potential (CGC)U(OAr)$_2$ byproduct was not observed (by ^{1}H NMR spectroscopy; vide infra), and filtration is therefore not required to obtain the analytically pure, microcrystalline orange **2-OAr** powder (excess ArOH is removed in vacuo at 10^{-6} Torr). This compound can also be prepared in situ and used directly in catalytic reactions with identical results. ^{1}H NMR (C$_6$D$_6$, 500 MHz, 20 °C): δ 48.76 (s, 3 H), 24.66 (s, 3 H), 23.69 (br s, 2 H, *meta*-C$_6$H$_3$), 18.03 (t, 1 H, J = 7.5 Hz, *para*-C$_6$H$_3$), 12.49 (s, 6 H, N(*CH$_3$*)$_2$), 2.11 (s, 18

H, (^{t}Bu)$_2$C$_6$H$_3$), -3.22 (s, 3 H), -15.62 (s, 3 H), -19.05 (s, 3 H), -30.09 (s, 3 H), -34.46 (s, 9 H, NC(CH$_3$)$_3$). Anal. Calcd. C, 50.53; H, 7.39; N, 3.80. Found: C, 50.22; H, 7.38; N, 3.55.

(CGC)Zr(NMe$_2$)Cl (3-Cl).   A 50 mL round-bottom flask was charged in the glovebox with a magnetic stir bar, (CGC)ZrCl$_2$ (0.415 g, 1.01 mmol), and LiNMe$_2$ (0.052 g, 1.02 mmol). Et$_2$O (40 mL) was condensed onto the solids in vacuo at -78 °C, and the mixture was slowly allowed to warm to 20 °C under Ar. After 4 h, volatiles were removed in vacuo and pentane (30 mL) was condensed onto the colorless solids at -78 °C. The suspension was next warmed to 20 °C under Ar and filtered to remove LiCl. The pale yellow filtrate was concentrated in vacuo to a total volume of ca. 10 mL, and slowly cooled in a -78 °C bath. The colorless **3-Cl** powder was isolated in 70% yield by filtration and drying under high vacuum (0.30 g, 0.71 mmol). ^{1}H NMR (C$_6$D$_6$, 500 MHz, 25 °C): δ 2.66 (S, 12 H, N(CH$_3$)$_2$), 2.16 (s, 3 H, C$_5$(CH$_3$)$_4$), 2.10 (s, 3 H, C$_5$(CH$_3$)$_4$), 2.00 (s, 3 H, C$_5$(CH$_3$)$_4$), 1.71 (s, 3 H, C$_5$(CH$_3$)$_4$), 1.34 (s, 9 H, NC(CH$_3$)$_3$), 0.57 (s, 3 H, Si(CH$_3$)$_2$), 0.53 (s, 3 H, Si(CH$_3$)$_2$). Anal. Calc. C, 48.59; H, 7.92; N, 6.67. Found: C, 48.23; H, 7.90; N, 6.33. Single crystals of **3-Cl** suitable for X-ray diffraction analysis were grown by cooling a concentrated pentane solution to -30 °C over several days.

Kinetic Studies of Hydroamination Reactions.

In a typical experiment, precatalyst (ca. 1-6 mg, 2-11 μmol) and internal standard tetra(p-tolyl)silane (ca. 2-5 mg, 5-12 μmol) were dissolved in C$_6$D$_6$ (0.80 mL) and added to a Teflon-valved NMR tube in the glove box. A preliminary ^{1}H NMR spectrum was recorded to verify the

relative concentrations of precatalyst and standard. The NMR tube was then attached to a high vacuum manifold via a glass adapter with a secondary Teflon valve and was placed in a -78 ℃ bath before evacuating to ca. 10^{-6} Torr and resealing. The upper portion of the valve was then backfilled with Ar, and a ca. 1 M solution of substrate in C_6D_6 (0.20 mL, ca. 200 μmol) was added via syringe to the adapter under an Ar flush and briefly degassed under static vacuum. The primary valve was next opened under positive Ar pressure, and the substrate solution was thereby pulled into the NMR tube, freezing the substrate solution just above the precatalyst solution. After evacuating and backfilling the tube with Ar three times, the valve was closed. The sample remained frozen in the -78 ℃ bath until thawing and placing directly into the Varian ^{UNITY}Inova 500 MHz NMR spectrometer, pre-equilibrated at 25.0 ℃ ($\pm$ 0.2 ℃; calibrated with an ethylene glycol standard). Data were obtained with a single transient to avoid saturation, and substrate or product concentration was determined relative to the intensity of an Si(p-tolyl)$_4$ resonance, typically downfield of C_6D_5H in the aromatic region (7.74 ppm), over three or more half-lives. All data were fit by least-squares analysis according to eq. 1, where C_0 is the initial concentration of substrate and t is time. The turnover frequency (N_t) was calculated according to eq. 2, where E is the normalized substrate:catalyst ratio, determined from the relative intensities of non-overlapping resonances in each ^{1}H NMR spectrum, typically with $\pm$ 5% precision. Representative plots of kinetic data are shown in Figures 2 and 3.

$$C = mt + C_0 \qquad\qquad (1)$$

$$N_t = \left(\frac{m}{-C_0} \right) E \qquad\qquad (2)$$

X-ray Diffraction Analyses.

Single crystals of complexes **1-Cl**, **2-Cl**, **3-Cl**, and **1-OAr** suitable for X-ray diffraction were grown by cooling concentrated pentane solutions in a -30 ºC freezer over a period of several days. The mother liquor was removed and the crystals were covered in Infineum V8512 (Paratone-N) oil in an N_2-filled glove box immediately prior to mounting on a goniometer head. Data were collected under a cold (-120 ºC) N_2 stream using a Bruker SMART-1000 CCD area detector with graphite monochromated MoK_α radiation. Complexes **1-Cl**, **2-Cl**, and **3-Cl** crystallize in space group $P\bar{1}$, while complex **1-OAr** crystallizes in space group $P2_1/c$ (Tables 1, 2). Structures were solved by direct methods and expanded using Fourier techniques, refined with full-matrix least-squares on F^2. Non-hydrogen atoms were refined anisotropically, while hydrogen atoms were included but not refined. All calculations and absorption corrections were performed using the Shelxtl for WindowsNT software package.[20] Centroid distances and angles were obtained using the program ORTEP-3 for Windows,[21] available as a free download.

Results

In this section we discuss the synthesis and structural characterization of a series of selectively substituted, electrophilic, tetravalent actinide and group 4 $(CGC)M(NR_2)X$ complexes and mechanistic studies of representative primary and secondary aminoalkene and aminoalkyne intramolecular HA/cyclization mediated by these complexes. Effects of catalyst substitution, metal ion, and ancillary ligation are presented along with relevant kinetic

parameters and deuterium KIE. It will be seen that chloride- and aryloxide-substituted complexes are highly active HA/cyclization catalysts that display kinetic and mechanistic signatures inconsistent with M=NR species in the catalytic cycle. A mechanistic pathway proceeding through an M–N σ-bonded species is proposed based on results presented herein.

Synthesis and Characterization of Chloride- and Aryloxide-Substituted (CGC)M(NR₂)X Complexes.

   (CGC)An[N(SiMe₃)₂]Cl complexes **1-Cl** and **2-Cl** are available in excellent yield and high purity from the corresponding AnCl₄ reagents via in situ generation of the tris(hexamethyldisilazido)actinide chlorides, An[N(SiMe₃)₂]₃Cl, followed by protodeamination with diprotic H₂CGC, evolving hexamethyldisilazane over 16 h at 70 °C (Scheme 4; Chart 1). Owing to unfavorable steric interactions that preclude An[N(SiMe₃)₂]₄ formation, the desired complexes are obtained without (CGC)An[N(SiMe₃)₂]₂ contamination. The analogous group 4 complex (CGC)Zr(NMe₂)(Cl) **3-Cl** was obtained by traditional salt metathesis from (CGC)ZrCl₂ and LiNMe₂ (Scheme 4; Chart 1). No evidence for amide-halide disproportion is observed by ¹H NMR spectroscopy at 25 °C over a period of days for any of the chloride-substituted complexes prepared for this study. Solid-state structures were defined by single-crystal X-ray diffraction, indicating that **1-Cl** is a bis(μ-chloro) dimer in the solid state, while **2-Cl** and **3-Cl** are monomeric (Tables 1-2, Figure 1a-c; vide infra).

   Aryloxide complexes (CGC)An(NMe₂)OAr, **1-OAr** and **2-OAr**, are cleanly obtained by protodeamination of (CGC)An(NMe₂)₂ complex **1** or **2** with excess of sterically hindered 2,6-di-

Table 1. Summary of structure refinement data for single crystal X-ray diffraction analysis of
[(CGC)Th[N(SiMe$_3$)$_2$](μ-Cl)]$_2$ (**1-Cl**), (CGC)U[N(SiMe$_3$)$_2$]Cl (**2-Cl**), (CGC)Zr(NMe$_2$)Cl (**3-Cl**),
and (CGC)Th(NMe$_2$)OAr (**1-OAr**) at -120 °C. See Supporting Information for complete listings.

	1-Cl	2-Cl	3-Cl	1-OAr
Empirical formula	C$_{21}$H$_{45}$ClN$_2$Si$_3$Th	C$_{21}$H$_{45}$ClN$_2$Si$_3$U	C$_{17}$H$_{33}$ClN$_2$SiZr	C$_{31}$H$_{54}$NOSiTh
Crystal system	Triclinic	Triclinic	Triclinic	Monoclinic
Space group	P$\bar{1}$	P$\bar{1}$	P$\bar{1}$	P2$_1$/c
Unit cell dimensions	a = 10.896(3) Å	a = 8.9653(8) Å	a = 8.465(4) Å	a = 9.929(6) Å
	b = 11.550(2) Å	b = 11.9961(15) Å	b = 8.780(2) Å	b = 10.039(7) Å
	c = 13.120(2) Å	c = 13.5399(10) Å	c = 15.839(6) Å	c = 32.12(2) Å
	α = 74.700(13)°	α = 99.175(7)°	α = 82.11(3)°	
	β = 83.260(10)°	β = 90.657(9)°	β = 74.85(3)°	β = 96.41(4)°
	γ = 63.205(16)°	γ = 95.203(8)°	γ = 63.74(4)°	
Volume	1421.6(5) Å^3	1431.1(2) Å^3	1018.6(6) Å^3	3182(4) Å^3
Absorption coefficient	5.475 mm^{-1}	5.900 mm^{-1}	0.729 mm^{-1}	4.749 mm^{-1}
F(000)	668	672	440	1464
Theta range for data collection	1.61° to 28.85°	1.52° to 28.61°	1.33 to 28.56°	1.28° to 28.87°
Reflections collected / unique	3208 / 2337 [R(int) = 0.0260]	13047 / 6466 [R(int) = 0.0841]	9247 / 4668 [R(int) = 0.0506]	28708 / 7692 [R(int) = 0.1252]
Completeness to theta = 28.85	89.2 %	88.2 %	89.7 %	91.9 %
Data / restraints / parameters	2337 / 0 / 268	6466 / 0 / 268	4668 / 0 / 211	7692 / 0 / 342
Goodness-of-fit on F^2	1.076	1.098	1.096	0.937
Final R indices [I > 2 (σ)]	R1 = 0.0200, wR2 = 0.0532	R1 = 0.0274, wR2 = 0.0726	R1 = 0.0449, wR2 = 0.1071	R1 = 0.0476, wR2 = 0.0875
R indices (all data)	R1 = 0.0206, wR2 = 0.0535	R1 = 0.0296, wR2 = 0.0738	R1 = 0.0534, wR2 = 0.1111	R1 = 0.0954, wR2 = 0.1007
Largest diff. peak and hole	0.918 and -0.730 e/Å^{-3}	1.785 and -1.594 e/Å^3	1.844 and -0.651 e/Å^3	2.838 and -1.673 e/Å^3

Figure 1. ORTEP depictions of solid-state structures of the following precatalysts at -120 °C (a) dimeric $[(CGC)Th[N(SiMe_3)_2](\mu-Cl)]_2$ (**1-Cl**), (b) $(CGC)U[N(SiMe_3)_2]Cl$ (**2-Cl**), (c) $(CGC)Zr(NMe_2)Cl$ (**3-Cl**), and (d) $(CGC)Th(NMe_2)OAr$ (**1-OAr**; $OAr = 2,6\text{-}^tBu_2C_6H_3$). Thermal ellipsoids are drawn at the 50% probability level. See Tables 2 and 3, Charts 1 and 2, and Supporting Information for complete structural data.
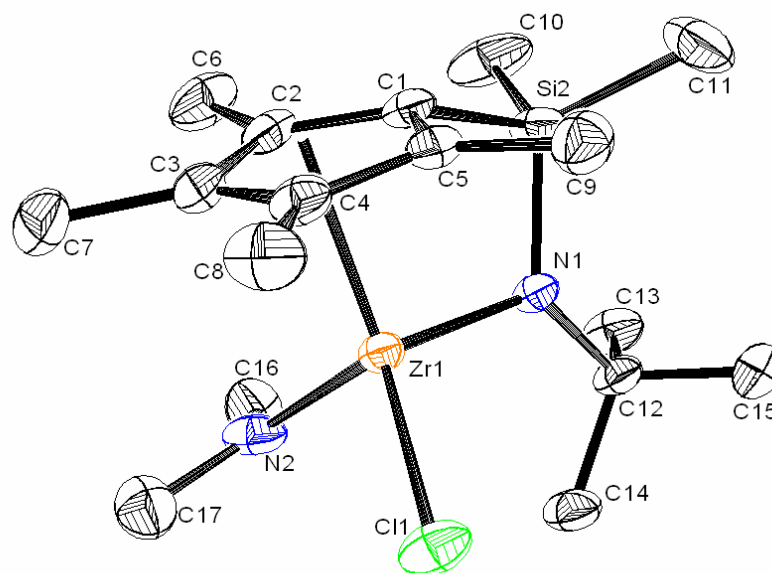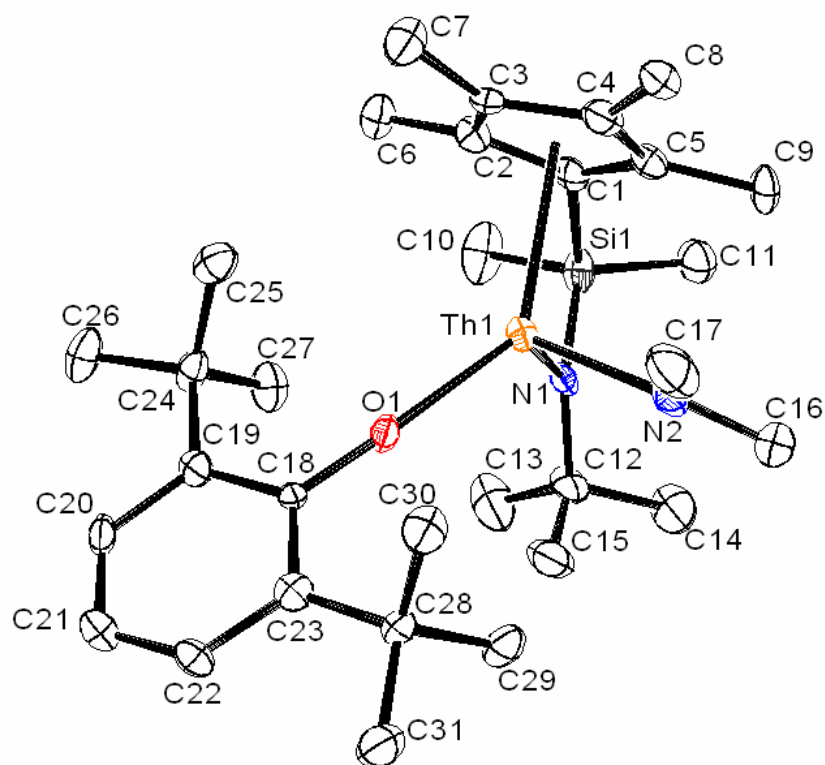
(a)
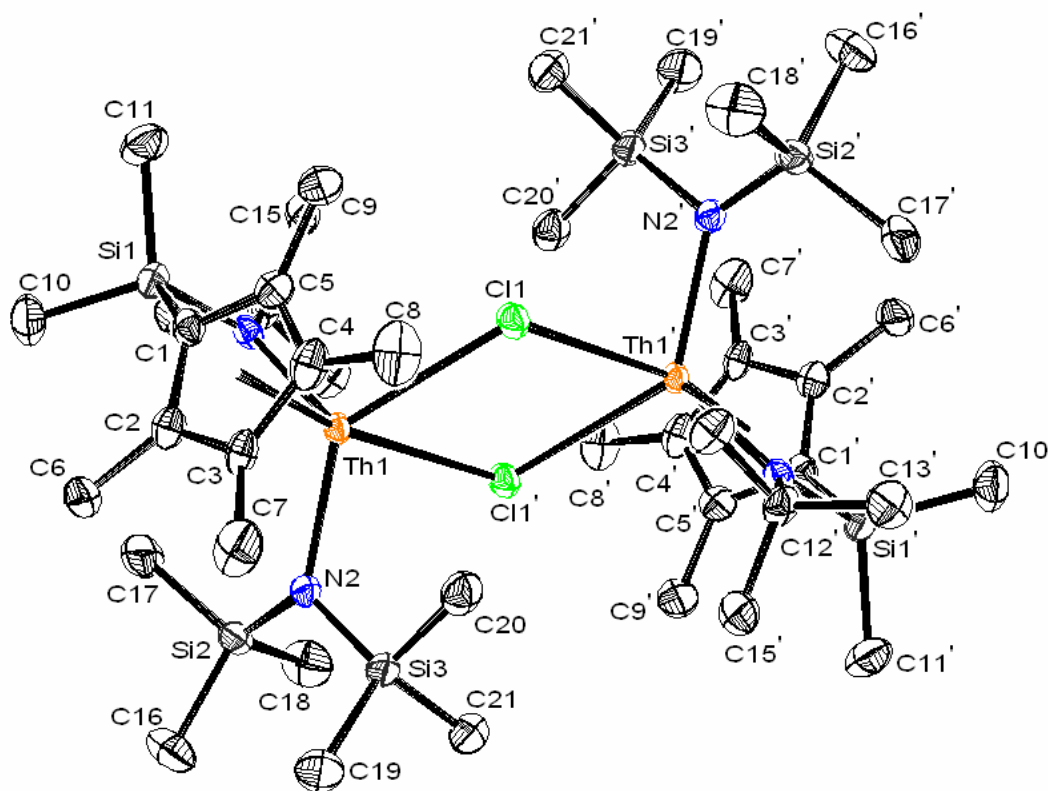
(b)
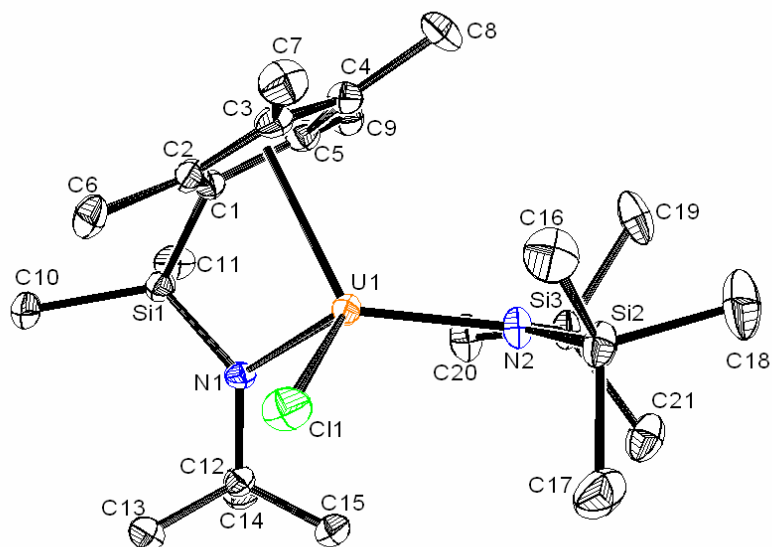
(c)

(d)

tert-butylphenol, ArOH (Scheme 4; Chart 1). In the case of An = U, treatment of **2** with 1.8 equiv. of ArOH leads to exclusive formation of **2-OAr**, leaving 0.8 equiv. unreacted ArOH. Initial ^{1}H NMR screening experiments indicate complete consumption of **2** within 30 min of dissolution in benzene-d_6 and negligible interaction between the paramagnetic U^{4+} ion and unreacted ArOH (as judged by negligible isotropic shifts of the resonances) up to temperatures of 90 °C. Similar experiments carried out with Th complex **1** and 1.2 equivalents of ArOH to generate **1-OAr** indicate further reaction and complete consumption of excess ArOH within 60 min at 25 °C. In preparative scale syntheses, the $(CGC)Th(OAr)_2$ byproduct is easily removed by filtration from concentrated pentane solutions of the otherwise pure monoaryloxide complex. When in situ-generated **1-OAr** containing 5-10% $(CGC)Th(OAr)_2$ is employed in catalytic HA experiments, results are identical to those obtained with analytically pure **1-OAr**. Complex **1-OAr** was also analyzed via single-crystal X-ray diffraction and shown to be monomeric in the solid state (Tables 1-2 and Figure 1d).

Catalytic Intramolecular Hydroamination/Cyclization Experiments

In this section, results of catalytic intramolecular HA/cyclization of representative aminoalkyne and aminoalkene substrates, mediated by precatalysts $(CGC)An(NMe_2)_2$ (An = Th, **1**; An = U, **2**), $[(CGC)Th(NR_2)(\mu\text{-}Cl)]_2$ (R = SiMe$_3$, **1-Cl**), $(CGC)M(NR_2)Cl$ (M = U, R = SiMe$_3$, **2-Cl**; M = Zr, R = Me, **3-Cl**), $(CGC)ZrMe_2$ (**3**), $(CGC)An(NMe_2)OAr$ (OAr = 2,6-di-*tert*-Bu-phenoxide; An = Th, **1-OAr**; An = U, **2-OAr**), $Me_2SiCp''_2U(CH_2Ph)_2$ (**4**), $Me_2SiCp''_2U(CH_2Ph)Cl$ (**4-Cl**), $Cp'_2An(CH_2SiMe_3)_2$ (An = Th, **5**; An = U, **6**), and

Chart 1

(CGC)Th(NMe$_2$)$_2$
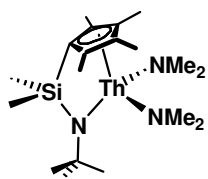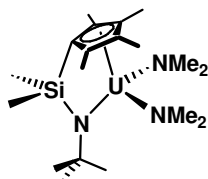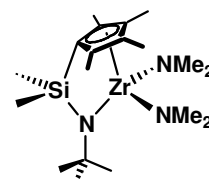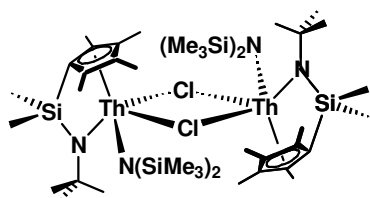**1**

(CGC)U(NMe$_2$)$_2$
2

(CGC)Zr(NMe$_2$)$_2$
3

[(CGC)Th(NMe$_2$)Cl]$_2$
1-Cl
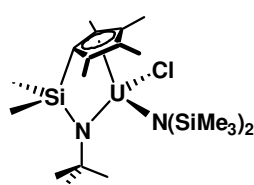
(CGC)U(NMe$_2$)Cl
2-Cl
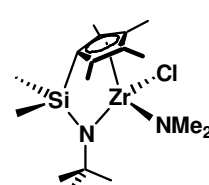
(CGC)Zr(NMe$_2$)Cl
3-Cl
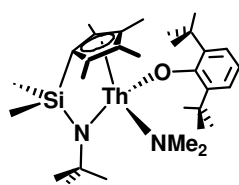
(CGC)Th(NMe$_2$)OAr
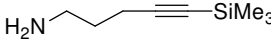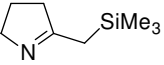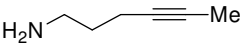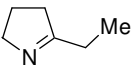**1-OAr**
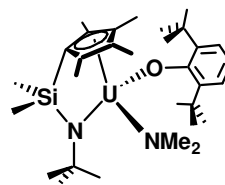
(CGC)U(NMe$_2$)OAr
2-OAr

Table 2. Selected bond distances (Å) and angles (°) for [(CGC)Th[N(SiMe$_3$)$_2$](μ-Cl)]$_2$ (**1-Cl**), (CGC)U[N(SiMe$_3$)$_2$]Cl (**2-Cl**), (CGC)Zr(NMe$_2$)Cl (**3-Cl**), and (CGC)Th(NMe$_2$)OAr (**1-OAr**). See Supporting Information for complete listings (Cp(cent) = Me$_4$C$_5$ ring centroid; X = Cl or OAr).

	1-Cl	2-Cl	3-Cl	1-OAr
Cp(cent)-M-N1	91.7	93.1	101.1	90.4
Cp(cent)-M-X	94.8/157.8	108.1	131.9	136.6
Cp(cent)-M-N2	108.8	122.1	104.4	106.9
N1-M-X	107.7(1)	100.52(7)	115.10(7)	115.9(2)
N1-M-N2	110.8(2)	123.8(1)	104.7(1)	102.0(2)
N2-M-X	133.6(1)	106.67(8)	104.06(8)	100.9(2)
Cp(cent)-M	2.53	2.41	2.30	2.55
M-N1	2.335(5)	2.223(3)	2.077(2)	2.293(6)
M-N2	2.334(5)	2.257(3)	2.078(3)	2.252(6)
M-X	2.883(2)/2.964(2)	2.6124(9)	2.437(1)	2.258(5)

Cp$'_2$An(CH$_2$SiMe$_3$)Cl (An = Th, **5-Cl**; An = U, **6-Cl**), are presented. Primary, *N*-unprotected substrates bearing C≡C and C=C unsaturations are presented first, followed by results with *N*-methyl substituted secondary amine substrates.

Primary Aminoalkyne Hydroamination. Intramolecular aminoalkyne HA/cyclization is effectively mediated by bisamido as well as "substituted" chloroamido and aryloxoamido complexes **1**-**6**. In some cases, substituted complexes promote **7** → **8** and **9** → **10** cyclizations with far greater catalytic efficiency than the unsubstituted congeners. For example, **7** → **8** conversion mediated by **1-Cl** proceeds at a rate more than double that mediated by **1** at 25 °C (N_t = 200 h^{-1} (**1-Cl**) vs. 82 h^{-1} (**1**); Table 3, entries 1, 2), and with a 5× greater rate vs. bulkier aryloxide-substituted **1-OAr** (N_t = 37 h^{-1}; Table 3, entry 3). Smaller ionic radius (CGC)U‹ derivatives display a similar trend, with **2-Cl** mediating **7** → **8** more rapidly than **2-OAr** (N_t = 280 h^{-1} (**2-Cl**) and 52 h^{-1} (**2-OAr**) at 25 °C; Table 3, entries 5, 6). This conversion becomes less rapid as ancillary ligation becomes less open, requiring mild heating to achieve moderate N_t values. Note that no difference in reactivity is observed between unaltered **4** and "substituted" **4-Cl** (N_t = 10 h^{-1} at 60 °C; Table 3, entries 7, 8). More sterically congested Cp$'_2$An(R)Cl complexes **5-Cl** and **6-Cl** also mediate this transformation, though catalytic activities are considerably lower than those of their Cp$'_2$AnR$_2$ congeners (N_t = 190 h^{-1} (**5**) and 1.2 h^{-1} at 60 °C (**5-Cl**); N_t = 16 h^{-1} (**6**) and 0.4 h^{-1} (**6-Cl**) at 60 °C; Table 3, entries 9-12).[22] Isolation of volatiles following complete **7** → **8** conversion with **5-Cl** or **6-Cl** and subsequent GC/MS and ^{1}H NMR spectroscopic

Table 3. Catalytic data for the intramolecular HA/cyclization of representative aminoalkyne substrates **7** and **9** mediated by the indicated actinide and group 4 complexes.

Entry	Substrate	Product[a]	Precatalyst[b]	N_t, h^{-1} (°C)[c]
1.			**1**, (CGC)Th(NMe$_2$)$_2$[d]	82 (25)
2.			**1-Cl**, [(CGC)Th(NR$_2$)Cl]$_2$	200 (25)
3.			**1-OAr**, (CGC)Th(NMe$_2$)OAr	37 (25)
4.			**2**, (CGC)U(NMe$_2$)$_2$[d]	3000 (25)
5.			**2-Cl**, (CGC)U(NR$_2$)Cl	280 (25)
6.	H$_2$N ⎯≡⎯SiMe$_3$	SiMe$_3$ (ring, N)	**2-OAr**, (CGC)U(NMe$_2$)OAr	52 (25)
7.			**4**, (Me$_2$SiCp''$_2$)UBn$_2$[d]	10 (60)
8.	**7**	**8**	**4-Cl**, (Me$_2$SiCp''$_2$)U(Bn)Cl	10 (60)
9.			**5**, Cp'$_2$ThR$_2$[d]	190 (60)
10.			**5-Cl**, Cp'$_2$Th(R)Cl[e]	1.2 (60)
11.			**6**, Cp'$_2$UR$_2$[d]	16 (60)
12.			**6-Cl**, Cp'$_2$U(R)Cl[e]	0.4 (60)
13.			**3**, (CGC)ZrMe$_2$	0.2 (60)
14.			**3-Cl**, (CGC)Zr(NMe$_2$)Cl	2.2 (25)
15.			**1**, (CGC)Th(NR$_2$)$_2$[d]	2.2 (25)
16.			**1-Cl**, [(CGC)Th(NR$_2$)Cl]$_2$	7.2 (25)
17.			**1-OAr**, (CGC)Th(NMe$_2$)OAr	0.5 (25)
18.	H$_2$N ⎯≡⎯Me	Me (ring, N)	**2**, (CGC)U(NR$_2$)$_2$[d]	170 (25)
19.			**2-Cl**, (CGC)U(NR$_2$)Cl	2.9 (25)
20.	**9**	**10**	**2-OAr**, (CGC)U(NMe$_2$)OAr	7.2 (25)
21.			**3**, (CGC)ZrMe$_2$	0.2 (60)
22.			**3-Cl**, (CGC)Zr(NMe$_2$)Cl	0.7 (60)

[a]Identified by ^{1}H NMR spectroscopy and GC/MS. [b]R = SiMe$_3$. [c]Determined in situ by ^{1}H NMR spectroscopy. [d]Ref. 11. [e]Isolated product from thermally-induced 1,3-sigmatropic shift, N-(trimethylsilyl)-2-exo-methylene-pyrrolidine (see ref. 21).
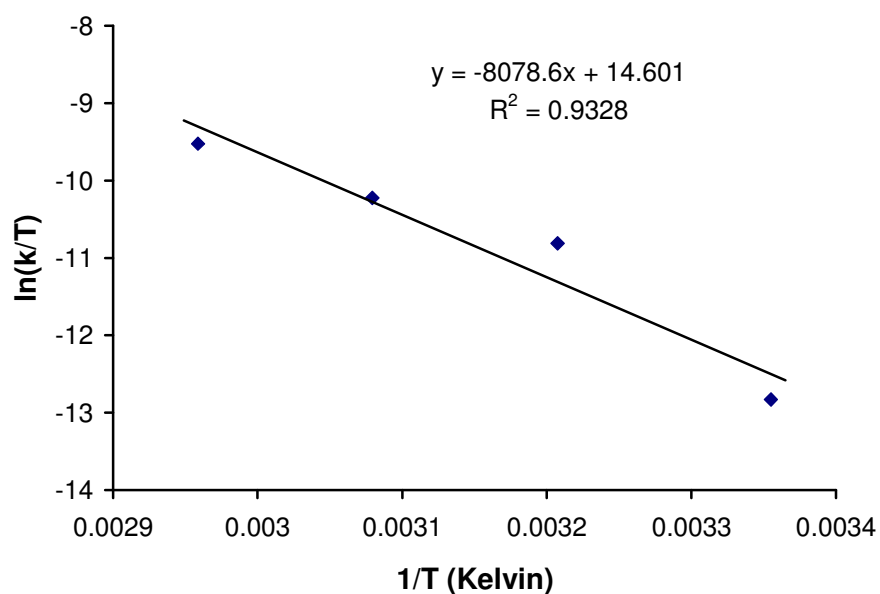
analyses provide no evidence for formation of free HCp′ (or its derivatives) during catalytic reactions.

Aminoalkyne transformation $9 \rightarrow 10$ is also mediated by the present complexes (Table 3). Again, complex **1-Cl** exhibits enhanced activity vs. **1** and **1-OAr** (N_t = 7.2 h^{-1} (**1-Cl**) vs. 2.2 h^{-1} (**1**) and 0.5 h^{-1} (**1-OAr**) at 25 °C; Table 2, entries 15-17). The (CGC)U‹-catalyzed intramolecular HA/cyclization of **9** is also efficient at 25 °C, with catalytic efficiencies **2** > **2-OAr** > **2-Cl** (N_t = 170 h^{-1} (**2**), 7.2 h^{-1} (**2-OAr**), 2.9 h^{-1} (**2-Cl**); Table 3, entries 18-20). Eyring and Arrhenius analyses[23] for $9 \rightarrow 10$ yield $\Delta H^{\ddagger}$ = 16(3) kcal/mol, $\Delta S^{\ddagger}$ = -18(9) eu, and E$_a$ = 17(3) kcal/mol when mediated by **2-Cl** from 24.9 °C to 64.8 °C with well-behaved kinetics (Figure 2). Furthermore, in situ determination of the solution magnetic moment of **2-Cl** by the Evans' method[24] in bezene-d_6 confirms that μ_{eff} for (CGC)U‹ complex **2-Cl** prior to activation with substrate **9** is identical to that of the major paramagnetic species present immediately following addition of **9**, as well as during and after complete conversion to **10** under typical HA conditions at 25 °C. Note that (CGC)MCl$_2$ complexes **1-Cl$_2$** (M = Th), **2-Cl$_2$** (M = U),[10] and **3-Cl$_2$** (M = Zr)[16] are *not* active catalysts for HA/cyclization $9 \rightarrow 10$ at 25 °C (M = Th, U) or 60 °C (M = Zr) in C$_6$D$_6$.
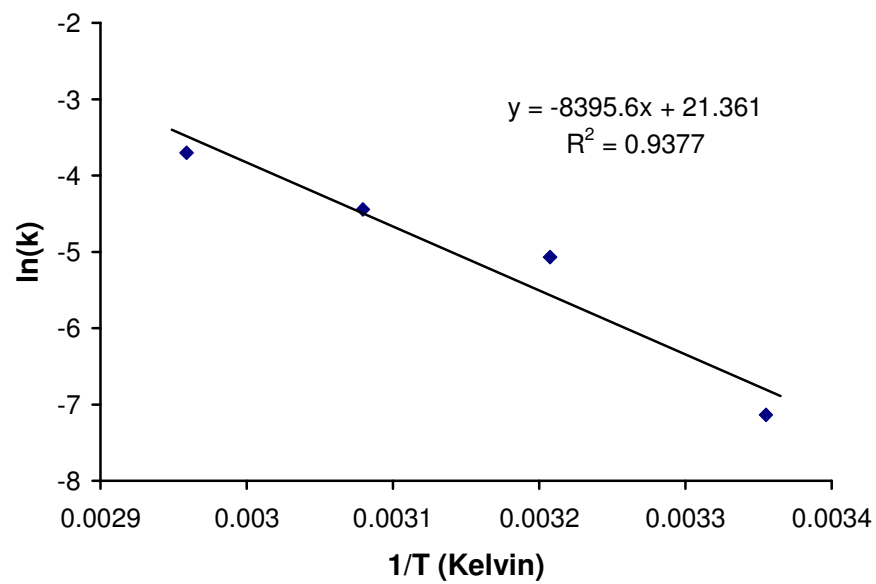
Intramolecular aminoalkyne HA/cyclizations $7 \rightarrow 8$ and $9 \rightarrow 10$ are efficient when catalyzed by (CGC)Zr‹ complexes **3** and **3-Cl**, although moderate heating is required to obtain activities comparable to the larger (CGC)An‹ complexes (Table 3). More reactive Me$_3$Si-substituted **7** is converted to exocyclic imine **8** with a markedly enhanced rate (ca. 100×) when mediated by **3-Cl** vs. **3** (N_t = 2.2 h^{-1} at 25 °C (**3-Cl**) vs. 0.2 h^{-1} at 60 °C (**3**); Table 3, entries 13,

Figure 2. (a) Eyring plot for conversion **9** → **10** catalyzed by (CGC)U[N(SiMe$_3$)$_2$]Cl (**2-Cl**) from 24.9 to 64.8 °C in C$_6$D$_6$ ($\Delta H^{\ddagger}$ = 16(3) kcal/mol, $\Delta S^{\ddagger}$ = -18(9) eu). (b) Arrhenius plot for conversion **9** → **10** catalyzed by **2-Cl** over a 40 °C range in C$_6$D$_6$ (E$_a$ = 17(3) kcal/mol). (c) Representative kinetic plot for conversion **9** → **10** catalyzed by **2-Cl** in C$_6$D$_6$ at 40 °C. (d) Representative kinetic plot for conversion **9** → **10** catalyzed by (CGC)U(NMe$_2$)OAr (**2-OAr**) at 25 °C in C$_6$D$_6$.

(a)

y = -8078.6x + 14.601
R^2 = 0.9328

(b)

$y = -8395.6x + 21.361$
$R^2 = 0.9377$

x-axis: **1/T (Kelvin)**
y-axis: **ln(k)**

(c)

$y = 2.6893x + 12.302$
$R^2 = 0.9972$

x-axis: **Time (min)**
y-axis: **% [10]/[U-Cl]**

(d)

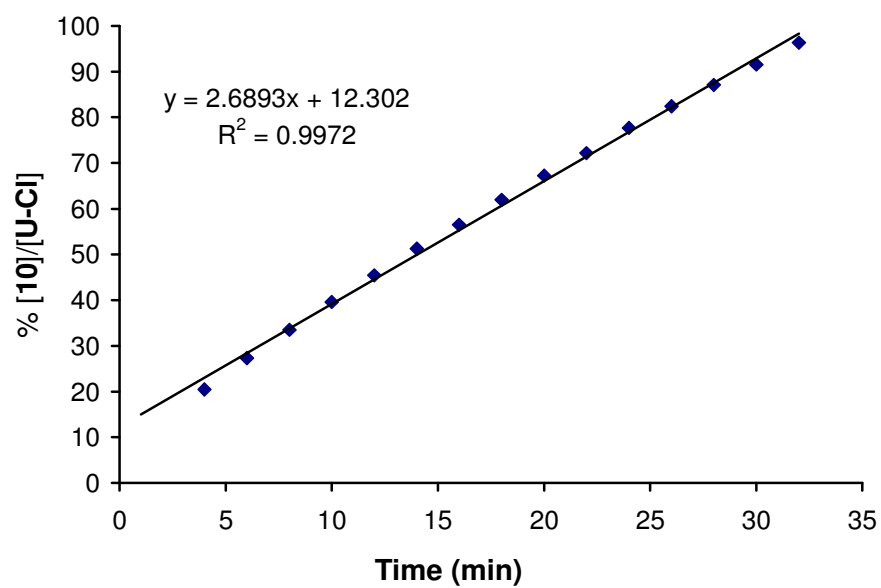$y = 0.2561x - 0.2169$

$R^2 = 0.9976$

Y-axis: % [10]/[U-OAr]

X-axis: Time (min)
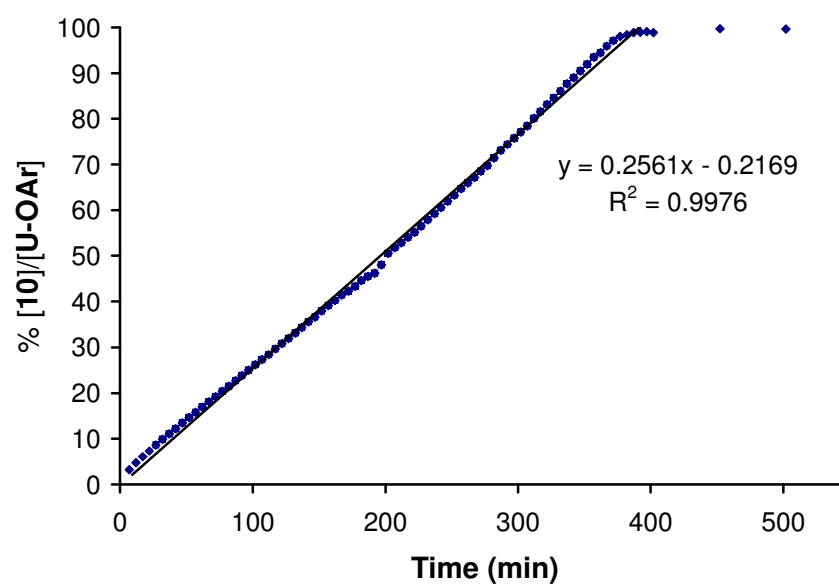
14). Catalytic conversion of Me-substituted aminoalkyne **9** proceeds with a similar although less pronounced **3-Cl** vs. **3** rate effect, i.e., a ca. 3× increase in activity is observed for **3-Cl** ($N_t = 0.7$ h^{-1} (**3-Cl**) vs. 0.2 h^{-1} (**3**) at 60 °C; Table 3, entries 21, 22). Eyring and Arrhenius analyses[23] for **7** → **8** mediated by **3-Cl** provide direct comparison to L$_2$An‹ and L$_2$Ln– catalysts, affording $\Delta H^{\ddagger} =$ 11(2) kcal/mol, $\Delta S^{\ddagger} = $ -35(7) eu, and E$_a$ = 12(2) kcal/mol from 24.8 °C to 67.3 °C displaying well-behaved kinetics (Figure 3).

Primary Aminoalkene Hydroamination. Intramolecular aminoalkene HA/cyclization of representative substrate **11** is effectively mediated by both "substituted" and unsubstituted bisamido complexes **1**-**3**. Comparison between Th complexes shows decreased activity for **1-Cl** vs. **1** at 25 °C (N_t = 3.3 h^{-1} (**1-Cl**) vs. 15 h^{-1} (**1**); Table 4, entries 1, 2), although dimeric **1-Cl** may remain intact and, therefore, sterically encumbered during catalysis. Precatalyst **1-Cl′**, generated by treatment of **1-Cl** with (non-cyclizable) neopentylamine at 25 °C in C$_6$D$_6$ for 24 h followed by removal of byproduct HN(SiMe$_3$)$_2$, exhibits identical N_t (vs. **1-Cl**) for cyclization **11** → **12** at 25 °C, suggesting that the structure of **1-Cl** in solution (monomer vs. dimer) does not change with a large amine excess. Aryloxide-substituted **1-OAr** and **2-OAr** exhibit diminished reactivity with moderate N_t at 60 °C (0.6 h^{-1} and 1.5 h^{-1}, respectively; Table 4, entries 3, 6). Interestingly, complex **2-Cl** promotes **11** → **12** cyclization with > 2× the catalytic efficiency of **2** at 25 °C (N_t = 6.2 h^{-1} vs. 2.5 h^{-1}; Table 4, entries 4, 5). This **2/2-Cl** trend maintains for **11**-d_2 → **12**-d_2, where deuterium KIE are significant at 25 °C, where k_H/k_D = 3.3(5) and 2.6(4), respectively (N_t = 0.8 h^{-1} (**2**) and 2.4 h^{-1} (**2-Cl**) at 25 °C). Likewise, organozirconium complex **3-Cl** exhibits greater

Figure 3. (a) Eyring plot for conversion **7** → **8** catalyzed by (CGC)Zr(NMe$_2$)Cl (**3-Cl**) from 24.8

°C to 67.3 °C in C$_6$D$_6$ ($\Delta H^{\ddagger}$ = 11(2) kcal/mol, $\Delta S^{\ddagger}$ = -35(7) eu). (b) Arrhenius plot for **7** → **8**

conversion catalyzed by **3-Cl** over 42 °C in C$_6$D$_6$ (E$_a$ = 12(2) kcal/mol). (c) Representative

kinetic plot for conversion **7** → **8** catalyzed by **3-Cl** in C$_6$D$_6$ at 25 °C.
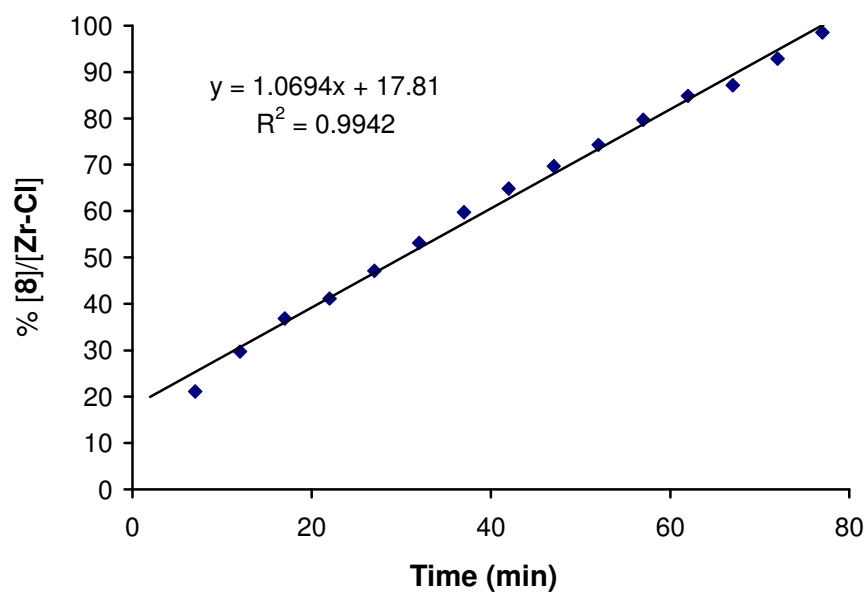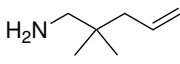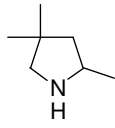
(a)
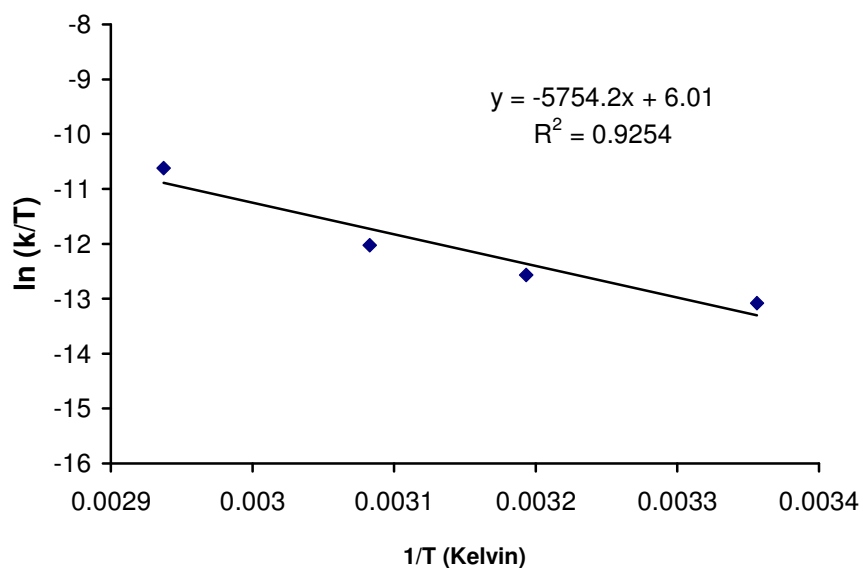
(b)
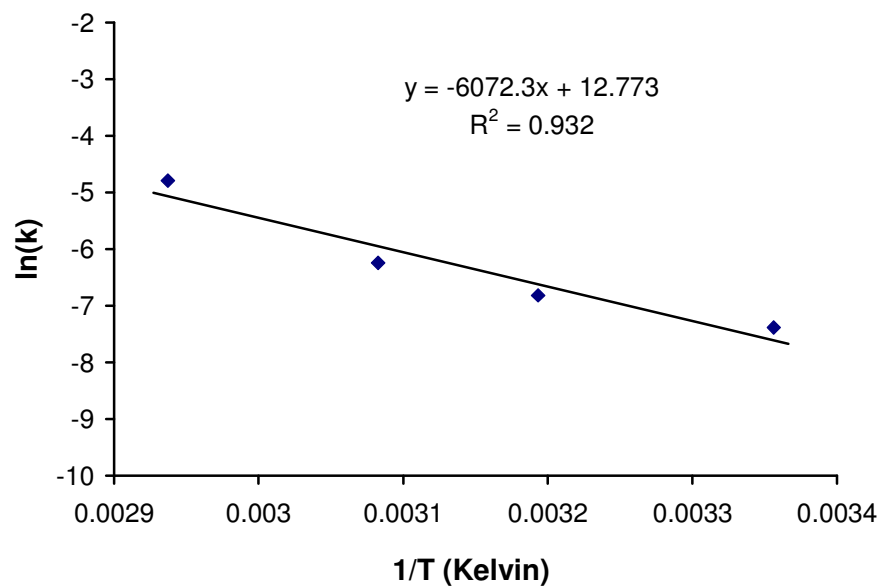
(c)

Table 4. Catalytic data for the intramolecular HA/cyclization **11** → **12** mediated by the indicated actinide and group 4 complexes.

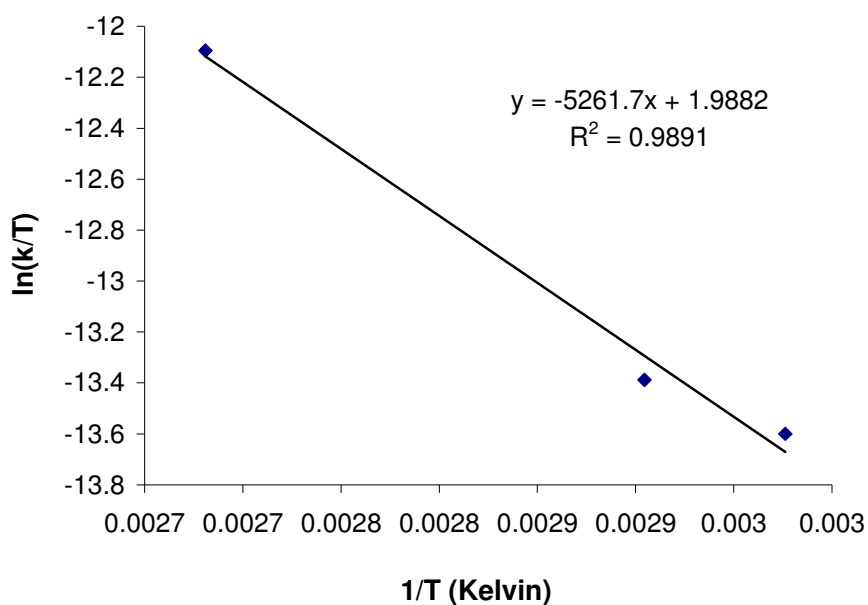| Entry	Substrate	Product[a]	Precatalyst[b]	N_t, h^{-1} (°C)[c]
1.			**1**, (CGC)Th(NMe$_2$)$_2$[d]	15 (25)
2.			**1**-**Cl**, [(CGC)Th(NR$_2$)Cl]$_2$	3.3 (25)
3.			**1-OAr**, (CGC)Th(NMe$_2$)OAr	0.6 (60)
4.	H$_2$N...**11**	...N-H ...**12**	**2**, (CGC)U(NMe$_2$)$_2$[d]	2.5 (25)
5.			**2-Cl**, (CGC)U(NR$_2$)Cl	6.2 (25)
6.			**2-OAr**, (CGC)U(NMe$_2$)OAr	1.5 (60)
7.			**3**, (CGC)ZrMe$_2$	0.07 (100)
8.			**3-Cl**, (CGC)Zr(NMe$_2$)Cl	0.14 (100)

[a]Identified by ^{1}H NMR spectroscopy and GC/MS. [b]R = SiMe$_3$. [c]Determined in situ by ^{1}H NMR spectroscopy. [d]Ref. 10.

catalytic activity than **3**, although rates are considerably more sluggish than for the Th analog (N_t = 0.14 h^{-1} (**3-Cl**) vs. 0.07 h^{-1} (**3**); Table 4, entries 7, 8). Although the (CGC)Zr‹ complexes exhibit sluggish cyclization rates and require elevated reaction temperatures, no reactions other than precatalyst protonolysis and CH$_4$/HNMe$_2$ evolution are observed by ^{1}H NMR spectroscopy below 100 °C. Furthermore, neither (CGC)Zr‹-mediated reaction evidences an induction period consistent with a disproportionation or equilibration phase preceding the catalytic cycle (vide infra). Eyring and Arrhenius analyses[23] for **11** → **12** yield $\Delta H^{\ddagger}$ = 10(3) kcal/mol, $\Delta S^{\ddagger}$ = -43(9) eu, and E$_a$ = 11(3) kcal/mol when mediated by **2-OAr** from 63 °C to 100 °C with well-behaved kinetics (Figure 4).
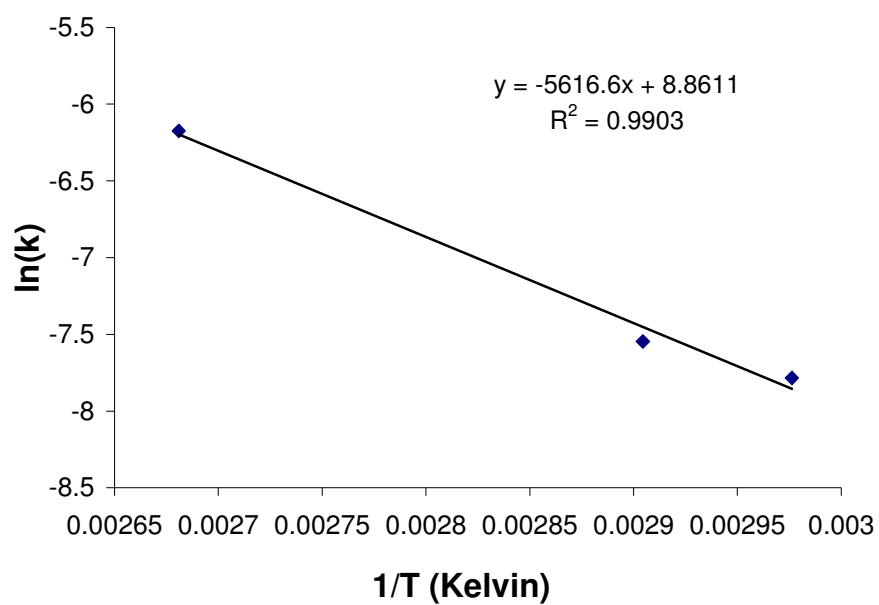
Secondary Aminoalkene and Aminoalkyne Hydroamination. Intramolecular aminoalkene and aminoalkyne HA/cyclization of representative secondary amines **13** and **15** is effectively mediated by unsubstituted and "substituted" complexes **1**-**3** and **1**-**3**, **5**-**6**, respectively. Chloride-substituted **3-Cl** mediates *N*-methylaminoalkene cyclization **13** → **14** significantly more rapidly than **3**, although considerably more sluggishly than do more reactive chloride-substituted organoactinide complexes (N_t = 0.1 h^{-1} (**1-Cl**) and 0.2 h^{-1} (**2-Cl**) at 60 °C vs. 0.1 h^{-1} (**3-Cl**) at 90 °C and 0.2 h^{-1} (**3**) at 120 °C; Table 5, entries 2, 5, 7-8). Cyclization **13** → **14** catalyzed by **1-OAr** or **2-OAr** proceeds more sluggishly, with comparable efficiencies observed at 120 °C (0.5 h^{-1}; Table 5, entries 3, 6). Mediated by **1** or **2** in the more polar 1:1 *ortho*-C$_6$H$_4$F$_2$:C$_6$D$_6$ solvent mixture, this transformation proceeds with considerably diminished catalytic efficiency (> 10× for **2**), although catalyst decomposition via F$^-$ abstraction may occur for **1** (An = Th).[25] Note that

Figure 4. (a) Eyring plot for conversion **11** → **12** catalyzed by (CGC)U(NMe$_2$)OAr (**2-OAr**) from 63 to 100 °C in C$_6$D$_6$ ($\Delta H^{\ddagger}$ = 10(3) kcal/mol, $\Delta S^{\ddagger}$ = -43(9) eu). (b) Arrhenius plot for conversion **11** → **12** catalyzed by **2-OAr** over a 40 °C range in C$_6$D$_6$ (E$_a$ = 11(3) kcal/mol). (c) Eyring plot for conversion **13** → **14** catalyzed by (CGC)Th(NMe$_2$)$_2$ (**1**) from 60 to 110 °C in C$_6$D$_6$ ($\Delta H^{\ddagger}$ = 9(3) kcal/mol, $\Delta S^{\ddagger}$ = -48(6) eu). (d) Arrhenius plot for conversion **13** → **14** catalyzed by **1** over a 50 °C range in C$_6$D$_6$ (E$_a$ = 10(3) kcal/mol).
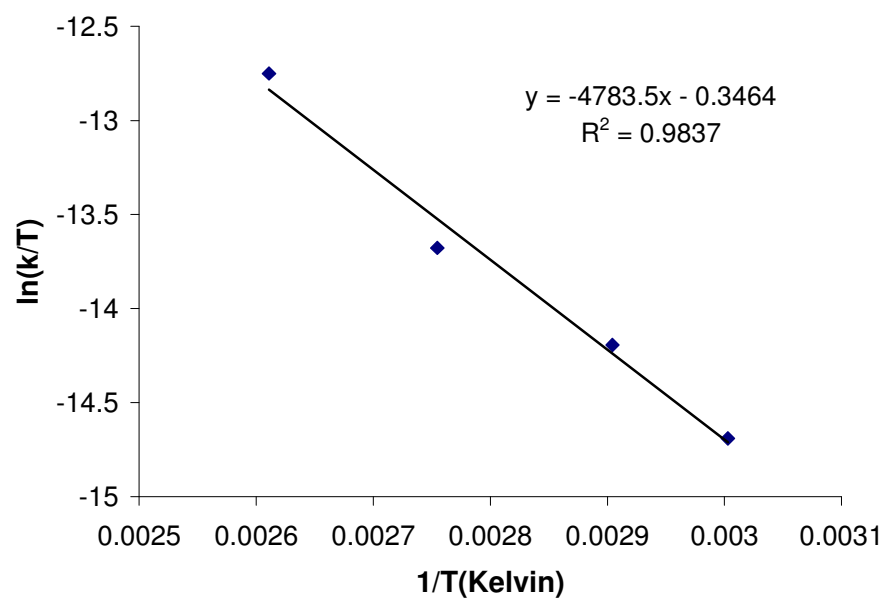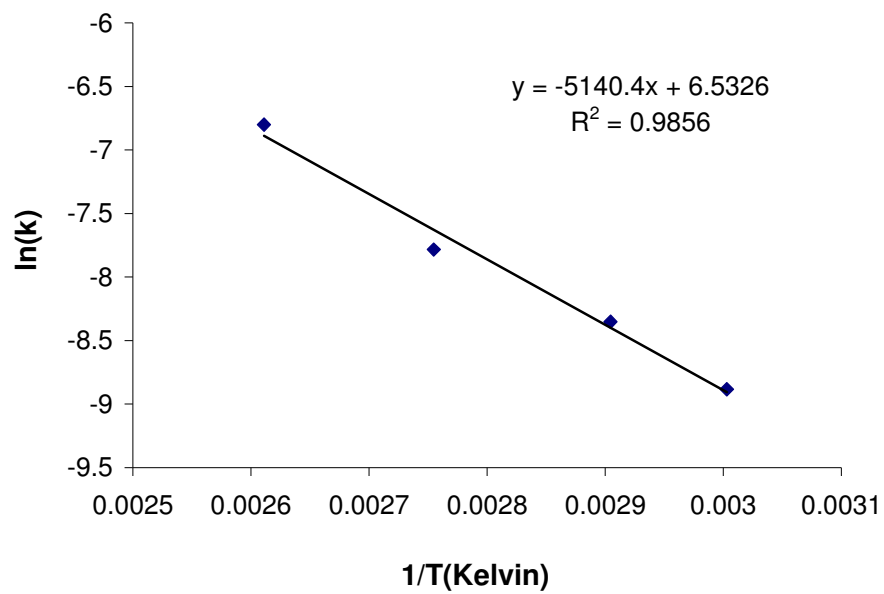
(a)

(b)

$y = -5616.6x + 8.8611$

$R^2 = 0.9903$

(c)

$y = -4783.5x - 0.3464$

$R^2 = 0.9837$

(d)

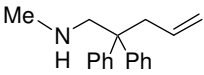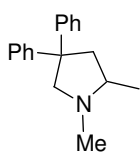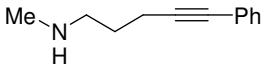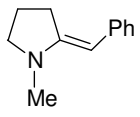$y = -5140.4x + 6.5326$

$R^2 = 0.9856$

ln(k) vs 1/T(Kelvin)

Table 5. Catalytic data for the intramolecular HA/cyclization of representative secondary aminoalkene **13** and secondary aminoalkyne **15** mediated by the indicated actinide and group 4 complexes.

Entry	Substrate	Product[a]	Precatalyst[b]	N_t, h^{-1} (°C)[c]
1.			**1**, (CGC)Th(NMe$_2$)$_2$[d]	0.5 (60)
2.			**1-Cl**, [(CGC)Th(NR$_2$)Cl]$_2$	0.1 (60)
3.			**1-OAr,** (CGC)Th(NMe$_2$)OAr	0.5 (120)
4.			**2**, (CGC)U(NMe$_2$)$_2$[d]	0.9 (60)
5.			**2-Cl,** (CGC)U(NR$_2$)Cl	0.2 (60)
6.			**2-OAr,** (CGC)U(NMe$_2$)OAr	0.5 (120)
7.			**3**, (CGC)ZrMe$_2$	0.2 (120)
8.			**3-Cl**, (CGC)Zr(NMe$_2$)Cl	0.4 (90)
9.			**1,** (CGC)Th(NMe$_2$)$_2$[d]	80 (25)
10.			**1-Cl,** [(CGC)Th(NR$_2$)Cl]$_2$	24 (60)
11.			**2,** (CGC)U(NMe$_2$)$_2$[d]	120 (25)
12.			**2-Cl**, (CGC)U(NR$_2$)Cl	33 (25)
13.			**3**, (CGC)ZrMe$_2$	0.3 (90)
14.			**3-Cl**, (CGC)Zr(NMe$_2$)Cl	0.02 (90)
15.			**5**, Cp'$_2$Th[CH$_2$(SiMe$_3$)]$_2$	7.4 (60)
16.			**6**, Cp'$_2$U[CH$_2$(SiMe$_3$)]$_2$	15 (60)

Substrate **13**, Product **14**; Substrate **15**, Product **16**.

[a]Identified by ^{1}H NMR spectroscopy and GC/MS. [b]R = SiMe$_3$. [c]Determined in situ by ^{1}H NMR spectroscopy. [d]Ref. 10b.

N_t values for **13** → **14** differ little between the **1**- and **2**-catalyzed processes and those catalyzed by the corresponding monochloro derivatives (Table 5, entries 1-2, 4-5). Eyring and Arrhenius analyses[23] for **13** → **14** yield $\Delta H^{\ddagger}$ = 9(3) kcal/mol, $\Delta S^{\ddagger}$ = -48(6) eu, and E_a = 10(3) kcal/mol when mediated by **1** from 60 °C to 110 °C with well-behaved kinetics (Figure 4).

N-methylaminoalkyne **15** is also converted to exocyclic pyrrolidine **16** by (CGC)An‹, (CGC)Zr‹, and Cp′$_2$An‹ complexes, although with considerably less efficiency when promoted by **3** (N_t = 80 h^{-1} (**1**) and 120 h^{-1} (**2**) at 25 °C, vs. N_t = 0.3 h^{-1} (**3**) at 90 °C; Table 5, entries 9, 11, 13). Metallocenes **5** and **6** are also effective precatalysts for this cyclization, with intermediate efficiency far less than **1** or **2** but considerably greater than **3** (N_t = 7.4 h^{-1} (**5**) and 15 h^{-1} (**6**) at 90 °C; Table 5, entries 15-16). Monoamidochloride complexes **1-3** also mediate **15** → **16** conversion effectively, though with marked reduction in efficiency (N_t = 24 h^{-1} (**1-Cl**) and 33 h^{-1} (**2-Cl**) at 60 °C, and 0.02 h^{-1} at 90 °C (**3-Cl**); Table 5, entries 10, 12, 14).

Discussion

In this section, the synthesis, structural characterization, and hydroamination/cyclization catalytic characteristics of bisamido and substituted, monoamido complexes **1-6** are discussed. Implications of these findings are presented in the context of plausible mechanistic pathways for actinide- vs. group 4-mediated intramolecular aminoalkene and aminoalkyne HA/cyclizations.

Synthesis and Characterization of Monosubstituted (CGC)M(NR$_2$)X Complexes.

Mono-substituted chloride and aryloxide complexes **1**-**3** are obtained in excellent yield and purity in a single step from known reagents (Scheme 4). Neutral, monomeric tris(amido)actinide chlorides, An[N(SiMe$_3$)$_2$]$_3$Cl,[14] are obtained quantitatively in toluene without competing formation of tris(amido)actinide hydrides[14a-b] or of potentially inhibitory, charged/solvated byproducts. Treatment in situ with H$_2$CGC cleanly affords chloroamido complexes **1-Cl** and **2-Cl** in up to 85% isolated yield. Note that the enhanced Lewis acidity of An[N(SiMe$_3$)$_2$]$_3$Cl vs. homoleptic Ln[N(SiMe$_3$)$_2$]$_3$ complexes (used in the synthesis of closely related (CGC)Ln–N(SiMe$_3$)$_2$ complexes; eq. 3)[3k] leads to significant rate enhancements in **1-Cl** and **2-Cl** generation, requiring markedly lower reaction temperatures and proceeding without periodic removal of evolved HN(SiMe$_3$)$_2$ (Scheme 4). ^{1}H NMR spectra of **1-Cl** and **2-Cl**
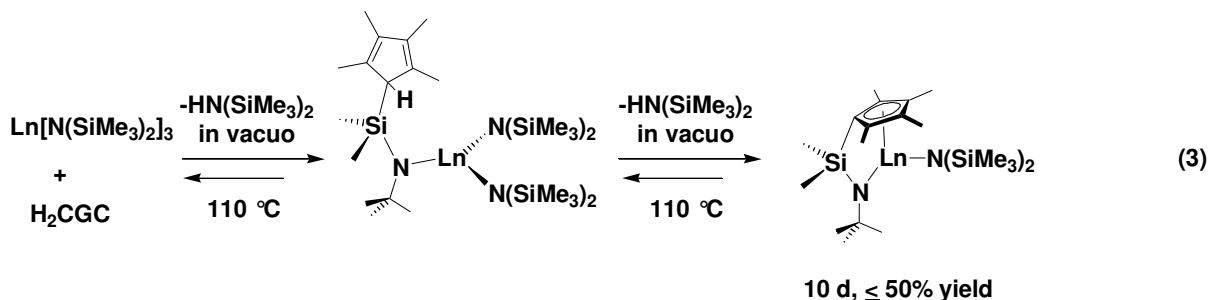
recorded in non-coordinating solvents at 20-80 °C are consistent with C_1 symmetry in solution, and evidence no detectable ligand redistribution or dynamic equilibria on the NMR timescale. Furthermore, the known insolubility of (CGC)AnCl$_2$ complexes in low-polarity solvents[10] and absence of **1-Cl/2-Cl**-derived precipitates over several days in C$_6$D$_6$ suggests that the bulky –N(SiMe$_3$)$_2$ moiety affords sufficient kinetic stabilization to prevent halide/amide redistribution.

Scheme 4. Syntheses of constrained geometry organoactinide and organozirconium complexes **1-Cl, 2-Cl, 3-Cl**, **1-OAr**, and **2-OAr**.
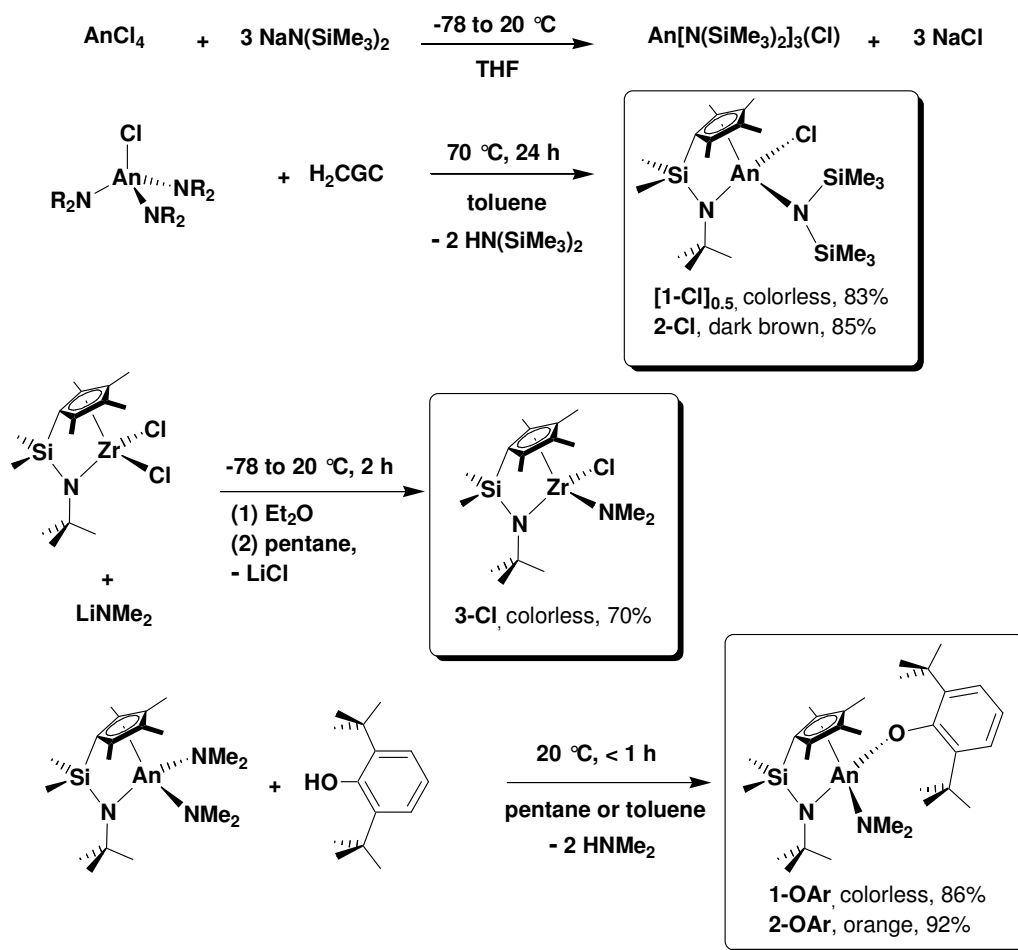
Interestingly, subtle An^{4+} ionic radius differences (9-coordinate: Th^{4+} 1.09 Å vs. U^{4+} 1.05 Å)[26] apparently result in Th complex **1-Cl** crystallizing as a C_2-symmetric bis(μ-chloro) dimer (Figure 1a). Single crystals of **1-Cl** (Table 1) contain planar, diamond-shaped $Th_2(\mu\text{-Cl})_2$ cores with Th–Cl–Th′ and Cl–Th–Cl′ angles of 113.66(5)° and 66.34(5)°, respectively, and a large Th····Th distance of 4.89(1) Å. The Cp(centroid)–Th–N(^{t}Bu) angle of 91.7° compares well with that in **1** (91.3°)[10] and **1-OAr** (90.4°; vide infra), indicating significant steric openness (Chart 2).[11,17,27] The 2.334(5) Å Th–N(SiMe_3)_2 bond distance in **1-Cl** is considerably longer than the 2.27(1) Å and 2.252(6) Å Th–NMe_2 distances in **1** (average) and **1-OAr**, respectively, but statistically comparable (< 3σ) to Th–N(^{t}Bu) distances in **1-Cl** (2.335(5) Å), **1** (2.315(4) Å), and **1-OAr** (2.293(6) Å), reflecting the electron-withdrawing capacity of the –SiMe_3 groups.[28] Bridging Th–Cl distances of 2.883(2) Å and 2.964(2) Å in **1-Cl** are quite similar to those of 2.874(2) Å and 2.933(2) Å in $[(CGC)Th(\mu\text{-Cl})_2(Cl)Li(OEt_2)_2]_2$.[26a] The similar U^{4+} dimer $[(N[CH_2CH_2N(SiMe_3)]_3)U(\mu\text{-Cl})]_2$ also displays a planar $U_2(\mu\text{-Cl})_2$ diamond core with U–Cl–U′ and Cl–U–Cl′ angles of 104.51(9)° and 75.49(8)°, respectively (Chart 2).[26c] Monomeric $(N[CH_2CH_2N(SiMe_3)]_3)UCl$ possesses a terminal U–Cl distance of 2.641(5) Å, roughly 10% shorter than in the corresponding dimer.[26b] The solid-state structures (Table 1) of monomeric **2-Cl** (Figure 1b) and **3-Cl** (Figure 1c) also display steric openness nearly identical to unsubstituted analogs **2** and **3**. Cp(centroid)–M–N(^{t}Bu) angles of 91.7° (**1-Cl**), 93.1° (**2-Cl**), and 101.1° (**3-Cl**) correlate with metal ionic radius,[26] evidencing greater coordinative unsaturation with increasing ion size. Also, note the comparatively short Th····C(20) distance of 3.18(1) Å in **1-Cl** vs. U····C(20) of 3.53(1) Å in **2-Cl**, suggesting agostic Si–C(α) bond stabilization in the larger Th

Chart 2

θ = 91.3°
1

θ = 93.3°
2

θ = 100.2°
3
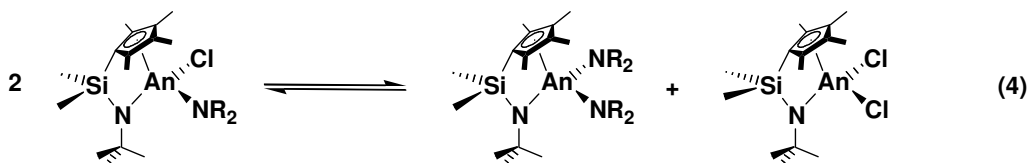
θ = 91.7°
1-Cl

θ = 93.1°
2-Cl

θ = 101.1°
3-Cl
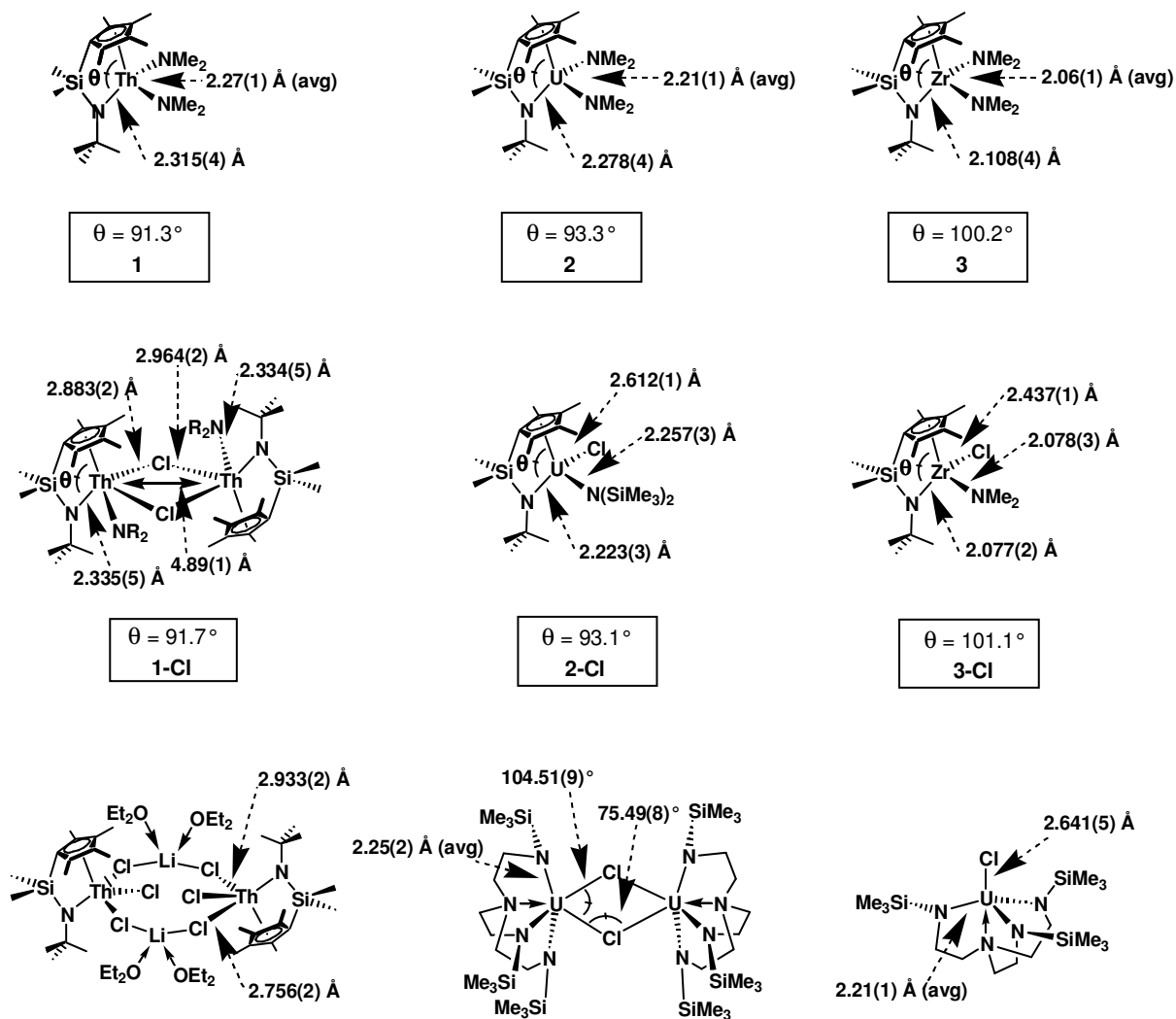
complex. [3k,29,30]
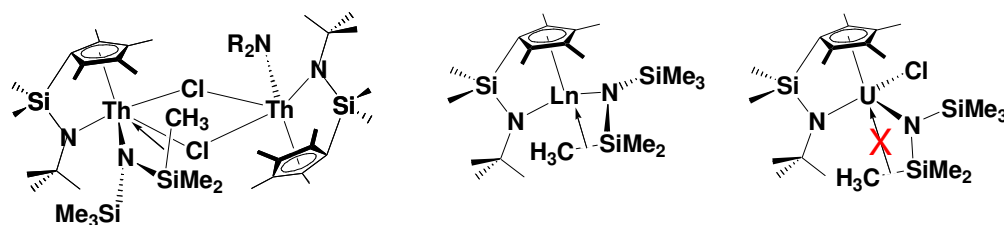
Redistribution processes analogous to eq. 4 are known to occur, especially in complexes with larger actinide ions in open ligation environments and in the absence of coordinating Lewis

(4)

bases. [28,31] To probe the importance of complicating (CGC)M(NR$_2$)Cl redistribution processes during catalytic reactions, aryloxide-substituted precatalysts **1-OAr** and **2-OAr** were generated via protodeamination of **1** and **2** with ArOH (2,6-di-^{t}Bu-phenol; Scheme 4). The disparity in An^{4+} ionic radii/covalency is evident where organouranium complex **2-OAr** does not undergo reaction with excess phenol up to 90 °C, whereas organothorium complex **1-OAr** rapidly forms (CGC)Th(OAr)$_2$ at 25 °C. In situ-generated precatalysts **1-OAr** and **2-OAr** exhibit near-identical catalytic properties vs. isolated precatalysts, and neither byproduct (CGC)Th(OAr)$_2$ nor unreacted ArOH significantly affect measured HA/cyclization N_t values, allowing convenient precatalyst generation. In the solid-state, **1-OAr** is monomeric and crystallizes in space group P2$_1$/c, displaying a pseudotetrahedral coordination geometry (Figure 1d). The near-linear 166.5(2)° Th–O–C$_{ipso}$ angle and Th–O distance of 2.258(5) Å in **1-OAr** are characteristic of the large –O-2,6-^{t}Bu$_2$C$_6$H$_3$ moiety (Chart 3). [32] Cp′An(OAr)$_n$R$_{3-n}$ complexes display An–O–C$_{ipso}$

Chart 3

2.258(5) Å

171.4(5) °

153.5(10) °

2.293(6) Å

166.5(2) °

2.14(1) Å avg

2.189(6) Å

θ = 90.4 °
1-OAr

123.5 °

2.53(1) Å

158.6(8) °

154.0(6) °

171.4(5) °

2.29(1) Å (avg)

2.135(4) Å

Chart 4

X = Cl, OAr
R = Me, SiMe$_3$
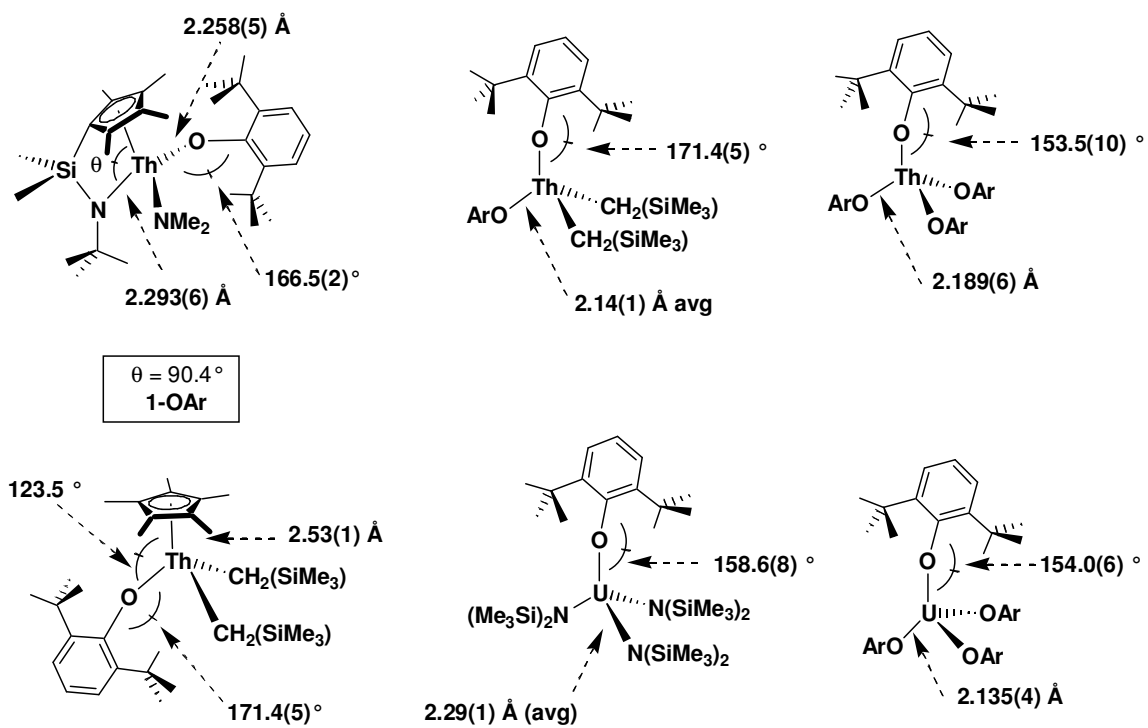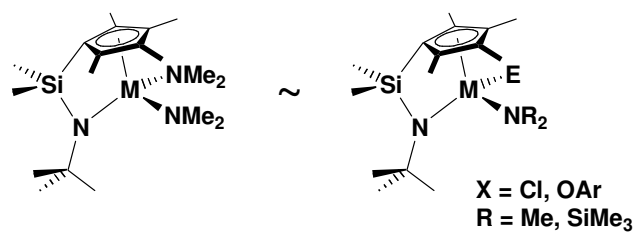
CGC Cp''(cent)-M-N1 angle	
Th^{4+}	91.3°
U^{4+}	93.3°
Sm^{3+}	95.3°
Zr^{4+}	100.2°
Lu^{3+}	100.9°
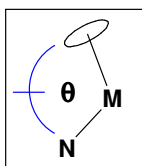
CGC Cp''(cent)-M(X)-N1 angle	
Th^{4+} (X = Cl; R = SiMe$_3$)	91.7°
Th^{4+} (X = OAr; R = Me)	90.4°
U^{4+} (X = Cl; R = SiMe$_3$)	93.1°
Zr^{4+} (X = Cl; R = Me)	101.1°

angles in the range 153.5(10)-171.4(5)°, along with An–O distances ranging from 2.14(1)-2.189(6) Å (Th^{4+})[30] and 2.135(4)-2.29(1) Å (U^{4+}).[30c] Again, the coordinative unsaturation imparted by the CGC ancillary ligation (Cp(centroid)–Th–N(^{t}Bu) = 90.4°) reflects the steric and electronic factors that promote unique catalytic properties in (CGC)M$^{3+/4+}$ complexes (Charts 3, 4).[3k,10,17, 33]

Related complexes **5-Cl** and **6-Cl** can be generated via traditional salt metathesis or an alternative redistributive synthesis (eq. 5).[16] The equilibrium lies ≥ 95% to the right for R =

$$\tag{5}$$
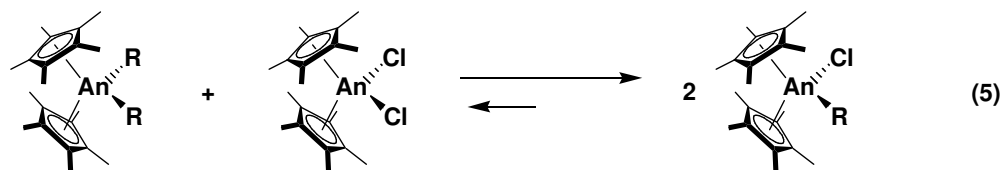
CH$_3$,[9b,16] although the present bulkier R = CH$_2$SiMe$_3$ substituents undergo such conproportionations more sluggishly. The reverse disproportionation is therefore expected to be of minor significance and is not detected by ^{1}H NMR spectroscopy of either **5-Cl** or **6-Cl** over several days at 25 °C or while heating at 90 °C for >36 h. Moreover, addition of ca. 10-100 equiv. of Lewis basic amine substrate likely forms a species such as **D** (eq. 6; as in Cp′$_2$Ln–catalysts),[1d;3a,v] suggesting further steric impediment to Cp′$_2$An[N(H)R]Cl redistribution.

$$\tag{6}$$

D
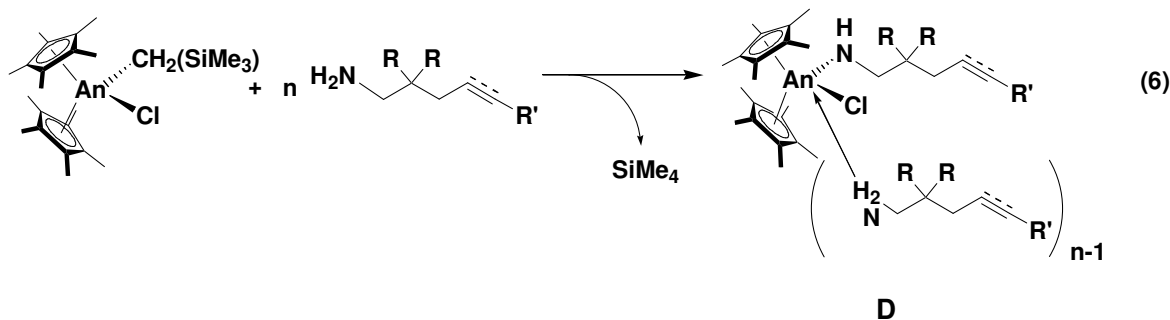
Monomeric imidoactinide complexes are typically stabilized by sterically screening ancillary ligation, e.g., $Cp'_2An‹$ as opposed to *ansa* scaffolds $Me_2SiCp''_2An‹$ and $(CGC)An‹$, with more open structures leading to dimeric/oligomeric species.[28,34] Imidoactinide complexes are generally formed under forcing conditions conducive to α-elimination (e.g., eq. 7) or under milder conditions employing reagents inducing oxidation to U^{6+}, stabilizing more open coordination environments (e.g., eq. 8). Computational studies implicate 6d and 5f orbital involvement in An=NR π–bonding with considerable positive charge at An (and negative charge buildup at =NR).[35] Moreover, $L_2An=NR$ complexes revert to bis(amido)actinide complexes in the presence of excess protic amines (e.g., $(^tBu_3Cp)_2An‹$ in eq. 9).[34a] Note that these synthetic routes appear generally inconsistent with the present catalytic reaction rates (25 °C, C_6D_6) and observed rate laws for aminoalkene and aminoalkyne HA/cyclizations (vide infra).

(7)

(8)

(9)
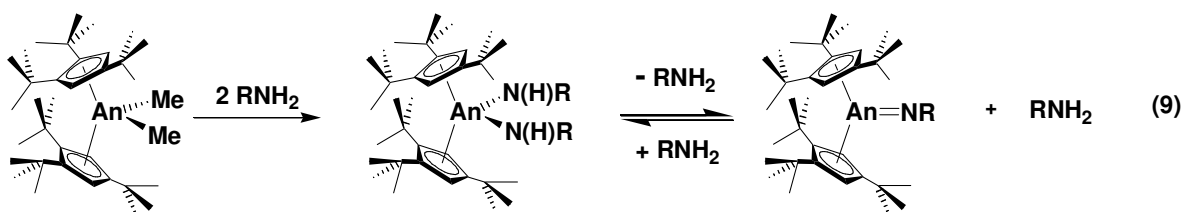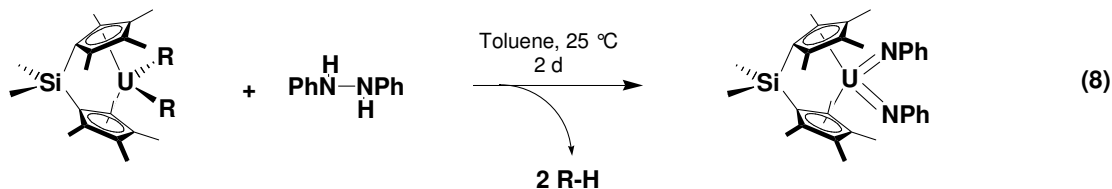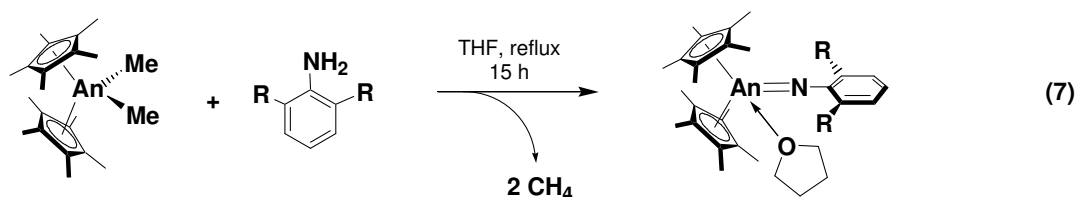
Catalytic Intramolecular Hydroamination/Cyclization and Mechanistic Considerations.

In this section, the key features of the two most plausible mechanistic scenarios, i.e., C=C/C≡C insertion into an M–N(H)R linkage (Scheme 1) vs. formation of a reactive M=NR intermediate (Scheme 2), followed by C=C/C≡C cycloaddition, are considered, followed by discussion of the data concerning intramolecular aminoalkyne and aminoalkene HA/cyclization pathways for representative primary and secondary amines mediated by (CGC)An‹ and (CGC)Zr‹ complexes. Effects of metal ionic radius as well as σ and π ancillary ligation are discussed along with kinetic parameters for C=C and C≡C unsaturations. L_2An‹ catalysts are discussed first, followed by extension to (CGC)Zr‹ catalysts. We begin with a summary of relevant mechanistic observations.

Summary of Mechanistically-Relevant Results.   Following is a summary of prominent features observed in HA/cyclization kinetics and reactivity studies carried out with $L_2M(NR_2)X$ catalysts **1**-**6**.

   (i)   Substituted $(CGC)M(NR_2)X$-derived catalysts are often more active than their traditional $(CGC)MR_2$ counterparts (Tables 3-5).

   (ii)   Complete precatalyst activation by primary amine substrates occurs within seconds at -78 °C in toluene-d_8 solutions, and bulkier secondary amine substrates are rapidly activated under HA/cyclization catalysis conditions. Induction periods are not observed with L_2MR_2 or $L_2M(R)X$ precatalysts (M = Zr, Th, U).

(iii) The observed rate law $\nu \sim [L_2M\iota]^1[\text{amine}]^0$ is the same for organo-4f- and (CGC)An‹-catalyzed HA/cyclizations (vide infra). Competitive binding/product inhibition of catalytic turnover is observed under high [product] conditions (Figures 2c-d, 3c).

(iv) Ionic radius/metal accessibility trends for aminoalkyne and aminoalkene HA/cyclization are conserved relative to known L_2Ln– and L_2An‹-catalyzed reactions (Tables 3-5).

(v) Both primary and secondary amine substrates are efficiently cyclized under mild reaction conditions (Tables 3-5). Secondary aminoalkene HA/cyclization rates are *not* accelerated in more polar solvent media.

(vi) Solution phase magnetic moments of major (diamagnetic or paramagnetic) catalyst species do not change upon precatalyst activation or during/after catalytic runs.

(vii) Activation parameters measured for (CGC)M‹-catalyzed aminoalkyne and aminoalkene HA/cyclization are very similar for both $(CGC)MR_2$ and $(CGC)M(NR_2)X$ catalysts (M = Th, U, Zr). Moderate $\Delta H^{\ddagger}$ and large negative $\Delta S^{\ddagger}$ values are characteristic of all L_2Ln– and (CGC)An‹-catalyzed HA/cyclizations (vide infra; Table 7, Figures 2, 3).

Mechanistic Considerations.   As noted above, the two most plausible scenarios for intramolecular aminoalkene and aminoalkyne HA/cyclization are presented in Schemes 1 and 2 (Table 6). In the former, trivalent organolanthanides proceed through highly polar, highly organized insertive four-center transition states (**A**). These reactions are characterized by

Table 6. Mechanistic characteristics of hydroamination pathways.

	M-N(R')R (Schemes 1,3)	M=NR (Scheme 2)
Rate law	$\nu \sim [M]^1[N\text{-}H]^{0\ a}$	$\nu \sim [M]^1[N\text{-}H]^{-1}[\text{alkyne}]^{1\ b}$
Induction period?	No	Yes
High [substrate]	No effect	Rate decrease
Low [substrate]	No effect	Rate increase
High [product]	Rate decrease^c	~No effect ^{c}
$\Delta H^{\ddagger}$	~ 10 kcal/mol	~ 12 kcal/mol ^{d}
$\Delta S^{\ddagger}$	~ -30 eu	~ -45 eu ^{d}
C-C substitution dependence?	Yes	Yes (M = Zr); No (M = An)
2° Amine substrates?	Yes	No

^{a} For hydroamination/cyclization. ^{b} The rate law $\nu \sim [M]^1[N\text{-}H]^0[\text{alkyne}]^0$ is predicted for scenario depicted in eq. 10b. Cp'$_2$An<-catalyzed *intermolecular* HA: $\nu \sim [M]^1[N\text{-}H]^{-1}[\text{alkyne}]^0$. ^{c} Bulky products unable to induce competitive binding/inhibition. ^{d} Measured for Cp'$_2$AnMe$_2$-catalyzed *intermolecular* alkyne HA.

moderate $\Delta H^{\ddagger}$ (ca. 12 kcal/mol) and large negative $\Delta S^{\ddagger}$ (ca. -30 eu) values, with their scope including primary and secondary amine substrates.[1d;3o,v] Although [amine] and [C–C] cannot be independently varied in *intramolecular* HA/cyclization kinetic studies, addition of non-cyclizable competing Lewis bases (e.g., THF or *n*-propylamine) to intramolecular reactions yield the rate law $\nu \sim [L_2Ln–]^1[base]^{-1}$ for large [base]:[substrate], consistent with competitive inhibition of C=C/C≡C insertion.[1d,3,4] From similar arguments, an analogous pathway was proposed for L_2Ln^{3+}-mediated *intermolecular* HA of alkenes, alkynes, and dienes, with the observed rate law $\nu \sim [catalyst]^1[alkyne]^1[amine]^0$, consistent with turnover-limiting C–C insertion into an Ln–N bond, independent of amine exchange.[1d,3f] Note that zero-order [amine] dependence is expected for $L_2Ln–$ catalysts incapable of forming charge-neutral $L_2Ln=NR$ species and is consistent with immediate catalyst activation/initiation of turnover by substrate and secondary amine reactivity. Also, the marked N_t dependence on ring size, substrate tether (α-alkyl and *gem*-dialkyl substitutions; Thorpe-Ingold effect),[36] and C–C substituent electronic effects (vs. steric bulk) for alkene, alkyne, allene, and diene unsaturations argue strongly against turnover-limiting heterocycle protonolysis *after* C–C insertion into M–N (i.e., $k_{protonolysis} > k_{insertion}$ appears operative here).[3a,x;5]

The *intermolecular* HA pathway of Scheme 2 proceeds via $L_2M=NR$ intermediate **B** that undergoes [2 + 2] cycloaddition with disubstituted (reversible)[8] or terminal (irreversible)[9] alkynes. This process typically displays a brief induction period and rate law consistent with rapid pre-equilibrium loss of RNH_2. $Cp_2Zr\!<$-catalyzed reactions require bulky amines able to stabilize the $Cp_2Zr=NR$ intermediate, although excessive alkyne steric bulk is unnecessary (eq.

10a). Cp′$_2$An‹-mediated *intermolecular* alkyne HA,[9] complicated by concomitant alkyne oligomerization processes, behaves somewhat differently, exhibiting a rate law $\nu \sim$ [Cp′$_2$An‹]^1[amine]$^{-1}$[alkyne]^0. In each case, the nature of the amine substituents dictates rate and regioselectivity. Note that, although Cp′$_2$An‹ catalysts are active with less bulky aliphatic amines, secondary amine HA does not proceed with either Cp$_2$Zr‹ or Cp′$_2$An‹ catalysts. Interestingly, however, cationic (Et$_2$N)$_3$U$^+$BPh$_4^-$ mediates the catalytic addition of secondary Et$_2$NH to alkynes.[9a] Although contradicted by synthetic L$_2$An=NR chemistry for sterically open ligands,[31] an alternative scenario where an M=NR species forms *irreversibly*, followed by rapid C≡C addition is conceivable (eq. 10b).[37] Key features and mechanistic implications that would
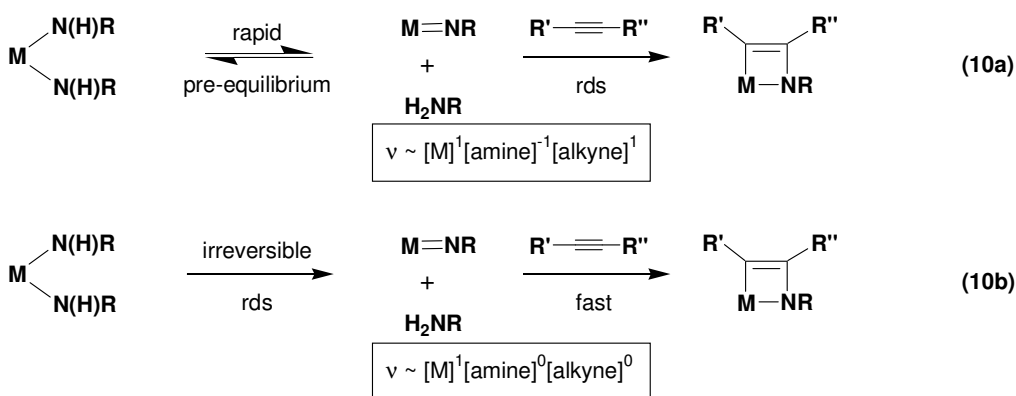
distinguish σ-bonded M–N(H)R vs. π-bonded M=NR L$_2$M‹ -catalyzed HA pathways based on mechanistic observations on L$_2$Ln– and Cp$_2$Zr‹ and L$_2$An‹ catalysts are summarized in Table 6. Beyond observed rate laws, the most strikingly different mechanistic characteristics concern the presence of an induction period -- during which catalyst generation occurs (eq. 10a) -- and an intrinsic inability to turn over secondary amines (vide infra) via an M=NR pathway. This scenario also exhibits a rate *increase* at low [amine] and rate *decrease* at high [amine], owing to

inhibition of M=NR formation during the rapid pre-equilibrium (eq. 10a). While an M–N(H)R pathway mediates secondary N–H bond addition to C–C unsaturations, competitive binding/product inhibition can lead to a moderate rate depression at high [product].

Ligand and Metal Effects. Intramolecular aminoalkyne HA/cyclization mediated by unsubstituted organoactinide complexes **1**, **2**, and **4**-**6** is broad in scope, with activity and selectivity dependent on An^{4+} ionic radius and ancillary ligation.[10] For less open $Me_2SiCp''_2An‹$ and $Cp'_2An‹$ complexes, primary N–H bond addition to terminal and disubstituted aminoalkyne substrates is generally more rapid for Th than for U complexes. The rate disparity is greatest for hindered metallocene $Cp'_2An‹$ frameworks and least for more coordinatively unsaturated $Me_2SiCp''_2An‹$ frameworks. Similar rate dependences on ancillary ligation are observed for Ln^{3+} catalysts, where *smaller* Ln^{3+} ions and less accessible metal centers yield more active catalysts. In contrast to organo-4f catalysts, trends for (CGC)An‹ complexes **1** and **2** typify the enhanced aminoalkyne catalytic activity imparted by CGC ancillary ligation,[33] with far greater catalytic efficiency for (CGC)An‹ vs. *less* open $L_2An‹$ complexes. Here the smaller U^{4+} ion in **2** achieves the most impressive N_t values, typically 10-100× greater than for organothorium complex **1**, retaining the ionic radius dependence observed with 4f catalysts and suggesting an intricate balance between coordinative unsaturation, metal ionic radius, bond covalency, and ligand/substrate electronic demands in organoactinide-mediated aminoalkyne HA/cyclization.[10]

In the present study, (CGC)M(NR$_2$)X-derived complexes (X = Cl, aryloxide) were investigated because the corresponding imido complexes (**E**) should not be readily accessible. It
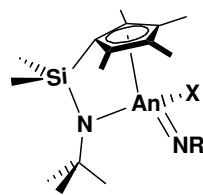
E

was found that HA/cyclization rates are generally comparable to or greater than those mediated

by (CGC)M(NR$_2$)$_2$ precatalysts, and within the context of a Schemes 1,3 scenario, the question

then arises as to what effects are expected from the X ligand. Alkyl hydrogenolysis and An–H

olefin insertion processes have been investigated for Cp$'_2$An(R)X complexes as a function of R

and X (X = OR$'$, Cl; eqs. 11, 12).[38] Here, electron-donating alkoxide co-ligands result in marked

(11)

(12)
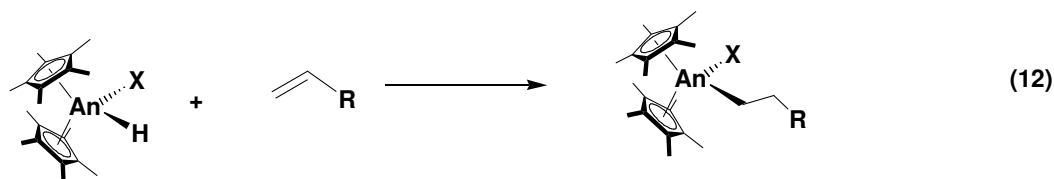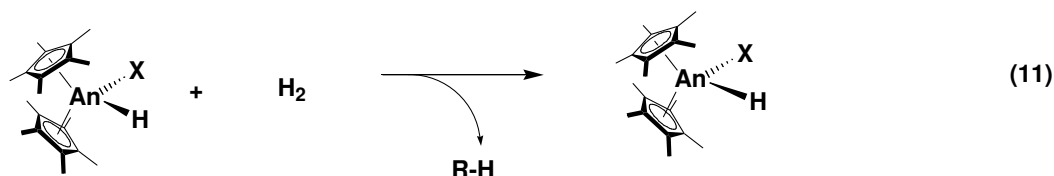
depression of reactivity, likely reflecting –OR$'$ π-donation effects on An electrophilicity (cf.,

resonance forms **F** and **G**) as well as steric impediments. Parallel trends are observed in both

stoichiometric and catalytic Cp$'_2$An(R)Cl complex reactivity, consistent with Cl-based π-

F   **G**
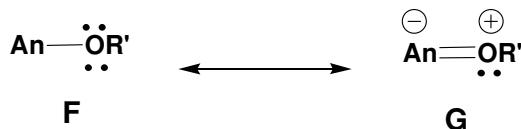
donation effects.[35] Computation and PES experiments also indicate strong dependence of non-Cp ligand σ–/π–donor properties on the extent of bond covalency in actinocenes, and argue that interactions with actinide 6d orbitals dominate π–bonding, consistent with observed effects on reactivity of electron-withdrawing X substituents.[35]

While monoamido complexes **1-Cl**, **2-Cl**, **1-OAr**, and **2-OAr** are effective precatalysts for aminoalkyne HA/cyclization, reactivity trends for $L_2An(R)X$ complexes appear dependent on a variety of factors, and direct comparisons of X effects are complicated by the interplay between steric and electronic factors.[10] Given the impact of An^{4+} ionic radius on intramolecular HA/cyclization rates ($Th^{4+} > U^{4+}$ for aminoalkenes vs. $U^{4+} > Th^{4+}$ for aminoalkynes) and greater metal center access afforded by the open CGC ancillary ligand (vs. $Me_2SiCp''_2An‹$ and $Cp'_2An‹$ catalysts),[10b,33] the HA/cyclization rate trends **1 > 1-Cl >> 1-OAr** and **2-Cl > 2 >> 2-OAr** observed for primary aminoalkene conversion **11 → 12** (Table 4) are similar to previously observed trends upon increasing metal center accessibility. The pattern $(CGC)An(NMe_2)_2 > (CGC)An(NMe_2)Cl > (CGC)An(NMe_2)OAr$ observed for **13 → 14** HA/cyclization (Table 5) is consistent with diminished importance of An^{4+} ionic radius with *secondary* aminoalkene substrates and reflects the substantial steric crowding afforded by the 2,6-di-*tert*-butylphenoxide ligand for an already congested C=C insertion into an M–N(R′)R bond (cf., $R^3 \neq H$ in **C**, Scheme 3). Note that although CGC-imposed geometric constraints are uniform, the presence of a relatively small, relatively non-labile chloride ligand as opposed to an encumbered, substrate-derived amido moiety should reduce HA transition state steric congestion. For aminoalkyne HA/cyclization, the general trend **1-Cl > 1 > 1-OAr** is observed for An = Th, while trends for An

= U (i.e., **2** >> **2-Cl** > **2-OAr**, R = SiMe$_3$, **7** → **8**; **2** >> **2-OAr** > **2-Cl**, R = Me, **9** → **10**) vary with alkyne substitution (Table 3), providing additional evidence for increased importance of transition state electronic demands in aminoalkyne HA/cyclization.[1d,3,4,10b] This is also seen with secondary aminoalkyne cyclization **15** → **16**, where the less hindered chloride ligand effects less rapid N_t with (CGC)M(NR$_2$)Cl for M = Zr, Th, U, though (CGC)An‹ retain there reactivity advantage[10,17,34] over Cp′$_2$An‹ catalysts (Table 5). Interestingly, with the exception of **15** → **16**, monoamido zirconium precatalyst **3-Cl** is a more efficient precatalyst than **3** in mediating the aminoalkene and aminoalkyne transformations investigated here, suggesting that decreased steric hindrance outweighs electronic demands for Zr-mediated *intramolecular* HA/cyclization.

Metallocenes **4/4-Cl** (Me$_2$SiCp″$_2$U‹), **5/5-Cl** (Cp′$_2$Th‹), and **6/6-Cl** (Cp′$_2$U‹) were also investigated as precatalysts in *aminoalkyne* **7** → **8** HA/cyclization. The catalytic activity of *ansa*-metallocenes **4** and **4-Cl** is largely unaffected by chloride incorporation. However, potential Cp″ ring detachment (eq. 13), previously observed for mixed-ring organolanthanide catalysts,[3r,s]
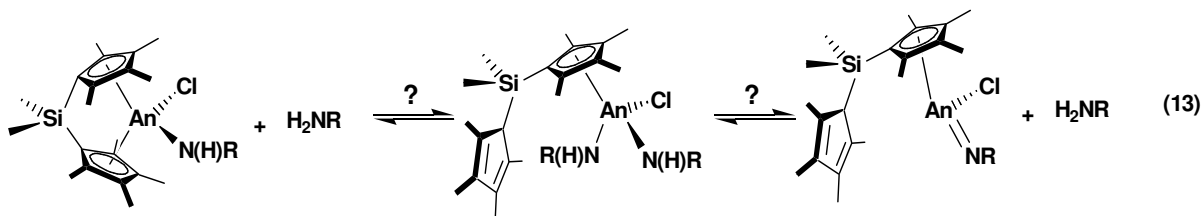

prompted more thorough investigation of the Cp′$_2$AnR$_2$ precatalysts, where reversible ring dissociation is less likely.[15,39] GC/MS and ^{1}H NMR analyses of reaction mixtures during and immediately following **7** → **8** cyclization give no sign of HCp′ or single-ring Cp′An‹ species, arguing that ring protonolysis is unlikely (eq. 14). Interestingly, a 100× *decrease* in activity is

$$\text{(14)}$$
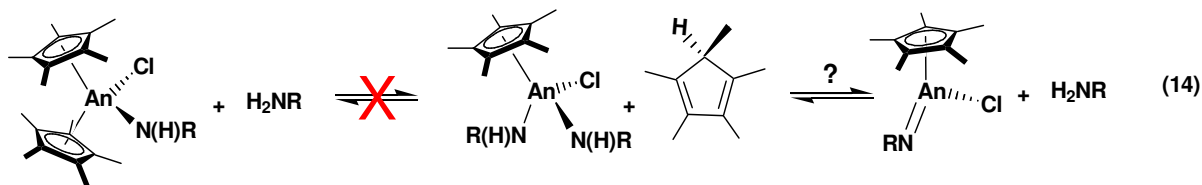
observed in these complexes vs. $Cp'_2An\langle$ for conversion $\textbf{7} \rightarrow \textbf{8}$ (Table 3), perhaps reflecting the pronounced deactivation by the chloride ligand electronic characteristics as discussed above for An–R hydrogenolysis/An–H olefin insertion processes (eqs. 11, 12).[38] Decreased electrophilicity could reduce alkyne insertion rates, depressing N_t vs. $Cp'_2An\langle$, $Me_2SiCp''_2An\langle$, and $(CGC)An\langle$ catalysts.[40] Alternatively, the agency of $Cp'_2An{=}NR$ species in the sterically protected Cp'_2 environment could explain diminished reactivity vs. more open ancillary ligation favoring M–N(H)R intermediates, especially in light of the reported difficulty of cycloadding C=C bonds to M=NR bonds (M = Ti, Zr).[1,41] However, that $Cp'_2An\langle$ complexes mediate intramolecular aminoalkyne HA/cyclization of primary *and* secondary amines with zero-order dependence on [amine] and without protonolytic HCp′ release argues for a σ-bonded M–N insertive pathway, even in sterically-congested environments.

A ligand dissociation/reattachment process analogous to eqs. 13 and 14 is in principal possible with CGC ancillary ligation (eq. 15). Although not spectroscopically observed, the chelating $({}^tBu)N–An^{4+}$ moiety in $(CGC)An\langle$ complexes *could* be displaced in the presence of a large excess of substrate molecules, enabling transient An=NR formation (eq. 15a, R′ = H) and, potentially, C=C/C≡C [2 + 2] cycloaddition. However, the catalytic activity of *any* $L_2M\langle$ complex with secondary amine substrates (eq. 15b, R′ ≠ H) with observed rate law ν ~

$[M]^1[amine]^0$, provides compelling evidence for an insertive M–N(R′)R pathway (Scheme 3), and the comparable competence of substituted and unsubstituted **1**-**2** in mediating such
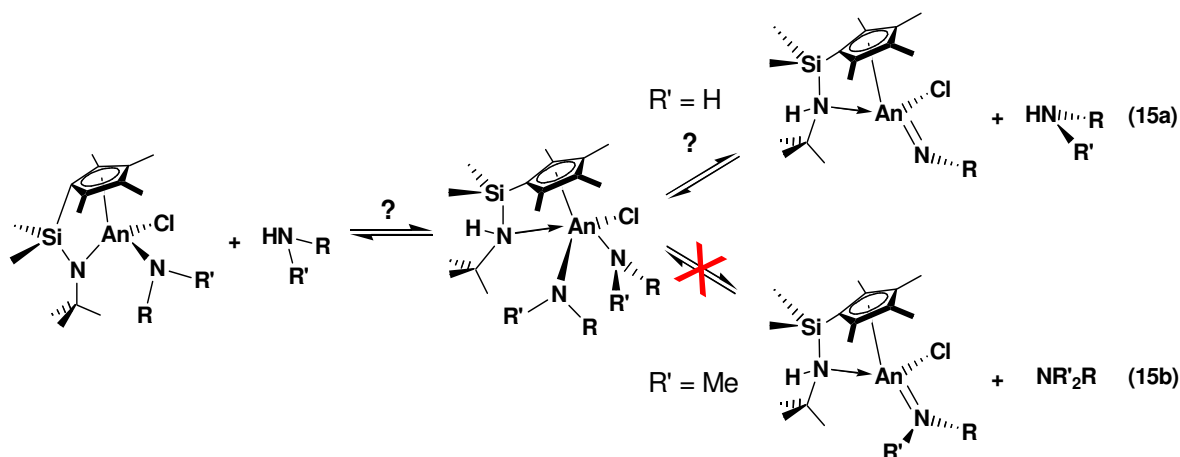
transformations argues that an $L_2An=NR$ imidoactinide intermediate (**B**) is not important. Passage through an $L_2M=NR$ reactive intermediate requires unprecedented high-energy species similar to **H** or **I** in lieu of more reasonable **J**. Salt-like structure **H** would presumably be generated via α-hydrogen abstraction[8,9,42] and involves hypervalent N bonded directly to M^{4+}, whereas zwitterionic **I** (via electron pair transfer from N to the An–N bond) places a formal
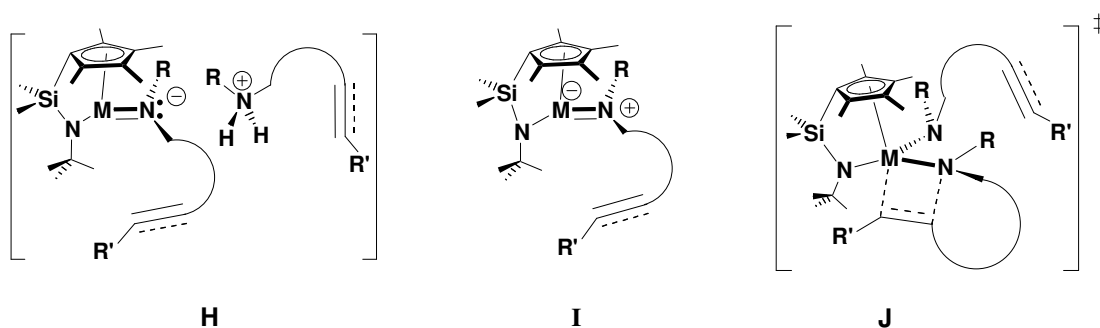
negative charge on An^{4+} or Zr^{4+} (no change in diamagnetism or μ_{eff} is observed during primary or secondary amine HA/cyclization). Moreover, species **H** or **I** should be stabilized in more polar

media, contrary to the observed N_t decrease for **2** (rapid catalyst decomposition occurs with **1**). Also note that the high yields and regioselectivity in the present aminoalkene and aminoalkyne HA/cyclizations are inconsistent with (chain) radical processes (eqs. 16, 17).[43] The required but energetically unfavorable $An^{4+} \rightarrow An^{3+}$ electron transfer/reduction process (particularly for An =

$$(16)$$

$$R = H, Me, Ph$$

$$(17)$$
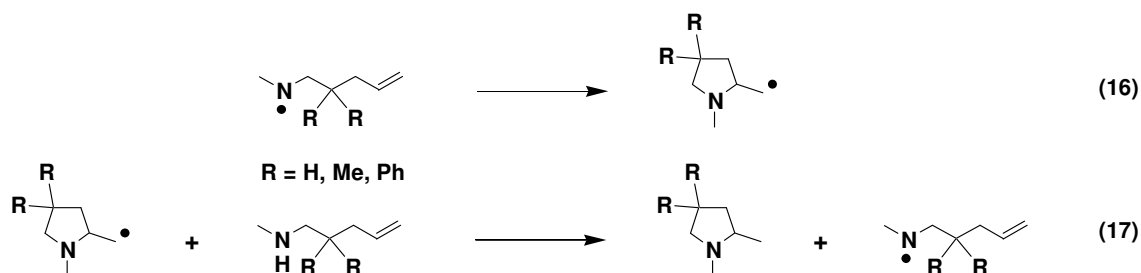
Th),[28] rate dependence on metal ionic radius, zero-order dependence on [substrate],[23] and pronounced effects of ancillary ligation on N_t and diastereoselectivity, all render radical pathways unlikely, particularly in light of reported trends in heterocycle yield and regioselectivity in radical-mediated aminoalkene cyclizations.[43b,c]

(CGC)Zr‹-Mediated Hydroamination. Initial intramolecular aminoalkyne HA/cyclization reports proposed the involvement of in situ-generated CpM=NR(Cl) species (M = Ti, Zr) at high catalyst loadings ($\geq$ 20 mol%), starting from CpM(CH$_3$)$_2$Cl or CpMCl$_3$ with 40 mol% ^{i}Pr$_2$NEt in THF.[7d,e] More recently, well-defined group 4 amidate, metallocene, and chelating diamide complexes have been applied to primary aminoalkyne (**K**; M = Ti, Zr; R = H, Me)[7a] and aminoalkene (**L**; 120-150 °C) HA/cyclizations, invoking similar M=NR pathways.[6a] Sterically

K   L
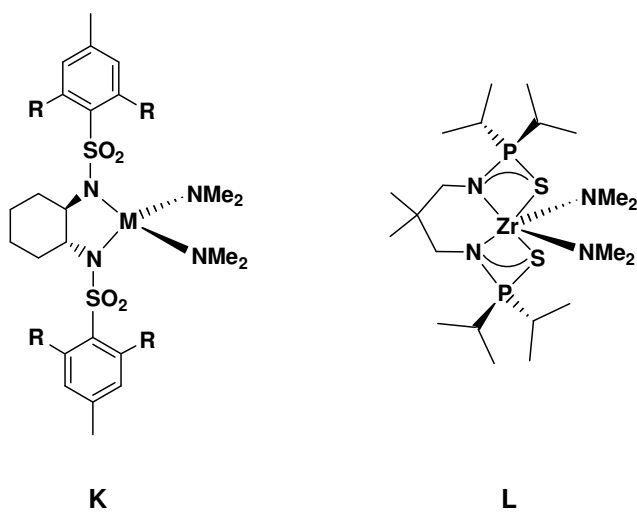
open homoleptic Ti(NMe$_2$)$_4$ also mediates intramolecular primary aminoalkene HA/cyclization.
[6b,44] Although it is again reasonable to expect electron-withdrawing chloride ligands to reduce

catalytic activity,[38] substituted **3-Cl** is typically the most efficient (CGC)Zr‹ precatalyst found in

this study. For the Me$_3$Si-substituted aminoalkyne conversion **7 → 8**, this difference is quite

pronounced (Table 3), and for transformations **9 → 10** and **11 → 12** (Tables 3, 4), the distinction

is again significant, displaying a roughly two- to three- fold enhancement vs. complex **3**. The

activities of **3-Cl** and **3** in mediating **11 → 12** at 100 °C are roughly 4× and 2× greater,

respectively, than electron-rich precatalyst **L**[6a] (Ti(NMe$_2$)$_4$ is ca. 2× less active than **L**).[6b]

Secondary amine **13 → 14** and **15 → 16** HA/cyclizations mediated by (CGC)Zr‹ are

considerably more sluggish than with (CGC)An‹ catalysts, reflecting metal accessibility effects

on N_t.[1,3,10b] The added steric hindrance in secondary vs. primary aminoalkenes **13** (Table 5) and

11 (Table 4), where cyclization rates are comparable, is offset by the enhanced transition state

orientation (Thorpe-Ingold effect)[36] of substrate chain *gem*-diphenyl vs. *gem*-dimethyl groups.

Furthermore, in light of the similar catalytic behavior of (CGC)An‹ and (CGC)Zr‹ catalysts, the N_t trends (**3-Cl > 3** for **11 → 12** vs. **3 > 3-Cl** for **15 → 16**) presumably reflects the importance of transition-state steric demands, where the small, rigid chloride ligand provides a less hindered site for C=C/C≡C insertion, perhaps outweighing electronic deactivation (cf., Scheme 1, **A** and Scheme 3, **C**). In addition, while cationic group 3 catalysts mediate intramolecular primary aminoalkene HA/cyclization,[4a,h] and $Cp_2ZrMe^+MeB(C_6F_5)_3^-$ effects more thermodynamically-favorable[1] primary aminoallene HA/cyclization,[7a] cationic $L_2M(R)^+XB(C_6F_5)_3^-$ (M = Ti^{4+}, Zr^{4+}; R = Me, Ch_2Ph; X = C_6F_5, R) catalysts are *only* active for secondary amine intramolecular HA/cyclizations.[41] Interestingly, the poisoning of these cationic catalysts by primary amine substrates has been rationalized as deactivation via *unreactive* neutral imido complex formation.[8,9,41,42] These observations, in conjunction with the present results, confirm that M=NR intermediates are unnecessary to invoke in intramolecular HA/cyclization reactions mediated by organozirconium catalysts and that a σ-bonded M–N mechanistic pathway is accessible, if not *favored*.

Activation Parameter Parallels. Activation parameters determined for intramolecular HA/cyclization mediated by monoamido (CGC)M(NR_2)X catalysts (M = An, Zr) are comparable to those for similar processes mediated by L_2AnR_2 and L_2LnR catalysts (Table 7). The moderate $\Delta H^\ddagger$ and large negative $\Delta S^\ddagger$ values are consistent with highly-ordered C=C/C≡C insertive transition states having considerable bond-forming accompanying bond-breaking.[45] The change in $\Delta S^\ddagger$ to more negative values with **11 → 12** conversion mediated by **2-OAr** ($\Delta S^\ddagger$ = -43(9) eu) is

Table 7. Experimental activation parameters for intramolecular aminoalkene and aminoalkyne HA/cyclization catalyzed by Cp′$_2$Ln–, (CGC)An‹, and (CGC)Zr‹ complexes over at least a 40 °C temperature range in C$_6$D$_6$.
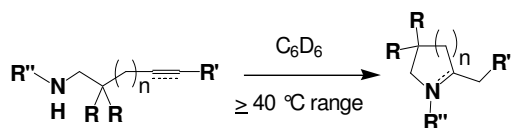
Unsaturation	Precatalyst	Substrate	$\Delta H^{\ddagger}$ (kcal/mol)	$\Delta S^{\ddagger}$ (eu)	E_a (kcal/mol)	ref.
aminoalkene	Cp'$_2$La[CH(SiMe$_3$)$_2$]	R = R' =R" = H, n = 1	12.7(5)	-27(2)	13.4(5)	*3v*
	(CGC)Th(NMe$_2$)$_2$	R = Ph, R' = R" = H, n = 2	12.6(5)	-30(1)	13.3(7)	*11*
	(CGC)U(NMe$_2$)OAr	R = Ph, R' = R" = H, n=1 (**11**)	10(3)	-43(9)	11(3)	*this work*
2° aminoalkene	(CGC)Th(NMe$_2$)$_2$	R = Ph, R' = H, R" = Me, n=1 (**13**)	9(3)	-48(6)	10(3)	*this work*
aminoalkyne	Cp'$_2$Sm[CH(SiMe$_3$)$_2$]	R = R' = R" = H, n = 1	11(8)	-27(6)	--	*3o*
	(CGC)Th(NMe$_2$)$_2$	R = R" = H, R' = Me, n = 1 (**9**)	14(2)	-27(5)	15(2)	*11*
	(CGC)U[N(SiMe$_3$)$_2$]Cl	R = R" = H, R' = Me, n = 1 (**9**)	16(3)	-18(9)	17(3)	*this work*
	(CGC)Zr(NMe$_2$)Cl	R = R" = H, R' = SiMe$_3$, n = 1 (**7**)	11(2)	-35(7)	12(2)	*this work*

consistent with the transition state ordering necessary to accommodate the steric hindrance of the large aryloxide ligand (**M**; cf., **C**, Scheme 3). A similar change in $\Delta S^{\ddagger}$ for HA/cyclization **13** → **14** mediated by **1** ($\Delta S^{\ddagger}$ = -48(6) eu) is also not surprising given the nonbonding repulsions engendered by the *N*-methyl group of **13** and substrate organization required prior to C=C insertion (**N**; cf., **C**, Scheme 3). To our knowledge, activation parameters have not been reported

M **N**
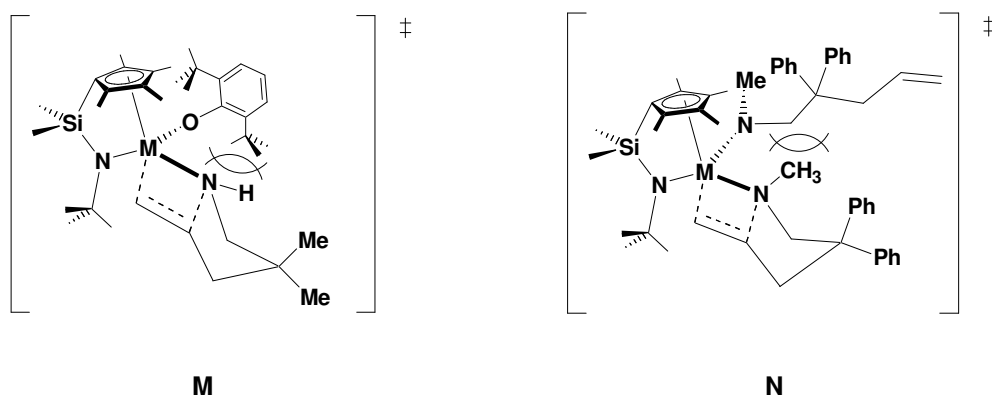
for group 4-mediated HA/cyclizations,[1,6,7] although *intermolecular* terminal alkyne + aliphatic amine HA mediated by Cp′$_2$AnMe$_2$ also displays comparable parameters, $\Delta H^{\ddagger}$ = 11.7(3) kcal/mol and $\Delta S^{\ddagger}$ = -44.5(8) eu.[46] That the present activation parameters parallel those for L$_2$Ln– and L$_2$An‹-catalyzed HA/cyclizations[1d,3,10] suggests that the mechanism and turnover-limiting steps in each process are very similar if not identical. Zero-order substrate dependence, characteristic of intramolecular HA (Table 6),[1] indicates that a rapid pre-equilibrium involving RNH$_2$ extrusion is *not* significant, while the ready cyclization of secondary amine substrates argues against the involvement of conventional M=NR species produced via α–H elimination.

Kinetic Isotope Effects. In similar organolanthanide aminoalkene HA/cyclization, substantial deuterium KIEs are observed in the range k_H/k_D = 2.7(4)-5.2(8), varying with substrate structure and temperature from 25-60 °C,[3v] while an analogous k_H/k_D = 4.2 is reported at 40 °C for chiral binaptholate Ln complexes.[4a] The marked HA/cyclization rate dependence on ring size and alkyl chain substitution in addition to other arguments[1d] suggest that the significant N–H/N–D KIE does *not* result from turnover-limiting protonolysis of completely cyclized aminoalkene, but rather that protonolysis may be concurrent with cyclization. In the present study, the observed k_H/k_D = 3.3(5) and 2.6(4) for **2** and **2-Cl**, respectively, is in excellent agreement with Ln-mediated aminoalkene HA/cyclization results (eq. 18), further supporting an

(18)

11-d_2 **12**-d_2

(CGC)U(NMe$_2$)$_2$ (**2**), k_H/k_D = 3.3(5)
(CGC)U[N(SiMe$_3$)$_2$]Cl (**2-Cl**), k_H/k_D = 2.6(4)
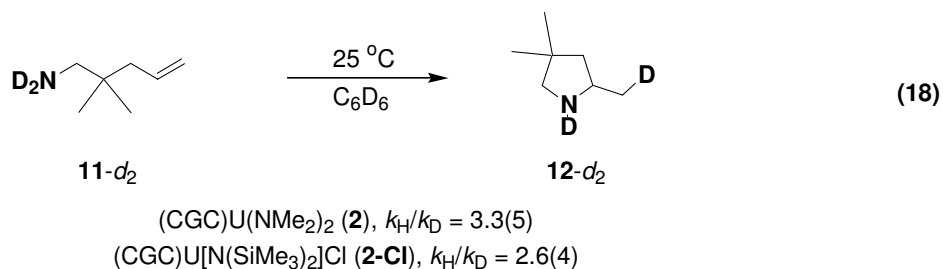
M–N σ-bonded mechanistic pathway (Scheme 1). To our knowledge, similar KIE studies have not been reported in group 4-catalysts, where aminoalkene HA is typically sluggish, limiting direct comparisons with organolanthanide catalysts. However, in the unimolecular α-elimination process shown in eq. 19, where an M=NR species is generated with bulky R = Si(^{t}Bu)$_3$ groups, a

(19)

M = Ti, k_H/k_D = 5.9(6)
M = Zr, k_H/k_D = 7.3(4)
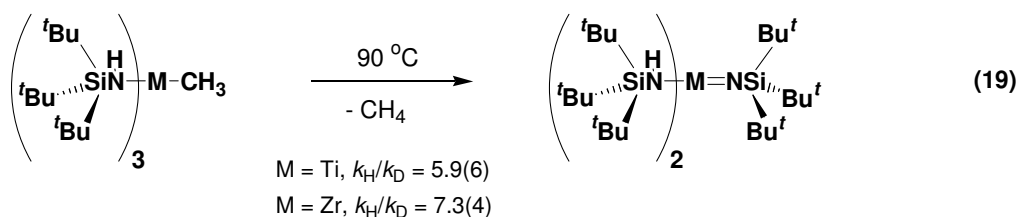
significantly larger KIE is observed with k_H/k_D = 5.9(6) and 7.3(4) for M = Ti, Zr, respectively.[47] This stark contrast in N–H/N–D KIE suggests that unimolecular M=NR formation is not significant in the turnover-limiting step of (CGC)An‹-mediated intramolecular HA/cyclization.

Mechanistic Summary. It is useful to briefly summarize the observations supporting the basic HA/cyclization pathway of Scheme 3. The present (CGC)M‹ catalysts could reasonably mediate intramolecular HA/cyclization via either of two plausible mechanistic scenarios: (1) a highly polar, highly organized four-centered, insertive transition state involving catalytically-active (CGC)M‹ species possessing two M–N(H)R σ-bonds ("Ln-like"; Scheme 1), or (2) a [2 + 2] cycloaddition probably following a rapid pre-equilibrium (step (i), Scheme 2) that generates L_2M=NR reactive intermediate **B**. Note that stable monomeric L_2An=NR complexes invoked in scenario (2) are challenging synthetic targets (vide supra), particularly with unencumbered ancillary ligation,[34] and that imidoactinide complexes typically revert to bis(amido)actinides in the presence of excess amine (cf., eq. 10b).[34a]

The data here support mechanistic scenario (1) (Scheme 3), with perhaps the strongest evidence opposing scenario (2) (eq. 10; Scheme 2) being the ability of (CGC)An(NMe$_2$)$_2$, (CGC)ZrMe$_2$, and (CGC)M(NR$_2$)X precatalysts **1-6** to effectively mediate secondary *N*-alkyl aminoalkene and aminoalkyne HA/cyclizations. The relative depression in N_t for secondary vs. primary substrates is consistent with trends previously observed for L_2Ln– catalysts, where diminished turnover frequencies can be attributed to unfavorable steric interactions.[1d,3,4] In the present study, secondary amine HA/cyclizations proceed without deviation from the observed

primary amine rate law, $\nu \sim [L_2M\langle]^1[\text{amine}]^0$, and with similar activation energetics, arguing that a mechanistic scenario similar to Scheme 3 is again operative. While a pathway proceeding through an active $L_2M=NR$ species (**B**) is conceivable in unsubstituted L_2MR_2 complexes with primary amine substrates, the mild reaction conditions, absence of required steric bulk in amine substrates, facile cyclization of 2° amine substrates, and lack of an induction period prior to catalytic turnover argue against scenario (2)/Scheme 2. Moreover, the $[\text{amine}]^{-1}$ kinetics seen in [2 + 2] cycloaddition pathways[8] differs from the present results, where high [product] depresses N_t owing to competitive binding/inhibition (Table 6).[1d,3v,11] Devoid of unlikely intermediates **H** or **I** and without detectable ancillary ligand detachment or rearrangement (eqs. 4, 5, 13-15), there are no obvious pathways from $L_2M(NR_2)X$ complexes **1-6** to the M=NR species required in scenario (2), making this pathway unlikely for either primary or secondary amine substrates.

Conclusions

Catalytic intramolecular HA/cyclization reactions mediated by selectively substituted 5f and d^0 complexes provide strong evidence for a mechanistic pathway proceeding via C=C/C≡C insertion at an M–N(H)R σ-bond (Schemes 1, 3), particularly with sterically open CGC ancillary ligation in the presence of excess amine substrate. The ability of $(CGC)MR_2$ and $(CGC)M(NR_2)X$ complexes to effectively promote HA/cyclization of *both* primary and secondary aminoalkyne and aminoalkene substrates with comparable rates and activation parameters argues that M=NR intermediates are unlikely and that a pathway involving insertion at an M–N σ-bonded intermediate is kinetically viable. Moreover, activities of selectively

substituted (CGC)M(NR$_2$)X complexes generally *exceed* those of (CGC)MR$_2$ precatalysts, further supporting passage through a transition state similar to **A** or **C** with a strong dependence on nonbonded interactions and C=C/C≡C insertion into an M–N(H)R σ-bonded intermediate (Scheme 3).

Supporting Information Available: Crystallographic Information Files and data tables for **1-Cl**, **2-Cl**, **3-Cl**, and **1-OAr** are available free of charge via the Internet at http://pubs.acs.org.

Appendix

Further Exploration into Hydroelementation Reactions Catalyzed by Highly Electrophilic Constrained Geometry 3d, 4f, and 5f Complexes. New Directions in C–N and P–P Bond-Forming Processes

Part 1

Scope and Mechanism of Intramolecular Aminoalkene and Aminoalkyne Hydroamination/ Cyclization Catalyzed by Constrained Geometry Titanium Complexes. In this section, a brief investigation of scope and mechanism of intramolecular aminoalkene and aminoalkyne hydroamination/cyclization catalyzed by tetravalent organotitanium complexes is presented.[1] The constrained geometry complex $(CGC)TiMe_2$ (**1**, $CGC = [Me_2Si(\eta^5-Me_4C_5)(^tBuN)]^{2-}$) is an active precatalyst for intramolecular primary and secondary aminoalkyne and aminoalkene HA/cyclization.[1d] Substrate reactivity trends reflect the considerably smaller ionic radius of Ti^{4+} (vs. An^{4+} and Ln^{3+}),[2] displaying markedly reduced N_t (Table 1). Interestingly, the tremendous rate enhancement normally observed and attributed to the electronic effects[3] and transition state stabilization[1d,4] of $-SiMe_3$ in **2** $\rightarrow$ **3** is not apparent with (CGC)Ti‹-catalyzed aminoalkyne HA/cyclization, where comparable efficiencies are seen for $-Me$ ($N_t \geq 1$ h^{-1}, 60 °C) and $-SiMe_3$ ($N_t = 0.2$ h^{-1}, 25 °C) substituted alkynes. The primary aminoalkene conversion **8** $\rightarrow$ **9** proceeds very sluggishly at 120 °C ($N_t < 0.1$ h^{-1}), consistent with previous reports of Ti-catalyzed aminoalkene HA/cyclization.

Of greatest interest here is the cyclization of the secondary aminoalkyne **6** $\rightarrow$ **7**. Though no induction period is observed, initial protonolysis of the Ti–CH$_3$ groups is exceedingly slow[5] preventing accurate N_t determination. However, > 95% yield is achieved at 90 °C over several weeks, without necessarily achieving complete protonolysis and catalyst activation, suggesting that a Ti–N σ-bonded mechanistic pathway, similar to that proposed for (CGC)An‹ and L_2Ln-

Scheme 1. Proposed σ-bond insertive mechanism for (CGC)Ti‹-catalyzed *intramolecular* HA/cyclization of aminoalkenes and aminoalkynes. When X = NR$_2$ or R, two substrate molecules enter the catalytic cycle and two HNR$_2$ are evolved during precatalyst activation (see ref. 6).
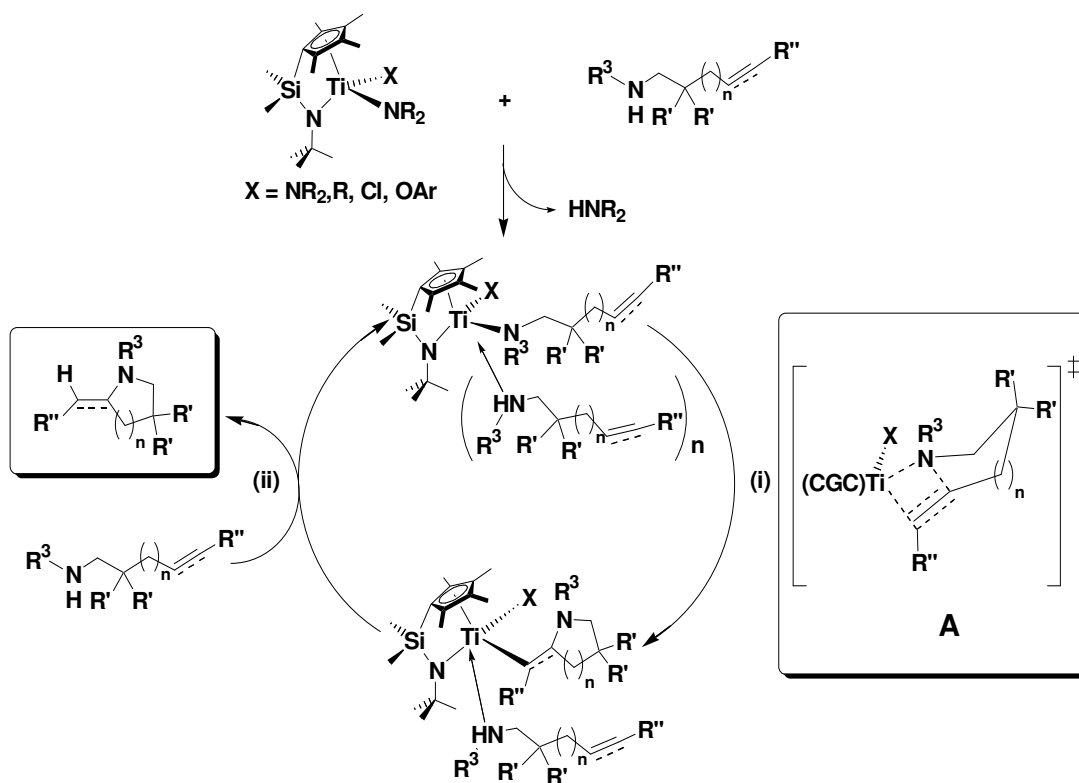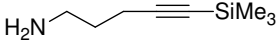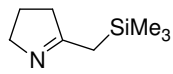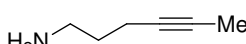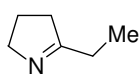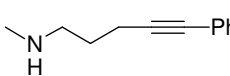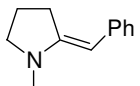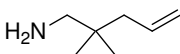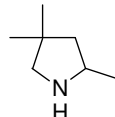
Table 1. Results of (CGC)Ti‹-mediated intramolecular aminoalkene and aminoalkyne HA/cyclization in C_6D_6.

Substrate	Product[a]	N_t, h^{-1} (°C)[b]
2	**3**	0.2 (25)
4	**5**	≥ 1 (60)
6	**7**	TBD
8	**9**	≤ 0.1 (120)

[a]Yields $\geq$ 95% by ^1H NMR spectroscopy and GC/MS.
[b]Determined by ^1H NMR spectroscopy.

mediated intramolecular HA/cyclization (Scheme 1),[1d,6] *can* be operative with coordinatively unsaturated organotitanium complexes. The extent of competition between pathways proceeding through Ti–N(H)R and Ti=NR intermediates is unclear in the absence of more rapidly activated precatalysts (e.g., (CGC)Ti(R)Cl and (CGC)TiH$_2$ or similar Me$_2$Si(η^5-C$_5$H$_4$)(^{t}BuN)TiR$_2$ complexes) necessary to probe these questions in greater detail. What is clear from these preliminary results is that there are many intriguing mechanistic nuances that remain to be elucidated for intramolecular HA/cyclization reactions.

Part 2

Catalytic Intermolecular Tetraphosphetane Formation Mediated by Constrained Geometry Organoactinide Complexes. In this section, the first catalytic synthesis of a tetraphosphetane is reported.[7] (CGC)An(NMe$_2$)$_2$ complexes (An = Th, 1; An = U, 2; CGC = [Me$_2$Si(η^5-Me$_4$C$_5$)(^{t}BuN)]$^{2-}$) catalytically consume H$_2$PCy in the presence of Me$_3$SiC≡CCH$_3$ to form (PCy)$_4$ (**3**) in C$_6$D$_6$, with organothorium complex **1** displaying considerably greater efficiency. In a typical experiment, precatalyst (ca. 4-6 mg, 8-11 μmol) and internal standard Si(p-tolyl)$_4$ (ca. 3-4 mg, 7-10 μmol) were dissolved in C$_6$D$_6$ (0.80 mL) and added to a Teflon-valved NMR tube in the glove box. A preliminary ^{1}H NMR spectrum was recorded to verify the relative concentrations of precatalyst and standard. On the high-vacuum line, the catalyst solution was frozen in a -78 °C bath and evacuated before adding 0.2 mL of neat CyPH$_2$ ($\geq$ 100× excess) by syringe as previously described.[6] In situ generation of the active species (eq. 1),
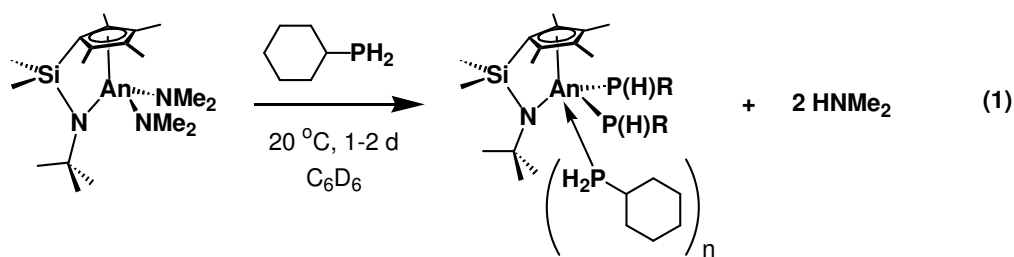
presumably (CGC)An[P(H)Cy]$_2$(H$_2$PCy)$_n$, was monitored by ^{1}H NMR spectroscopy. For An = Th, activation and loss of HNMe$_2$ is complete in 1 d at 20 °C, forming a golden solution, however, activation was not fully achieved for An = U, even after several days at 20 °C and periodic removal of the HNMe$_2$ byproduct. (CGC)U‹-catalyzed reaction mixtures display characteristic darkening of solutions upon heating at 100 °C. Product formation is observed

spectroscopically, with sluggish rates tied to partial catalyst activation. Attempts to isolate more

readily exchanged bis(phosphido)uranium (CGC)U(PR$_2$)$_2$ complexes by salt metathesis (eq. 2)
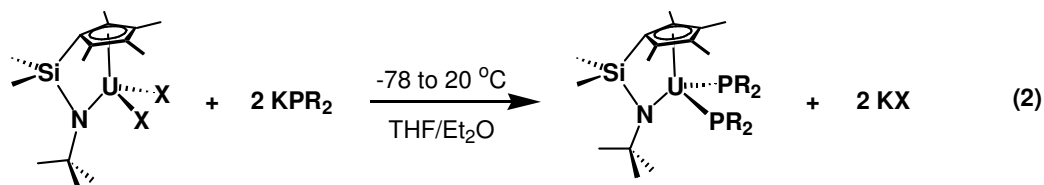
were unsuccessful, but moderate heating during in situ catalyst activation would likely be

tolerated (catalysis T = 100 °C) and should be investigated further as it would likely accelerate

protodeamination. On the high-vacuum line, the (activated) catalyst solution was again frozen in

a -78 °C bath and degassed prior to the addition of neat Me$_3$SiC≡CCH$_3$ (0.2 mL) in the usual

manner.[6] While heating to 100 °C for 7 d, reaction progress was monitored by ^{1}H NMR

spectroscopy, with N_t determination complicated by the precipitation of a colorless, flocculent

solid. Upon cooling to 20 °C, the solids re-dissolved, and tetraphosphetane **3** slowly precipitated

from C$_6$D$_6$ solution as a very large single, hard, colorless crystal, as well as a considerable build-

up of pressure in the reaction vessel, presumably owing to H$_2$ evolution. The identity of **3** was

confirmed by single-crystal X-ray diffraction for the reaction catalyzed by **1**. From these

observations, it is unclear what role Me$_3$SiC≡CCH$_3$ plays (if any), suggesting that the net

reaction depicted in eq. 3 is operative.
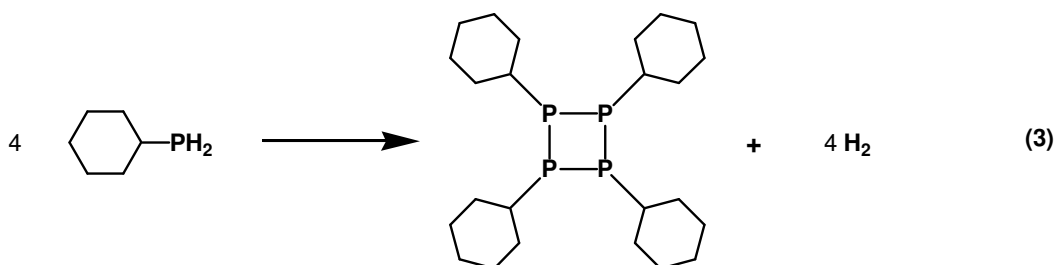
Future studies are necessary to explore the scope and selectivity of this interesting reaction, elucidate mechanistic details, and improve the characterization and generation of the activated catalyst species. Although detailed mechanistic studies of catalytic HA/cyclization mediated by **1** and **2** favor an An–N σ-bonded intermediate,[1] little is known about the chemistry of σ-bonded An–P species and the stability and reactivity properties of An=PR species (including radical intitiation processes) particularly with coordinatively unsaturated ancillary ligands. With these fascinating questions, it is clear that a rich chemistry may exist for An–P species and (CGC)An‹-catalyzed inter- and intramolecular hydrophosphination reactions.

Part 3

Catalytic Intermolecular Aminoalkyne Hydroamination Mediated by Constrained Geometry Organo-f-element Complexes. Towards Medium- to Large-Ring Nitrogen Heterocycle Formation.   Medium- to large-ring heterocycles (7-10 members) are attractive synthetic targets in the organic and biological chemistry of natural products with potential applications in the pharmaceutical industry.[8] Hydroamination,[1] the atom-economical and catalytically efficient addition of N–H bonds across C–C unsaturations, is a particularly attractive route to such products, without multi-step syntheses or restrictions to product symmetry. One plausible route (Scheme 2) proceeds via initial *intermolecular* coupling of amine substrates, followed by *intramolecular* cyclization to afford the desired diazacycle (Scheme 2). An alternative pathway mediated by binuclear catalysts is currently under investigation.[9]

In this section, progress toward these interesting products is summarized for catalytic reactions mediated by mononuclear constrained geometry organoactinide (CGC)An(NMe$_2$)$_2$ (An = Th, **1**; An = U, **2**; CGC = [Me$_2$Si(η^5-Me$_4$C$_5$)(^{t}BuN)]$^{2-}$) and organolanthanide (CGC)Sm–N(SiMe$_3$)$_2$ (**3**) complexes. A series of catalytic intermolecular aminoalkene and aminoalkyne hydroamination reactions mediated by **1-3** are presented for substrates bearing short alkyl chain tethers –(CH$_2$)$_n$– (n = 1, 2) to prevent endocyclic intramolecular HA/cyclization byproducts (eq. 4 and Chart 1). In a typical experiment, precatalyst (ca. 4-9 mg, 8-16 μmol) and internal standard Si(*p*-tolyl)$_4$ (ca. 2-5 mg, 5-12 μmol) were dissolved in C$_6$D$_6$ (0.80 mL) and added to a Teflon-valved NMR tube in the glove box. A preliminary ^{1}H NMR spectrum was recorded to verify the relative concentrations of precatalyst and standard. A neat (for C–H/C–D bond activation studies

Scheme 2. Catalytic cycle envisioned for symmetric heterocycle formation.

Chart 1

$$2 \ H_2N \overset{(\ )_n}{\diagdown} \overset{R}{\diagup} \quad \xrightarrow{\quad \times \quad} \quad 2 \ R \overset{H}{\underset{N}{\diagdown \triangle (\ )_n}} \qquad (4)$$

$$n = 1, 2$$
$$R = H, Me, Ph, SiMe_3$$
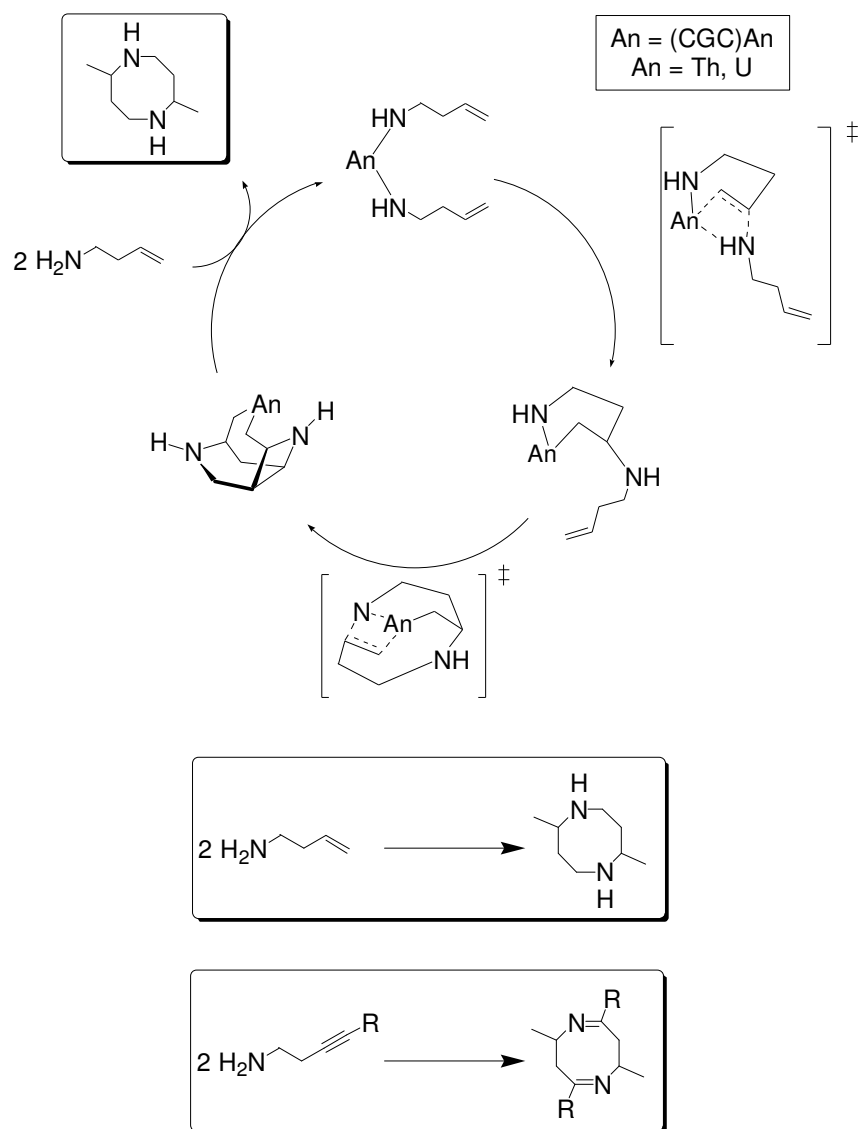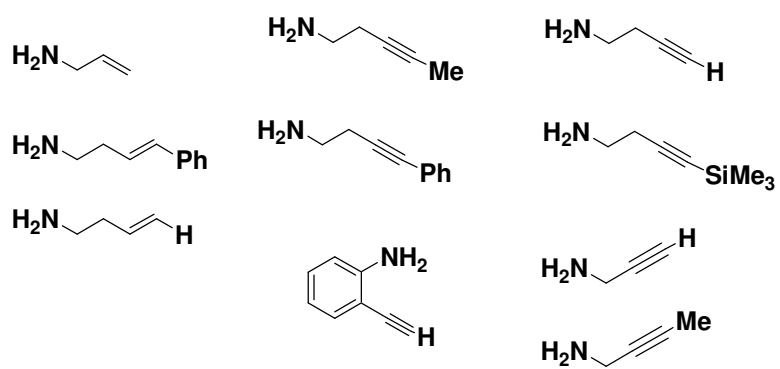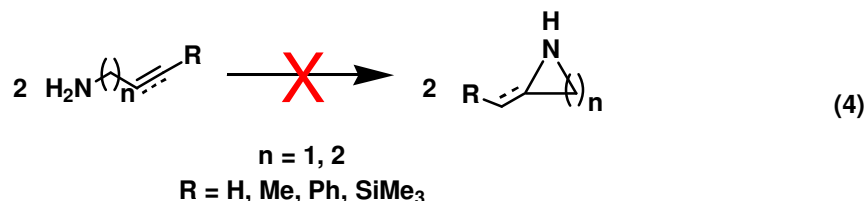
in C_6D_{12}) or 1 M C_6D_6 substrate solution (0.20 mL) was then added to the catalyst solution on the high-vacuum line as previously described[6] or at 20 °C in the glovebox. While heating in constant temperature oil baths (up to 140 °C), reaction progress was monitored by ^{1}H NMR spectroscopy, typically with up to ca. 70% substrate consumption and $N_t < 0.1 \ h^{-1}$. Among the aminoalkenes investigated (Chart 1), allyl amine underwent significant coupling, while 3-buten-1-amine and 4-phenyl-3-buten-1-amine afforded very little or no intermolecular HA coupled product. Propargyl amines and 2-ethynylaniline (Chart 1) underwent rapid color change upon heating with precatalyst **1** or **2**, leading to substrate decomposition. The more robust 3-butyn-1-amine substrates were investigated in greater detail, displaying similar conversion rates and yields, with far less pronounced electronic effects when vary alkyne substituents $-C{\equiv}CR$ (R = H, Me, Ph, SiMe_3). Although each conversion is limited by catalyst death (vide infra), 4-phenyl-3-butyn-1-amine couples slightly more efficiently than R = SiMe_3, Me, or H. Reaction products were isolated by vacuum transfer of volatiles or by passage through a silica plug, then analyzed using GC/MS and standard 1-D and 2-D ^{1}H and ^{13}C NMR spectroscopic techniques. Interestingly, alkyne coupling occurs in an anti-Markovnikov fashion ($\geq$ 90% selectivity) *without* subsequent cyclization to afford the intermediate Schiff base products generalized in eq. 5. Prolonged heating of reaction mixtures in C_6D_6,

$$2 \ H_2N(\ )_n{-}{\equiv}{-}R \longrightarrow \qquad \cdots\cdots\rightarrow \qquad (5)$$

(n = 1, 2)
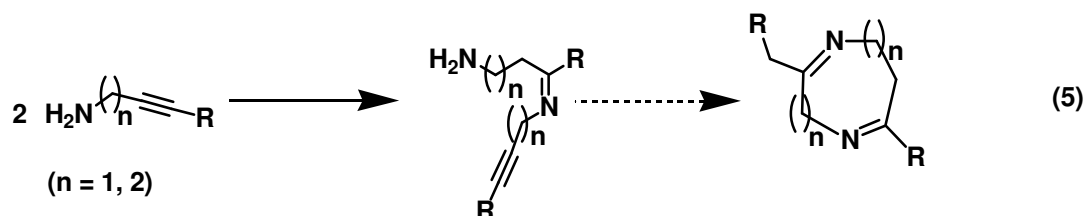
C_7D_8, or C_6D_{12} afforded identical results, suggesting that catalyst decomposition via C–H/C–D bond activation is unlikely under these conditions.[4,10] Significant decomposition was, however, observed with most substrates, indicated by the presence of free H_2CGC in ^{1}H NMR spectra., contrary to other (CGC)M-catalyzed intramolecular HA/cyclization.[1d,6] One likely route to decomposition proceeds via protonolysis of bound CGC^{2-} by several chelating intermediates as shown here for coupled 3-butyn-1-amines (R = H, Me, Ph, SiMe$_3$). This pathway would likely
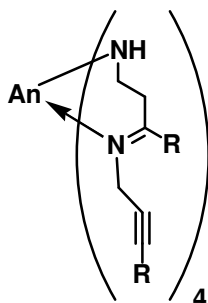
proceed more rapidly at higher temperatures (in agreement with experimental results) and may be less significant for binuclear ligand scaffolds and/or smaller ionic radius metals (vs. An^{4+}).[2,9]

Conversions mediated by **1-3** yield identical products at similar rates, suggesting that aminoalkyne and aminoalkene coupling occur in an entropically unfavorable bimolecular process (Scheme 3) rather than a unimolecular "cross-over" C=C/C≡C insertion from one covalently bonded substrate into a neighboring An–N σ-bond in **1** or **2** (Scheme 2). Given the prolonged reaction times and harsh reaction conditions employed, a pathway proceeding through an

Scheme 2. Proposed mechanism for intermolecular aminoalkyne HA/coupling mediated by (CGC)An‹ **1-2** and (CGC)Sm– **3** catalysts.
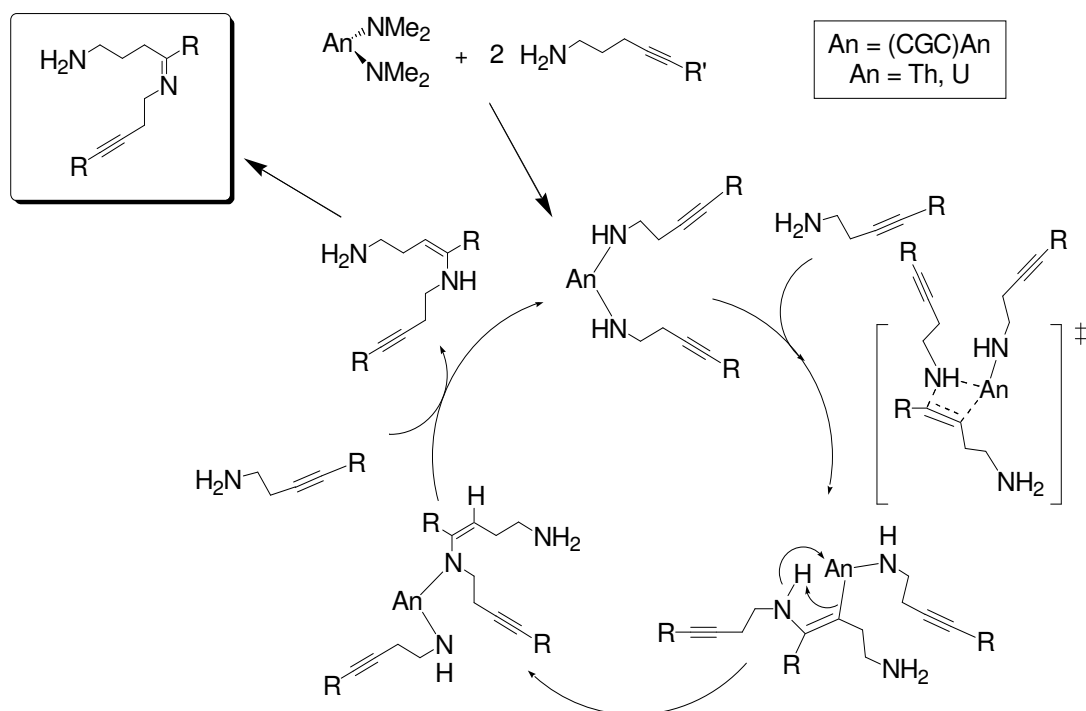
An=NR species, though unlikely in light of the coordinative unsaturation of (CGC)An‹ complexes,[6] cannot be precluded at this time.

   In summary, the selective intermolecular HA of aminoalkenes and aminoalkynes mediated by (CGC)An‹ and (CGC)Sm– catalysts has been achieved with limited success. Further substrate exploration might also prove beneficial, particularly with terminal allenes where variable ring closures have been observed with group 4 and lanthanide catalysts for intramolecular HA/cyclization (eq. 6). The elevated reaction temperatures necessary for initial
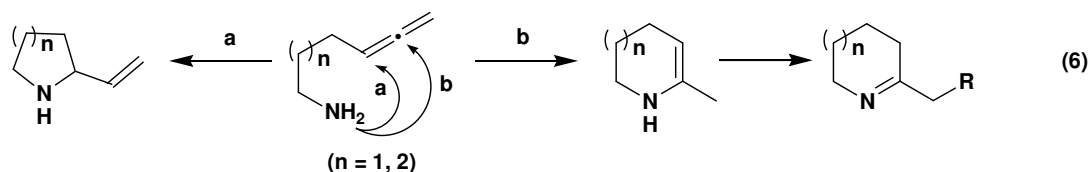
coupling and the inability of these complexes to mediate concomitant cyclization of coupled intermediates indicates that further catalyst development is needed for successful generation of medium- to large-ring diazacycles.

References

Chapter 1 and Chapter 2

Appendix

Chapter 1

1. For general C–N bond-formation references, see: (a) Beller, M.; Seayad, J.; Tillack, A.; Jiao, H. *Angew. Chemie, Int. Ed.* **2004**, *43*, 3368-3398. (b) Beller, M.; Tillack, A.; Seayad, J. *Catalytic Amination Reactions of Olefins and Alkynes*; 2nd ed., 2004; Vol. 2. (c) Hartwig, J. F. *Science* **2002**, *297*, 1653-1654. (d) Beller, M.; Riermeier, T. H. *Transition Metals for Organic Synthesis* **1998**, *1*, 184-194. (e) Hegedus, L. S. *Angew. Chemie, Int. Ed.* **1988**, *27*, 1113-1126.

2. For general hydroamination reviews, see: (a) Odom, A. L. *Dalton Trans.* **2005**, 225-233. (b) Hultzsch, K. C. *Adv. Synth. Cat.* **2005**, *347*, 367-391. (c) Hultzsch, K. C.; Gribkov, D. V.; Hampel, F. *J. Organometallic Chem.* **2005**, *690*, 4441-4452. (d) Hong, S.; Marks, T. J. *Acc. Chem. Res.* **2004**, *37*, 673-686. (e) Doye, S. *Synlett* **2004**, 1653-1672. (f) Beller, M.; Seayad, J.; Tillack, A.; Jiao, H. *Angew. Chemie, Int. Ed.* **2004**, *43*, 3368-3398. (g) Roesky, P. W.; Mueller, T. E. *Angew. Chemie, Int. Ed.* **2003**, *42*, 2708-2710. (h) Pohlki, F.; Doye, S. *Chem. Soc. Rev.* **2003**, *32*, 104-114. (i) Bytschkov, I.; Doye, S. *Eur. J. Org. Chem.* **2003**, *2003*, 935-946. (j) Seayad, J.; Tillack, A.; Hartung, C. G.; Beller, M. *Adv. Synth. Cat.* **2002**, *344*, 795-813. (k) Togni, A. In *Catalytic Heterofunctionalization*; 1st ed.; Togni, A., Gruetzmacher, H., Eds.; Wiley-VCH: New York, 2001; pp 91-141. (l) Nobis, M.; Drießen-Holscher, B. *Angew. Chemie, Int. Ed.* **2001**, *40*, 3983-3985. (m) Eisen, M. S.; Straub, T.; Haskel, A. *J. Alloys Comp.* **1998**, *271-273*, 116-122. (n) Mueller, T. E.; Beller, M. *Chem. Rev.* **1998**, *98*, 675-703.

3. (a) Seyam, A. M.; Stubbert, B. D.; Jensen, T. R.; O'Donnell, J. J., III; Stern, C. L.; Marks, T. J. *Inorg. Chim. Acta* **2004**, *357*, 4029-4035. (b) Ryu, J.-S.; Marks, T. J.; McDonald, F. E. *J. Org. Chem.* **2004**, *69*, 1038-1052. (c) Hong, S.; Kawaoka, A. M.; Marks, T. J. *J. Am. Chem. Soc.* **2003**, *125*, 15878-15892. (d) Hong, S.; Tian, S.; Metz, M. V.; Marks, T. J. *J. Am. Chem. Soc.* **2003**, *125*, 14768-14783. (e) Ryu, J.-S.; Li, G. Y.; Marks, T. J. *J. Am. Chem. Soc.* **2003**, *125*, 12584-12605. (f) Hong, S.; Marks, T. J. *J. Am. Chem. Soc.* **2002**, *124*, 7886-7887. (g) Ryu, J.-S.; Marks, T. J.; McDonald, F. E. *Org. Lett.* **2001**, *3*, 3091-3094. (h) Arredondo, V. M.; Tian, S.; McDonald, F. E.; Marks, T. J. *J. Am. Chem. Soc.* **1999**, *121*, 3633-3639. (i) Arredondo, V. M.; McDonald, F. E.; Marks, T. J. *Organometallics* **1999**, *18*, 1949-1960. (j) Tian, S.; Arredondo, V. M.; Stern, C. L.; Marks, T. J. *Organometallics* **1999**, *18*, 2568-2570. (k) Arredondo, V. M.; McDonald, F. E.; Marks, T. J. *J. Am. Chem. Soc.* **1998**, *120*, 4871-4872. (l) Li, Y.; Marks, T. J. *J. Am. Chem. Soc.* **1998**, *120*, 1757-1771. (m) Roesky, P. W.; Stern, C. L.; Marks, T. J. *Organometallics* **1997**, *16*, 4705-4711. (n) Li, Y.; Marks, T. J. *J. Am. Chem. Soc.* **1996**, *118*, 9295-9306. (o) Li, Y.; Marks, T. J. *Organometallics* **1996**, *15*, 3770-3772. (p) Li, Y.; Marks, T. J. *J. Am. Chem. Soc.* **1996**, *118*, 707-708. (q) Giardello, M. A.; Conticello, V. P.; Brard, L.; Gagne, M. R.; Marks, T. J. *J. Am. Chem. Soc.* **1994**, *116*, 10241-10254. (r) Giardello, M. A.; Conticello, V. P.; Brard, L.; Sabat, M.; Rheingold, A. L.; Stern, C. L.; Marks, T. J. *J. Am. Chem. Soc.* **1994**, *116*, 10212-10240. (s) Li, Y.; Fu, P.-F.; Marks, T. J. *Organometallics* **1994**, *13*, 439-440. (t) Gagne, M. R.; Brard, L.; Conticello, V. P.; Giardello, M. A.; Stern, C. L.; Marks, T. J. *J. Am. Chem. Soc.* **1992**, *11*, 2003-2005. (u) Gagne, M. R.; Stern, C. L.; Marks, T. J. *J. Am. Chem. Soc.* **1992**, *114*, 275-94. (v) Gagne, M. R.; Marks, T. J. *J. Am. Chem. Soc.* **1989**, *111*, 4108-9. (w) Motta, A.; Lanza, G.; Fragala, I. L.; Marks, T. J. *Organometallics*, in press.

4.   For additional examples of group 3- and lanthanide-catalyzed HA, see: (a) Gribkov, D. V.; Hultzsch, K. C.; Hampel, F. *J. Am. Chem. Soc.* **2006**, *128*, 3748-3759. (b) Panda, T. K.; Zulys, A.; Gamer, M. T.; Roesky, P. W. *Organometallics* **2005**, *24*, 2197-2202. (c) Collin, J.; Daran, J.-C.; Jacquet, O.; Schulz, E.; Trifonov, A. *Chem. Eur. J.* **2005**, *11*, 3455-3462. (d) Kim, J. Y.; Livinghouse, T. *Org. Lett.* **2005**, *7*, 4391-4393. (e) Kim, J. Y.; Livinghouse, T. *Org. Lett.* **2005**, *7*, 1737-1739. (f) Molander, G. A.; Hasegawa, H. *Heterocycles* **2004**, *64*, 467-474. (g) Lauterwasser, F.; Hayes, P. G.; Brase, S.; Piers, W. E.; Schafer, L. L. *Organometallics* **2004**, *23*, 2234-2237. (h) Hultzsch, K. C.; Hampel, F.; Wagner, T. *Organometallics* **2004**, *23*, 2601-2612. (i) O'Shaughnessy, P. N.; Gillespie, K. M.; Knight, P. D.; Munslow, I. J.; Scott, P. *Dalton Trans.* **2004**, 2251-2256. (j) O'Shaughnessy, P. N.; Scott, P. *Tetrahedron Asym.* **2003**, *14*, 1979-1983. (k) O'Shaughnessy, P. N.; Knight, P. D.; Morton, C.; Gillespie, K. M.; Scott, P. *Chem. Comm.* **2003**, 1770-1771. (l) Kim, Y. K.; Livinghouse, T.; Horino, Y. *J. Am. Chem. Soc.* **2003**, *125*, 9560-9561. (m) Molander, G. A.; Pack, S. K. *Tetrahedron* **2003**, *59*, 10581-10591. (n) Molander, G. A.; Pack, S. K. *J. Org. Chem.* **2003**, *68*, 9214-9220. (o) Kim, Y. K.; Livinghouse, T. *Angew. Chemie, Int. Ed.* **2002**, *41*, 3645-3647. (p) Bürgstein, M. R.; Berberich, H.; Roesky, P. W. *Chem. Eur. J.* **2001**, *7*, 3078-3085. (q) Kim, Y. K.; Livinghouse, T.; Bercaw, J. E. *Tetrahedron Lett.* **2001**, *42*, 2933-2935. (r) Molander, G. A.; Dowdy, E. D. *J. Org. Chem.* **1999**, *64*, 6515-6517. (s) Molander, G. A.; Dowdy, E. D. *J. Org. Chem.* **1998**, *63*, 8983-8988.

5.   For group 4 catalysts see: (a) Esteruelas, M. A.; Lopez, A. M.; Mateo, A. C.; Onate, E. *Organometallics* **2006**. (b) Bexrud, J. A.; Beard, J. D.; Leitch, D. C.; Schafer, L. L. *Org. Lett.* **2005**, *7*, 1959-1962. (c) Esteruelas, M. A.; Lopez, A. M.; Mateo, A. C.; Onate, E. *Organometallics* **2005**, *24*, 5084-5094. (d) Kim, H.; Lee, P. H.; Livinghouse, T. *Chem. Comm.* **2005**, 5205-5207. (e) Hoover, J. M.; Petersen, J. R.; Pikul, J. H.; Johnson, A. R. *Organometallics* **2004**, *23*, 4614-4620. (f) Gribkov, D. V.; Hultzsch, K. C. *Angew. Chem. Int. Ed.* **2004**, *43*, 5542-5546. (g) Knight, P. D.; Munslow, I.; O'Shaughnessy, P. N.; Scott, P. *Chem. Comm.* **2004**, 894-895. (h) Li, C.; Thompson, R. K.; Gillon, B.; Patrick, B. O.; Schafer, L. L. *Chem. Comm.* **2003**, 2462-2463. (i) Ackermann, L.; Bergman, R. G. *Org. Lett.* **2002**, *4*, 1475-1478. (j) Ackermann, L.; Bergman, R. G.; Loy, R. N. *J. Am. Chem. Soc.* **2003**, *125*, 11956-11963.

6.   See for example: (a) Krogstad, D. A.; Cho, J.; DeBoer, A. J.; Klitzke, J. A.; Sanow, W. R.; Williams, H. A.; Halfen, J. A. *Inorg. Chim. Acta* **2006**, *359*, 136-148. (b) Zhang, J.; Yang, C.-G.; He, C. *J. Am. Chem. Soc.* **2006**, *128*, 1798-1799. (c) Kadzimirsz, D.; Hildebrandt, D.; Merz, K.; Dyker, G. *Chem. Comm.* **2006**, 661-662. (d) Bajracharya, G. B.; Huo, Z.; Yamamoto, Y. *J. Org. Chem.* **2005**, *70*, 4883-4886. (e) Field, L. D.; Messerle, B. A.; Vuong, K. Q.; Turner, P. *Organometallics* **2005**, *24*, 4241-4250. (f) Bender, C. F.; Widenhoefer, R. A. *J. Am. Chem. Soc.* **2005**, *127*, 1070-1071. (g) Zulys, A.; Dochnahl, M.; Hollmann, D.; Löhnwitz, K.; Herrmann, J.-S.; Roesky, P. W.; Blechert, S. *Angew. Chemie Int. Ed.* **2005**, *44*, 7794-7798. (h) Lutete, L. M.; Kadota, I.; Yamamoto, Y. *J. Am. Chem. Soc.* **2004**, *126*, 1622-1623. (i) Schlummer, B.; Hartwig, J. F. *Org. Lett.* **2002**, *4*, 1471-1474.

7.   Crimmin, M. R.; Casely, I. J.; Hill, M. S. *J. Am. Chem. Soc.* **2005**, *127*, 2042-2043.

8.   (a) Kadzimirsz, D.; Hildebrandt, D.; Merz, K.; Dyker, G. *Chem. Comm.* **2006**, 661-662. (b) Zhang, J.; Yang, C.-G.; He, C. *J. Am. Chem. Soc.* **2006**, *128*, 1798-1799. (c) Muller, T. E.; Grosche, M.; Herdtweck, E.; Pleier, A.-K.; Walter, E.; Yan, Y.-K. *Organometallics* **2000**, *19*, 170-183.

9.   For reviews of enantioselective catalysis with lanthanides, see: (a) Aspinall, H. C. *Chem. Rev.* **2002**, *102*, 1807-1850. (b) Inanaga, J.; Furuno, H.; Hayano, T. *Chem. Rev.* **2002**, *102*, 2211-2225. (c) Molander, G. A. *Pure Appl. Chem.* **2000**, *72*, 1757-1761.

10.   Shannon, R. D. *Acta Cryst.* **1976**, *A32*, 751-67.

11.   For reviews of constrained geometry catalysts, see: (a) Gromada, J.; Carpentier, J.-F.; Mortreux, A. *Coord. Chem. Rev.* **2004**, *248*, 397-410. (b) Okuda, J. *Dalton Trans.* **2003**, 2367-2378. (c) Arndt, S.; Okuda, J. *Chem. Rev.* **2002**, *102*, 1953-1976. (d) Britovsek, G. J. P.; Gibson, V. C.; Wass, D. F. *Angew. Chemie, Int. Ed.* **1999**, *38*, 428-447.

12. For reviews of 4f- and 5f-element chemistry, see: (a) Burns, C. J.; Neu, M. P.; Boukhalfa, H.; Gutowski, K. E.; Bridges, N. J.; Rogers, R. D. *Comprehensive Coordination Chemistry II* **2004**, *3*, 189-345. (b) Edelmann, F. T.; Freckmann, D. M. M.; Schumann, H. *Chem. Rev.* **2002**, *102*, 1851-1896. (c) Molander, G. A.; Dowdy, E. D. *Topics in Organometallic Chemistry* **1999**, *2*, 119-154. (d) Edelmann, F. T. *Angew. Chemie, Int. Ed.* **1995**, *34*, 2466-88. (e) Edelmann, F. T. In *Comprehensive Organometallic Chemistry II*; Abel, E. W., Stone, F. G. A., Wilkinson, G., Eds.; Pergamon: New York, 1995; Vol. 4; pp 11-213. (f) Schaverien, C. J. *Adv. Organomet. Chem.* **1994**, *36*, 283-362. (g) Molander, G. A. *Chem. Rev.* **1992**, *92*, 29-68. (h) *The Chemistry of the Actinide Elements*; Katz, J. J.; Seaborg, G. T.; Morss, L. R., Eds.; Chapman and Hall: New York, 1986. (i) *Fundamental and Technological Aspects of Organo-f-Element Chemistry*; Marks, T. J.; Fragalà, I. L., Eds.; Reidel: Dordrecht, 1985. (j) Marks, T. J.; Ernst, R. D. In *Comprehensive Organometallic Chemistry*; Abel, E. W., Stone, F. G. A., Wilkinson, G., Eds.; Pergamon: New York, 1982; Vol. 3; pp 173-270. (k) Marks, T. J. *Progress in Inorganic Chemistry* **1979**, *25*, 223-333. (l) Marks, T. J. *Progress in Inorganic Chemistry* **1979**, *25*, 223-333.

13. (a) Cotton, F. A.; Wilkinson, G.; Murillo, C. A.; Bochmann, M. *Advanced Inorganic Chemistry*; 6th ed.; John Wiley & Sons, Inc.: New York, 1999. (b) Kettle, S. F. A. *Physical Inorganic Chemistry: A Coordination Chemistry Approach*; Oxford University Press: New York, 1998. (c) Huheey, J. E.; Keiter, E. A.; Keiter, R. L. *Inorganic Chemistry: Principles of Structure and Reactivity*; 4th ed.; HarperCollins College Publishers: New York, 1993.

14. See, for example: (a) Barnea, E.; Eisen, M. S. *Coord. Chem. Rev.* **2006**, *250*, 855-899. (b) Burns, C. J. *Science* **2005**, *309*, 1823-1824. (c) Evans, W. J.; Kozimor, S. A.; Ziller, J. W. *Science* **2005**, *309*, 1835-1838. (d) Castro-Rodriguez, I.; Meyer, K. *J. Am. Chem. Soc.* **2005**, *127*, 11242-11243. (e) Evans, W. J.; Kozimor, S. A.; Ziller, J. W.; Kaltsoyannis, N. *J. Am. Chem. Soc.* **2004**, *126*, 14533-14547. (f) Castro-Rodriguez, I.; Nakai, H.; Zakharov, L. N.; Rheingold, A. L.; Meyer, K. *Science* **2004**, *305*, 1757-1760. (g) Castro-Rodriguez, I.; Nakai, H.; Gantzel, P.; Zakharov, L. N.; Rheingold, A. L.; Meyer, K. *J. Am. Chem. Soc.* **2003**, *125*, 15734-15735. (h) Diaconescu, P. L.; Arnold, P. L.; Baker, T. A.; Mindiola, D. J.; Cummins, C. C. *J. Am. Chem. Soc.* **2000**, *122*, 6108-6109.

15. Stubbert, B. D.; Stern, C. L.; Marks, T. J. *Organometallics* **2003**, *22*, 4836-4838.

16. Stubbert, B. D.; Marks, T. J., companion manuscript.

17. Bagnall, K. W. In *Topics in Inorganic Chemistry*; Robinson, P. L., Ed.; Elsevier Publishing Co.: Amsterdam, 1972; pp 93-95.

18.   Hermann, J. A.; Suttle, J. F. *Inorg. Synth.* **1957**, *5*, 143-5.

19.   Jamerson, J. D. Ph.D. Thesis, University of Alberta, 1974.

20.   (a) Bagnall, K. W.; Yanir, E. *J. Inorg. Nucl. Chem.* **1974**, *36*, 777-9. (b) Watt, G. W.; Gadd, K. F. *Inorg. Nucl. Chem. Lett.* **1973**, *9*, 203-5.

21.   (a) Fendrick, C. M.; Schertz, L. D.; Day, V. W.; Marks, T. J. *Organometallics* **1988**, *7*, 1828-1838. (b) Fendrick, C. M.; Mintz, E. A.; Schertz, L. D.; Marks, T. J. *Organometallics* **1984**, *3*, 819-21.

22.   Schnabel, R. C.; Scott, B. L.; Smith, W. H.; Burns, C. J. *J. Organometallic Chem.* **1999**, *591*, 14-23.

23.   Fagan, P. J.; Manriquez, J. M.; Maatta, E. A.; Seyam, A. M.; Marks, T. J. *J. Am. Chem. Soc.* **1981**, *103*, 6650-6667.

24.   Shapiro, P. J.; Schaefer, W. P.; Labinger, J. A.; Bercaw, J. E.; Cotter, W. D. *J. Am. Chem. Soc.* **1994**, *116*, 4623-40.

25.   (a) Kondo, T.; Okada, T.; Mitsudo, T. *J. Am. Chem. Soc.* **2002**, *124*, 186-187.   (b) Tamaru, Y.; Hojo, M.; Higashimura, H.; Yoshida, Z. *J. Am. Chem. Soc.* **1988**, *110*, 3994-4002.

26.   Tokuda, M.; Fujita, H.; Suginome, H. *Tetrahedron Lett.* **1990**, *31*, 5353-5356.

27.   Molinaro, C.; Jamison, T. F. *J. Am. Chem. Soc.* **2003**, *125*, 8076-8077.

28.   Shelxtl for WindowsNT: Crystal Structure Analysis Package, Bruker (1997).

29.   ORTEP-3 for Windows v. 1.075. Farrugia, L.J. *J. Appl. Cryst.* **1997**, *30*, 565.

30.   Gillespie, R. D.; Burwell, R. L., Jr.; Marks, T. J. *Langmuir* **1990**, *6*, 1465-1477.

31.   Espenson, J. H. *Chemical Kinetics and Reaction Mechanisms*; 2nd ed.; McGraw-Hill, Inc.: New York, 1995.

32.   (a) Berthet, J. C.; Ephritikhine, M. *Coord. Chem. Rev.* **1998**, *178-180*, 83-116. (b) Kuhlman, R. *Coord. Chem. Rev.* **1997**, *167*, 205-232. (c) Bradley, D. C.; Chisholm, M. H. *Acc. Chem. Res.* **1976**, *9*, 273-80.

33. (a) Ossola, F.; Rossetto, G.; Zanella, P.; Arudini, A.; Jamerson, J. D.; Takats, J.; Dormond, A. *Inorg. Synth.* **1992**, *29*, 234-8. (b) Arduini, A. L.; Takats, J. *Inorg. Chem.* **1981**, *20*, 2480-5. (c) Arduini, A. L.; Jamerson, J. D.; Takats, J. *Inorg. Chem.* **1981**, *20*, 2474-9. (d) Arduini, A. L.; Edelstein, M.; Jamerson, J. D.; Reynolds, J. G.; Schimd, K.; Takats, J. *Inorganic Chemistry* **1981**, *20*, 2470-2474. (e) Jamerson, J. D.; Takats, J. *J. Organometallic Chem.* **1974**, *78*, C23-C25. (f) Jones, R. G.; Karmas, G.; Martin, G. A., Jr.; Gilman, H. *J. Am. Chem. Soc.* **1956**, *78*, 4285-4286.

34. (a) Taft, R. W.; Bordwell, F. G. *Acc. Chem. Res.* **1988**, *21*, 463-469. (b) Bordwell, F. G. *Acc. Chem. Res.* **1988**, *21*, 456-463. (c) Bordwell, F. G.; Bausch, M. J. *J. Am. Chem. Soc.* **1983**, *105*, 6188-6189.

35. (a) Trnka, T. M.; Bonanno, J. B.; Bridgewater, B. M.; Parkin, G. *Organometallics* **2001**, *20*, 3255-3264. (b) Roussel, P.; Alcock, N. W.; Boaretto, R.; Kingsley, A. J.; Munslow, I. J.; Sanders, C. J.; Scott, P. *Inorg. Chem.* **1999**, *38*, 3651-3656. (c) Straub, T.; Frank, W.; Reiss, G. J.; Eisen, M. S. *Dalton Trans.* **1996**, 2541-2546. (d) Scott, P.; Hitchcock, P. B. *Dalton Trans.* **1995**, 603-609. (e) Gilbert, T. M.; Ryan, R. R.; Sattelberger, A. P. *Organometallics* **1988**, *7*, 2514-2518.

36. (a) Brinkman, E. A.; Berger, S.; Brauman, J. I. *J. Am. Chem. Soc.* **1994**, *116*, 8304-8310. (b) Hopkinson, A. C.; Lien, M. H. *J. Org. Chem.* **1981**, *46*, 998-1003.

37. See for example: Basolo, F. *New J. Chem.* **1994**, *18*, 19-24.

38. (a) Evans, W. J.; Kozimor, S. A.; Hillman, W. R.; Ziller, J. W. *Organometallics* **2005**, *24*, 4676-4683. (b) Jantunen, K. C.; Burns, C. J.; Castro-Rodriguez, I.; Da Re, R. E.; Golden, J. T.; Morris, D. E.; Scott, B. L.; Taw, F. L.; Kiplinger, J. L. *Organometallics* **2004**, *23*, 4682-4692.

39. Carpenetti, D. W.; Kloppenburg, L.; Kupec, J. T.; Petersen, J. L. *Organometallics* **1996**, *15*, 1572-81.

40. See for example: Fagan, P. J.; Manriquez, J. M.; Marks, T. J.; Day, C. S.; Vollmer, S. H.; Day, V. W. *Organometallics* **1982**, *1*, 170-80, and references therein.

41. Golden, J. T.; Kazul'kin, D. N.; Scott, B. L.; Voskoboynikov, A. Z.; Burns, C. J. *Organometallics* **2003**, *22*, 3971-3973.

42. For general reviews, see: (a) Barron, A. R. *Metallocene-Based Polyolefins* **2000**, *1*, 33-67. (b) Chen, E. Y.-X.; Marks, T. J. *Chem. Rev.* **2000**, *100*, 1391-1434, and references therein.

43. Where necessary, N_t values at 25 °C estimated based on activation parameters determined in the lead reference.

44. Induction periods have been reported in support of a [2 + 2] cycloaddition pathway proceeding via a rapid pre-equilibrium for *intermolecular* HA mediated by group 4 and An metals. The proposed active species, $L_2M=NR$, is postulated to form via α-elimination from $L_2M[N(H)R]_2$ species (see ref. 2a, h-n and 16 for details).

45. Stubbert, B. D.; Marks, T. J., unpublished results. Prolonged reaction times and forcing conditions (T > 120 °C) in alkane and aromatic solvents do not induce catalyst decomposition with similar 1° and 2° amine substrates.

46. Sammes, P. G.; Weller, D. J. *Synthesis* **1995**, 1205-22.

47. (a) Motta, A.; Lanza, G.; Fragala, I. L.; Marks, T. J. *Organometallics* **2004**, *23*, 4097-4104. (b) (a) Motta, A.; Lanza, G.; Fragala, I. L.; Marks, T. J. *Organometallics*, in press.

48. (a) Tobisch, S. *Dalton Trans.* **2006,** (35), 4277-4285. (b) Tobisch, S. *Chem. Eur. J.* **2006**, *12*, 2520-2531. (c) Tobisch, S. *J. Am. Chem. Soc.* **2005**, *127*, 11979-11988.

49. March, J. Advanced Organic Chemistry: Reactions, Mechanisms, and Structure; 4th ed.; John Wiley & Sons: New York, 1992.

50. See for example: (a) Shakhnovich, E. I. *Nat. Struct. Biol.* **1999**, *6*, 99-102. (b) Stryer, L. *Biochemistry*; 4th ed.; W. H. Freeman and Company: New York, 1995; pp 181-206.

51. Hazari, N.; Mountford, P. *Acc. Chem. Res.* **2005**, *38*, 839-849.

52. (a) Walton, J. C.; Studer, A. *Acc. Chem. Res.* **2005**, *38*, 794-802. (b) Kemper, J.; Studer, A. *Angew. Chemie, Int. Ed.* **2005**, *44*, 4914-4917. (c) Newcomb, M.; Burchill, M. T.; Deeb, T. M. *J. Am. Chem. Soc.* **1988**, *110*, 6528-6535.

53. Note that the dependence on ring size and significant C–C substituent electronic effects for alkene, alkyne, allene, and diene unsaturations seem to preclude turnover-limiting heterocycle protonolysis *after* C–C insertion into M–N (i.e., $k_{protonolysis} > k_{insertion}$ appears operative here).

54. (a) Illuminati, G.; Mandolini, L. *Acc. Chem. Res.* **1981**, *14*, 95-102. (b) Mandolini, L. *J. Am. Chem. Soc.* **1978**, *100*, 550-554.

55. (a) Baranger, A. M.; Walsh, P. J.; Bergman, R. G. *J. Am. Chem. Soc.* **1993**, *115*, 2753-2763. (b) Walsh, P. J.; Baranger, A. M.; Bergman, R. G. *J. Am. Chem. Soc.* **1992**, *114*, 1708-1719.

56. (a) Straub, T.; Haskel, A.; Neyroud, T. G.; Kapon, M.; Botoshansky, M.; Eisen, M. S. *Organometallics* **2001**, *20*, 5017-5035. (b) Haskel, A.; Straub, T.; Eisen, M. S. *Organometallics* **1996**, *15*, 3773-3775.

57. For the following pathway ([A] = [M=NR]):

$$\frac{d[A]}{dt} = k_1[M(NHR)_2] - k_2[A][RNH_2] - k_3[A][C{\equiv}C] = 0$$

$$\implies k_2[A][RNH_2] + k_3[A][C{\equiv}C] = k_2[M(NHR)_2]$$

$$\therefore [A] = \frac{k_1[M(NHR)_2]}{k_2[RNH_2] + k_3[C{\equiv}C]}$$

If the rate of product formation is

$$\nu = k_3[A][C{\equiv}C],$$

$$\text{then } \nu = \frac{k_1 k_3[M(NHR)_2][C{\equiv}C]}{k_2[RNH_2] + k_3[C{\equiv}C]}$$

Therefore: (i) for k_3 very large, $\nu \sim [M(NHR)_2]^1[RNH_2]^0[C{\equiv}C]^0$
(ii) for k_2 very large, $\nu \sim [M(NHR)_2]^1[RNH_2]^{-1}[C{\equiv}C]^1$
(iii) for k_3 very small, $\nu \sim [M(NHR)_2]^1[RNH_2]^{-1}[C{\equiv}C]^1$

58. Wang, J.; Dash, A. K.; Kapon, M.; Berthet, J.-C.; Ephritikhine, M.; Eisen, M. S. *Chem. Eur. J.* **2002**, *8*, 5384-5396.

Chapter 2

1. For general hydroamination reviews, see: (a) Odom, A. L. *Dalton Trans.* **2005**, 225-233. (b) Hultzsch, K. C. *Advanced Synthesis & Catalysis* **2005**, *347*, 367-391. (c) Hultzsch, K. C.; Gribkov, D. V.; Hampel, F. *J. Organometallic Chem.* **2005**, *690*, 4441-4452. (d) Hong, S.; Marks, T. J. *Acc. Chem. Res.* **2004**, *37*, 673-686. (e) Doye, S. *Synlett* **2004**, 1653-1672. (f) Beller, M.; Seayad, J.; Tillack, A.; Jiao, H. *Angew. Chemie, Int. Ed.* **2004**, *43*, 3368-3398. (g) Roesky, P. W.; Mueller, T. E. *Angew. Chemie, Int. Ed.* **2003**, *42*, 2708-2710. (h) Pohlki, F.; Doye, S. *Chem. Soc. Rev.* **2003**, *32*, 104-114. (i) Bytschkov, I.; Doye, S. *Eur. J. Org. Chem.* **2003**, *2003*, 935-946. (j) Seayad, J.; Tillack, A.; Hartung, C. G.; Beller, M. *Adv. Synth. Cat.* **2002**, *344*, 795-813. (k) Togni, A. In *Catalytic Heterofunctionalization*; 1st ed.; Togni, A., Gruetzmacher, H., Eds.; Wiley-VCH: New York, 2001; pp 91-141. (l) Nobis, M.; Drießen-Holscher, B. *Angew. Chemie, Int. Ed.* **2001**, *40*, 3983-3985. (m) Eisen, M. S.; Straub, T.; Haskel, A. *J. Alloys Comp.* **1998**, *271-273*, 116-122. (n) Mueller, T. E.; Beller, M. *Chem. Rev.* **1998**, *98*, 675-703.

2. For general C–N bond-formation references, see: (a) Beller, M.; Seayad, J.; Tillack, A.; Jiao, H. *Angew. Chemie, Int. Ed.* **2004**, *43*, 3368-3398. (b) Beller, M.; Tillack, A.; Seayad, J. *Catalytic Amination Reactions of Olefins and Alkynes*; 2nd ed., 2004; Vol. 2. (c) Hartwig, J. F. *Science* **2002**, *297*, 1653-1654. (d) Beller, M.; Riermeier, T. H. *Transition Metals for Organic Synthesis* **1998**, *1*, 184-194. (e) Hegedus, L. S. *Angew. Chemie, Int. Ed.* **1988**, *27*, 1113-1126.

3.	(a) Motta, A.; Lanza, G.; Fragala, I. L.; Marks, T. J. *Organometallics* **2004**, *23*, 4097-4104. (b) Seyam, A. M.; Stubbert, B. D.; Jensen, T. R.; O'Donnell, J. J., III; Stern, C. L.; Marks, T. J. *Inorg. Chim. Acta* **2004**, *357*, 4029-4035. (c) Ryu, J.-S.; Marks, T. J.; McDonald, F. E. *J. Org. Chem.* **2004**, *69*, 1038-1052. (d) Hong, S.; Kawaoka, A. M.; Marks, T. J. *J. Am. Chem. Soc.* **2003**, *125*, 15878-15892. (e) Hong, S.; Tian, S.; Metz, M. V.; Marks, T. J. *J. Am. Chem. Soc.* **2003**, *125*, 14768-14783. (f) Ryu, J.-S.; Li, G. Y.; Marks, T. J. *J. Am. Chem. Soc.* **2003**, *125*, 12584-12605. (g) Hong, S.; Marks, T. J. *J. Am. Chem. Soc.* **2002**, *124*, 7886-7887. (h) Ryu, J.-S.; Marks, T. J.; McDonald, F. E. *Org. Lett.* **2001**, *3*, 3091-3094. (i) Arredondo, V. M.; Tian, S.; McDonald, F. E.; Marks, T. J. *J. Am. Chem. Soc.* **1999**, *121*, 3633-3639. (j) Arredondo, V. M.; McDonald, F. E.; Marks, T. J. *Organometallics* **1999**, *18*, 1949-1960. (k) Tian, S.; Arredondo, V. M.; Stern, C. L.; Marks, T. J. *Organometallics* **1999**, *18*, 2568-2570. (l) Arredondo, V. M.; McDonald, F. E.; Marks, T. J. *J. Am. Chem. Soc.* **1998**, *120*, 4871-4872. (m) Li, Y.; Marks, T. J. *J. Am. Chem. Soc.* **1998**, *120*, 1757-1771. (n) Roesky, P. W.; Stern, C. L.; Marks, T. J. *Organometallics* **1997**, *16*, 4705-4711. (o) Li, Y.; Marks, T. J. *J. Am. Chem. Soc.* **1996**, *118*, 9295-9306. (p) Li, Y.; Marks, T. J. *Organometallics* **1996**, *15*, 3770-3772. (q) Li, Y.; Marks, T. J. *J. Am. Chem. Soc.* **1996**, *118*, 707-708. (r) Giardello, M. A.; Conticello, V. P.; Brard, L.; Gagné, M. R.; Marks, T. J. *J. Am. Chem. Soc.* **1994**, *116*, 10241-10254. (s) Giardello, M. A.; Conticello, V. P.; Brard, L.; Sabat, M.; Rheingold, A. L.; Stern, C. L.; Marks, T. J. *J. Am. Chem. Soc.* **1994**, *116*, 10212-10240. (t) Li, Y.; Fu, P.-F.; Marks, T. J. *Organometallics* **1994**, *13*, 439-440. (u) Gagné, M. R.; Brard, L.; Conticello, V. P.; Giardello, M. A.; Stern, C. L.; Marks, T. J. *J. Am. Chem. Soc.* **1992**, *11*, 2003-2005. (v) Gagné, M. R.; Stern, C. L.; Marks, T. J. *J. Am. Chem. Soc.* **1992**, *114*, 275-94. (w) Gagné, M. R.; Marks, T. J. *J. Am. Chem. Soc.* **1989**, *111*, 4108-9. (x) Motta, A.; Lanza, G.; Fragala, I. L.; Marks, T. J. *Organometallics*, ASAP, October 12, 2006.
.

4. For additional examples of group 3- and lanthanide-catalyzed intramolecular HA, see: (a) Bambirra, S.; Tsurugi, H.; van Leusen, D.; Hessen, B. *Dalton Trans.* **2006**, 1157-1161. (b) Gribkov, D. V.; Hultzsch, K. C.; Hampel, F. *J. Am. Chem. Soc.* **2006**, *128*, 3748-3759. (c) Panda, T. K.; Zulys, A.; Gamer, M. T.; Roesky, P. W. *Organometallics* **2005**, *24*, 2197-2202. (d) Collin, J.; Daran, J.-C.; Jacquet, O.; Schulz, E.; Trifonov, A. *Chem. Eur. J.* **2005**, *11*, 3455-3462. (e) Kim, J. Y.; Livinghouse, T. *Org. Lett.* **2005**, *7*, 4391-4393. (f) Kim, J. Y.; Livinghouse, T. *Org. Lett.* **2005**, *7*, 1737-1739. (g) Molander, G. A.; Hasegawa, H. *Heterocycles* **2004**, *64*, 467-474. (h) Lauterwasser, F.; Hayes, P. G.; Brase, S.; Piers, W. E.; Schafer, L. L. *Organometallics* **2004**, *23*, 2234-2237. (i) Hultzsch, K. C.; Hampel, F.; Wagner, T. *Organometallics* **2004**, *23*, 2601-2612. (j) O'Shaughnessy, P. N.; Gillespie, K. M.; Knight, P. D.; Munslow, I. J.; Scott, P. *Dalton Trans.* **2004**, 2251-2256. (k) O'Shaughnessy, P. N.; Scott, P. *Tetrahedron Asym.* **2003**, *14*, 1979-1983. (l) O'Shaughnessy, P. N.; Knight, P. D.; Morton, C.; Gillespie, K. M.; Scott, P. *Chem. Comm.* **2003**, 1770-1771. (m) Kim, Y. K.; Livinghouse, T.; Horino, Y. *J. Am. Chem. Soc.* **2003**, *125*, 9560-9561. (n) Molander, G. A.; Pack, S. K. *Tetrahedron* **2003**, *59*, 10581-10591. (o) Molander, G. A.; Pack, S. K. *J. Org. Chem.* **2003**, *68*, 9214-9220. (p) Kim, Y. K.; Livinghouse, T. *Angew. Chemie, Int. Ed.* **2002**, *41*, 3645-3647. (q) Bürgstein, M. R.; Berberich, H.; Roesky, P. W. *Chem. Eur. J.* **2001**, *7*, 3078-3085. (r) Kim, Y. K.; Livinghouse, T.; Bercaw, J. E. *Tetrahedron Lett.* **2001**, *42*, 2933-2935. (s) Molander, G. A.; Dowdy, E. D. *J. Org. Chem.* **1999**, *64*, 6515-6517. (t) Molander, G. A.; Dowdy, E. D. *J. Org. Chem.* **1998**, *63*, 8983-8988.

5. A slightly modified pathway arguing in favor of turnover-limiting heterocycle protonolysis in intramolecular aminoallene and aminodiene HA/cyclization was proposed from DFT calculations. (a) Tobisch, S. *Chem. Eur. J.* **2006**, *12*, 2520-2531. (b) Tobisch, S. *J. Am. Chem. Soc.* **2005**, *127*, 11979-11988.

6. (a) Kim, H.; Lee, P. H.; Livinghouse, T. *Chem. Comm.* **2005**, 5205-5207. (b) Bexrud, J. A.; Beard, J. D.; Leitch, D. C.; Schafer, L. L. *Org. Lett.* **2005**, *7*, 1959-1962.

7. (a) Ackermann, L.; Bergman, R. G.; Loy, R. N. *J. Am. Chem. Soc.* **2003**, *125*, 11956-11963. (b) Li, C.; Thompson, R. K.; Gillon, B.; Patrick, B. O.; Schafer, L. L. *Chem. Comm.* **2003**, 2462-2463. (c) Ackermann, L.; Bergman, R. G. *Org. Lett.* **2002**, *4*, 1475-1478. (d) McGrane, P. L.; Livinghouse, T. *J. Org. Chem.* **1992**, *57*, 1323-1324. (e) McGrane, P. L.; Jensen, M.; Livinghouse, T. *J. Am. Chem. Soc.* **1992**, *114*, 5459-5460.

8. (a) Baranger, A. M.; Walsh, P. J.; Bergman, R. G. *J. Am. Chem. Soc.* **1993**, *115*, 2753-2763. (b) Walsh, P. J.; Baranger, A. M.; Bergman, R. G. *J. Am. Chem. Soc.* **1992**, *114*, 1708-1719.

9.   (a) Wang, J.; Dash, A. K.; Kapon, M.; Berthet, J.-C.; Ephritikhine, M.; Eisen, M. S. *Chem. Eur. J.* **2002**, *8*, 5384-5396. (b) Straub, T.; Haskel, A.; Neyroud, T. G.; Kapon, M.; Botoshansky, M.; Eisen, M. S. *Organometallics* **2001**, *20*, 5017-5035. (c) Haskel, A.; Straub, T.; Eisen, M. S. *Organometallics* **1996**, *15*, 3773-3775.

10.   (a) Stubbert, B. D.; Stern, C. L.; Marks, T. J. *Organometallics* **2003**, *22*, 4836-4838. (b) Stubbert, B. D.; Marks, T. J., companion manuscript.

11.   Bagnall, K. W. In *Topics in Inorganic Chemistry*; Robinson, P. L., Ed.; Elsevier Publishing Co.: Amsterdam, 1972; pp 93-95.

12.   Hermann, J. A.; Suttle, J. F. *Inorg. Synth.* **1957**, *5*, 143-5.

13.   (a) Simpson, S. J.; Turner, H. W.; Andersen, R. A. *Inorg. Chem.* **1981**, *20*, 2991-2995. (b) Turner, H. W.; Simpson, S. J.; Andersen, R. A. *J. Am. Chem. Soc.* **1979**, *101*, 2782. (c) Turner, H. W.; Andersen, R. A.; Zalkin, A.; Templeton, D. H. *Inorg. Chem.* **1979**, *18*, 1221-1224. (d) Bradley, D. C.; Ghotra, J. S.; Hart, F. A. *Inorg. Nucl. Chem.* **1974**, *10*, 209-211.

14.   Schnabel, R. C.; Scott, B. L.; Smith, W. H.; Burns, C. J. *J. Organomet. Chem.* **1999**, *591*, 14-23.

15.   Fagan, P. J.; Manriquez, J. M.; Maatta, E. A.; Seyam, A. M.; Marks, T. J. *J. Am. Chem. Soc.* **1981**, *103*, 6650-6667.

16.   Carpenetti, D. W.; Kloppenburg, L.; Kupec, J. T.; Petersen, J. L. *Organometallics* **1996**, *15*, 1572-1581.

17.   Shapiro, P. J.; Schaefer, W. P.; Labinger, J. A.; Bercaw, J. E.; Cotter, W. D. *J. Am. Chem. Soc.* **1994**, *116*, 4623-40.

18.   Tamaru, Y.; Hojo, M.; Higashimura, H.; Yoshida, Z. *J. Am. Chem. Soc.* **1988**, *110*, 3994-4002.

19.   Smith, J. K.; Bergbreiter, D. E.; Newcomb, M. *J. Org. Chem.* **1985**, *50*, 4549-4553.

20.   Shelxtl for WindowsNT: Crystal Structure Analysis Package, Bruker (1997).

21.   ORTEP-3 for Windows v. 1.075. Farrugia, L.J. *J. Appl. Cryst.* **1997**, *30*, 565.

22.   Isolated as the *exo*-methylene product from thermally-induced 1,3-sigmatropic shift (–SiMe$_3$ migration to N; see also ref. 3p).

H$_2$N · · · Me$_3$Si — (Cp'$_2$An(R)Cl) → (N, SiMe$_3$) — 60 °C → (N, SiMe$_3$)
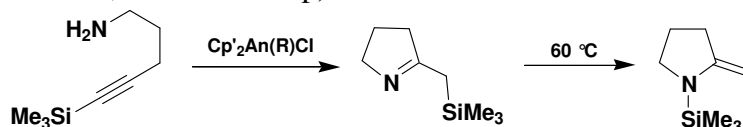
23.   Espenson, J. H. *Chemical Kinetics and Reaction Mechanisms*; 2nd ed.; McGraw-Hill, Inc.: New York, 1995.

24.   (a) Schubert, E. M. *J. Chem. Ed.* **1992**, *69*, 62. (b) Evans, D. F. *J. Chem. Soc.* **1959**, 2003-2005.

25.   Heating (CGC)Th(NMe$_2$)$_2$ in a 1:1 *ortho*-C$_6$H$_4$F$_2$:C$_6$D$_6$ solvent mixture to 60 °C in the absence of substrate leads to rapid decomposition of **1** and formation of an uncharacterized product.

26.   Shannon, R. D. *Acta Cryst.* **1976**, *A32*, 751-67.

27.   (a) Golden, J. T.; Kazul'kin, D. N.; Scott, B. L.; Voskoboynikov, A. Z.; Burns, C. J. *Organometallics* **2003**, *22*, 3971-3973. (b) Roussel, P.; Alcock, N. W.; Boaretto, R.; Kingsley, A. J.; Munslow, I. J.; Sanders, C. J.; Scott, P. *Inorg. Chem.* **1999**, *38*, 3651-3656. (c) Scott, P.; Hitchcock, P. B. *Dalton Trans.* **1995**, 603-609.

28.   (a) Brinkman, E. A.; Berger, S.; Brauman, J. I. *J. Am. Chem. Soc.* **1994**, *116*, 8304-8310. (b) Hopkinson, A. C.; Lien, M. H. *J. Org. Chem.* **1981**, *46*, 998-1003.

29.   For recent reviews on the chemistry of 4f- and 5f-elements, see: (a) Burns, C. J.; Neu, M. P.; Boukhalfa, H.; Gutowski, K. E.; Bridges, N. J.; Rogers, R. D. In *Comprehensive Coordination Chemistry II*; Abel, E. W., Stone, F. G. A., Wilkinson, G., Eds.; Pergamon: New York, 1995; Vol. 4; pp 189-345. (b) Edelmann, F. T.; Freckmann, D. M. M.; Schumann, H. *Chem. Rev.* **2002**, *102*, 1851-1896. (c) Molander, G. A.; Dowdy, E. D. *Topics in Organometallic Chemistry* **1999**, *2*, 119-154. (d) Edelmann, F. T. *Angew. Chemie, Int. Ed.* **1995**, *34*, 2466-88. (e) Edelmann, F. T. In *Comprehensive Organometallic Chemistry II*; Abel, E. W., Stone, F. G. A., Wilkinson, G., Eds.; Pergamon: New York, 1995; Vol. 4; pp 11-213. (f) Schaverien, C. J. *Adv. Organomet. Chem.* **1994**, *36*, 283-362.

30.   Klooster, W. T.; Brammer, L.; Schaverien, C. J.; Budzelaar, P. M. H. *J. Am. Chem. Soc.* **1999**, *121*, 1381-1382.

31. See, for example: (a) Turner, L. E.; Thorn, M. G.; Fanwick, P. E.; Rothwell, I. P. *Organometallics* **2004**, *23*, 1576-1593. (b) Rothwell, I. P. *Chem. Comm.* **1997**, 1331-1338. (c) Zambrano, C. H.; Profilet, R. D.; Hill, J. E.; Fanwick, P. E.; Rothwell, I. P. *Polyhedron* **1993**, *12*, 689-708. (d) Rothwell, I. P. *Acc. Chem. Res.* **1988**, *21*, 153-159. (e) Lateskey, S.; Keddington, J.; McMullen, A. K.; Rothwell, I. P.; Huffman, J. C. *Inorg. Chem.* **1985**, *24*, 995-1001, and references therein.

32. (a) Clark, D. L.; Grumbine, S. K.; Scott, B. L.; Watkin, J. G. *Organometallics* **1996**, *15*, 949-57. (b) Butcher, R. J.; Clark, D. L.; Grumbine, S. K.; Scott, B. L.; Watkin, J. G. *Organometallics* **1996**, *15*, 1488-96. (c) Berg, J. M.; Clark, D. L.; Huffman, J. C.; Morris, D. E.; Sattelberger, A. P.; Streib, W. E.; Van der Sluys, W. G.; Watkin, J. G. *J. Am. Chem. Soc.* **1992**, *114*, 10811-21.

33. For reviews of constrained geometry catalysts, see: (a) Gromada, J.; Carpentier, J.-F.; Mortreux, A. *Coord. Chem. Rev.* **2004**, *248*, 397-410. (b) Okuda, J. *Dalton Trans.* **2003**, 2367-2378. (c) Arndt, S.; Okuda, J. *Chem. Rev.* **2002**, *102*, 1953-1976. (d) Britovsek, G. J. P.; Gibson, V. C.; Wass, D. F. *Angew. Chemie, Int. Ed.* **1999**, *38*, 428-447.

34. For examples of $L_2An=NR$ complexes and their reactivity, see: (a) Zi, G.; Blosch, L. L.; Jia, L.; Andersen, R. A. *Organometallics* **2005**, *24*, 4602-4612. (b) Arney, D. S. J.; Burns, C. J. *J. Am. Chem. Soc.* **1995**, *117*, 9448-60. (c) Brennan, J. G.; Andersen, R. A.; Zalkin, A. *J. Am. Chem. Soc.* **1988**, *110*, 4554-4558. (d) Morris, D. E.; DaRe, R. E.; Jantunen, K. C.; Castro-Rodriguez, I.; Kiplinger, J. L. *Organometallics* **2004**, *23*, 5142-5153. (e) Jantunen, K. C.; Burns, C. J.; Castro-Rodriguez, I.; Da Re, R. E.; Golden, J. T.; Morris, D. E.; Scott, B. L.; Taw, F. L.; Kiplinger, J. L. *Organometallics* **2004**, *23*, 4682-4692.

35. (a) Bursten, B. E.; Strittmatter, R. J. *Angew. Chemie, Int. Ed.* **1991**, *30*, 1069-1085. (b) Pepper, M.; Bursten, B. E. *Chem. Rev.* **1991**, *91*, 719-741. (c) Burns, C. J.; Bursten, B. E. *Comm. Inorg. Chem.* **1989**, *9*, 61-93.

36. Sammes, P. G.; Weller, D. J. *Synthesis* **1995**, 1205-22.

37. For the following pathway, where [A] = [M=NR]:
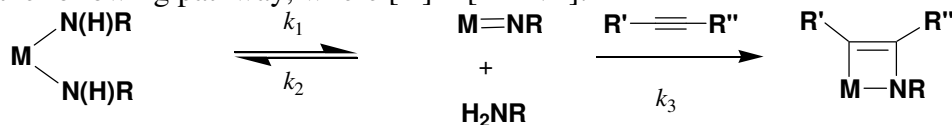
$$\frac{d[A]}{dt} = k_1[M(NHR)_2] - k_2[A][RNH_2] - k_3[A][C\equiv C] = 0$$

$$\implies k_2[A][RNH_2] + k_3[A][C\equiv C] = k_2[M(NHR)_2]$$

$$\therefore \quad [A] = \frac{k_1[M(NHR)_2]}{k_2[RNH_2] + k_3[C\equiv C]}$$

If the rate of product formation is

$$v = k_3[A][C\equiv C],$$

then $$v = \frac{k_1 k_3[M(NHR)_2][C\equiv C]}{k_2[RNH_2] + k_3[C\equiv C]}$$

Therefore: (i) for k_3 very large, $v \sim [M(NHR)_2]^1[RNH_2]^0[C\equiv C]^0$

(ii) for k_2 very large, $v \sim [M(NHR)_2]^1[RNH_2]^{-1}[C\equiv C]^1$

(iii) for k_3 very small, $v \sim [M(NHR)_2]^1[RNH_2]^{-1}[C\equiv C]^1$

38. (a) Lin, Z.; Marks, T. J. *J. Am. Chem. Soc.* **1990**, *112*, 5515-5525. (b) Lin, Z.; Le Marechal, J.-F.; Sabat, M.; Marks, T. J. *J. Am. Chem. Soc.* **1987**, *109*, 4127-4129. (c) Lin, Z.; Marks, T. J. *J. Am. Chem. Soc.* **1987**, *109*, 7979-7985.

39. (a) Arduini, A. L.; Edelstein, M.; Jamerson, J. D.; Reynolds, J. G.; Schimd, K.; Takats, J. *Inorg. Chem.* **1981**, *20*, 2470-2474. (b) Fagan, P. J.; Manriquez, J. M.; Vollmer, S. H.; Day, C. S.; Day, V. W.; Marks, T. J. *J. Am. Chem. Soc.* **1981**, *103*, 2206-2220.

40. (a) Lanza, G.; Fragala, I. L.; Marks, T. J. *Organometallics* **2002**, *21*, 5594-5612. (b) Lanza, G.; Fragala, I. L.; Marks, T. J. *Organometallics* **2001**, *20*, 4006-4017. (c) Lanza, G.; Fragala, I. L.; Marks, T. J. *J. Am. Chem. Soc.* **2000**, *122*, 12764-12777.

41. (a) Gribkov, D. V.; Hultzsch, K. C. *Angew. Chemie, Int. Ed.* **2004**, *43*, 5542-5546. (b) Knight, P. D.; Munslow, I.; O'Shaughnessy, P. N.; Scott, P. *Chem. Comm.* **2004**, 894-895.

42. An analogous mechanism is invoked in imidotitanium synthesis: Hazari, N.; Mountford, P. *Acc. Chem. Res.* **2005**, *38*, 839-849.

43. (a) Walton, J. C.; Studer, A. *Acc. Chem. Res.* **2005**, *38*, 794-802. (b) Kemper, J.; Studer, A. *Angew. Chemie, Int. Ed.* **2005**, *44*, 4914-4917. (c) Newcomb, M.; Burchill, M. T.; Deeb, T. M. *J. Am. Chem. Soc.* **1988**, *110*, 6528-6535.

44. (a) Kawaoka, A. M.; Douglass, M. R.; Marks, T. J. *Organometallics* **2003**, *22*, 4630-4632. (b) Kim, Y. K.; Livinghouse, T.; Bercaw, J. E. *Tetrahedron Lett.* **2001**, *42*, 2933-2935.

45. (a) Illuminati, G.; Mandolini, L. *Acc. Chem. Res.* **1981**, *14*, 95-102. (b) Mandolini, L. *J. Am. Chem. Soc.* **1978**, *100*, 550-554.

46. Experimentally-determined $\Delta S^{\ddagger}$ = -44.5(8) eu for intermolecular HA is representative of a bimolecular C≡C insertion process, as opposed to the unimolecular insertion proposed for intramolecular HA/cyclization ($\Delta S^{\ddagger}$ ca. -30 eu). See ref. 1d for details.

47. (a) Cummins, C. C.; Schaller, C. P.; Van Duyne, G. D.; Wolczanski, P. T.; Chan, A. W. E.; Hoffman, R. *J. Am. Chem. Soc.* **1991**, *113*, 2985-2994. (b) Cummins, C. C.; Baxter, S. M.; Wolczanski, P. T. *J. Am. Chem. Soc.* **1988**, *110*, 8731-8733.

Appendix

1. For general hydroamination reviews, see: (a) Odom, A. L. *Dalton Trans.* **2005**, 225-233. (b) Hultzsch, K. C. *Advanced Synthesis & Catalysis* **2005**, *347*, 367-391. (c) Hultzsch, K. C.; Gribkov, D. V.; Hampel, F. *J. Organometallic Chem.* **2005**, *690*, 4441-4452. (d) Hong, S.; Marks, T. J. *Acc. Chem. Res.* **2004**, *37*, 673-686. (e) Doye, S. *Synlett* **2004**, 1653-1672. (f) Beller, M.; Seayad, J.; Tillack, A.; Jiao, H. *Angew. Chemie, Int. Ed.* **2004**, *43*, 3368-3398. (g) Roesky, P. W.; Mueller, T. E. *Angew. Chemie, Int. Ed.* **2003**, *42*, 2708-2710. (h) Pohlki, F.; Doye, S. *Chem. Soc. Rev.* **2003**, *32*, 104-114. (i) Bytschkov, I.; Doye, S. *Eur. J. Org. Chem.* **2003**, *2003*, 935-946. (j) Seayad, J.; Tillack, A.; Hartung, C. G.; Beller, M. *Adv. Synth. Cat.* **2002**, *344*, 795-813. (k) Togni, A. In *Catalytic Heterofunctionalization*; 1st ed.; Togni, A., Gruetzmacher, H., Eds.; Wiley-VCH: New York, 2001; pp 91-141. (l) Nobis, M.; Drießen-Holscher, B. *Angew. Chemie, Int. Ed.* **2001**, *40*, 3983-3985. (m) Eisen, M. S.; Straub, T.; Haskel, A. *J. Alloys Comp.* **1998**, *271-273*, 116-122. (n) Mueller, T. E.; Beller, M. *Chem. Rev.* **1998**, *98*, 675-703.

2. Shannon, R. D. *Acta Cryst.* **1976**, *A32*, 751-767.

3. (a) Brinkman, E. A.; Berger, S.; Brauman, J. I. *J. Am. Chem. Soc.* **1994**, *116*, 8304-8310. (b) Hopkinson, A. C.; Lien, M. H. *J. Org. Chem.* **1981**, *46*, 998-1003.

4. (a) Stubbert, B. D.; Marks, T. J. *J. Am. Chem. Soc.* In press. (b) Stubbert, B. D.; Marks, T. J. submitted to *J. Am. Chem. Soc.* (c) See also Chapters 1 and 2.

5. Slow protonolytic precatalyst activation has also been noted for bulky secondary *N*-benzyl amine substrates in organoactinide-mediated HA/cyclization. See ref. 4a for full details.

6. (a) Stubbert, B. D.; Marks, T. J. *J. Am. Chem. Soc.* In press. (b) Stubbert, B. D.; Marks, T. J. submitted to *J. Am. Chem. Soc.* (c) See also Chapters 1 and 2.

7. The tetraphosphetane (PCy)$_4$ has been prepared stoichiometrically from an organomolybdenum complex: Felsberg, R.; Blaurock, S.; Junk, P. C.; Kirmse, R.; Voigt, A.; Hey-Hawkins, E. *Zeit. Anorg. Allg. Chemie* **2004**, *630*, 806-816.

8. (a) Klapars, A.; Parris, S.; Anderson, K. W.; Buchwald, S. L. *J. Am. Chem. Soc.* **2004**, *126*, 3529-3533. (b) Nubbemeyer, U. *Top. Curr. Chem.* **2001**, *216*, 125. (c) Maier, M. E. *Angew. Chem., Int. Ed.* **2000**, *39*, 2073. (d) Evans, P. A.; Holmes, B. *Tetrahedron* **1991**, *47*, 9131.

9.   Rate enhancements are observed with binuclear catalysts. Yuen, H. F.; Marks, T. J. Experiments in progress.

10.   For more detailed studies of thermal decomposition of coordinatively unsaturated organolanthanides, see: Ryu, J.-S.; Li, G.; Marks, T. J. *J. Am. Chem. Soc.* **2003**, *125*, 12584-12605.

Curriculum Vitae

Bryan D. Stubbert

2145 Sheridan Road
Department of Chemistry
Northwestern University
Evanston, IL 60208-3113
(847) 491-2982
bstubby@chem.northwestern.edu

EDUCATION

Northwestern University, Evanston, IL
Ph.D. in Chemistry (December 2006)
- Advisor: Professor Tobin J. Marks, Vladimir N. Ipatieff Professor of Catalytic Chemistry, Professor of Materials Science and Engineering
- Thesis title: Constrained Geometry Organoactinide Complexes: Scope and Mechanism of Intramolecular Hydroamination/Cyclization of Primary and Secondary Amines

University of California, Berkeley, CA
B.S. in Chemistry, May 1999
- Undergraduate research under the guidance of Professor Andrew Streitwieser, Jr.
- Undergraduate research apprentice with Professor Herbert L. Strauss

RESEARCH EXPERIENCE

University of Rochester, Rochester, NY
- Postdoctoral research with Professor Patrick L. Holland
  - Investigation of low-coordinate iron complexes as nitrogenase models

Northwestern University, Evanston, IL
- Synthesis of highly air- and moisture-sensitive organoactinide and organolanthanide complexes
  - Small-molecule catalytic (hydroelementation) reactions
  - Solid-state synthesis of f-element oxides and halides
  - Organic synthesis of proligands and substrate molecules
- Summer research prior to matriculation in the Graduate School
  - Synthesis of highly strained organic monomers for use in Ring-Opening Ziegler Polymerization (ROZP)

University of California, Berkeley, CA
- Undergraduate and post-graduate research with Professor Andrew Streitwieser, Jr.
  - Organic and organometallic synthesis

Affiliations
- American Chemical Society, 1999-present
  - Division of Inorganic Chemistry
  - Bioinorganic and Organometallic Chemistry subdivisions
- Chicago Local Section of the American Chemical Society, 2000-present
- Phi Lambda Upsilon, Chemistry Honor Society, 2002-present
- California Alumni Association, University of California, Berkeley, 1999-present
- National Association for the Advancement of Science, 2002-2003
- American Institute of Chemical Engineers, 1995-1997

Publications
- Bryan D. Stubbert and Tobin J. Marks "Constrained Geometry Organoactinides as Versatile Catalysts for the Intramolecular Hydroamination/Cyclization of Primary and Secondary Amines Having Diverse Tethered C–C Unsaturation" Accepted as an Article in *J. Am. Chem. Soc*.

- Bryan D. Stubbert and Tobin J. Marks "Mechanistic Investigation of Intramolecular Aminoalkene and Aminoalkyne Hydroamination/Cyclization Catalyzed by Highly Electrophilic, Tetravalent Constrained Geometry 4d and 5f Complexes. Evidence for an M–N σ-Bonded Insertive Pathway" Submitted as an Article to *J. Am. Chem. Soc*.

- A. M. Seyam, B. D. Stubbert, T. R. Jensen, J. J. O'Donnell III, C. L. Stern, and T. J. Marks "Organolanthanide constrained geometry complexes modified for catalysis: synthesis, structure, and aminoalkene hydroamination properties of a pyrrolidine-substituted constrained geometry organolutetium complex." *Inorg, Chim. Acta* **2004**, *357* (13), 4029-4035.

- Bryan D. Stubbert, Charlotte L. Stern, and Tobin J. Marks "Synthesis and Catalytic Characteristics of Novel Constrained Geometry Organoactinide Complexes. The First Example of Actinide-Mediated Intramolecular Hydroamination." *Organometallics* **2003**, *22* (24), 4836-4838.

Meetings and Presentations
- Bryan D. Stubbert and Tobin J. Marks "Synthesis and Catalytic Reactivity of Novel Organoactinide Complexes for Inter- and Intramolecular Hydroamination." Gordon Research Conference on Organometallic Chemistry, Salve Regina University, Newport, RI, July 11th-16th, 2004.

- Bryan D. Stubbert and Tobin J. Marks "Synthesis and Catalytic Characteristics of Novel Constrained Geometry Organoactinide Complexes." International Symposium on Relationships Between Heterogeneous and Homogeneous Catalysis XI, Evanston, IL, July 20th-25th, 2003.

- Tryg R. Jensen, Bryan D. Stubbert, and Tobin J. Marks "Ring-Opening Polymerization of Methylenecycloalkanes. Scope and Mechanism." Abstract of Papers, American Chemical Society, 221st National Meeting, San Diego, CA, March 30th-April 4th, 2001.

TEACHING EXPERIENCE

- **BIPmeister**, Northwestern University Department of Chemistry, Evanston, IL, 2004-2005. Volunteered to host, organize, schedule speakers, and coordinate weekly informal student seminar, primarily involving the Inorganic Division of the Department. (Please contact Prof. Basolo for more information).

- **Laboratory Mentor**, Northwestern University Department of Chemistry (Marks group), Evanston, IL, September 2001 to present (instructed and mentored graduate students, one post-doc, and one visiting scholar).

- **Teaching Assistant**, Northwestern University Department of Chemistry, Evanston, IL, September 2000 to June 2001 and January 2002 to March 2002.

- **Undergraduate Assistant Teaching Assistant**, University of California, Berkeley, Department of Chemistry, Berkeley, CA, January 1999 to May 1999.

REFERENCES

The faculty members from the Chemistry Department at Northwestern University listed below have offered to send a letter of support upon request.

- Tobin J. Marks, Doctoral Advisor
  Vladimir N. Ipatieff Professor of Catalytic Chemistry and
  Professor of Materials Science and Engineering
  Northwestern University, Chemistry Department
  t-marks@northwestern.edu
  (847) 491-5658

- Fred Basolo
  Professor Emeritus
  Northwestern University, Chemistry Department
  basolo@chem.northwestern.edu
  (847) 491-3793

- Hilary A. Godwin, Department Chair
  Howard Hughes Medical Institute Professor
  Northwestern University, Chemistry Department
  h-godwin@northwestern.edu
  (847) 467-3543

- James A. Ibers, Thesis Committee
  Charles E. and Emma H. Morrison Professor of Chemistry
  Northwestern University, Chemistry Department
  ibers@chem.northwestern.edu
  (847) 491-5449

- Thomas J. Meade
  Eileen M. Foell Professor
  Northwestern University (also BMBCB; Neurobio. & Physiology; Radiology)
  tmeade@northwestern.edu
  (847) 491-2481